QUANTIFYING SOIL FERTILITY PARAMETERS WITH ELECTROMAGNETIC INDUCTION, INFRARED REFLECTANCE SPECTROSCOPY AND CONVENTIONAL CHEMISTRY PROCEDURES FOR WHEAT AND MAIZE UNDER IRRIGATION IN ARID CLIMATE

By

Isaac Gura

Submitted in fulfilment of the academic requirements for the degree of the Doctor of Philosophy

(Soil Science)

Department of Soil, Crop and Climate Sciences

Faculty of Natural and Agricultural Sciences

University of the Free State

Bloemfontein

April 2021

Promoters: Prof CC du Preez

Prof LD van Rensburg

Co-promoter: Dr JH Barnard

DECLARATION

I, **Isaac Gura**, declare that the research work reported in this thesis hereby submitted for the degree of Doctor of Philosophy at the University of the Free State is my own work and has not been previously submitted at another University. I also relinquish copyright of the thesis to the University of the Free State.

Signature……

Date: April, 2021

Place: University of the Free State, Bloemfontein, South Africa.

ACKNOWLEDGEMENTS

Firstly, I want to acknowledge and thank Almighty God for His sufficient grace that enabled this research work to be accomplished. Secondly, my heartfelt gratitude goes to my supervisors, Professor C.C. du Preez and Dr J.H. Barnard for their valuable guidance, insights and support towards the consummation of this work. It would not have been possible without your valuable inputs. I also want to acknowledge Professor L.D. van Rensburg for his inputs and efforts toward this work and the broader Water Research Commission project. A special thank you to Dr E. Kotze for her assistance with the operation of the iS50 FTIR spectrophotometer and moral support. I would also want to thank the Water Research Commission and University of the Free State Postgraduate Research Development Centre for their financial contributions towards my upkeep, field and laboratory work. A special mention goes to my research colleague, Mr C. Mc Lean for his friendship and support during this study. His assistance is greatly appreciated. I would also want to acknowledge the members of staff in the Department of Soil, Crop and Climate Sciences: Professor A. Franke, Professor J.J. VanTol, Professor C.W. van Huyssteen, Mrs D. Terblanche Dr A. Mengistu, Dr C. Tfwala, Dr Z. Bello, Dr S.W. Mavimbela, Mr A. Rukudzo-Dzvene, Mr M. Mamera, Ms J. Edeh, to name just a few. Thank you all for your support. Finally, I want to acknowledge and appreciate the support I received from my family; my wife Erita and son Comfie during the course of this research work. Thank you very much for your patience and I say: *this is our accomplishment! To God be the glory!*

GENERAL ABSTRACT

Current global challenges, such as food security and soil quality, cannot be solved without up-to-date, high-quality, high-resolution, spatio-temporal, and continuous soil and environmental data that characterize soil and cropping ecosystems. Therefore, accurate and precise assessments of soil and crop characteristics are critical for site-specific management, vibrant soil condition and environmental sustainability. The inability to evaluate soil and crop characteristics quickly and inexpensively remains one of the main challenges of precision agriculture. Therefore, the ultimate aim of this study was to evaluate the use of soil sensors, *viz* the mid-infrared (MIR) sensor and the apparent electrical conductivity (EC_a) sensor, in quantifying multiple soil fertility properties and their variability under irrigation. The study also attempted to apply the sensor data fusion approach to improve the assessment of multiple soil quality indicators and the overall soil quality under irrigation using the Soil Management Assessment Framework (SMAF).

The established international EC_a-directed soil sampling design approach was employed at each of the seven fields of interest by measuring apparent soil electrical conductivity (EC_a) with a Geonics EM38-MK2 sensor (non-invasive geophysical electromagnetic induction, EMI). A “Response Surface Sampling Design” (RSSD) sampling methodology in the “Electrical Conductivity Sampling Assessment and Prediction” (ESAP) software was used to direct soil and crop sampling based on the degree of EC_a variability. This methodology reduced sampling points from each field to 12 sampling points after an initial EC_a survey. Soil samples from each field were analysed in the laboratory for various soil properties that are related to soil fertility. Wheat and maize were also sampled from the EC_a directed sampling points at each field at the end of the winter 2016 season and 2016/17 summer season, respectively. The MIR spectra was obtained in the laboratory from the soil and crop samples from each field using a sensor iS50 Nicolet Fourier Transform Infrared (FTIR) (Thermo Fisher Scientific Inc., Waltham, MA) equipped with an accessory for attenuated reflectance acquisition (iS50 FTIR-ATR).

The MIR sensor and EM38 sensor showed different levels of accuracy with respect to predicting soil fertility properties under irrigation. The study results demonstrated the effectiveness and usefulness of the MIR attenuated total reflectance (ATR) technique coupled with partial squares least regression (PLSR) in quantitative analysis of soil fertility properties. In contrast, the EM38 sensor modelled accurately only a few soil properties per site at a given sampling time. Comparatively, the model results from both sensors show that the MIR sensor produced better prediction models for most of the measured soil fertility properties than the EM38 sensor. For quantifying nutrient accumulation in wheat and maize, the MIR sensor technique produced more excellent predictive models for the nutrient concentrations in wheat samples than in maize. The results from the in-field spatial characterization of plant nutrient levels and crop yields at the study sites showed that although EC_a readings may be useful for the spatial characterization of some soil fertility properties in non-saline and non-sodic soils in South Africa, the results showed many inconsistencies between sites and between the centre pivots.

The limitations of quantifying soil properties and overall soil quality using a single soil sensor can be overcome by integrating data from conceptually different sensing techniques to improve model accuracy and robustness. The findings in this study demonstrated that models for most of the soil properties obtained based on step-wise multiple linear regression (SMLR) fusion of data from MIR sensor and EM38 sensor measurements were more robust as compared to models from individual sensors. The SMLR sensor fusion technique failed to improve the models of some soil properties at the selected fields as well as the overall SMAF soil quality index at the Douglas 40 ha field. A more robust fusion technique such as PLSR can be used to implement the data fusion for these properties. The sensor data fusion results demonstrate the superiority and efficiency of the sensor data fusion approach in the measurement of soil fertility properties and overall soil quality in irrigation systems of South Africa. Based on the findings of this study, for soil fertility evaluation and quantification, it is recommended to use the MIR technique coupled with PLSR and alternatively, the EC_a

measurements as complementary information to provide extended attribute coverage and increased capacity of the sensor data fusion.

Key words soil sensors; mid-infrared spectroscopy; apparent electrical conductivity; sensor fusion; soil fertility evaluation; in-field spatial variability; partial least square regression; step-wise multiple linear regression; principal component regression

TABLE OF CONTENTS

CHAPTER 1. MOTIVATION, OBJECTIVES AND HYPOTHESIS

1.1 Motivation

Current global challenges, such as food security and soil quality, cannot be solved without up-to-date, high-quality, high-resolution, spatio-temporal, and continuous soil and environmental data that characterizes cropping ecosystems (Grunwald *et al.,* 2011; 2015). Therefore, precise assessment and quantification of soil properties at different spatial scales is critical for management of soil quality. There is also need to evaluate the impact of land use changes and disturbances on soils in irrigated agriculture; however, the rapidity, robustness and efficiency of the existing direct and indirect methods to monitor these changes across large spatial scales need to be improved. Monitoring the changes in irrigated agriculture require the quantification of soil quality parameters which consist of multiple chemical, physical and biological soil properties (Veum *et al.*, 2017). Measurement of these soil properties often involves costly and labour-intensive laboratory analyses, which hinders the production of spatially dense, field scale data that is critical in site-specific management (Veum *et al.*, 2017). In contrast, on-the-go sensor technology has the potential to provide high-resolution spatial data quickly at low cost (Hummel *et al.,* 1996; Grunwald *et al.,* 2011; 2015).

Soil sensors have been widely used not only to estimate individual but multiple soil properties concomitantly and a sensor fusion approach has been applied successfully to improve estimates of multiple soil attributes (Wetterlind *et al*., 2015; Grunwald *et al.,* 2015; Veum *et al.,* 2015; 2017). There is sufficient evidence that sensor-derived and sensor-fusion models provide more cost effective solutions for spatial and temporal monitoring of soil properties when compared to traditional lab/field-based soil surveying specifically over large regions (Grunwald *et al*., 2015). Sensor fusion technology has the potential to provide high-resolution soil quality assessment data for better informed, site-specific management decisions. Hence, studies that deals with the fusion of data derived from various sensor technologies demands

special attention. The focus of this study is on the use of infrared reflectance spectroscopy and electromagnetic induction to assess and quantify selected soil properties from irrigated fields for site-specific management.

Soil test results are essential inputs to the effective application of fertilizer, lime, and other amendments (Adamchuk *et al*., 2004). A standard soil test usually includes determination of extractable phosphorous (P), exchangeable potassium (K), calcium (Ca) and magnesium (Mg), cation exchange capacity (CEC) and lime requirement when the pH is below the threshold of 5.5 (Adamchuk *et al*., 2004). The following measurements are also included to these primary measurements by some laboratories such as organic matter (OM) content, salinity, nitrate (NO_3^-), sulphate (SO_4^{2-}), certain micronutrients and heavy metals (Foth and Elis, 1998). The conventional option to determine these soil properties is mainly based on chemical methods which involves extraction or digestion before determining the relevant parameter by colorimetry or atomic absorptiometry (Fainthfull, 2002). The chemical methods are useful tools for soil characterization, but are very often time-consuming, which makes them unsuitable for fast or *in situ* evaluation of soil fertility as well as bulk analysis of soil samples that is required in precision agriculture (McCarty and Reeves, 2006; Ortega and Santibanez, 2007).

Infrared reflectance spectroscopy can be used as an alternative to conventional laboratory analyses as the measurement of soil or plant samples take just few seconds and several constituents can be analysed simultaneously with only one spectra (Shepherd and Walsh, 2002; Bauer *et al.*, 2008). This procedure has advantages over some of the conventional techniques of soil analysis, e.g., they are rapid, timely, and less expensive, and hence are more efficient when a large number of samples must be analysed (McCarty and Reeves, 2006; Nanni and Dematte, 2006). Spectral analysis is very important when infrared reflectance spectroscopy is used in the evaluation of soil fertility. Because of the interference of multi-components in the soil, multi-calibration should be involved for extracting the needed

information of the targeted nutrients in the soil spectra. Partial least square regression (PLSR) and principal component regression (PCR) are some of the important multivariate statistical methods that can be used to achieve this objective. However, there is a lack of published research information regarding interactions between infrared (IR) spectral data with soil fertility properties in South Africa.

Research has demonstrated that precision agriculture in the form of site-specific nutrient management can increase crop yield and in some cases, reduce the amount of fertilizer or lime applied (Heiniger *et al.,* 2003). Precision agriculture (PA) has been defined as farming with preciseness (Kitchen *et al.*, 1996) or as targeting the inputs of arable crop production according to crop requirement on a localised basis (Stafford, 1996). Whelan and Taylor (2013) defines PA as an integrated information- and production-based farming system that is designed to increase long-term, site-specific and whole farm production efficiency, productivity and profitability while minimising unintended impacts on wildlife and the environment. Site-specific crop management is possibly the most promising approach for achieving sustainable irrigation, which is predicated on a delicate balance of maximising crop productivity to maintain economic stability, while minimizing the use of natural resources and unfavourable environmental impacts (Corwin *et al*., 1999).

Generally, farmers manage agricultural fields as uniform units ignoring spatial and temporal variability and hence site-specific crop management (Venter *et al.*, 2004). This is not the most effective management strategy as some areas in the field receive too much application of resources and some areas receiving less, resulting in observed crop yield variation. Site-specific crop management is recommended as it ensures efficient use of resources and maximization of profit in irrigated agriculture. Site-specific crop management focus on management of soil spatial variability by applying inputs such as fertilizers in accordance with the site-specific requirements of a specific soil and crop (Fraisse *et al.,* 1999; Whelan and Taylor, 2013). Whelan and Taylor (2013) defines site-specific crop management as a form of

PA whereby decisions on resource application and agronomic practices are improved to better match soil and crop requirements as they vary in the field. Improved decision-making through site specific crop management will provide economic, social and environment benefits. However, site-specific crop management demands the identification of subfield regions with homogeneous characteristics, *viz* management zones. Determining subfield areas is difficult because of complex correlations and the spatial variability of soil properties responsible for variations in crop yields within the field (Corwin and Scudeiro, 2016). Therefore, efficient methods for accurately measuring within-field variability of soil properties such as plant nutrients are required in order to successfully implement site-specific management.

There are a variety of sensor-based methods for potentially characterizing soil spatial variability including ground penetrating radar, aerial photography, multi- and hyper-spectral imagery, time-domain reflectometry and apparent soil electrical conductivity (EC_a) (Corwin and Scudeiro, 2016). Another method that can be used to characterize soil spatial variability is grid soil sampling. However, this method is not viable because a large number of soil samples would be required in order to achieve a good representation of the nutrient levels. The geospatial measurement of EC_a is a sensor-based method that can be used to accurately measure in-field variability. The EC_a can be intensively recorded in an easy and inexpensive way, and it is usually related to various soil physico-chemical properties across a wide range of soils (Sudduth *et al.,* 2005), because it depends on the clay content, chemical composition of the soil solution and exchangeable ions, and the interaction between non-exchangeable and exchangeable ions (Rhoades *et al.,* 1989). Most of these ions are essential plant nutrients.

The measurement of EC_a is complicated by the interaction effects of several site-specific soil properties. Primary soil properties that principally influence EC_a measurements at a particular site include temperature, salinity, water content, texture, bulk density and organic matter. Secondary influences such as metal, surface roughness, soil compaction and surface geometry also affects the EC_a variability. The ability to measure a particular target property or

properties with EC_a depends on the property or properties dominating the EC_a measurement at the specific site of measurement. For this reason, it is necessary to determine the dominant soil properties influencing the EC_a measurements at the specific site of interest to interpret the information obtained from the map generated from measurement of EC_a (Corwin and Lesch, 2003). However, recent research on the applications of geospatial EC_a measurements in homogeneous management zones showed weak and inconsistent relationships between EC_a and plant nutrients (Corwin and Lesch, 2003; Heiniger *et al.,* 2003; Sudduth *et al.,* 2005; Peralta and Costa, 2013). These inconsistencies could have been due to complex inter-relationships between EC_a and soil properties at study sites. Nonetheless, other studies also have demonstrated that EC_a measurements can also be used as a surrogate measurement of some plant nutrients. Bronson *et al.,* (2005) reported that some extractable nutrients such as Ca^{2+}, Mg^{2+}, Na^{+} and CEC correlated with EC_a geospatial measurements. Peralta and Costa (2013) argue that if EC_a could be used to produce accurate spatial maps of site-specific management zones with differences in soil properties and nutrient concentrations designated, then this tool could be used for variable rate seeding and fertilization. The application of EC_a measurement in precision agriculture context has been intensively studied in the areas of soil salinity, water content and texture (Corwin and Scudiero, 2016) but limited studies have concentrated on the application of EC_a measurements in nutrient management in irrigated production systems. This study aims to investigate the use of EC_a in studying the spatial variability of plant nutrients that affects crop yield across an irrigated field for variable rate nutrient application.

Irrigation presents an effective tool that can be used to increase the yield potential of the arable lands in South Africa. However, a major objective in modern irrigated agriculture is to maximise the efficiency of irrigated crop production. It is critical for the irrigation farmers to refine their soil and crop management practices in improving crop yield, production efficiency and profitability in a sustainable manner. Moreover, the delineation of homogeneous management zones using soil sensor technology to improve nutrient management has not been adequately

studied in irrigated soils of South Africa. Hence, achievement of sustainability in irrigation systems can be enhanced by efficient nutrient management through the use of soil sensing technology in quantifying soil properties and their spatial variability which is an important nexus in precision agriculture.

1.2 Objectives

The objective of the study is to investigate the use of soil sensors in estimating multiple soil fertility parameters under irrigation. Specifics aims are:

- to determine the predictive capabilities of the mid-infrared (MIR) spectral datasets obtained with an iS50 FTIR spectrophotometer for predicting nutrients in soils and plants samples under irrigation.
- to determine whether EC_a can serve as an efficient estimator of plant nutrient levels for the demarcation of site-specific management zones in irrigated fields.
- to spatially characterize within-field variability of plant nutrients and crop yield under irrigation in wheat-maize cropping sequence.
- to characterize the spatial variability of seasonal nutrient removal by wheat and maize crops for formulating nutrient replacement strategies under irrigation.
- to evaluate a sensor data fusion approach on soils from irrigated fields using MIR spectra in conjunction with EC_a data to estimate multiple soil quality indicators, soil management assessment framework (SMAF) scores and overall soil quality.

1.3 Hypothesis

- An iS50 FTIR spectrophotometer can be used to measure nutrients in soils and plants indirectly after appropriate calibration and validation.

- Measurements of apparent electrical conductivity with electromagnetic induction (EM38) is an efficient estimator of plant nutrients and crop yield and can be a tool for the demarcation of site-specific management zones.
- Spatial plant nutrient variability have an influence on the performance of irrigated maize and wheat crops and will ultimately influence crop yield.
- Spatial variability maps of seasonal nutrient removal can be used effectively in formulating nutrient replacement strategies under irrigation.
- Sensor data fusion technique can best extract useful information from an iS50 FTIR-ATR sensor and EM38 sensor and will improve the accuracy of predictions of measurable soil quality indicators and SMAF scores as compared to either of the individual sensors.

CHAPTER 2. LITERATURE REVIEW

2.1 Introduction

Soil fertility is a commonly used concept that involves the function of soil properties, including soil minerals, water, organic matter, and plant nutrients among others (Desbiez *et al.,* 2004). Therefore, soil fertility is very all-inclusive, which cannot be measured directly but can be evaluated by some other soil properties such as plant nutrients and soil organic matter. Evidently, soil fertility and its variability at field scale is very important to sustainable agriculture; thus it is indispensable to know how to efficiently quantify variability of soil fertility for evaluation to optimise productivity (Du and Zhou, 2009). The achievement of sustainable agriculture through the application of precision agriculture requires the development of innovative new methodologies to assess and quantify soil fertility as well as its spatial and temporal variability. In particular, the use of spectroscopic techniques like infrared spectroscopy and the geospatial measurements of apparent electrical conductivity (EC_a) offer the potential to quickly and inexpensively characterize soil fertility and its variability in precision agriculture.

2.2 Irrigation management and soil fertility

Plant nutrient variability at field scale generally plays a prominent role among the factors responsible for spatial and temporal yield variability and is a major input resource for precision management (Smith *et al*., 2009). Fortunately, spatial variability of soil properties can be managed and the efficiency of nutrient use can be increased by spatial variable application of fertilizers to meet the specific needs of management zones. The cost of any uniformity in applications of resources through irrigation is presumed to be reduced yield and lower efficient use of resources. Uniform application of fertilizers assumes that the requirements of each

plant are exactly the same by ignoring differences in crop nutrient requirements due to spatial differences in soil hydraulic properties, fertility and other inputs (Smith *et al*., 2009).

Incorporating effective water and fertilizer management strategies is very important for optimizing crop productivity and maximizing the economic net return to maintain production sustainability in irrigated systems (Djaman *et al.,* 2013). Plant nutrients such as N, P, K, Ca, and Mg are indispensable elements for plant growth and development. Proper fertilizer management is therefore critical for food production, sustainability, and reducing adverse impacts of nutrients on the environment. Applications of nitrogen fertilizer that exceed crop requirements for maximum crop yield can result in residual soil nitrate (NO_3) that may leach or denitrify, which will reduce the efficiency of crop production (Djaman *et al.,* 2013). Farmers use a variety of methods when deciding on crop fertilizer requirements, ranging from traditional amounts of fertilizer application to imitating other farmers involved in the same farming trade. Ferguson *et al.* (2002) reported the advantage of site-specific N management and concluded that the spatial application of the existing recommendation algorithms developed for uniform application might be ineffective and that unique recommendation equations for specific soils and climatic regions may be necessary to achieve significant increases in N use efficiency.

Limited knowledge and data exist in terms of how water application affects plant nutrient uptake and the availability of soil residual nutrients in order to establish effective fertilizer management under irrigation to prevent undesirable environmental impacts. Generally, farmers assume that fertilizer needs across the entire field are uniform (Venter *et al.*, 2004). However, variability in soil properties, non-uniform irrigation applications, changes in the field landscape, non-uniform crop emergence, irrigation levels (e.g. full irrigation vs. limited irrigation), and other factors may result in spatially varying fertilizer requirements, nutrient uptake, and residuals (Djaman *et al.,* 2013). Hence, field studies are required to investigate the effects of the variability in irrigation management on plant nutrient availability and uptake to establish effective fertilizer management strategies.

Kumar and Dey (2011) reported that N, P, and K uptake was positively affected by irrigation method and the amount of water applied. They found that maximum nutrient uptake occurred in a fully irrigated treatment, while the rain-fed treatment had the least nutrient uptake. Research by Djaman *et al.* (2013) showed that irrigation variability significantly influenced maize above ground biomass production and maize grain yield. Maize biomass and grain yield increased with increasing irrigation amounts. The study also noted that while N uptake was similar in the two years of study, there was greater P and K uptake in the wetter year. In the same study, Djaman *et al.* (2013) also observed a decrease in grain N concentration with increasing irrigation and the observation was attributed to N dilution in the increasing dry matter, which increased with irrigation amounts. It was also noted that grain nutrient uptake was influenced by the irrigation regime and that N, P, and K uptake increased with irrigation amounts. Higher amounts of irrigation also increased soil K. Zeng and Brown (2000) reported that the mobility of soil K increased significantly with soil water content. Low soil water status has been found to restrict K ion diffusivity and its uptake as a result of impedance (Kuchenbuch *et al.,* 1986).

Research has demonstrated that differences in soil fertility can influence the amounts of N, P, and K taken up by maize plants, but not the seasonal pattern of uptake and distribution of these nutrients in the plants (Bender, 2012). Pandey *et al.* (2000) found that N uptake was more dependent on applied N than water supply, although N uptake decreased with greater water and N deficits. Irrigation frequency marginally influenced nutrient concentration and accumulation in maize, but increased frequency significantly increased the concentration and accumulation of certain nutrients (Hussaini *et al.,* 2008). These studies have demonstrated that crop growth, development and yield response to fertilizer varies substantially under various water management conditions. The driving factors for crop response to fertilizer is similar to those of crop response to water because both responses are driven primarily by climate, soil type, and especially specific soil and crop management practices. Studies have also demonstrated that the crop response to nutrient uptake varies considerably among

varying soil locations. Thus, the variations in crop nutrient uptake that manifested in crop growth and development and hence yield justify the developing of robust strategies to determine the crop response to nutrient management under irrigation management practices.

One important nutrient management principle is the importance of maximising crop productivity to increase the quantity of applied nutrient recovered by the crop (Havlin *et al.,* 2014). This reduces the quantity of the applied nutrient in the soil after harvest and thus, reduces the impact of nutrient use on the environment. Therefore, studies to understand the nutrient uptake dynamics and to determine the best nutrient management practices under irrigation are needed to aid farmers in increasing the efficiency of crop production and to protect the quality of soil and water resources. In South Africa, limited field data exist in terms of how agronomic management practices under irrigation affects spatial and temporal variability of plant nutrient availability and removal which is an important aspect in fertility management.

Information on the amounts of nutrients taken up by plants is of great practical interest in assessing the nutrient requirements of crops. Thus, soils should be able to supply sufficient nutrients without exhaustion. Information on nutrient uptake is also of importance in understanding the absorption of nutrients by crops to produce a certain yield, the ratio in which major nutrients are absorbed and the partitioning of absorbed nutrients in the plant (Tandon and Muralidharudu, 2010). Despite the complexity of nutrient management, improving producer's understanding of nutrient use and removal by wheat and maize plants and its variability under irrigation presents opportunities to optimize water and fertilizer application rates. This re-evaluation of plant nutrient uptake and partitioning under irrigation can provide the basis for refinement of nutrient management practices as farmers aim for increased yields and profitability.

2.3 Sensor fusion technology

Characterization of spatial and temporal variability of soil properties within a field is essential within precision farming model (Mahmood *et al.,* 2012). Due to high costs in conventional soil sampling and laboratory analysis for accurate establishment of spatial variability within landscapes, more efficient and cost-effective alternative methods are being explored to replace the conventional methods. Advances in remote and proximal soil sensing methods have made it possible to acquire large volume of soil and crop data rapidly for efficient and effective management. However, the accuracy of only using one soil sensor to predict soil properties is often low. The inability of a single-sensor based system can be overcome by integrating data from differing soil sensing methods (Adamchuk *et al.,* 2011; Mahmood *et al.,* 2012). This technique is termed data fusion or sensor fusion technology. The aim of the sensor fusion approach is to obtain target information with better quality and reliability. Sensor data integration may perform inferences that are potentially more accurate than those achieved by a single sensor (Mahmood *et al.,* 2009). Sensor fusion technology plays a pivotal role in soil modelling because it allows producing dense space-time data sets, is cost-effective and rapid, and facilitates to infer on multiple soil properties concomitantly. Hence, the fusion of data derived from various sensor technologies demands special attention (Grunwald *et al.,* 2015). Veum *et al*. (2017) asserts that modern agriculture has a challenge of attaining a balance of agronomic productivity with long-term sustainability and sensor fusion technology has the potential to address this challenge by providing high-resolution soil quality data for better informed, site-specific management decisions.

2.3.1 Sensor performance assessment

Majority of sensors used in agriculture provide signal output that is affected by more than one agronomic soil characteristic. Adamchuk *et al*. (2011) grouped the soil sensing methods into

categories as shown in Table 2.1 based on the principle of assessment. Table 2.1 also shows the soil properties that have been targeted using each sensing technique. Although a number of sensors are under development, only electrical and electromagnetic sensors have been widely used in precision agriculture (Adamchuk *et al*., 2004). These sensors give substantial information about soil spatial similarities and differences which is an important aspect in site-specific management. In many instances, an acceptable correlation between sensor output and particular agronomic soil property was found for a specific soil type or when the variation of interfering properties was insignificant. In most cases, the current sensing techniques have not been fully correlated with some important soil fertility properties such as micro-nutrients as shown in Table 2.1. It has not been thoroughly established in literature which sensor combinations could be used concurrently to describe the spatial variability of several agronomic soil properties in diverse cropping systems (Adamuchuk *et al*., 2004; Grunwald *et al*., 2015). Literature reports different levels of results on the assessments of the performance of a specific sensor in measuring soil properties. Precision and accuracy have been used as the standard quantitative assessments of sensor performance (Vaughan, 1999; Adamchuk *et al*., 2004). In this context, precision refers to the ability of the sensor to repeat its own measurement in the same location and time whereas accuracy denotes how well the sensor measurements correlate to an actual soil property that is determined using the conventional measurement technique. Both assessment methods define how well given soil properties can be predicted based on sensor output. Most of the studies in literature report these correlation relationships using Pearson's coefficient of correlation (r) or coefficient of determination (R^2). However, both values may depend on a range of soil properties used during evaluation and may vary in different locations (Adamchuk *et al*., 2004).

Table 2.1: Soil properties targeted with various soil sensing techniques (modified table adapted from Adamchuk *et al*., 2011)

Soil property[1]	Sensor type							
	Gamma-ray	X-ray	Optical	Microwave	Radio wave	Electrical	Electrochemical	Mechanistic
Chemical								
Total carbon	D	D	D					
Organic carbon	I		D					
Inorganic carbon	I		D					
Total nitrogen	D	D	D					
Total phosphorous	D	D	I					
Extractable phosphorous								
Total potassium	D	D	D					
Extractable potassium			I				I	
Other major nutrients	D	D	D					
Micronutrients	D	D	D					
Total Iron	D	D	D		I			
Iron oxides	I		D		I			
Heavy metals	D	D	I					
CEC	I		I			I		
Soil pH	I		I		D		D	
Buffering capacity and LR			I				I	
Salinity and sodicity					D	D	D	
Physical								
Color			D					
Water content	D			D	D	D		I
Particle size distribution	I				I	I		I
Clay minerals	I	D				I		I
Bulk density	I				D			I
Porosity								D
Soil strength								D

[1] – soil properties directly (D) or indirectly (I) predictable using different types of proximal soil sensors

2.3.2 Proximal soil sensors

Proximal soil sensing has been defined as “the use of field-based sensors to obtain signals from the soil when the sensor’s detector is in contact with or close to (within 2 m) the soil” (Viscarra Rossel *et al.,* 2011). Soil sensors have been used to cost-efficiently augment the number of observation sites in order to better characterize the spatial variation of physical and chemical soil properties. Applications of proximal soil sensors in soil and related sciences include soil mapping and monitoring, precision agriculture and farm decision making, environmental pollution assessment, among others (Grunwald *et al.,* 2015). There are a number of sensors that can be used in soil science but in this study, the focus will be on electrical conductivity sensors of electromagnetic induction (EMI) and MIR attenuated reflectance sensors of infrared reflectance (IR) spectroscopy. A brief discussion on other sensors that could be useful in soil sensing technology in literature will also be presented.

2.3.2.1 Electrical conductivity sensors

Soil electrical conductivity (soil EC) is the ability of soil to conduct an electrical current. Soil is a three-phase system composed of water, air, and organic and mineral solids that offer multiple pathways with different EC and an undefined boundary for electrical current to flow (Grunwald *et al.,* 2015). In this case, it is practical to measure the apparent electrical conductivity (EC_a) of the soil. Soil electrical conductivity (EC) is affected by a number of soil properties such as soil moisture, soil texture, and ion concentration among other properties. EC_a measurements has been used to estimate soil salinity (Li *et al*., 2013), cation exchange capacity (CEC) (Bronson *et al*., 2005; Sudduth *et al*., 2005), ion concentrations (Bronson *et al*., 2005), and soil water content (Sudduth *et al*., 2005). EC_a has also been used to estimate a number of soil physical and chemical properties such as particle size distribution (Bronson *et al*., 2005; Sudduth *et al*., 2005; Heil and Schmidhalter, 2012), topsoil depth (Sudduth *et al*., 2013), depth to clay layer (Saey *et al*., 2011), compaction (Al-Gaadi, 2012), water holding

capacity (Abdu *et al*., 2008), and organic matter or carbon (Sudduth *et al*., 2005). A study by Ekwue and Bartholomew (2011) predicted EC_a as a linear function of bulk density, clay, peat and water content, obtaining an R^2 of 0.89. In another study, Peralta and Costa (2013) proposed the use of EC_a to demarcate management zones. They predicted EC_a as a function of principal components derived from pH, CEC, organic matter, EC, and nutrients data also obtaining good results ($R^2 > 0.90$).

2.3.2.2 Ground penetrating radar and reflectometers

Ground penetrating radar (GPR), time-domain reflectometer (TDR), and frequency-domain reflectometer (FDR) measure the relative permittivity or dielectric constant of soil, which describes how easily an electric field is generated in the soil when electric current is applied to it (Grunwald *et al.,* 2015). These techniques follow the same principle of EC_a sensors, but their operation is based on electric field instead of electric current. Time-domain reflectometer measures the time it takes for the emitted electric pulse to interact with the soil and to return back. Frequency-domain reflectometer measures the frequency differences between the emitted electric pulse and the received pulse after interaction with the soil. The GPR does not require penetration of the soil, but instead it emits and receives a microwave (radar) pulse that interacts with the soil and is modified depending on the electrical conductivity (EC) and di-electric constant of the soil, where the depth of reading is inversely proportional to the EC. The operation of the GPR requires hauling it across a soil surface to produce a continuous cross-sectional profile of the soil plotting the distance versus depth. GPR, TDR, and FDR sensors have been used to estimate soil properties such as volumetric water content (VΘ), EC_a, NO_3^-, pore water salinity, and bulk density (ρb) (Grunwald *et al.,* 2015).

2.3.2.3 Infrared reflectance sensors

Visible (VIS), near-infrared (NIR) and mid-infrared (MIR) reflectance spectrometers measure the reflectance of the soil, that is, the proportion of the incoming light that is reflected by the soil. The reflectance of the soil depends on how its components interact with the received energy and is affected by the minerals, organic matter and water in soil and its particle size distribution as well as other soil-related factors (Grunwald *et al.,* 2015). The most common spectral ranges recognised by reflectance sensors include the visible (VIS ~ 400-700 nm), near-infrared (NIR ~ 700-2500 nm), and mid-infrared (MIR ~ 2500-25,000 nm). Ultraviolet (~200-400 nm) and far-infrared (~25,000-350,000 nm) sensors are less frequently used in soil assessments. The amount of soil preparation differs depending on the technology employed. VIS-NIR-MIR reflectance sensors produce spectra data containing hundreds to thousands of reflectance data that can be useful in a number of ways to estimate multiple soil properties (Grunwald *et al.,* 2015).

Lab-based VIS-NIR-MIR spectra have been successfully used to predict soil total carbon (McDowell *et al.,* 2012), soil carbon fractions (Vasques *et al*., 2008; Knox *et al*., 2015), and concurrently multiple soil properties (Shepherd and Walsh, 2002; Pirie *et al*., 2005; Viscarra Rossel *et al*., 2006; Ma *et al*., 2019). Field-based VIS-NIR-MIR techniques have been used effectively to predict soil clay, water, organic matter, carbon, phosphorus and sum of bases contents (Maleki *et al*., 2007; Viscarra Rossel *et al*., 2009; Minasny *et al*., 2009a). A study by Kodaira and Shibusawa (2013) used a mobile real-time VIS-NIR (305-1700 nm) sensor and partial least squares regression (PLSR) to estimate water, organic matter, pH, EC, CEC, C, N and P in soil, obtaining R^2 for prediction with range of 0.45-0.93. However, it is expected that spectral data obtained under laboratory conditions correlate better with other soil properties than those measured in the field under a less controlled environment (Grunwald *et al.,* 2015).

2.3.2.4 Gamma-ray sensors

Gamma-ray spectrometers measure the energy emitted by the soil in the form of gamma radiation. Multivariate techniques are employed in the analysis of gamma-ray spectra which can be analysed either as a whole or at the specific energy levels allowing the calculation of the concentrations of specific elements in the soil (Grunwald *et al.,* 2015). Gamma-ray spectroscopy has received attention in soil sensing technology because of its potential to characterize and correlate with soil parent material. Gamma sensors are being used to predict various soil properties, including soil texture, potassium and organic carbon and many other properties (Spadoni and Voltaggio, 2013; Dierke and Werban, 2013; Mahmood *et al*., 2013). Viscarra Rossel *et al.* (2007) analysed gamma-ray spectra to evaluate multiple soil properties using bagging and partial least squares regression (PLSR). The study found adjusted R^2 > 0.70 for clay, coarse sand and iron contents at 0-15 cm, and pH and coarse sand content at 15-50 cm respectively. However, the study also indicated that significant amounts of pre-processing were essential to obtain these results.

2.3.2.5 Magnetic susceptibility sensors

Magnetic susceptibility sensors measure how much soil is magnetized upon application of a magnetic field (Grunwald *et al.,* 2015). The magnetic susceptibility of soils depends on the type and concentration of minerals that can be magnetized, mainly iron minerals. The most common iron minerals in the soil with high magnetic susceptibility are magnetite and maghemite, but other iron minerals with low magnetic susceptibility also appear in higher concentration in soils, including hematite and goethite (Grunwald *et al.,* 2015). These magnetic iron minerals are associated with other soil mineral and organic constituents, and their concentrations relate to the original concentrations in the parent material. Moreover, the formation and dissolution of these magnetic iron minerals are controlled by soil pH and soil drainage properties such as water regime and texture. Magnetic susceptibility is also closely

related to electrical conductivity. Therefore, the magnetic susceptibility of soils can be used to estimate the concentration of soil iron minerals and other soil constituents using correlation (Grunwald *et al.,* 2015). Magnetic susceptibility has been used as a soil sensing technique to assess the concentration of heavy metals close to pollution sites (Lu *et al*., 2008), and soil deposition (Jong *et al*., 1998), but also to separate landscape segments (Barrios *et al*., 2012) and soil drainage classes (Wang *et al*., 2008). It has also been related to soil color and elemental mobility (Kumaravel *et al*., 2010). However, there is limited research on the influence of soil water on magnetic susceptibility (Grunwald *et al.,* 2015). Therefore, there should be more interest in investigating the inter-influence among soil water, magnetic susceptibility, electrical conductivity and permittivity.

2.3.2.6 X-ray sensors

Two field portable X-ray sensors, the X-ray diffractometer and X-ray fluorescence spectrometer, are commercially available and they have great potential to contribute to field assessments of soil mineralogical and elemental compositions (Grunwald *et al.,* 2015). X-ray diffractometers measure the diffraction of an X-ray beam upon contact with crystalline minerals in the soil. Generally, each mineral diffracts in a specific direction depending on its structure. X-ray diffractometers can be used for mineral identification and to semi-quantitatively estimate the concentration of minerals based on the peak intensities of the X-ray diffraction pattern (Grunwald *et al.,* 2015). X-ray fluorescence spectrometers measure the energy emitted by the soil in the form of fluorescent X-rays upon receiving high-intensity radiation from an artificial source (Grunwald *et al.,* 2015). Practically, these X-ray sensors are usually calibrated to quantify the most common of the elements in the soil such as Mg, Al, Si, P, S, Cl, K, Ca, Fe, etc., as well as trace elements of environmental concern e.g., Cr, Cd, Ag and Pb. X-ray fluorescence sensors have been used to measure heavy metals (Ridings *et al*., 2000; Wu *et al*., 2012) and estimate particle size contents indirectly by measuring multiple soil elements,

with R^2 as high as 0.98 (Zhu *et al*., 2011). More frequently, laboratory X-ray fluorescence instruments have been used to predict multiple soil elements (Towett *et al*., 2013).

2.3.2.7 Other proximal soil sensors

Other proximal sensing techniques are available with applications in soil science. These includes ion-selective electrodes (Adamchuk *et al*., 2005), photoacoustic spectroscopy (Changwen *et al*., 2013), laser-induced breakdown spectroscopy (Martin *et al*., 2010), laser-induced fluorescence spectroscopy (Milori *et al*., 2006) and inelastic neutron scattering (Wielopolski *et al*., 2011). Mechanical sensors that quantify penetration resistance of soil have also been used widely and are often combined with other sensors to quantify soil properties in precision agriculture (Grunwald *et al*., 2015; Veum *et al*., 2017).

2.3.3 Sensor data fusion

Even though studies on individual sensors show promising results, no one single sensor is able to fully characterize the spatial and temporal complexity of soils. It has been recognized that for many applications the information provided by individual sensors are incomplete, inconsistent, or imprecise (Simone *et al*., 2002). Mahmood *et al*. (2012) asserts that the accuracy of a single soil sensor is often low because most of the proximal soil sensors respond to more than one soil property of interest. Hence, additional sources may provide complementary data, and fusion of different information can produce a better understanding of the observed soil characteristics by decreasing the uncertainty related to a single sensor (Simone *et al.,* 2002). Sensor fusion can be a realistic alternative to integrate different scales of soil variation and different soil properties (Grunwald *et al.,* 2015). Overcoming the limitations imposed by uncertainties contained in any single data set such as data gaps, biases, inaccurate processing algorithms, nonlinear dynamics, model error, and surface heterogeneity is one of the purposes of the sensor fusion approach (Renzullo *et al*., 2008). There are three

major types of sensor fusion: (1) proximal sensor fusion, where only proximal sensors are used together; (2) proximal and remote sensor fusion, where proximal sensor(s) are used together with remote sensor(s); and (3) remote sensor fusion, where only remote sensors are fused. All three share in common that often additional environmental variables are used along fused sensor data to predict multiple soil properties (Grunwald *et al.,* 2015). Adamchuk and Christensen (2005) demonstrated a soil sensor fusion system that concurrently measures soil mechanical resistance, optical reflectance and capacitance. Fusing the three sensors addressed spatial variability in soil organic matter, water content and compaction. A proximal crop sensor fusion system that integrates crop canopy reflectance sensing with crop height evaluation using ultrasonic sensors concurrently with crop canopy temperature sensors was demonstrated by Shiratsuchi *et al.* (2005).The need for such a system can be explained by the difference in crop physiological properties when either N or water stress are observed (Adamchuk *et al.,* 2011).

To demonstrate the effectiveness of the sensor data fusion technique, a few preliminary studies have been conducted. For example, Wong *et al.* (2010) successfully used a dual EM38-gamma-ray soil sensing approach with a rule-base method to predict topsoil depth and soil pH with better accuracy than the single-based sensor approach. Taylor *et al.* (2010) made an attempt towards data fusion using a gamma-ray spectrometer and an EM38 sensor to predict topsoil clay content and concluded that soil property models based on both sensors predicted topsoil clay content better than models based on either of the sensors. Schirrmann *et al.* (2011) investigated a sensor fusion approach comprising a pH sensor, a VIS-NIR spectrometer and an EC_a sensor for mapping plant macro-nutrients in soil. The conclusion was that only the prediction of pH was improved by combining the data from all three sensors. These reviews showed that there is potential to get better soil property estimates using sensor data fusion, although this approach has not been extensively tested for predicting multiple soil quality indicators. Veum *et al*. (2017) applied a sensor-based approach to estimate soil quality indicators and SMAF scores using VNIR spectroscopy in conjunction with apparent electrical

conductivity (EC_a) and penetration resistance measured by a cone penetrometer. They found improved models for estimates of the individual physical, chemical and biological soil quality scores, demonstrating reductions in RMSE from individual sensors. If improved soil quality data from sensor fusion can be obtained at high spatial and temporal resolution, rather than from few selected sampling locations, soil quality maps can be generated for site-specific management applications, reducing the need for costly laboratory analysis (Karlen *et al*., 2019).

As indicated above, sensor data fusion may provide many possible benefits, such as robust accuracy, extended attribute coverage and complementary information on certain soil properties (Mahmood *et al.,* 2009). Nevertheless, limited research has been done on this topic that can be taken as reference for complementary sensor data fusion in the framework of precision agriculture (Mahmood *et al.,* 2012). Furthermore, as data fusion is a new field of research (Grunwald *et al*., 2015) literature so far has not provided guidelines on the best statistical and geostatistical data handling and analysis techniques for sensor data fusion to get the maximum benefit from this approach (Mahmood *et al.,* 2012). Hence it is of interest to compare different statistical data handling tools in assessing the efficiency of the sensor data integration approach in predicting multiple soil properties. Current sensor fusion research is focused on improvements in estimation of multiple soil properties using the data fusion approaches with an emphasis on in-situ data collection (Karlen *et al*., 2019).

2.4 Infrared spectroscopy for soil fertility evaluation

The determination of soil fertility in the laboratory usually includes determination of pH, extractable phosphorous (P), exchangeable potassium (K), calcium (Ca), and magnesium (Mg), as well as cation exchange capacity (CEC) (Adamchuk *et al*., 2004). Some laboratories include more soil fertility parameters such as salinity and contents of organic matter, nitrate,

sulphate, certain micronutrients and heavy metals (Foth and Elis, 1998). In addition, crop growth is affected by soil texture, soil compaction, water content, and other soil physical properties. The conventional option to determine these soil properties is mainly based on chemical methods, in which sample pre-treatment, such as soil extraction and soil digestion, and sample processing, such as colorization, are needed (Fainthfull, 2002).

Evaluation of soil fertility is now becoming a routine for soil and crop management in precision agriculture. However, laboratory analysis of soil properties is costly and time-consuming, which is not suitable for precision agriculture. Hence, infrared spectroscopy (IR) appears as an alternative technique to measure soil fertility parameters (Du and Zhou, 2009). Infrared transmission and reflectance spectroscopy are both useful in soil analysis. Infrared transmission spectroscopy is usually used in soil qualitative analysis, such as identification of soil organic matter, and reflectance spectroscopy can be used in soil quantitative analysis. Infrared reflectance spectroscopy has advantages over some of the conventional techniques of soil analysis, e.g. they are rapid, timely, and less expensive, and hence are more efficient when a large number of analyses are required (McCarty and Reeves, 2006; Nanni and Dematte, 2006; Du and Zhou, 2009). This technique's main advantages in precision agriculture application is speed, a high degree of automation, medium resolution, and cost-effectiveness (Bauer *et al.,* 2008). Moreover, spectroscopic techniques do not require expensive and time-consuming sample pre-processing or the use of chemical extractants that may be environmentally harmful (Du and Zhou, 2009). Another advantage is the potential adaptability of the techniques for field use (Viscarra Rossel and McBratney, 1998). These are principally important benefits knowing that there is an increasing global need for larger amounts of good-quality, inexpensive spatial soil data to be used in environmental monitoring and site-specific management (Mouazen *et al.,* 2007).

Spectral analysis is very important when infrared spectroscopy is used in the evaluation of soil fertility. Because of the interference of multi-characteristics in the soil, multi-calibration should

be involved for obtaining the needed information of soil fertility in the soil spectra. Sufficient soil samples with adequate variance are also needed for a good multivariate calibration of soil properties. A proper library of soil spectra should be assembled which would be a useful information system in the estimation of soil properties (Du and Zhou, 2009). This spectral information system will provide rapid and *in-situ* evaluation of soil properties, which will be beneficial for sustainable agriculture.

2.4.1 Infrared techniques and soil fertility measurements

Infrared spectroscopic techniques are highly sensitive to both the organic and inorganic phases of soil, making them useful in agricultural and environmental application. Intense fundamental molecular frequencies related to soil components occur mostly in the MIR wavelengths between 2,500 and 25,000 nm (Viscarra Rossel *et al.,* 2006; Du and Zhou, 2009). Infrared spectroscopy is based on the vibrations of atoms of a molecule. An infrared spectrum is generally obtained by passing infrared radiation through a soil sample and determining what fraction of the incident radiation is absorbed at a specific energy (Bauer *et al*., 2008). The energy at which any peak in an absorption spectrum appears to correspond to the frequency of a vibration of a characteristic of a soil sample, which makes infrared spectroscopy an alternative method in quantification of soil fertility properties (Dematte *et al.,* 2004; Du and Zhou, 2009). No two samples of different structure have exactly the same IR absorption pattern; thus, the IR spectrum of a sample can be described as a molecular fingerprint characteristic of a specific chemical or biochemical substance (Bauer *et al.,* 2008).

For the past three decades, NIR techniques have received more attention as a major tool for analytical purposes than MIR. The popularity of the NIR techniques was mainly due to the primary requirement of KBr as a diluting agent for MIR quantitative analysis (Pirie *et al*., 2005). However, the MIR technique have been developed and research have shown that dilution of soil samples is no longer necessary. The main benefits of near-Infrared (NIR) spectroscopy

are low absorptivity and low reflectivity (Bauer *et al.,* 2008). Low absorptivity permits energy to pass easily through samples without rapid attenuation. Therefore, sample path lengths can be much longer than for mid-infrared analysis (up to 10 cm), allowing sample analysis without the need for sample pre-treatment. Low reflectivity permits NIR energy to penetrate the surface of even visually dense samples. Generally, mid-infrared (MIR) soil spectral data are easier to interpret than information obtained from the UV–VIS and NIR spectral data. The reason for this is the existence of absorption bands for many soil constituents in the MIR region (Reeves *et al.,* 2001; Pirie *et al.,* 2005; Viscarra Rossel *et al*., 2006). Even though advanced IR spectroscopic techniques have been accepted strongly and has led to many applications in quantitative analysis, two critical factors are still problematic *viz*. accuracy and scale (Bauer *et al.,* 2008). The reliability of the results is directly proportional to the extent to which the samples adequately represent the sites from which they were taken; hence representative sampling is critical (Bauer *et al.,* 2008).

2.4.2 Calibration and model validation of spectral data

The application of infrared (IR) techniques in soil fertility is mostly dependent on spectra pre-treatment and multivariate calibration due to strong interferences in the spectra (Du and Zhou, 2009). Partial least square regression (PLSR) and principle component regression (PCR) are the most widely used mathematical tools in the prediction of soil properties from spectral data, and more mathematical tools-combined models will benefit the prediction performance (Viscarra Rossel *et al*., 2006; Bauer *et al.,* 2008; Du and Zhou, 2009). Furthermore, some of the regression methods that can be used to relate soil spectra data to conventional soil measurements are multiple linear regression (MLR), stepwise multiple linear regression (SMLR), multivariate adaptive regression splines (MARS), radial basis function networks (RBFN) and artificial neural networks (ANN) (Viscarra Rossel *et al*., 2006; Du and Zhou, 2009). During calibration, a model is related to the available data in such a way that it describes the data as reliable as possible. Validation establishes the model accuracy and precision and thus

how well a model will perform for independent samples collected from the same site as the calibration samples (Esbensen, 2002; Bauer *et al.,* 2008). When several soil properties are to be calibrated to the IR spectra data, calibration requires selection of the most relevant spectral wavelengths first, followed by informed use of multivariate calibration to optimize the calibration equations for each of the different soil characteristics (Bauer *et al.,* 2008; Du and Zhou, 2009). The strength of the calibration models are usually expressed using correlation coefficient, R^2. The squared correlation coefficient R^2 is used as a goodness-of-fit measure; the closer R^2 is to 1, the better is the prediction ability of the model. Another set of samples is required to validate the accuracy, precision, and robustness of an established calibration model. In regression, model validation allows for an estimation of the average prediction error and the outcome of the validation stage is the root mean square error of prediction (RMSEP) which is a measurement of the average difference between predicted and reference values at the validation or prediction stage, and it is expressed in the same units as the original soil characteristic values (Bauer *et al.,* 2008). The lower the RMSEP of a model, the higher the prediction power of the model performance. Some researchers suggested that using R^2 and RMSEP alone to compare the different models is not sufficient (Batten, 1998; Islam *et al.,* 2003, 2004a; Ward *et al.,* 2011). These researchers suggested to further use residue prediction deviation (RPD) along with R^2 and RMSEP to assess the prediction power of a model. The RPD is the standard deviation (SD) of data divided by the root mean square error of prediction (RMSEP), thus representing the average error on predicted values. However, there is no critical level of RPD for the application of IR analysis in the prediction of soil fertility properties and acceptable values depend on the intended use of the predicted variables. An approach suggested by Chang *et al.,* (2001) has been considered satisfactory where the RPD values are grouped into three categories. Using this approach, calibration models with RPD > 2 are considered excellent, those with RPD 1.4-2.0 are considered acceptable and lastly calibration models having RPD < 1.4 are considered unacceptable or requiring further improvements using various strategies.

2.4.3 Infrared spectra based plant nutrient analyses

Macronutrients such as C, N, P, K, Ca, Mg and micronutrients such as Cu, Zn, Fe, Mn, are required by plants and these elements play the most important role in soil fertility (Du and Zhou, 2009). Usually the nutrients content are determined through laboratory analysis. Many of the existing methods of soil and plant analysis are resource intensive and are not convenient for use when analysing a large number of samples usually required for site-specific management. It is possible to evaluate the nutrients' content in plants and soils using infrared spectroscopy. This technique of infrared spectroscopy could be a faster, cheaper, and more reasonable way in the evaluation of plant nutrients in soil and plants (Du and Zhou, 2009; Van Maarchalkerweerd and Husted, 2015). Viscarra Rossel *et al.* (2006) provided a review of some literature comparing quantitative predictions of plant nutrients using various multivariate techniques and reflectance spectra response in the infrared region of the spectrum. The content of soil C and N are mainly studied because they are more sensitive to infrared radiation. The calibration coefficients (R^2) were in the region of 0.80–0.98, and the root mean square errors (RMSE) were reasonable for fast evaluation of soil fertility. Soil C can be spectrally predicted with a reasonable accuracy level, depending on the type of instrument and environmental conditions, with RMSE ranging from 1 to 15 g C kg^{-1} (Du and Zhou, 2009). The calibration coefficient (R^2) was more than 0.8 and soil size particle has a strong influence on the model development. Mineralization of C was also studied using diffuse reflectance spectra (Mutuo *et al.,* 2006). Infrared studies of soil C source materials such as humic acids, fulvic acids, and their interaction products have been studied by Byler *et al.,* (1987) and Francioso *et al.,* (2007). Soil nitrate concentration has been measured directly using MIR ATR spectroscopy (FTIR-ATR) through the correlation between nitrate concentration and the vibration band around 1,350 cm^{-1} (Verma and Deb, 2007b). Shaviv *et al.* (2003) demonstrated that MIR-ATR can be used for direct determination of nitrate concentration in water, soil extracts, or soil pastes. A study by Linker *et al.* (2004) improved the nitrate determination accuracy using PCR and PLSR chemometric techniques. They managed to overcome some

of the interferences associated with soil pastes. However, the correlation was soil dependent, due mostly to varying contents of carbonate (Linker *et al.,* 2004, 2005). Linker *et al.* (2005) suggested the use of a two-stage method: (1) determination of the soil type and (2) determination of the nitrate concentration using the model related to a particular soil type. The suggested approach led to prediction errors significantly lower than those reported earlier (Shaviv *et al.,* 2003; Linker *et al.,* 2004), and prediction errors ranged from 6.2 to 13.0 mg kg^{-1}, depending on the soil type, with the lowest errors for light sandy soils. These errors were considerably smaller than those obtained using a single model calibrated with all the data (Linker *et al.,* 2006).

For the estimation of the other macronutrients such as P, K, and micronutrients the calibration model results are not stable, which mostly depends on the variability and capacity of the calibration set (Du and Zhou, 2009). A study by He *et al.* (2007) showed that NIR was not a good technique for P and K estimations, with R^2 values of 0.47 and 0.68, and RMSE values of 33.70 and 26.54, respectively and future research should be focussed on developing calibrations for open populations (Du and Zhou, 2009). However, in some instances the MIR technique have been demonstrated to be more superior to the NIR technique in the prediction of some soil properties (Pirie *et al.,* 2005; Viscarra Rossel *et al.,* 2006). Usually, infrared reflectance spectroscopy is used in the quantitative analysis of soil properties, but there are certain limits especially in the sample pre-treatment. Studies by Du and Zhou (2007) as well as Du *et al.* (2009) used infrared photoacoustic spectroscopy to quantify soil fertility and better calibration results were obtained for soil C, N, P and K. Ma *et al.* (2019) used diffuse reflectance spectroscopy (DRF), attenuated total reflectance spectroscopy (ATR) and fourier transform infrared photoacoustic spectroscopy (PAS) to evaluate soil pH, soil organic matter, total N and available P to explore their features in the MIR region. The study results demonstrated good performance of the ATR spectra for the prediction of pH, DRF spectra exhibited the greatest accuracy of prediction for soil organic matter and total N, but all three MIR techniques performed poorly regarding the prediction of available P. They further on

asserted that the efficiency of each technique might be affected by the contact between the sensor and soil sample, light paths, the position of soil particles for detection by infrared incident angles, peak interference and the prediction model. They concluded that future studies should investigate the respective advantages of each technique for evaluation of the properties of various other soils. These MIR techniques usually do not need sample pre-treatment, and a fast and *in situ* monitoring of soil nutrients can be reached, which is promising in the evaluation of soil fertility.

Using the technique of infrared spectroscopy combined with geographic information system (GIS) and geostatistical methods, the C, N, P and K spatial variability within a field can be obtained (Wetterlind *et al.,* 2008b; Christy, 2008), and spatial maps for C, N, P and K can be drawn (He *et al.,* 2005), in which spatial variability of plant nutrient status can be directly indicated. The reference maps for the predicted and measured values of C and N are usually the same due to the successful prediction of these parameters. The same cannot said for P and K due to the non-successful prediction of these soil components. However, there is a potential to develop a P sensing system using diffuse reflectance of soil for soil P testing and based on this technique a spectral map could be drawn, in which P spatial variability could be well represented and would be useful in site-specific management (Bogrekci and Lee, 2005b). The maps resulting from the IR spectra data are encouraging, and the potential for developing a cost-effective approach to map soil fertility from infrared spectra data at field-scale is considerable (Wetterlind *et al.,* 2008b).

There is a lack of more published research data regarding interactions between IR spectral data and soil fertility for local irrigation fields that could be critical in a site-specific management context in South Africa. MIR spectroscopy applications for irrigated soils in South Africa are almost non-existent. Thus, such lack of more accessible knowledge allows greater possibilities of researching application of MIR reflectance spectroscopy in soil fertility from a South African perspective. To make MIR data more reliable for soil survey, management and conservation,

it is important to prove their efficiency by comparing to conventional laboratory analyses and predictions with the MIR data. The key point is that there are few studies about spectral modelling of soil properties in South Africa and agriculture claims for efficient methods to predict soil properties with good accuracy which is more convenient in precision agriculture.

2.5 Apparent electrical conductivity (EC_a) measurements for site-specific nutrient management

Apparent electrical conductivity (EC_a) is a sensor-based parameter that reflects from the cumulative current applied by the device over a specific depth range (Edeh, 2017). The standard units of measure of EC_a are milliSiemens per meter (mSm^{-1}). Initially, the measurement of EC_a with electromagnetic induction (EMI) was regarded as the most practical method for the measurement of the spatial variability of soil salinity at field scales and larger (Rhoades *et al.,* 1999; Corwin and Lesch, 2003). Measurement of EC_a with EMI has the greatest potential for application to precision agriculture because of its reliability, accuracy, large volume of measurements and relative ease of obtaining the measurements (Corwin and Lesch, 2003). The primary soil properties that control the measurements of EC_a at field scale consist of soil water content, soil salinity, soil clay content, cation exchange capacity (CEC) and temperature. Other soil properties associated with EC_a measured by EMI sensors are bulk density, soil organic content, plant nutrients and the concentration of ions in a solution (Friedman, 2005).

2.5.1 Protocols for a field-scale EC_a surveys

More details on protocols for conducting an EC_a survey to characterize soil spatial variability at field scale were outlined by Corwin and Scudeiro (2016). The protocols consist of eight stages: (i) site description and EC_a survey design, (ii) EC_a data collection with mobile GPS-

based equipment, (iii) soil sampling design, (iv) soil core sampling, (v) laboratory analysis, (vi) calibration of EC_a to EC_e, (vii) spatial statistical analysis and (viii) GIS database development and graphic display. Corwin and Lesch (2005c) demonstrated the application of the EC_a survey protocols by conducting a soil quality assessment of a 32.4 ha field in California's San Joaquin Valley. The results clearly demonstrated the effectiveness of geospatial EC_a measurements for characterizing the spatial variability of certain soil properties at field scales. The protocols provide guidelines to assure the reliability, consistency and compatibility of EC_a survey measurements and their interpretation.

2.5.2 Determination of dominant soil properties influencing EC_a measurements

The fact that EC_a is a function of several soil properties (i.e. soil salinity, water content and texture) is often overlooked in the application of EC_a measurements obtained with EMI and ER to precision agriculture. Precision agriculture studies relating EC_a to crop yield have met with inconsistent results due to the fact that a combination of factors influence EC_a measurements to varying degrees across units of management, thereby confounding interpretation (Heiniger *et al.,* 2003). These factors include soil salinity, water content, saturation percentage, and bulk density. In areas of saline soils, salinity dominates the EC_a measurements, and interpretations are often more straightforward. To use spatial measurements of EC_a in a precision agriculture context, it is necessary to understand what factors are most significantly influencing the EC_a measurements within the field of study.

Corwin and Scudeiro (2016) asserts that the ability to measure a particular target property or properties with EC_a depends on the property or properties dominating the EC_a measurement at the specific site of measurement. For this reason, it is necessary to determine the dominant soil properties influencing the EC_a measurements at the specific site of interest to interpret what information is being conveyed by the information from the map generated from measurement of EC_a (Corwin and Lesch, 2003). Corwin and Scudeiro (2016) further

elaborated on the importance of determining dominant factors influencing spatial measurements of EC_a within the field of study in a soil quality or site-specific management context. For example, when salinity is sufficiently high (i.e. EC_a > 1-2 dSm^{-1}) to dominate the EC_a measurement, the influence of other soil properties (i.e. mineralogy, texture, bulk density, water, OM, CEC) becomes insignificant. In these instances, EC_a is principally measuring only soil salinity. However, when there is little significant effect of salinity on the EC_a measurement (i.e. EC_a < 1 dS m^{-1}), then the interpretation of the meaning of the EC_a measurement can only be established directly from soil samples using a relationship between EC_a and all potential soil properties influencing EC_a. In an EC_a range of 1 to 2 dS m^{-1}, it is likely that several soil properties are influencing EC_a in a significant manner (Corwin and Scudeiro, 2016). In this scenario, geospatial EC_a measurements can be used as a surrogate of soil spatial variability to direct soil sampling when mapping target soil properties at field scale and larger spatial scales.

2.5.3 Agricultural applications potential of geospatial EC_a measurement

Increased interest in precision agriculture has led to the vast application of EC_a in agriculture. EC_a measurement is considered as the best method to spatially determine soil salinity (Rhoades *et al.*, 1999; Corwin and Lesch, 2003). Strong correlation between soil water content and EC_a measurement has long been an established fact (Edeh, 2017). Some studies have also evaluated EC_a to describe several soil properties that can possibly influence crop yield (Johnson *et al.*, 2001; Corwin *et al*., 2003a). A few studies have been conducted on the EC_a measurements application to field assessment with respect to a full spectrum of soil fertility properties. The use of geospatial EC_a measurements can improve the characterization of the spatial pattern of edaphic properties that influence soil fertility properties such as plants nutrients which in turn can be used to define site-specific crop management units (Moral *et al.,* 2010).

2.5.3.1 Quantification and evaluation of plant nutrient variability

Soils vary widely in their nutrient contents and in their ability to supply sufficient macronutrients and micronutrients for optimal crop production. The spatio-temporal variability of plant nutrients may be affected by soil type, land forms, vegetation, climate, and anthropogenic activities. Therefore, plant nutrient content, distribution, and availability can vary widely among soils both within and between fields as well as seasonally (Corwin and Lesch, 2003). If EC_a could be used to produce accurate maps of zones with the differences in the plant nutrient concentrations indicated, it could be a useful tool for variable- rate seeding and for fertilizer producers and users (Peralta and Costa, 2013). The reason is that, the effect most soil properties imposed on EC_a are to an extent fixed; while, some show seasonal changes. Thus, EC_a measurements have been consecutively applied to understand soil variability, both spatially and temporally (Brocca *et al.*, 2009, 2010). Eigenberg *et al.* (2002) related time structured EC_a data to temporal changes with the hypothesis that EC_a measurements might be used as an indicator of soluble nitrogen gain and loss in the soil over time.

Plant nutrients such as N and K directly affect the electrical conductivity of the isolated soil solution. Therefore, geospatial EC_a measurements could be used to measure the available nutrient content in soil, thereby eliminating the need for time consuming and expensive soil sample acquisition (Heiniger *et al.,* 2003). The most important factor influencing EC_a is the volumetric water content of the soil and changes in volumetric water content tend to mask differences in other factors influencing EC_a (Rhoades *et al.,* 1989; Nadler, 1982; Heiniger *et al.,* 2003). Another major factor influencing EC_a is soil salinity (Malicki and Walczak, 1999; Heiniger *et al.,* 2003). At high Na concentration, the conductivity of the soil solution is greater than that of the bulk soil (Heiniger *et al*., 2003). However, in non-saturated and non-saline soils, the conductivity of the bulk soil is greater due to the contribution of adsorbed ions. In most productive agricultural fields, salinity does not have a major influence on EC_a. Therefore, under non-saturated conditions changes in nutrient levels will most likely influence EC_a by

changing electrical conductivity of soil solids through differences in the type and number of cations held by the soil particles (Heiniger *et al.,* 2003). Hence cations commonly associated with binding sites on the soil particles such as Ca, Mg, or K could influence EC_a by changing electrical conductivity of soil solids. However, the common assumption is that, in most field conditions, the influence that changing levels that cations have on electrical conductivity of the soil is minor compared with the influence associated with changes in soil bulk density and texture (Lund *et al.,* 1999). A study by Bronson *et al* (2005) reported that soil properties that correlated with EC_a included silt, extractable and soluble Ca^{2+}, Mg^{2+}, Na^{+} and CEC. Hence geospatial EC_a measurements can be used as a surrogate measurement of some plant nutrients in soil.

Differences in plant nutrient contents could also potentially influence EC_a through changes in the conductivity of the soil solution. Under saturated conditions, changes in nutrient levels could influence EC_a by changing electrical conductivity of the soil solution (Rhoades *et al.,* 1989; Heiniger *et al.,* 2003). Therefore, dissolved nutrients such as N and S should have more influence on EC_a under saturated conditions than when the soil is close to the wilting point. Unfortunately, large differences in volumetric water content across a field will likely mask small differences that changing nutrient levels will have on electrical conductivity of the mobile soil solution. Heiniger *et al.* (2003) strongly suggests that taking consideration of the factors contributing to EC_a, it may be difficult to directly measure site-specific changes in nutrient content using electrical conductivity. Furthermore, they suggest that a close analysis of the factors contributing to EC_a suggests that EC_a might be used along with other measurements of soil properties such as texture, water-holding capacity, pH and CEC to determine nutrient levels in the soil. Chang *et al.* (2001) suggested that if spatial differences in water-holding capacity and salt concentration were taken into account, there would be a good relationship between plant nutrient levels and EC_a. Another study by Doolittle *et al.* (1994) suggests that EC_a could be used to determine depth to a clay layer and that these measurements identified

areas where EC_a was related to plant nutrient contents. Because soil properties such as texture and CEC are static over time, a model that include these measurements along with EC_a could be developed to predict plant nutrient contents (Heiniger *et al.,* 2003).

A study by Sudduth *et al.* (2005) examined the relationship of EC_a with various soil physico-chemical properties across a wide range of soil types, management practices and climatic conditions. For all fields, clay content and CEC presented the highest correlation with EC_a. The implication of this work is that it may be feasible to develop relationships between EC_a and either clay or CEC that are applicable across a wide range of soil and climatic conditions. Apparent soil electrical conductivity could also be used to indirectly determine field sites where plant nutrient levels differ. Depth of topsoil, texture, soil water content and CEC are all good indicators of crop productivity (Jaynes *et al.,* 1995; Sudduth *et al.,* 1996). Because EC_a is able to measure these soil properties directly, it has the potential to identify management zones with differing crop productivity and nutrient requirements. Several researchers have reported that EC_a was useful in identifying field sites with different soil properties (Sudduth *et al.,* 1999; Franzen and Kitchen, 1999). Sudduth *et al* (1996) found that EC_a was correlated with depth to clay. Because depth to clay was the primary factor influencing yield at different field sites, EC_a proved to be a valuable tool in determining site-specific N requirements. These studies indicate that EC_a could indirectly provide a useful measure of plant nutrient levels.

2.5.3.2 Delineation of site-specific management units

Site-specific crop management (SSCM) is a form of precision agriculture whereby resource application and agronomic practices are improved to better match soil and crop requirements as they vary across the field (Whelan and Taylor, 2013). SSCM enables the identification of management zones within the area that usually have the same soil characteristics such as topography and nutrient levels (Kitchen *et al.,* 2005). Site-specific management (SSM) relies

heavily upon information and electronic technologies to improve the management of soils, crops and pests in a site-specific manner. Characteristics of SSM involves the following: (i) quantification of yield variability in small areas of the field, (ii) quantification of the spatial variability of soil properties influencing yield and (iii) amendment of inputs such as fertilizer, pesticides and seeding rates based on the soil and yield variability (Atherton *et al.,* 1999). Hence, accurate and efficient methods for measuring the spatial and temporal variability of soil characteristics that influence yield are required to make SSCM a reality (Bullock and Bullock, 2000). The geospatial measurements of EC_a is one of the technologies that can be used to achieve SSM. Measurements of EC_a helps in identification and analysis of sampling locations based on a sampling plan in order to characterize the spatial and temporal variability of soil properties that influences crop yield (Corwin and Scudeiro, 2016).

A study by Kitchen *et al.* (2005) applied EC_a measurements to SSM by observing whether homogeneous zones can be delineated using EC_a and elevation measurements on Missouri clay-pan soil fields. Homogeneous zones were zones of similar yield and useful for making management decisions based upon reliable estimates of expected yield. Unsupervised fuzzy-c means clustering was used on yield data to demarcate ground-truth homogeneous zones with combinations of EC_a and elevation data to define hypothetical management zones. A comparison of the ground-truth and hypothetical management zones using an overall accuracy statistical model, the Kappa coefficient showed that there was a 60–70% agreement when combined EC_a and elevation data are used. Homogeneous management zones were also researched by Jaynes *et al.* (2005). In this study, the demarcation of homogeneous management zones was based on a series of profiling steps in combination with cluster analysis to determine the relationship between yield clusters and easily measured field properties of elevation, simple terrain attribute data such as slope and aspect and EC_a. EC_a and the terrain characteristics were effective in identifying soybean yield clusters. This allowed easily measured field attributes to be used to estimate soybean management zones in similar fields where yield data was not be available.

The research by Kaffka *et al.* (2005) highlighted the effectiveness of using EC_a measurements to establish the relationship between soil properties and crop yield for resource management which is crucial to direct SSM. With the resultant SSM information, the study explored the relationship between yield and profit to consider the option of taking those areas of the field that were a net loss to the producer out of production. The greatest agricultural application of EC_a measurements in the short term is for directing soil sampling to characterize site-specific spatial and temporal variability of soil properties. However, the characterization of soil spatio-temporal variability is an essential component in site-specific management and the geospatial EC_a measurements will likely continue to serve a major role in future research.

2.6 Conclusions

Soil fertility and its variability is a decisive soil property in crop production and very important concept in sustainable agriculture. Soil fertility is usually illustrated by soil properties such as plant nutrients level, soil organic matter and water; therefore, the related soil properties should be first determined and then a model based on the soil properties is made to give an evaluation of soil fertility. The conventional technique of soil fertility evaluation is based on laboratory analysis and is costly and time-consuming which is not suitable for precision agriculture. The use of soil sensors such as infrared spectroscopy (IR) and electromagnetic induction (EMI) sensors offer alternative techniques that can be used for the evaluation of soil fertility and its variability in precision agriculture.

Although a number of sensors are under development, only electrical and electromagnetic sensors have been widely used in precision agriculture because of their ability to provide valuable information about soil spatial differences which is an important aspect in site-specific management. Numerous attempts have been made to evaluate soil fertility using infrared spectroscopy; however accuracy and scale are still critical factors that need to be improved. Because of the interference of multi-components in the soil matrix, multi-variate statistical

techniques should be involved for extracting the required information in the soil spectra data. Hence, choosing the multi-variate statistical method is a critical step in spectral data analysis and subsequent model development. Several researchers have demonstrated the usefulness of EC_a measurements in site-specific management; however limited studies have concentrated on the application of EC_a measurements in nutrient management to improve yields.

Even though studies on individual soil sensors show promising results, no one single sensor is able to fully characterize the spatial and temporal complexity of soils. As a result, the integration of different measurements concepts in interpreting and mapping agronomic soil properties is one of the current subjects of research (Karlen *et al.,* 2019). The fusion of data from different sensors is believed to better predict selected agronomic soil attributes and support site-specific management. An example of sensor data fusion is the coupling of MIR spectra with EC_a data to determine differences in soil quality indicators in diverse cropping systems. Furthermore, an EC_a map can be used along with soil pH measurements to prescribe variable rate lime applications. However, it has not been thoroughly established which sensor fusion methods could be used to describe the spatial variability of several agronomic soil properties in diverse cropping systems. Therefore, more studies investigating the sensor data fusion approach are still needed to help in making useful management decisions in precision agriculture.

CHAPTER 3. MATERIALS AND METHODS

3.1 Study sites

This study is part of the Water Research Commission (WRC) project on developing management guidelines for technology transfer to reduce salinization of irrigated land with precision agriculture. Three sites were selected for this study. The sites are situated near Douglas (Northern Cape), Luckhoff (Free State) and Hofmeyr (Eastern Cape).

3.1.1 Location

The fields at the three sites were irrigated with centre pivot irrigation systems. The first study site is a 30 ha field situated on Zoutpansdrift farm, about 20 km northwest of Douglas. This field is irrigated by water abstracted from the Lower Riet River. The second study site is on De Kroon farm, about 40 km south west of Luckhoff. The farm is located along the Settlement section of the Orange-Riet Irrigation Scheme and irrigated with water from the Orange River. Four centre pivot irrigated fields from this farm were used for this study. The third study site on Juriesbaken farm is located along the Fish River near Hofmeyr. On this farm, two fields that were irrigated with water from the Gariep Dam, via the Orange-Fish Tunnel which stretches from the Gariep Dam to Teebus were investigated.

3.1.2 Climatic conditions

The climate at Douglas is classified as hot semi-arid according to the Köppen-Geiger classification system and receives little rainfall throughout the year. In the Luckhoff area, the climate is classified as cold semi-arid and also with little rainfall. Similarly, the climate near Hofmeyr is also classified as cold semi-arid with little rainfall throughout the year. Weather conditions were obtained from the DeHoek weather station, 34 km west of Douglas; Rust

station, 33 km south of Luckhoff and the Grootfontein station, 49 km west of Hofmeyr for the 2016 winter season and 2016/17 summer season (Table 3.1).

Table 3.1 Weather data for the 2016 winter and 2016/17 summer seasons at the study sites (Van Heerden and Walker, 2016)

Season	Weather Characteristic	Douglas	Luckhoff	Hofmeyr
2016 winter	Mean Max Temp	24.3	23.0	20.9
	Mean Min Temp	6.3	6.7	4.5
	Mean Max RH(%)	84.6	85.4	*
	Mean Min RH(%)	19.5	20.6	20.5
	Mean Total Radiation (MJm^{-2})	19.2	19.9	18.8
	Mean Wind Speed (ms^{-1})	1.9	2.0	1.2
	Total Rainfaill (mm)	80	91	110
	ETo (mm/day)	3.9	5.3	3.9
2016/17 summer	Mean Max Temp	29.3	28.7	-
	Mean Min Temp	13.1	13.5	-
	Total Rainfaill (mm)	260	234	-
	ETo (mm/day)	5.1	4.9	-

*No information available

3.1.3 Soil types

The soils of the fields at all the study sites were classified according to the South African Taxonomic Soil Classification System (Soil Classification Working Group, 1991). The Douglas site is dominated by soil forms ranging between Augrabies, Montagu, Brandvlei, Addo, Clovelly and Molopo. These soils are characterized by orthic A-horizons followed by mainly calcium carbonate containing subsoils indicating low external drainage rates. The Montagu soil form is described as having unspecified material with signs of wetness in the C horizon which confirms poor drainage. Soils at the Luckhoff site are wind-blown sands deposited on rock, hard and soft carbonates. The soils at this site are dominated by the Hutton soil form. At the Hofmeyr site, the soils are of Oakleaf, Mispah, Hutton, Glenrosa, Clovelly and Valsrivier forms, with Oakleaf being the dominant soil form. The Glenrosa and Mispah soil forms at this site indicates the presence of shallow and marginal soils.

3.1.4 Agronomic management

Standard agronomic management practices such as irrigation scheduling, fertilizer application and pest control were adopted by the farmers at the study sites. There were no special amendments made for the sake of the project during the study period. Some of the relevant soil and crop management practices implemented by the farmers during the course of this study are given in Tables 3.2 and 3.3. A wheat-maize sequence was implemented at all sites except for Hofmeyr where only wheat was planted. A wheat crop was grown during the 2016 winter season and a maize crop during the 2016/17 summer season. The wheat was planted with a row spacing of 20.0 cm and 27.5 cm at Luckhoff and Hofmeyr respectively; however, at Douglas, the wheat crop was sown. The row spacing for maize was 76.0 cm at both Luckhoff and Douglas sites, respectively. Agronomic management practices were mostly the same at the different study sites and some differences were noted at Luckhoff. Firstly, the 20 ha field was irrigated with drainage water from the other two 60 ha fields. The amount of NPK fertilizer applied during the summer on the 40 ha pivot was different from the other three centre pivots. Crop residue management implemented on most of the centre pivots at Luckhoff was burning. Before planting of wheat, all the residues under the centre pivots were burnt after harvest except under the 40 ha pivot where the residues were retained. Likewise, before the planting of maize, the residues under all the centre pivots were also burned except the upper 60 ha NE field where the residues were retained after harvest.

Table 3.2: Agronomic practices applied on four centre pivots at Luckhoff study site during the 2016 winter and 2016/17 summer growing seasons

	20ha		40ha		60ha (Upper NE)		60ha (Lower NW)	
	Jun-Dec 16	Dec-May 17	Jun-Dec 16	Dec-May 17	Jun-Dec 16	Dec-May 17	Jun-Dec 16	Dec-May 17
Crop	Wheat	Maize	Wheat	Popcorn	Wheat	Maize	Wheat	Maize
Cultivar	SST 835	PAN 6126	SST 835	427	SST 835	PAN 6126	SST 835	PHB 32B07BR
Planting density	100kg/ha	85 000	100kg/ha	80 000	100kg/ha	90 000	100kg/ha	90 000
Planting date	20-June-16		16-June-16		10-June-16		22-June-16	
First harvest date			29-Nov-16					
Second harvest date								
Post-harvest crop residue management	Burn	Burn	Retained	Burn	Burn	Retained	Burn	Burn
Pest management	Lice sprayed	Red spider mite and worms sprayed	Spray for lice	Red spider mite and worms sprayed	*	*	Lice sprayed	Red spider mite and worms sprayed
Weed management	Spray for weeds before wheat covers soil surface	Spray for weeds; johnson grass	Spray for weeds before wheat covers soil surface	Spray for weeds; johnson grass	*	*	Spray for weeds before wheat covers soil surface	Spray for weeds; johnson grass
Cultivation practices	Plough to 300 mm depth, followed by tillage to 300 mm depth	Plant immediately after wheat was burnt	Plough to 300 mm depth, followed by tillage to 300 mm depth	Plant immediately after wheat was burnt	Deep till to 300-500mm depth followed by disc till to 200-300 depth	Strip till to 200-300mm depth followed by ortman cultivation	Deep till to 300-500mm depth followed by disc till combination to 200-300 depth	Deep till to 300-500mm depth followed by disc till combination to 200-300 depth
Fertilizer type ($kgha^{-1}$)	Plant mixture and then 'straights	Plant mixture and then 'straights	Plant mixture and then 'straights	Plant mixture and then 'straights	*	*	Plant mixture and then 'straights	Plant mixture and then 'straights
Total kg N ha^{-1}	252	280	252	280	252	284	250	284
Total kg P ha^{-1}	42	53	42	53	42	53	42	53
Total kg K ha^{-1}	52	65	52	65	52	65	52	65
Method of fertilizer application	Fertigation through centre pivot	Fertigation through centre pivot	Fertigation through centre pivot	Fertigation through centre pivot	*	*	Fertigation through centre pivot	Fertigation through centre pivot

*No information available

Table 3.3: Agronomic practices applied at Douglas and Hofmeyr study sites during the 2016 winter and 2016/17 summer growing seasons

	Douglas		Hofmeyr
	Jun-Dec 16	Dec –May 17	Jun-Dec 2016
Crop	Wheat	Maize	Wheat
Cultivar	PAN 3497	PHB 32Y27	SST 884
Planting density	80 kg/ha	88 000	130kg/ha
Planting date	07-Jul-16	03-Dec-16	03-Aug-16
First harvest date	07-Dec-16	28-May-17	10-Dec-16
Post-harvest crop residue management	Burn	Strip till	Retain
Weed management	MCPA/Resolve	Primagram	Spray for weeds before wheat covers soil surface
Cultivation practices	CLG to 450 mm depth	Strip till to 300mm depth	Burn and plant
Type of fertilizer applied ($kgha^{-1}$)	Plant 350 2:3:2	Plant 350 2:3:2	*
Total kg N ha^{-1}	280	310	*
Total kg P ha^{-1}	55	65	42
Total kg K ha^{-1}	85	90	52
Method of fertilizer application	Granular fertilizer with plant; Liquid fertilizer rest of the season	Granular fertilizer with plant; Liquid fertilizer rest of the season	Band application of planter-mixture and fertigation thereafter
Total irrigation water applied (mm)	540	600	*

*No information available

3.1.5 Irrigation water quality

The quality of the water the farmers used for irrigation at the study sites during the winter 2016 and the summer 2016/17 seasons are shown in Table 3.4.

Table 3.4: Irrigation water quality at the three study sites during the two growing seasons (Huizenga *et al.,* 2013)

	Douglas		Luckhoff		Hofmeyr
	Winter-16	Summer-16/17	Winter-16	Summer-16/17	Winter-16
EC ($mS\ m^{-1}$)	180 (SD=152)	105 (SD = 33)	17.9 (SD=2.3)	18.5 (SD=2.4)	16
SAR	<5	<5	<1	<1	_

EC = Electrical conductivity; SAR = Sodium adsorption ratio

3.2 Sampling points selection

The established international EC_a-directed soil sampling design approach was employed at each of the seven fields by measuring apparent soil electrical conductivity (EC_a) with the Geonics EM38-MK2 (non-invasive geophysical electromagnetic induction, EMI). The full details on the collection of the EC_a data at the study sites is outlined in Section 3.5.2. With the approach soil sample point selection is based on the spatial variation of geo-referenced EC_a measurements with a model-based response-surface sampling design (RSSD) to minimise the number of points needed to characterise the spatial variation of soil properties (Corwin and Lesch, 2010). The Electrical Conductivity Sampling Assessment and Prediction software (ESAP-95 Version 2.01R) was used to choose the reduced sampling points from each field to 12 sampling points per field after an initial EC_a survey. With the initial EC_a data collected at the start of the winter cropping season in 2016, 12 soil sampling points were identified for each study site using the ESAP-RSSD sampling methodology (Corwin and Lesch, 2003; 2010). These sampling points were used for the collection of soil samples at different time intervals during the course of the 2016 winter and 2016/17 summer growing seasons.

3.3 Soil and plant sampling

3.3.1 Soil sampling and preparation for analysis

Georeferenced EC_a readings were taken at each of the sampling points with an EM38-MK2 sensor as outlined in section 3.5.2 before the collection of the samples. At each of the 12 identified points, 4 samples were collected from the 1 m^2 area and were composited. A soil auger was used and samples were taken in 0.3 m depth increments to 1.5 m because the EM38-MK2 sensor measures to this depth in the vertical orientation (Corwin and Lesch, 2005b). However, only the 0 – 0.3 m samples were analysed to achieve the study objectives. The composite soil samples were placed in a drying room maintained at 40 ^oC to remove

moisture for 48 hrs. After 48 hrs, the soil samples were ground, sieved (< 2 mm) and stored for analysis

3.3.2 Plant sampling and preparation for analysis

Wheat-maize rotation was implemented by the irrigation farmers at the study sites for the duration of the study period. The wheat and maize crops were harvested from the 12 EC_a-directed sampling points at the end of the 2016 winter and 2016/17 summer growing season, respectively. At the end of the 2016 winter season, the wheat crop was harvested by harvesting four subplots (replicates) of 1 m^2. The entire wheat plants were cut at the soil surface just above the root zone and the above-ground components were collected. The harvested wheat was dried at 68 ^{0}C in an oven until the samples reached a constant weight and weighed. Then the grain harvest was separated from the stem and leaves and the grain seeds were separated from the husks (awn + glume + spike) in preparation for analysis. Thus, the wheat samples were fragmented into three separate components: stem-leaves, husks (awn + glume + spike) and grain (seeds). All the fragmented samples were grinded in preparation for analysis. The maize crop was also harvested from the 12 EC_a-directed sampling points by harvesting four replicates of 4 m^2. After drying to determine the dry matter of the samples, representative samples were fractionated into five different components: leaves, stems, husks (leaves covering the grain/seed), cobs and grain (seed). The stem and leaves data were treated as one component during data analysis. The fractionated maize and wheat samples were ground for chemical analysis. All the ground samples were placed in a freezer at -12 ^{0}C before analysis to limit chemical decomposition of the samples.

3.4 Soil and plant analyses

3.4.1 Soil analyses

Bulk density was determined by driving a coring metal ring of known mass and volume into the soil using a core sampler. Three samples were obtained from the sampling area. Excess soil was trimmed and soil was dried at 105 °C for 24 hrs and the dry mass was determined. Water content was determined using the gravimetric method. Particle size distribution was determined by using a pipette method as outlined by The Non-Affiliated Soil Analysis Work Committee (1990). Soil pH (pH_w) was determined using a standard pH meter in a 1:2.5 (v/v) soil water suspension without temperature adjustments as outlined by AgriLASA (2004). Electrical conductivity (EC_e) and pH (pH_e) of the saturated paste was measured with a standard pH and EC meter after a saturated soil paste was prepared for each sample by mixing 250 g dry soil with deionized water (United States Salinity Laboratory Staff, 1954). Extractable cations (Na K Ca and Mg), extractable nutrients (P, Cu Fe Mn and Zn) were obtained in solution using a modified Ambic 2 method (Thompson, 1995) and determined with an Inductively Coupled Plasma Emission Spectrograph (ICP–OES) (Varian 710-ES). Total soil C and N were determined in the air-dried soil samples by dry combustion using a LECO Truspec – CNS analyzer (LECO, 2003).

3.4.2 Plant analyses

All fractionated wheat and maize samples were digested using the closed tube digestion technique (Wheal *et al.*, 2011) and analysed for concentrations of Ca, Mg, K, Na, P, Cu, Fe, Mn, Zn and B with an Inductively Coupled Plasma Emission Spectrograph (ICP–OES) (Varian 710-ES).

3.5 Soil and plant measurements with sensors

3.5.1 MIR spectra data acquisition

MIR spectral data in the range 4000 – 400 cm^{-1} were measured by a sensor iS50 Nicolet Fourier Transform Infrared (FTIR) (Thermo Fisher Scientific Inc., Waltham, MA) equipped with an accessory for attenuated reflectance acquisition (Attenuated Total Reflectance). The equipment uses laser as lighting source positioned internally and with a calibration standard for each wavelength. The spectra for the samples was acquired with spectral resolution of 1.2 nm and 16 scans every second for spectrum. Approximately 1 cm^3 of soil and plant sample were placed on the built-in diamond iS50 ATR sampling station for spectral analysis. Soil and plant samples were not pre-processed. This direct technique enables propagation of the infrared radiation to pass at an angle that allows internal reflectance from the diamond crystal. Before each scan, the background spectrum of the reference plate was obtained for sensor calibration. A diamond plate was used as reference removing the background radiation from sample spectrum. The diamond plate was cleaned with acetone and deionized water following each successive spectrum sampling.

3.5.2 EMI measurements

All EC_a measurements were taken with the Geonics EM38-MK2 instrument (Geonics Limited, Mississauga, Ontario, Canada) at a transect width of about 10 m. Each measurement were georeferenced with a Trimble R4 RTK GNSS surveying system. Metal objects were removed from wrists, fingers, neck and pockets and standard procedures used, as described in the EM38-MK2 ground conductivity meter operation manual (Geonics Limited, 2008), when preparing the instrument for survey operation, namely (i) battery test, (ii) initial Inphase nulling (iii), instrument zero and (iv) final Inphase nulling. At each field the EC_a survey design was similar i.e. one geo-referenced EC_a reading was taken per second while the instrument was

pulled behind an off-road vehicle (Quade bike) at a speed of approximately 8 km hour^{-1} (Sudduth *et al.,* 2001). A reference 50 m transect to the side of each field was measured at the beginning and end of the survey.

Luckhoff 20 ha and 40 ha sites were surveyed three times i.e. June 2016 (first survey), December 2016 (second survey) and June 2017 (final survey). At Luckhfoff 60 ha NE and 60 ha NW fields, the total area under the centre pivot were surveyed only once; the other times only 30 ha (half) was surveyed. Douglas and Hofmeyr fields were surveyed only twice, first and a final survey. It is important to note that the instrument read a non-linear depth-weighted soil electrical conductivity and that EC_a readings were obtained for two effective depth ranges with the EM38-MK2. This is possible because of the two-transmitter receiver coil separations at 1 and 0.5 m. In the vertical dipole orientation of the instrument the effective depth range was 0-1.5 m (EC_a deep) and the horizontal orientation the depth range was 0-0.75 m (EC_a shallow), which was used at all fields accept the two fields near Hofmeyr. For these fields the instrument was used in the horizontal dipole mode of orientation with an effective depth range of 0-0.75 m (EC_a deep) and 0-0.35 m (EC_a shallow). All material below 1.5 m (1 m coil separation) and 0.75 m (0.5 m coil separation) contributes about 30% to the EC_a reading in the vertical dipole orientation. In the horizontal dipole orientation all material below 0.75 m (1 m coil separation) and 0.35 m (0.5 m coil separation) contributes about 30% to the EC_a reading. These values are based on the cumulative response functions provided in the EM38-MK2 ground conductivity meter operation manual (Geonics Limited, 2008).

3.6. Evaluating soil quality with Soil Management Assessment Framework (SMAF)

A soil quality index calculated using the Soil Management Assessment Frameowork (Andrews *et al*., 2004) in conjunction with EC_a and MIR data fusion was used to evaluate and quantify the impact of soil and crop management in this study. Six soil quality indicators used in this tool were transformed via scoring algorithms into unit less scores (0 to 1) that reflected the

level of function of that indicator in a soil or crop management system, taking into account the differing soil and climatic factors that are known to influence the performance of the indicators. The use of six indicators was consistent with the SMAF general guidelines. The general SMAF guidelines recommend the use of a minimum of five indicators, provided at least one of each represents soil physical, chemical and biological properties and processes (Cherubin *et al.,* 2016). A score of 1 for an indicator represents the highest potential that a soil quality parameter could reach in that particular soil and crop management system. The six soil quality indicators (bulk density (ρb), EC, SOC, pH, extractable P and K) were used to calculate a SMAF soil quality index. To facilitate the interpretation of the results the scored indicators were grouped into different categories. The physical group included the SMAF scores for bulk density. The chemical group included scores for the reactivity indicators pH and EC. The biological group included scores for soil C, while the nutrient group comprised of the mean scores for extractable P and exchangeable K. An overall soil quality index (SMAF index) for each field was calculated for the 0-0.3m soil depth by summing weighted scores of six soil quality indicators and dividing the summed score by the number of the indicators.

3.7 Data processing and statistical analysis

3.7.1 Modelling soil fertility parameters and nutrient concentrations in wheat and maize with mid-infrared (MIR) spectroscopy

Descriptive statistical analyses was applied to characterize the variability of the soil and plant data sets. If the data was not normally distributed based on values of kurtosis and skewness, the analytical data was transformed to achieve data normality. These transformations aimed to obtain approximate normally distributed values and to maximize the prediction algorithm performances. Initially, the spectral data was grouped into 7 data sets based on the sample site location to compare the performances of the regression models with respect to a specific site and management system. The modelling of the soil and plant spectral data was achieved

using the TQ analyst software. Four regression methods were used *viz.* classical least square regression (CLSR), step-wise multiple linear regression (SMLR), partial least squares regression (PLSR) and principal component regression (PCR). The CLS method is a regression technique that is based on the least square algorithm. This method can handle MIR spectral baselines that may vary from sample to sample. PLSR method performs a principal component analysis decomposition in such a way that reference data is used for an optimal decomposition of MIR data and then performs regression equations; while PCR uses only MIR spectral information in constructing principle components for regression purposes. Calibration statistics including the root mean square error of calibration (RMSEC), the coefficient of determination in calibration (R^2), root mean square error of prediction (RMSEP), coefficient of determination in prediction (R^2_v), and residue prediction deviation (RPD) were employed for the statistical evaluation of the modelling performances of the MIR spectral ranges. The regression models was classified into three categories of quality for comparison purposes considering prediction reliability according to variation of R^2 values: a) $R^2 > 0.75$: well-fitted models to accurately predict soil and plant properties; b) $0.50 \leq R^2 \leq 0.75$: fair models that can be improved; and c) $R^2 < 0.50$: unreliable models without any prediction abilities. An approach suggested by Chang *et al*., (2001) was used to interpret the RPD values. Three categories were distinguished: category A with a RPD >2.0 for excellent models, category B with RPD between 1.4 and 2.0 for models that have acceptable accuracy which could be improved, and category C with RPD <1.4 for models that may not be reliable for prediction.

3.7.2 Modelling soil fertility and crop yield parameters with apparent electrical conductivity (EC_a)

Calibrations of EC_a with conventional measurements of plant nutrients to determine whether EC_a can serve as an efficient estimator of plant nutrient levels for the delineation of site-specific management zones were achieved using the Electrical Conductivity Sampling Assessment and Prediction software (ESAP)-Calibrate software program. The measured soil and crop

parameters related to soil fertility in irrigated agriculture were calibrated against geospatial EC_a measurements. Calibrations of EC_a with crop yield parameters were also developed. Soil and plant analysis samples were determined as outlined in Sections 3.4.1 and 3.4.2, respectively. The calibrations were developed by obtaining targeted soil and crop attribute data from 12 EC_a measurement points and an appropriate stochastic-prediction model was estimated using spatial multiple linear regression (MLR). The stochastic approach uses spatial regression to directly predict the soil targeted property from EC_a survey data. In this approach the models are dynamic (i.e the model parameters are estimated using the soil sample data collected during the EC_a survey). Using the remaining EC_a data in conjunction with the established model, the calibrated properties can then be predicted at all of the remaining non-sampled, measurement locations. The stochastic calibration approach is described in detail by Lesch *et al* (1995a, 1995b, 2000) and incorporated into the ESAP software (Lesch *et al*., 2000).

3.7.3 Characterizing spatial variability of plant nutrients and crop yield in a wheat-maize cropping systems

Descriptive statistics that were calculated include: mean, minimum, maximum, range, standard deviation, and co-efficient of variation for 0-0.3 m soil depth over the depth measurement of EC_a. To use spatial measurements of EC_a in a site-specific management context, it is necessary to understand what factors are most significantly influencing EC_a measurements within a field. Pearson correlation coefficient (*r*) was used to determine the predominant factors affecting EC_a measurement. The calculation of the correlation coefficient between EC_a and mean value of each soil property over multiple sample points determines those soil properties that correlates best with EC_a and those soil properties that are spatially represented by the EC_a-directed sampling design.

Crop yield monitoring data in conjunction with EC_a survey data is used from a site-specific crop management perspective to (i) identify those soil properties influencing yield and (ii) delineate site-specific management units (Corwin and Scudeiro, 2016). For site-specific crop management, an understanding of the influence of spatial variation in soil properties on within-field crop-yield variation is required. To accomplish this, the relation of crop yield with EC_a within a field was determined. Using ESAP-Calibrate software, a spatial linear regression was formulated that related EC_a as the independent variable to crop yield as the dependent or response variable. The correlations between crop yield, physical and chemical soil properties were also established. The organization, manipulation, and graphic display in form of maps of spatial soil attributes, crop yields and EC_a data was accomplished using the ESAP-SaltMapper software. The kernel size for the interpolation was 6%.

3.7.4 Characterizing spatial variability of seasonal nutrient removal by wheat and maize crops

The accumulation of nutrients by the wheat crop during the 2016 winter growing season and maize crop during the 2016/17 summer growing season was quantified using the following parameters from the measured data:

Total grain nutrient content = yield (kg/ha) x nutrient content Equation 3.1

Wheat total nutrient uptake = ∑ [grain nutrient content + husks nutrient content + [stem and leaf] nutrient content] Equation 3.2

Maize total nutrient uptake = ∑ [grain nutrient content + cob nutrient content + husk nutrient content + [stem and leaf] nutrient content Equation 3.3

Dry weight harvest index = $\frac{Grain\ Dry\ weight}{Total\ Aboveground\ Biomass}$ x 100 Equation 3.4

The total amount of nutrient removals by a crop was calculated as shown in Equation 3.2 and 3.3. From these, estimated nutrient removal maps can be produced that can act as the basis for nutrient replacement rates in a field. The EC_a-nutrient removal calibrations, spatial analyses and graphic display in form of spatial total nutrient uptake/removal maps were performed as outlined in Sections 3.7.2 and 3.7.3.

3.7.5 Assessing soil quality using sensor data fusion approach

The fusion of data measured with the MIR and EM38 sensors for soil quality assessment was achieved using the step-wise multiple linear regression (SMLR) fusion technique. Identification of the MIR wavebands from the spectral data that were used in the SMLR fusion was done using the derivative analysis (Melendez-Pastor *et al*., 2008; Mahmood *et al*., 2012). Derivative analysis has been identified as the best method to eliminate baseline effects and improves the weak features of the significant dips in the spectra (Duckworth, 1998). Only the first derivative of the original spectrum was computed that shows the slope of the spectra curve at every point (Duckworth, 1998). The first derivative was then adapted to the absorption values. The identification of highly correlated MIR wavebands of the first derivative of absorbance and soil properties was carried out as follows: (i) for each soil sample Pearson correlation coefficients (r) were computed between individual soil parameter and the corresponding absorbance values for the first derivative; (ii) for each soil parameter highly correlated wavebands were identified and selected for the absolute $r > 0.75$. Moreover, for each soil parameter, high significant bilateral correlations ($p < 0.01$) were used.

The SMLR fusion method was used to develop models using the selected MIR wavenumbers or wavebands and EC_a as the predictor variables and soil quality indicators and SMAF scores as the response variables. The performance of individual and data fusion methods to predict soil quality indicators and SMAF scores were assessed using coefficient of determination (R^2)

and root-mean squared error (RMSE). The SMLR models selected for each soil parameter were those that showed lower RMSE values. The accuracy of model predictions using the data fusion methods was also compared with those measured with the individual soil sensors.

3.7.6 Statistical analysis

General descriptive statistics were used to analyse and interpret the soil, crop and EC_a data. The differences in measured soil and plant properties among the sites were compared using a one-way ANOVA, followed by Tukey's tests for mean separations. IBM SPSS statistics version 26 was used for all statistical analysis. All the soil data were calibrated, analysed and presented for each season separately.

CHAPTER 4: QUANTIFYING SOIL FERTILITY PARAMETERS UNDER IRRIGATION USING CONVENTIONAL CHEMISTRY PROCEDURES, INFRARED REFLECTANCE SPECTROSCOPY AND ELECTROMAGNETIC INDUCTION

4.1 Introduction

Optimum crop growth and development depends inter alia on adequate supply of plant nutrients. The quantity of nutrients required by plants varies depending on many inter-relating factors such as crop characteristics, soil properties, environmental conditions, yield potential and management practices (Havlin *et al.,* 2014). Thorough knowledge of crop nutrient requirement and potential nutrient supply by the soil is therefore essential to determine optimum nutrient application. Diagnostic techniques, including visual deficiency symptoms, soil and plant analyses, and remote sensing techniques, are generally used to determine potential nutrient stress and quantity of nutrients required for optimum crop growth and development (Havlin *et al.,* 2014). In-order to accomplish this objective, site-specific information is required.

Results from conventional plant and soil analyses are essential inputs to the effective application of fertilizer, lime, and other amendments (Adamchuk *et al*., 2004). However, these conventional options are time-consuming, which makes the approach unsuitable for fast or *in situ* evaluation of soil fertility as well as bulk analysis of soil samples that is needed for site-specific management (McCarty and Reeves, 2006; Ortega and Santibanez, 2007). Moreover, there is a need for high-quality, high resolution, spatio-temporal soil data to characterise and monitor changes under irrigation systems for site-specific management. Rapid, robust and effective techniques to monitor these changes are urgently needed to achieve these objectives at field scale. As a response to these research needs, soil sensing techniques has been widely accepted over the last few decades, for example visible-near-infrared (VIS-NIR) and mid infrared (MIR) reflectance spectroscopy as well as electromagnetic induction (EMI).

Infrared spectroscopy (IR) is one of the techniques commonly used in quantitative and qualitative soil research. Infrared spectroscopic techniques (visible (VIS), near-infrared (NIR) and mid-infrared (MIR) spectroscopy) are highly sensitive to both the organic and inorganic phases of soil, making them quite relevant in agricultural and environmental research (Viscarra Rossel *et al*., 2006). The use of the MIR in quantitative soil analysis is of particular interest in this study to evaluate and quantify soil fertility parameters under irrigation. Mid-infrared spectroscopy (4000–400 cm^{-1}) has been used frequently to predict soil properties such as soil organic carbon (SOC), total carbon (TC), soil organic matter (SOM), cation exchange capacity (CEC), Ca, Mg, clay, sand, silt and others (Viscarra Rossel *et al.,* 2006; Knox *et al.,* 2015; Terra *et al.,* 2015; Ma *et al*., 2019). Estimation of other important soil properties such as pH_w, P, K, Na, Cu, Fe, Mn and Zn has been less stable (Viscarra Rossel *et al.,* 2006; Du and Zhou, 2009). The full IR spectrum can be used to assess soil properties; however, the benefits from a full cover of the ranges are compromised by multi-collinearity and noise (Vohland and Emmerling, 2011; Ma *et al.,* 2019). A comparison of the performance of NIR and MIR has indicated that MIR provides a better potential spectral range for measurements of soil properties (McCarty *et al*., 2002; Pirie *et al.,* 2005; Vohland *et al*., 2014; Terra *et al*., 2015). Viscarra Rossel *at al.* (2006) noted that the reason for the better performance of MIR in quantitative and qualitative soil analysis is that intense fundamental molecular frequencies related to soil properties occur in the MIR wavelength of 2500 to 25 000 nm.

Quantitative analysis of the spectral data obtained from IR spectroscopy requires the use of advanced statistical techniques to obtain soil information from spectral characteristics. Different statistical methods have been used depending on the study objectives. Ben-Dor and Banin (1995) used multiple regression analysis (MRA) to extract specific soil information from NIR bands. On the other hand, Shibusawa *et al.* (2001) relied on step-wise multiple linear regression (SMLR) for the quantification of various soil properties from the NIR spectra soil data acquired from a field using on-the-go soil sensing system. A study by Shepherd and

Walsh (2002) employed multivariate adaptive regression splines (MARS) for the estimation of soil properties from spectral libraries. Terra *et al.* (2015) used principal component regression (PCR) to predict soil properties from NIR and MIR spectral data obtained from scanning tropical Brazilian soils. Knox *et al*. (2015) applied partial least squares regression (PLSR) and tree regression to model soil carbon fractions from visible NIR and MIR spectra datasets. Despite analysing data from MIR spectral data generally giving more accurate results, Viscarra Rossel *et al.* (2006) noted that the technology is more complex and expensive than that used for VIS and NIR measurements. Although infrared spectroscopy allows for rapid, cost effective and intensive sampling, one of the difficulties is the model scale (global, continental, regional, country, local and field) vs. accuracy (Mouazen *et al*., 2010). One of the most recommended solutions to this problem is the successful selection of a multivariate analysis method and subsequent calibration for model development. In conjunction with the finding of the predictive abilities of MIR datasets, this study seeks to compare the performance of multi-variate statistical techniques in predicting the soil parameters related to soil fertility under irrigation.

Apparent electrical conductivity (EC_a) measurements is another sensor-based technique that could be used to measure the available nutrient content of soil, thereby eliminating the need for time consuming and expensive soil sample acquisition (Heiniger *et al.,* 2003). Measurements of EC_a using geophysical techniques such as electrical resistivity (ER) and electromagnetic induction (EMI) play a major role in addressing the issue of field-scale spatial variability (Corwin and Scudiero, 2016). EC_a is a measure of bulk soil conductivity and is affected by any edaphic factor that affects bulk soil conductance. Hence, EC_a measurement is complex because it reflects the influence of the interaction of several soil physical and chemical properties (Corwin and Scudiero, 2016). At field-scale, the effects of soil properties on EC_a are separated statistically on a field-by-field basis using soil samples obtained from an EC_a-directed soil sampling design to develop a field-specific model to calibrate EC_a to a specific soil property (Lesch *et al.,* 2005).

Measurements of EC_a have been used successfully to measure soil salinity, clay and water content (Rhoades *et al.*, 1989a; Corwin and Lesch, 2003 Rhoades *et al.*, 1976; Hendricks, 1992; Heiniger *et al.,* 2003). Under certain field conditions, soil properties such as volumetric water content and salinity tend to mask the influence of plant nutrients on EC_a. However, in most agricultural fields under non-saturated conditions, changes in nutrient levels will most likely influence EC_a by changing electrical conductivity of soil solids through differences in the type and number of cations held by the soil particles (Heiniger *et al.,* 2003). Hence, cations commonly associated with binding sites on soil particles such as Ca, Mg, or K could influence EC_a by changing electrical conductivity of soil solids. A study by Bronson *et al* (2005) reported that soil properties that correlated with EC_a included silt, CEC, extractable Ca^{2+}, Mg^{2+}, Na^{+} and soluble salts and concluded that EC_a measurements can be used as a surrogate measurement of some plant nutrients. Other studies have shown weak and inconsistent relationships between EC_a and some plant nutrients (Corwin and Lesch, 2003; Heiniger *et al.,* 2003; Sudduth *et al.,* 2005; Peralta and Costa, 2013). These inconsistent relationships could have been due to complex inter-relationships between EC_a and soil properties at the particular study sites.

This study aimed to investigate the use of MIR and EC_a measurements as surrogate measurements of soil fertility parameters of irrigated fields for the purpose of site-specific management. The specific objectives of the study are: (i) to determine the predictive capabilities of spectral datasets for predicting various soil properties, and (ii) to determine whether EC_a can serve as an estimator of soil properties related to soil fertility under irrigation.

4.2 Procedure

The study sites' characteristics, soil sampling and analysis, data processing and statistical analysis are described in detail in Chapter 3, and therefore not repeated in this chapter.

4.3 Results and discussions

4.3.1 Exploratory analysis of soil properties across study sites during the study period

The descriptive statistics for the measured soil properties for all study sites are presented in Table 4.1 to 4.7. Generally, the temporal trend from June 2016 to June 2017 is a decrease in the mean of most parameters at the Douglas 40 ha centre pivot except for a significant increase in EC_a and slight increase in pH_e (Table 4.1). This observation indicates overall nutrient mining by the wheat and maize crops during the study period. At the Hofmeyr site, the 55 ha lower centre pivot (SE) recorded a decrease in the mean of the most parameters (pH_e, pH_w, C, K, Ca, Mg, Na, Zn, Mn) and an increase in some of the parameters (EC_e, N, P, Cu and Fe) from June 2016 to December 2016 (Table 4.3). The 55 ha upper pivot (NW) showed an increase in C, P, K, Zn, Cu, and Fe and a decrease in EC_a, EC_e, pH_e, pH_w, Ca, Mg, Na and Mn. Nitrogen (N) remained fairly constant during the same period (Table 4.2).

At the Luckhoff site, for the 20 ha centre pivot the mean of the most of the parameters (EC_e, pH_e, pH_w, C, P, K, Ca, Mg, Na, Zn, Cu and Fe) increased while EC_a significantly and Mn slightly decreased from June 2016 to June 2017 (Table 4.4). Under this centre pivot, N remained fairly constant after two seasons. In contrast, the 60 ha (NE) centre pivot experienced a decrease in most parameters (EC_e, C, P, K, Ca, Mg, Na, Zn, Cu and Fe) and only an increase in pH_e, pH_w and Zn for the same period (Table 4.6). However, Mg remained fairly constant on this centre pivot. For the 40 ha centre pivot, the macronutrients Ca, Mg and Na as well as pH_e and pH_w increased and the other parameters decreased (EC_a, EC_e, C, N, P, K, Zn, Mn, Cu and Fe) after two seasons (Table 4.5). The 60 ha (NW) centre pivot recorded an increase in EC_e, pH_w, C, N, P, Zn, Cu and Fe and a decrease in EC_a, pH_e, K, Ca, Mg, Na and Mn in the winter season from June 2016 to December 2016.

Field-scale variation of the soil properties is indicated by the coefficient of variation (CV) for each study site. The magnitude of the variability at a study site for the soil fertility parameters was deduced by using the standard criteria suggested by Wilding *et al.* (1994): CV from 0 to 15%; 15 to 35% and 35 to 100% characterizing low, medium and high variability, respectively. Based on this criterion, EC_a, EC_e, C, N, P, K, Mg and Na exhibited medium to high field scale variability for the Douglas 40 ha centre pivot (Table 4.1) except for N and Mg in the last season which was low. The micronutrients Zn, Mn, Fe for this centre pivot showed high variability across the study period except Cu which had during the second and third sampling times medium variability and high variability at the first sampling time (Table 4.1). Only pH_e, pH_w and exchangeable Ca exhibited low variability at the Douglas pivot across the study period. The physical properties (clay and gravimetric water content) showed medium variability (Table 4.1) except for the gravimetric water content in June 2017 which showed low variability.

On the 55 ha upper centre pivot (NW) at the Hofmeyr site C, N, K, Ca, Mg and Cu exhibited medium field-scale variability during the study period where as EC_a, pH_e, pH_w and Na showed low variability (Table 4.2). However, EC_e showed lower variability in June 2016 and significantly higher variability in December 2016. The parameters P, Zn, Mn and Fe showed higher variability for the study period (Table 4.2). Clay and gravimetric water content showed medium variability (Table 4.2). Some of the parameters on the 55 ha lower centre pivot (SE) showed the same trend with only a few exceptions as on the upper centre pivot with respect to field-scale variability. C, N, K, Ca and Cu exhibited medium field-scale variability in both June 2016 and December 2016 (Table 4.3). The nutrients *viz*. P, Zn, and Fe showed higher variability whereas EC_a, pH_e and pH_w showed low variability during the study period (Table 4.3). However, EC_e and Mn exhibited low field-scale variability in June 2016 but high in December 2016. Magnesium (Mg) showed high variability in June 2016, but medium variability in December 2016. The variability of Na showed medium in June 2016 and low in December 2016 (Table 4.3). The coefficient of variation for the most soil properties of the centre pivots

at Luckhoff changed significantly during the two growing seasons when compared to the centre pivots at Douglas and Hofmeyr.

At the 20 ha centre pivot, the field-scale variability of EC_e, C, P, Ca, Mg and Zn decreased from high to medium (Table 4.4). The Zn and Mn variability decreased from high to medium for June 2016 to December 2016 and then increased again to high in June 2017 (Table 4.4). However, EC_a, K and Cu exhibited medium variability whereas pH_e, pH_w and Na showed low variability from June 2016 to June 2017. At the 40 ha centre pivot, EC_e, Zn and Cu variability increased from medium to high whereas the variability of N decreased from high to medium for June 2016 to June 2017 (Table 4.5). The variability of P and Mn decreased from high to medium variability from June 2016 to December 2016 and then increased again to high in June 2017 (Table 4.5). On the other hand, EC_a, K, Ca and Mg exhibited medium variability whereas pH_e, pH_w and Na showed low variability from June 2016 to June 2017. Only C and Fe exhibited high field scale variability on the 40 ha centre pivot during the study period.

Table 4.1: Descriptive statistics for soil properties from the 40 ha centre pivot at Douglas site at different sampling times

Soil property	mean	Min	max	SD	CV	range	mean	min	max	SD	CV	range	mean	min	max	SD	CV	range
	June 2016						Dec 2016						May 2017					
EC_a, mS/m	95.3	51.4	159.1	34.7	36	107.7	-	-	-	-	-	-	121.2	49.4	293.0	70.2	58	243.6
EC_e, mS/m	447.6	269	1129	235.2	53	860.0	211.8	90.0	344.0	55.0	26	254.0	115.0	77.0	145.0	19.8	17	68.0
pH_e	7.77	7.32	8.15	0.28	4	0.83	7.47	7.08	8.00	0.29	4	0.92	7.89	7.26	8.47	0.42		1.21
pH_w	8.34	8.11	8.69	0.14	2	0.58	8.27	7.7	8.55	0.20	2	0.85	8.32	8.12	8.58	0.13	2	0.46
C, (%)	1.16	0.56	1.52	0.27	23	0.96	1.34	0.41	3.30	0.83	62	2.89	1.10	0.64	1.66	0.29	26	1.02
N, (%)	0.10	0.06	0.13	0.02	20	0.07	0.09	0.05	0.18	0.04	44	0.13	0.09	0.07	0.11	0.01	11	0.04
P, mg/kg	2.01	0.50	3.58	0.79	39	3.08	1.20	0.50	2.59	0.60	50	2.09	1.48	0.50	3.10	0.65	44	2.60
K, mg/kg	553.1	264.0	947.9	164.6	30	683.9	413.7	179.6	706.4	115.7	38	526.78	493.9	336.8	754.9	104.7	21	418.1
Ca, mg/kg	3330	2593	4308	433.8	13	1715.0	3056	2408	3589	220.5	7	1181	3109	3505	3865	288.8	9	1360
Mg, mg/kg	500.3	334.6	700.6	95.1	19	366.0	553.8	357.5	850.4	116.7	21	493.0	459.2	321.1	650.4	65.5	14	329.4
Na, mg/kg	376.3	198.2	659.7	126.8	34	461.6	499.9	330.2	653.4	75.5	15	323.2	289.1	192.9	478.9	77.2	27	285.9
Zn, mg/kg	6.73	2.84	13.5	2.88	42	10.6	4.19	0.05	9.82	2.60	62	9.77	5.33	0.78	11.87	3.09	58	11.09
Mn, mg/kg	26.7	1.83	74.0	17.3	65	72.2	13.7	3.29	28.3	7.53	55	25.1	15.1	1.83	35.7	9.62	64	33.8
Cu, mg/kg	4.47	1.83	10.4	2.19	49	8.08	3.91	2.25	6.63	0.98	25	4.38	3.43	1.80	5.30	0.76	22	3.50
Fe, mg/kg	10.1	0.50	63.01	18.8	186	62.5	0.64	0.50	3.61	0.55	86	3.11	0.66	0.50	3.69	0.63	95	3.19
Clay, (%)	24.4	16.6	32.8	5.03	21	16.2	27.9	19.8	56.2	9.44	34	36.4	-	-	-	-	-	-
GΘ, (%)	13.1	10.2	17.1	2.17	17	6.84	13.3	9.72	20.1	2.79	21	10.4	9.53	7.65	10.8	1.00	10	3.13

GΘ – gravimetric water content

Table 4.2: Descriptive statistics for soil properties from the 55 ha upper pivot (NW) at Hofmeyr at different sampling times

Soil property	mean	min	max	SD	CV	range	mean	min	max	SD	CV	range
	June 2016						Dec 2016					
EC_a, mS/m	59.7	48.42	74.4	8.33	14	26.0	40.9	34.5	47.9	4.61	11	13.5
EC_e, mS/m	93.4	71.0	117	13.1	14	46.0	84.1	62.0	173.0	29.8	35	111.0
pH_e	7.72	7.03	8.11	0.37	5	1.08	7.34	6.07	8.08	0.51	7	2.01
pH_w	6.61	5.48	7.26	0.31	5	1.78	6.52	5.76	7.14	0.36	6	1.38
C, (%)	0.60	0.39	0.91	0.15	25	0.52	0.62	0.40	0.92	0.14	23	0.53
N, (%)	0.12	0.08	0.14	0.02	17	0.06	0.12	0.08	0.16	0.02	17	0.08
P, mg/kg	2.39	0.50	5.48	1.43	60	4.98	4.74	1.89	9.51	2.34	49	7.62
K, mg/kg	300.4	194.1	445.7	55.3	18	251.6	324.1	153.1	600.7	90.8	28	447.6
Ca, mg/kg	3073	1765	4543	725.0	24	2778	2715	1518	4154	633.7	23	2637
Mg, mg/kg	726.5	453.2	1032.1	153.8	21	578.8	589.1	369.0	758.7	96.0	16	389.7
Na, mg/kg	240.4	195.5	314.2	29.0	12	118.7	224.7	193.4	277.8	23.5	10	84.4
Zn, mg/kg	5.71	1.88	13.5	3.24	57	11.6	9.62	3.80	20.8	4.54	47	17.0
Mn, mg/kg	72.7	5.79	206.6	57.6	79	200.9	57.6	62.5	168.5	50.9	88	162.2
Cu, mg/kg	4.10	1.62	6.50	1.18	29	4.88	4.23	2.55	6.45	0.93	22	3.90
Fe, mg/kg	54.9	0.50	209.6	52.5	96	209.1	66.3	4.39	146.6	43.2	65	142.2
Clay, (%)	34.2	25.0	44.0	5.86	17	19.0	28.2	21.6	38.4	5.21	18	16.8
GΘ, (%)	9.39	4.17	14.1	2.81	30	9.97	8.61	4.92	14.0	2.70	31	9.11

GΘ – gravimetric water content

Table 4.3: Descriptive statistics for soil properties from the 55 ha lower pivot (SE) at Hofmeyr at different sampling times

Soil property	mean	min	max	SD	CV	range	mean	min	max	SD	CV	range
	June 2016						Dec 2016					
EC_a, mS/m	71.3	56.3	86.5	9.61	13	30.2	-	-	-	-	-	-
EC_e, mS/m	84.7	70.0	112.0	10.9	13	42.0	96.3	51.0	257.0	60.0	62	206.0
pH_e	7.47	7.22	7.92	0.22	3	0.70	7.35	6.34	8.08	0.59	8	1.74
pH_w	7.17	6.56	8.02	0.47	7	1.46	6.77	6.40	7.11	0.23	3	0.70
C, (%)	0.64	0.41	0.91	0.15	23	0.50	0.58	0.39	1.00	0.17	29	0.61
N, (%)	0.12	0.07	0.14	0.02	17	0.07	0.13	0.05	0.18	0.03	23	0.14
P, mg/kg	3.34	0.50	7.48	2.47	74	6.98	4.07	0.84	7.65	2.52	62	6.81
K, mg/kg	497.4	303.6	696.6	125.5	25	393.0	397.5	259.0	576.5	99.5	25	317.5
Ca, mg/kg	3340	2000	4591	861.0	26	2589	3049	2169	4288	716.5	23	2119
Mg, mg/kg	905.0	502.1	1780	422.1	47	1277	709.3	550.9	1060.0	139.8	20	509.1
Na, mg/kg	244.6	199.0	365.4	47.0	19	166.4	238.0	204.6	265.0	18.0	8	60.4
Zn, mg/kg	5.78	1.87	10.6	2.96	51	8.71	5.48	1.17	9.90	2.68	49	8.73
Mn, mg/kg	87.0	27.9	173.9	38.3	4	146.1	64.3	13.6	128.7	36.3	56	115.1
Cu, mg/kg	3.88	2.76	6.01	0.91	23	3.26	4.94	3.13	8.04	1.37	28	4.91
Fe, mg/kg	32.9	0.50	133.6	45.9	139	3.26	4.94	0.58	89.5	33.1	71	88.9
Clay, (%)	32.0	12.2	49.2	11.5	36	37.0	32.4	21.0	40.4	6.01	29	19.4
GΘ, (%)	11.2	6.64	17.1	3.56	32	10.5	7.88	4.72	12.9	2.92	37	8.20

GΘ – gravimetric water content

Table 4.4: Descriptive statistics for soil properties from the 20 ha centre pivot at Luckhoff site at different sampling times

Soil property	mean	min	max	SD	CV	range	mean	min	max	SD	CV	range	mean	min	max	SD	CV	range
	June 2016						Dec 2016						May 2017					
EC_a, mS/m	51.8	43.7	62.2	7.39	14	18.6	26.7	19.5	30.3	4.27	16	10.8	30.1	16.4	42.1	8.91	30	25.7
EC_e, mS/m	103.0	48.0	152.0	45.7	44	104.0	172.5	117.0	264.0	51.7	30	147.0	104.3	82.0	160.0	28.4	27	78.0
pH_e	7.24	6.43	7.97	0.57	8	1.54	6.99	6.40	7.41	0.36	5	1.01	7.49	6.63	7.93	0.46	6	1.30
pH_w	6.35	4.94	7.52	0.99	16	2.58	6.18	4.52	7.08	0.88	14	2.56	6.55	5.32	7.22	0.66	10	1.91
C, (%)	0.32	0.08	0.59	0.19	59	0.51	0.43	0.28	0.54	0.09	32	0.27	0.44	0.38	0.56	0.07	16	0.18
N, (%)	0.06	0.03	0.09	0.02	33	0.07	0.08	0.06	0.12	0.02	25	0.06	0.06	0.05	0.07	0.008	13	0.02
P, mg/kg	6.07	0.53	9.90	4.20	69	9.37	15.4	4.96	50.0	17.2	112	45.0	10.4	8.02	15.2	2.77	27	7.22
K, mg/kg	311.0	203.6	459.7	95.8	31	256.1	435.7	197.2	617.8	136.2	31	420.6	404.3	309.6	663.6	132.4	33	354.0
Ca, mg/kg	1204	689.5	2591	710.3	59	1901	1355	856.7	1917	406.4	93	1061	1383	965.3	1922	373.2	27	957.1
Mg, mg/kg	266.2	146.3	459.8	118.5	45	313.6	287.9	175.4	353.0	68.5	24	177.6	283.9	213.6	357.3	47.4	17	143.7
Na, mg/kg	165.0	147.1	196.4	16.8	10	49.3	194.8	172.6	215.7	15.9	8	43.1	204.6	174.3	224.9	17.4	9	50.6
Zn, mg/kg	3.17	0.78	5.41	1.79	56	4.63	5.84	3.73	9.14	2.18	37	5.41	5.14	3.35	6.07	0.93	18	2.72
Mn, mg/kg	64.0	15.6	141.2	46.9	73	125.6	60.2	35.6	76.9	13.8	23	41.3	55.8	36.5	102.7	24.3	44	66.2
Cu, mg/kg	1.85	1.37	2.68	0.50	27	1.31	2.70	1.88	3.24	0.54	20	1.36	2.36	1.76	3.33	0.55	23	1.57
Fe, mg/kg	62.6	9.71	184.8	66.6	106	175.1	154.6	120.0	215.2	36.0	23	95.3	94.5	53.3	141.6	41.4	44	88.3
Clay, (%)	11.5	8.60	15.2	2.24	19	6.60	9.27	5.20	12.4	2.65	29	7.20	14.4	8.40	20.6	5.10	35	12.2
GΘ, (%)	7.24	5.18	10.5	1.75	24	5.27	9.87	5.79	13.0	2.65	27	7.19	-	-	-	-	-	-

GΘ – gravimetric water content

Table 4.5: Descriptive statistics for soil properties from 40 ha centre pivot at Luckhoff at different sampling times

Soil property	mean	min	max	SD	CV	range	mean	min	max	SD	CV	range	mean	min	max	SD	CV	range
	June 2016						Nov 2016						May 2017					
EC_a, mS/m	48.3	36.6	62.8	8.27	17	26.2	23.2	13.7	39.3	6.99	30	25.5	30.2	17.3	51.9	9.74	32	34.7
EC_e, mS/m	106.3	70.0	165.0	30.1	28	95.0	78.3	50.0	141.0	24.3	31	91.0	66.1	30.0	132.0	24.9	38	102.0
pH_e	7.43	7.14	7.86	0.25	3	0.72	7.09	6.61	7.36	0.23	3	0.75	7.59	7.33	8.08	0.27	4	0.75
pH_w	6.57	5.87	7.40	0.42	6	1.54	6.68	6.39	7.02	0.18	3	0.63	6.86	6.15	7.43	0.36	5	1.28
C, (%)	0.49	0.19	1.43	0.32	65	1.24	0.45	0.30	0.93	0.17	38	0.64	0.42	0.13	0.69	0.17	40	0.56
N, (%)	0.07	0.03	0.19	0.04	57	0.16	0.06	0.05	0.10	0.01	17	0.06	0.06	0.03	0.10	0.02	33	0.07
P, mg/kg	10.00	6.05	28.25	5.05	51	22.2	9.59	6.13	13.0	1.92	20	6.91	8.04	0.57	15.15	4.61	57	15.2
K, mg/kg	470.2	303.2	677.5	90.4	19	373.3	451.6	281.5	795.7	124.2	28	514.2	428.5	230.6	582.2	79.1	18	351.6
Ca, mg/kg	1575	1000	2654	380.2	24	1654	1515	1131	2179	288.7	19	1048	1615	1150	2428	329.2	20	1278
Mg, mg/kg	303.7	211.6	436.4	0.42	0.1	224.8	309.2	211.2	468.1	60.4	20	256.9	342.4	231.9	534.5	77.2	23	302.6
Na, mg/kg	157.7	144.5	175.6	6.88	4	31.14	170.0	150.7	190.1	9.72	6	39.4	177.4	157.0	215.6	11.5	6	58.6
Zn, mg/kg	7.60	4.29	13.6	2.53	33	9.33	7.96	4.74	13.2	1.65	21	8.42	5.88	0.66	11.3	3.10	53	10.6
Mn, mg/kg	57.7	1.69	108.0	30.3	53	106.3	68.5	47.6	98.8	12.5	18	51.2	44.8	13.0	88.6	18.5	41	75.6
Cu, mg/kg	2.53	1.36	4.68	0.71	28	3.32	2.98	1.48	9.72	1.40	47	8.24	2.44	1.27	3.82	0.74	303	2.55
Fe, mg/kg	94.4	37.0	552.8	105.3	112	515.8	92.6	36.1	314.8	72.1	78	278.7	74.9	9.79	243.6	57.4	77	233.8
Clay, (%)	11.5	8.20	16.4	2.51	22	8.20	13.3	9.30	16.4	2.63	20	7.10	11.9	8.40	18.4	3.15	26	10.0
GΘ, (%)	5.66	1.58	9.64	2.06	36	8.07	9.24	5.60	13.0	2.46	27	7.40	-	-	-	-	-	-

GΘ – gravimetric water content

Table 4.6: Descriptive statistics for soil properties from the 60 ha (NE) centre pivot at Luckhoff site at different sampling times

Soil property	mean	min	max	SD	CV	range	mean	min	max	SD	CV	range	mean	min	max	SD	CV	range
	June 2016						Nov 2016						May 2017					
EC_a, mS/m	39.8	34.8	45.2	3.32	8	10.3	14.1	7.17	19.7	4.30	30	12.5	17.3	12.2	22.2	3.50	20	10.0
EC_e, mS/m	71.3	43.0	51.0	15.5	22	43.0	85.0	67.0	102.0	12.6	15	35.0	56.7	45.0	65.0	7.87	14	20.0
pH_e	7.40	6.88	7.83	0.27	4	0.95	7.29	6.75	7.69	0.37	5	0.94	7.63	7.38	8.04	0.25	3	0.66
pH_w	6.87	6.14	8.19	0.62	9	2.05	6.66	6.28	7.03	0.32	5	0.75	6.95	6.67	7.26	0.25	4	0.59
C, (%)	0.63	0.26	2.97	0.75	119	2.71	0.34	0.26	0.37	0.04	12	0.11	0.42	0.30	0.73	0.16	38	0.43
N, (%)	0.07	0.04	0.10	0.75	107	0.06	0.06	0.03	0.07	0.01	17	0.04	0.06	0.04	0.07	0.008	13	0.02
P, mg/kg	7.17	2.62	11.9	3.57	50	9.29	4.80	3.26	6.69	1.47	31	3.43	4.42	2.68	5.98	1.37	31	3.30
K, mg/kg	330.3	240.5	435.0	63.9	19	194.5	272.8	231.6	349.5	43.0	16	117.8	313.0	253.6	393.7	55.6	18	140.1
Ca, mg/kg	1681	1026	3441	730.6	43	2415	1381	1220	1671	221.8	16	450.3	1426	1005	1818	303.1	22	812.9
Mg, mg/kg	255.6	136.6	412.2	64.0	25	275.6	272.3	237.9	315.3	32.6	12	77.4	256.1	204.1	296.6	38.2	15	92.5
Na, mg/kg	185.6	165.6	222.1	15.4	8	56.5	202.6	185.2	217.4	10.3	5	32.2	182.0	176.1	185.4	3.73	2	9.32
Zn, mg/kg	6.77	5.49	7.98	0.81	12	2.49	8.08	5.59	10.9	1.76	22	5.31	7.80	6.08	9.99	1.43	18	3.91
Mn, mg/kg	56.8	15.0	107.5	21.9	39	92.5	39.5	13.1	68.1	21.5	54	55.0	49.7	40.9	57.9	5.95	12	16.9
Cu, mg/kg	3.27	1.90	11.2	2.56	79	9.31	3.27	2.16	4.00	0.77	24	1.84	2.83	2.26	3.72	0.51	18	1.46
Fe, mg/kg	63.5	0.50	251.0	64.9	102	250.5	44.8	22.2	83.0	22.3	50	60.8	59.4	24.8	101.7	31.5	53	77.0
Clay, (%)	8.31	5.75	12.8	2.28	27	7.00	-	-	-	-	-	-	9.25	7.00	12.1	1.88	20	5.10
GΘ, (%)	8.68	5.61	14.7	2.63	30	9.12	11.4	10.1	15.0	1.97	17	4.90	-	-	-	-	-	-

GΘ – gravimetric water content

Table 4.7: Descriptive statistics for soil properties from the 60 ha (NW) pivot at Luckhoff at different sampling times

Soil property	mean	min	max	SD	CV	range	mean	min	max	SD	CV	range
	June 2016						Dec 2016					
EC_a, mS/m	50.8	37.3	68.0	9.32	18	30.7	24.1	15.3	32.1	5.46	23	16.8
EC_e, mS/m	76.6	50.0	139.0	27.3	36	89.0	84.2	52.0	156.0	39.1	46	104.0
pH_e	7.93	7.21	8.73	0.51	6	1.52	7.37	7.20	7.64	0.17	2	0.44
pH_w	6.61	5.67	7.29	0.41	6	1.62	6.77	6.41	7.42	0.44	6	1.01
C, (%)	0.43	0.11	0.96	0.25	58	0.86	0.47	0.29	0.59	0.12	26	0.30
N, (%)	0.05	0.02	0.08	0.02	40	0.06	0.07	0.04	0.10	0.02	29	0.06
P, mg/kg	4.98	0.51	9.71	2.37	48	9.20	5.90	3.32	14.8	4.44	75	11.5
K, mg/kg	372.7	254.8	558.9	95.2	26	304.1	306.7	190.2	386.8	72.8	24	196.5
Ca, mg/kg	1360	991.1	1796	243.6	18	805.1	1347	1017	2153	425.7	32	1135
Mg, mg/kg	355.7	199.9	608.8	128.8	36	409.0	306.1	213.5	475.8	97.3	32	262.2
Na, mg/kg	187.8	169.8	238.2	20.2	11	68.4	178.7	168.5	188.6	7.16	4	20.1
Zn, mg/kg	8.31	0.71	14.5	3.98	48	13.77	8.78	6.02	6.13	1.95	22	6.02
Mn, mg/kg	40.9	4.30	73.8	22.8	56	69.5	27.8	3.26	43.5	14.3	51	40.2
Cu, mg/kg	2.54	1.73	3.74	0.58	23	2.01	3.36	1.64	7.19	2.00	60	5.55
Fe, mg/kg	70.1	10.3	111.5	29.2	42	101.3	91.2	51.4	180.0	46.0	50	128.5
Clay, (%)	8.82	5.20	11.9	2.07	23	6.65	-	-	-	-	-	-
GΘ, (%)	6.68	4.84	8.55	0.99	15	3.72	9.43	6.34	16.0	3.65	39	9.68

GΘ – gravimetric water content

At the 60 ha centre pivot of Luckhoff (NE), P, Ca and Cu variability decreased from high to medium whereas the variability of EC_a and Zn increased from low to medium from June 2016 to June 2017 (Table 4.6). The variability of C decreased from high to low variability from June 2016 to December 2016 and then increased to high in June 2017 whereas N variability decreased from high to low during the same period. From June 2016 to June 2017, EC_e, K, Mg, clay and gravimetric water content exhibited medium variability whereas pH_e, pH_w and Na showed low variability. Only Fe exhibited high field scale variability at this centre pivot for the entirety of the study period. The field-scale variability of the soil properties on the other 60 ha centre pivot (NW) were less than at the other three pivots. The parameters EC_a, K, Ca, Mg, clay content and gravimetric water content exhibited medium variability whereas pH_e, pH_w and Na showed low variability from June 2016 to December 2016 (Table 4.7). A high variability was observed only with EC_e, P, Mn and Fe for the same duration. However, the variability of C, N and Zn decreased from high to medium at the end of the 2016 winter season and the variability of Cu increased significantly from medium to high variability. These observations for the field scale variability at the Luckhoff centre pivots reflected that the soil and crop management practices implemented by the farmer over the two seasons were highly variable (Table 3.2).

At the 60 ha centre pivot of Luckhoff (NE), P, Ca and Cu variability decreased from high to medium whereas the variability of EC_a and Zn increased from low to medium from June 2016 to June 2017 (Table 4.6). The variability of C decreased from high to low variability from June 2016 to December 2016 and then increased to high in June 2017 whereas N variability decreased from high to low during the same period. From June 2016 to June 2017, EC_e, K, Mg, clay and gravimetric water content exhibited medium variability whereas pH_e, pH_w and Na showed low variability. Only Fe exhibited high field scale variability at this centre pivot for the entirety of the study period. The field-scale variability of the soil properties on the other 60 ha centre pivot (NW) were less than at the other three pivots. The parameters EC_a, K, Ca, Mg,

clay content and gravimetric water content exhibited medium variability whereas pH_e, pH_w and Na showed low variability from June 2016 to December 2016 (Table 4.7). A high variability was observed only with EC_e, P, Mn and Fe for the same duration. However, the variability of C, N and Zn decreased from high to medium at the end of the 2016 winter season and the variability of Cu increased significantly from medium to high variability. These observations for the field scale variability at the Luckhoff centre pivots reflected that the soil and crop management practices implemented by the farmer over the two seasons were highly variable (Table 3.2).

The coefficients of variation of the selected soil fertility properties indicated medium to high spatial variability at the study sites, suggesting the importance of considering site-specific nutrient management. High field-scale variability of the soil fertility properties at the study sites is probably the consequence of the interaction of soil formation processes, meteorological processes, and anthropogenic influences (Peralta and Costa, 2013). Soil formation processes are the result of complex interactions between physical, chemical and biological mechanisms acting on a parent material over time and influenced by topography (Moral *et al*., 2010).

4.3.2 Soil fertility comparisons across study sites during study period

Tables 4.8 to 4.10 presents the mean comparisons for the soil properties from the study sites over two growing seasons. Most of the parameters differed significantly ($p < 0.05$) showing significance at 0.001 probability level indicating strong differences in soil properties between the study sites. The soil texture for the Douglas and Hofmeyr sites were sandy clay loam. The soils of the 20 ha and 40 ha centre pivots at the Luckhoff site had the same soil texture namely, loamy sand. Both the 60 ha centre pivots (NE and NW) had sandy soils. The soil texture at the centre pivots influenced to a certain extent the soil fertility significant differences. For example, the soils at Douglas and Hofmeyr had higher clay contents that resulted in

significantly higher nutrient contents than the soils at Luckhoff which had lower clay contents. Despite the fact that soils at Hofmeyr had significantly higher clay contents than the soils at Douglas, the Douglas soils had significantly higher values for the majority of the measured parameters (Tables 4.8-4.10). Significantly higher EC_a, EC_e, pH_w, pH_e, C, N, K, Ca, Na, and GΘ values were observed at Douglas across two seasons. This observation may be attributed to the presence of significantly higher C contents at the Douglas site. Higher C contents indicates higher OM at Douglas site and OM is a key factor in optimising soil fertility. Generally, soil C observed at the study sites were below the critical level of 1.9% found by Musinguzi *et al.* (2016) to be necessary for achieving optimal grain yield responses from applied N. This observation suggests that an opportunity to optimize crop productivity still exists at the study sites through soil and crop management practices that ensures OM build-up over time.

Generally, Ca and Mg across the study sites were adequate for optimum crop growth. Extractable P was significantly lower at Douglas and Hofmeyr than at Luckhoff (Tables 4.8 – 4.10). This observation can be explained probably by the higher clay contents of the Douglas and Hofmeyr soils which tend to fix P and making it unavailable for plant uptake. According to the critical values accepted for optimum plant growth published by Landon (1991), P was low across all centre pivots except at the 20 ha and 40 ha centre pivots of Luckhoff where it was barely adequate for optimum plant growth. Hence, supplementary additions of P are necessary to soils of all the centre pivots to avoid yield loss.

Generally, at the Hofmeyr and Luckhoff sites the micronutrients Zn, Mn, Cu and Fe were adequate for optimum plant growth. Due to inhibitory effect of high pH_w on the availability of some micro-nutrients, the mean values for Fe and Mn at Douglas were in some cases below the critical values (Landon, 1991). However, the mean values for Zn and Cu were above the critical levels The soils at the study sites were classified as neither saline nor sodic because the calculated SAR, EC_e and pH were below the suggested salinity parameter norms (Reeve and Fireman, 1967) However, according to Landon (1991) soils with Na contents greater than

230 mg/kg indicates a potential for sodicity development. The soils of Douglas and Hofmeyr sites recorded significantly higher Na contents in most instances indicating potential sodicity problems in future.

4.3.3 Multivariate modelling of MIR and soil properties

Table 4.11 shows the correlation metrics obtained from the regression modelling of soil properties from each centre pivot using the principal component regression method. At Douglas, most of the parameters (EC_a, pH_e, P, Ca, Mg, Na, Zn, Mn, Cu, Fe and clay) were fairly correlated (R^2 = 0.51 - 0.75). However, pH_w, EC_e, C, N and K were well correlated (R^2 = 0.76 - 0.95). For Hofmeyr, the parameters pH_w, pH_e, N, P, Ca, Mg, Na, Mn, Cu, Fe and clay were well correlated (R^2 = 0.75 - 0.97) at both centre pivots. The parameters EC_a and EC_e were fairly correlated at the 55 ha upper centre pivot (NW) with R^2 values of 0.72 and 0.66 respectively. However, EC_e was poorly correlated at the lower centre pivot (SE) with R^2 value of 0.32. Carbon (C) was accurately (R^2 = 0.79) and fairly (R^2 = 0.69) modelled at the upper (NW) and lower (SE) centre pivots respectively. K and Zn were well correlated (R^2 = 0.81 – 0.85) at the lower centre pivot (SE) and moderately correlated (R^2 = 0.67 - 0.73) at the upper centre pivot (NW) respectively.

The parameters pH_w, EC_a, Mg and Mn values were well correlated at Luckhoff's 20 ha centre pivot (R^2 = 0.78 - 0.87). However, pH_e, EC_e, C, N, P, K, Ca, Na, Zn, Cu, Fe and clay were moderately correlated (R^2 = 0.53 - 0.74). At the 40 ha centre pivot of Luckhoff, EC_a, P, Ca, Mg, Zn and Mn were well correlated (R^2 = 0.78 - 0.87). The MIR models for pH_w, pH_e, EC_e, C, N, K, Na, Cu, Fe and clay showed moderate predictive abilities with R^2 ranging from 0.52 to 0.70.

Table 4.8: Mean comparisons for the soil properties of the centre pivots on the study sites in June 2016

Field		pH_w	pH_e	EC_a	EC_e	Clay	C	N	P	K	Ca	Mg	Na	Zn	Mn	Cu	Fe
				mS/m			%						mg/kg				
Douglas	40ha	8.34a	7.77a	95.3a	447a	24.4b	1.16a	0.10a	2.01c	553.1a	3330a	500.3b	376.3a	6.73a	26.7b	4.47a	10.1c
Hofmeyr	55ha NW	6.61b	7.73a	59.7c	93.4b	34.2a	0.60b	0.12a	2.39bc	300.4c	3073a	726.5ab	240.4b	5.71ab	72.7a	4.10a	54.9bc
	55ha SE	7.17b	7.48b	71.3b	84.7b	32.0a	0.64b	0.12a	3.34b	497.4ab	3340a	905.0a	244.6b	5.78ab	87.0a	3.88a	32.9bc
Luckhoff	20ha	6.35b	7.24b	51.8cd	103b	11.5c	0.32b	0.06c	6.07b	311.0c	1203b	266.2c	165.0c	3.17b	64.0a	1.85c	62.6ab
	40ha	6.57b	7.43b	48.3de	106b	11.5c	0.49b	0.07b	10.0a	470.2b	1574b	303.7c	157.7c	7.60a	57.7a	2.53abc	94.4a
	60ha NE	6.87b	7.40b	39.8e	71.3b	8.31c	0.63b	0.07b	7.17b	330.4c	1681b	255.6c	185.6c	6.77a	56.8a	3.27ab	63.5ab
	60ha NW	6.61b	7.93a	50.8d	87.5b	8.82c	0.44b	0.05c	4.98b	372.7c	1359b	355.7c	187.8c	8.31a	8.31b	2.54ac	70.1ab
P-value		***	***	***	***	***	***	***	***	***	***	***	***	0.02*	0.003**	0.002**	0.03*

ns – means not significant at 0.05 probability level; *, **,*** - means significant at the 0.05,0.01 and 0.001 probability level respectively. Means in the same column with the same letters are not significantly different.

Table 4.9: Mean comparisons for the soil properties of the centre pivots on the study sites in December 2016

Field		pH_w	pH_e	EC_a	EC_e	GΘ	C	N	P	K	Ca	Mg	Na	Zn	Mn	Cu	Fe
				mS/m			%			mg/kg							
Douglas	40ha	8.27a	7.47a	-	211.8a	13.0a	1.34a	0.09b	1.20c	413.6a	3056a	553.8b	499.9a	4.19b	13.7c	3.91b	0.64d
Hofmeyr	55ha NW	6.52bc	7.34ab	40.9a	84.1b	8.16b	0.62b	0.12a	4.74c	324.1b	2715a	589.1b	224.7bc	9.62a	57.5ab	4.23ab	66.3bc
	55ha SE	6.77 b	7.35ab	-	96.3b	7.88b	0.58b	0.13a	4.07c	397.5ab	3049a	709.3a	238.0b	5.48b	64.3ab	4.94a	46.8c
Luckhoff	20ha	6.18c	6.99b	26.7b	173.5a	9.87b	0.43b	0.08bc	15.4a	435.7a	1355b	287.9c	194.8cd	5.84b	60.2ab	2.70c	154.6a
	40ha	6.68b	7.09b	23.2b	78.3b	9.24b	0.45b	0.06d	9.59b	451.6a	1515 b	309.2c	170.0d	7.96ab	68.5a	2.98c	92.6b
	60ha NE	6.66b	7.29ab	14.1c	108.7b	11.4ab	0.34b	0.06d	4.80bc	272.8b	1381b	272.3c	202.6cd	8.08ab	39.5bc	3.27bc	44.8c
	60ha NW	6.77b	7.37ab	24.1b	84.2b	9.43b	0.47b	0.07bcd	5.90bc	306.7b	1347b	306.1c	178.7d	8.78a b	27.8c	3.36ab	91.2b
P-value		***	0.17ns	***	***		***	***	***	0.003**	***	***	***	***	***	***	***

GΘ – gravimetric water content; ns – means not significant at 0.05 probability level; *, **, *** - means significant at the 0.05, 0.01 and 0.001 probability level respectively. Means in the same column with the same letters are not significantly different.

Table 4.10: Mean comparisons for the soil properties of the centre pivots on the study sites in June 2017

Field		pH_w	pH_e	EC_a	EC_e	C	N	P	K	Ca	Mg	Na	Zn	Mn	Cu	Fe
				mS/m		%		mg/kg								
Douglas	40ha	8.32a	7.89a	121.2a	115.2a	1.01a	0.09a	1.48c	493.7a	3109a	459.2a	289.1a	5.33a	15.1b	3.43a	0.66b
Luckhoff	20ha	6.55b	7.49b	30.1b	104.3a	0.44b	0.06b	10.4a	404.3ab	1382b	283.9bc	204.6b	5.14a	55.8a	2.36b	94.5a
	40ha	6.86b	7.59ab	30.2b	65.2b	0.42b	0.06b	8.04a	428.5a	1615b	342.4b	177.4b	5.88a	44.8a	2.44b	74.9a
	60ha NE	6.95b	7.63ab	17.3c	56.7b	0.42b	0.06b	4.42b	313.0b	1426b	256.1c	182.0b	7.80a	49.7a	2.83ab	59.4a
P-value		***	0.103ns	***	***	***	***	***	0.005**	***	***	***	0.28ns	***	0.002**	***

ns – means not significant at 0.05 probability level; *, **,*** - means significant at the 0.05,0.01 and 0.001 probability level respectively. Means in the same column with the same letters are not significantly different.

The parameters pH_w, C, N, Ca, Mg, Fe and clay at Luckhoff's 60 ha centre pivot (NE) were well correlated with MIR (R^2 = 0.75 - 0.98). Moreover, pH_e, EC_a, P, K, Na, Zn, Mn and Cu were fairly predicted by the MIR models with R^2 ranging from 0.51 to 0.71 and EC_e was poorly predicted with R^2 of 0.41. At the other 60 ha centre pivot (NW), pH_w,P, K, Mg, Na and Zn produced well-fitted models with R^2 in the range from 0.78 to 0.95. However, the models for pH_w, EC_e, C, Ca, Mn, Cu and Fe showed moderate predictive abilities (R^2=0.60 - 0.74).

The classical least square regression (CLSR) method produced models with higher R^2 values for the soil properties from each centre pivot at the study sites (results not shown). However, these models had lower RPD values as compared to the PCR models. This observation showed that the CLSR technique produced overfitting models at each centre pivot at the study sites. The correlation results of modelling soil properties with MIR using combined soils from all the seven centre pivots are given in Table 4.12. Four regression methods *viz* classical least squares regression (CLSR), step-wise multiple linear regression (SMLR), partial least squares regression (PLSR) and principal component regression (PCR), were used to estimate various soil properties related to soil fertility from the MIR spectral datasets. The PLSR and PCR are the most commonly used sophisticated techniques for spectral calibration and prediction.

The model accuracy of the CLSR technique was greatly reduced when the soils from all centre pivots were combined with the R^2 of most of the soil properties reduced. This probably demonstrates the importance of considering specific information like soil type when performing multi-variate spectral statistical analysis (Shaviv *et al.,* 2003; Linker *et al*., 2004; 2005). The parameters EC_a, EC_e, N, K, Na, Zn, Mn and Cu were moderately modelled by the CLSR with R^2 in the range of 0.54 to 0.72. However, CLSR produced accurate models for C, Ca, Mg and clay with high R^2 values of 0.79, 0.81, 0.80 and 0.89 respectively. These accurate models had lower RPD values (RPD < 2) which demonstrates that this technique may in some instances produce overfitting models as stated before. The parameters pH_e, pH_w, P and Fe were poorly

modelled by CLSR with R^2 values of 0.28, 0.47, 0.43 and 0.46 respectively. Step-wise multiple linear regression (SMLR) produced moderately accurate models for EC_a, EC_e, N and Cu with R^2 values of 0.69, 0.61, 0.70 and 0.52 respectively. Soil pH_e, P, K, Zn, Mn and Fe were poorly modelled by SMLR (R^2 ranged from 0.40 to 0.49). In contrast, pH_w, C, Ca, Mg and clay were accurately modelled by SMLR with R^2 values of 0.75, 0.85, 0.88, 0.92 and 0.92 respectively. Partial least square regression (PLSR) produced moderately accurate models for EC_e, N, K, Mn, Cu and Fe (R^2 = 0.52 - 0.66) and poorly accurate models for pH_e, P and Zn (R^2 = 0.36 - 0.44). Accurate models were produced for EC_a, pH_w, C, Ca, Mg, Na and clay (R^2 values in the range of 0.77 to 0.96). Principal component regression (PCR) produced poor models for pH_e, P and Zn with R^2 values of 0.41, 0.46 and 0.42 respectively. Moderately accurate models were produced for EC_e, N, K, Mn, Cu and Fe with R^2 in the range of 0.52 to 0.71. However, EC_a, pH_w, C, Ca, Mg, Na and clay were accurately modelled by the PCR with R^2 in the range of 0.75 to 0.94.

Comparing the modelling techniques using R^2, RMSEP and RPD model statistical values shows that the PLSR and PCR performed better as compared to the CLSR and SMLR methods. Furthermore, PLSR performed slightly better than PCR method as indicated by the slightly higher R^2 and RPD as well as lower RMSEP values (Table 4.12). Viscarra Rossel *et al.* (2006) infer that PLSR is capable of handling multi-collinearity, it is robust in terms of data noise and missing values. Unlike the PCR, PLSR balances two objectives of explaining response and predictor variation thus calibrations and predictions are more robust. Comparisons of the five multi-variate techniques *viz* SMLR, PCR, PLSR, regression tree and committee trees by Vasques *et al.* (2008) in predicting soil carbon showed the PLSR as the best technique. For this study, the PLSR technique was also the best model predicting soil fertility properties which is in agreement with other studies (Viscarra Rossel *et al*., 2006; Vasques *et al*., 2008).

4.3.4 Regression modelling of EC_a and soil properties

Tables 4.13 to 4.15 provides the statistical analysis and summary statistics of the spatial multiple linear regression (MLR) models between EMI measured EC_a and soil parameters over the 0 - 0.3 m soil depth for the study sites in June 2016, December 2016 and June 2017 respectively. A significance test was performed to determine if a specific calibration model significantly represented the target soil parameter with the given spatial MLR model. Moreover, each parameter in the model was also tested for significance. However, only the significance of the parameter β_1 in the MLR model was reported since this parameter highlights the influence of the soil target property on EC_a variability. The proportion of variation in the soil parameters as explained by the different independent variables at the study sites was presented using the co-efficient of determination (R^2) of the spatial MLR models.

In June 2016, significant models were obtained for parameters EC_e, C, N, P, K, Ca and GΘ at the Douglas site (Table 4.13). Moderate to high R^2 values (0.50 - 0.93) were obtained for EC_e, N, P, K, Ca and GΘ models. However, only EC_e, C, Ca and GΘ significantly influenced the EC_a survey data. At Hofmeyr site, significant models were found in the 55 ha upper centre pivot (NW) for EC_e, N and clay whereas in the 55 ha lower centre pivot (SE), only models for pH_w and GΘ were significant. Moderate to high R^2 values (0.50 – 0.84) were obtained for both C and pH_w at the upper centre pivot (NW) as well as Zn and Mn at the lower centre pivot (SE) but the models for these soil properties were not significant. At the Hofmeyr site, only EC_e, N and clay in the 55 ha upper centre pivot significantly influenced the EC_a survey measurements.

Table 4.11: Correlation metrics between MIR and selected measured soil fertility parameters of the centre pivots at the study sites using the PCR regression

Field		Statistic	pH_w	pH_e	EC_a	EC_e	clay	C	N	P	K	Ca	Mg	Na	Zn	Mn	Cu	Fe
Douglas	40ha	R^2	0.85	0.62	0.69	0.76	0.57	0.95	0.81	0.60	0.84	0.72	0.63	0.69	0.58	0.71	0.51	0.64
		RMSEC	0.07	0.26	0.93	70.0	3.93	0.09	0.01	0.52	69.0	221.0	55.9	79.8	2.34	9.28	1.35	10.1
Hofmeyr	55ha NW	R^2	0.76	0.75	0.72	0.66	0.93	0.79	0.80	0.87	0.67	0.93	0.97	0.87	0.73	0.81	0.87	0.82
		RMSEC	0.20	0.31	0.19	20.7	2.86	0.09	0.01	1.14	66.6	275.0	57.7	12.8	3.04	30.9	0.47	31.9
	55ha SE	R^2	0.78	0.74	-	0.32	0.94	0.69	0.79	0.88	0.85	0.93	0.94	0.83	0.81	0.84	0.93	0.89
		RMSEC	0.23	0.30	-	38.1	3.99	0.11	0.02	1.12	64.2	421.0	84.5	12.3	1.41	17.6	0.43	17.8
Luckhoff	20ha	R^2	0.90	0.73	0.78	0.67	0.73	0.54	0.69	0.68	0.53	0.74	0.83	0.54	0.72	0.87	0.59	0.73
		RMSEC	0.37	0.32	0.25	32.1	2.54	0.10	0.01	8.67	103.0	356.0	40.2	19.5	1.40	16.0	0.47	38.8
	40ha	R^2	0.67	0.65	0.81	0.52	0.69	0.70	0.69	0.82	0.58	0.78	0.87	0.65	0.84	0.87	0.68	0.54
		RMSEC	0.22	0.23	0.26	25.7	2.09	0.23	0.03	2.60	88.5	195.0	29.6	8.96	1.44	11.3	0.60	51.4
	60ha NE	R^2	0.85	0.65	0.63	0.41	0.75	0.98	0.78	0.51	0.54	0.92	0.80	0.63	0.71	0.52	0.64	0.76
		RMSEC	0.27	0.24	0.43	61.3	2.56	0.12	0.01	2.48	53.2	247.0	32.3	12.3	0.98	15.5	1.31	30.1
	60ha NW	R^2	0.79	0.69	-	0.72	-	0.73	0.49	0.78	0.83	0.64	0.94	0.95	0.80	0.74	0.60	0.73
		RMSEC	0.28	0.35	-	19.2	-	0.12	0.02	1.75	33.4	215.0	39.6	5.59	1.74	12.8	1.01	25.0

PCR – principal component regression; R^2 – coefficient of determination of calibration; RMSEC – root mean square error of calibration

Table 4.12: Model statistics between MIR and selected measured soil fertility parameters for all the pivots using four (4) different regression techniques

Regression	Statistic	pH_w	pH_e	EC_a	EC_e	clay	C	N	P	K	Ca	Mg	Na	Zn	Mn	Cu	Fe
CLSR	R^2	0.47	0.28	0.61	0.70	0.89	0.79	0.65	0.43	0.54	0.81	0.80	0.72	0.56	0.56	0.54	0.46
	RMSEP	1.84	1.54	0.68	88.3	6.72	0.21	0.04	17.5	127.0	688.0	245.0	65.0	2.78	32.8	2.20	181.0
	RPD	0.42	0.28	0.82	0.93	1.58	1.77	0.75	0.31	1.00	1.40	1.00	1.16	1.12	1.08	0.63	0.35
SMLR	R^2	0.75	0.44	0.69	0.61	0.92	0.85	0.70	0.45	0.40	0.88	0.92	0.74	0.41	0.49	0.52	0.49
	RMSEP	0.29	0.38	0.31	32.5	3.99	0.09	0.02	2.73	82.5	413.0	68.0	20.4	1.20	14.3	0.82	71.2
	RPD	2.69	1.14	1.78	2.51	2.66	4.26	1.92	2.01	1.53	2.32	3.59	3.68	2.60	2.48	1.70	0.88
PLSR	R^2	0.80	0.37	0.77	0.60	0.95	0.91	0.66	0.44	0.60	0.89	0.96	0.82	0.40	0.57	0.52	0.53
	RMSEP	0.30	0.42	0.28	29.8	4.20	0.14	0.02	3.00	65.5	386.0	89.7	12.3	1.16	12.6	0.76	70.8
	RPD	2.60	1.04	2.00	2.74	2.52	2.57	1.97	1.83	1.93	2.49	2.72	6.11	2.69	2.82	1.83	0.89
PCR	R^2	0.80	0.42	0.75	0.61	0.94	0.85	0.71	0.45	0.51	0.90	0.90	0.79	0.42	0.62	0.54	0.55
	RMSEP	0.33	0.42	0.29	35.4	3.85	0.13	0.02	3.25	72.0	395.0	57.1	11.3	2.84	14.4	0.83	76.3
	RPD	2.39	1.04	1.87	1.21	2.75	2.82	1.80	1.69	1.75	2.43	4.27	5.65	1.10	2.57	1.67	0.83

CLSR – classical least squares regression; SMLR – step-wise multiple linear regression; PLSR – partial least squares regression; PCR – principal components regression; R^2 – coefficient of determination of calibration; RMSEP – root mean square error of prediction; RPD – residue prediction deviation

At the Luckhoff site, high R^2 values (0.68 – 0.80) were obtained for models of parameters pH_e, EC_e, K, Ca, GΘ and clay for the 20 ha centre pivot, but none of these models were significant. Moreover, none of the measured soil parameters significantly influenced EC_a readings at this centre pivot. Significant models were obtained for pH_w, C, N, P, Mn, Fe and GΘ at the 40 ha centre pivot, but only C, N, P and Mn significantly influenced the EC_a measurements. Furthermore, at this centre pivot relatively moderate R^2 values (0.50 – 0.69) were obtained for EC_e, K and Zn models but these models were not significant.

The models for pH_e, P, K, Mg and Na were significant at the 60 ha centre pivot (NE) but none of these soil properties significantly influenced the EC_a measurements. Although high R^2 values were obtained for Ca and pH_w (0.67 and 0.91 respectively) at this centre pivot, the models for these soil properties were not significant. Even though models for C, N, Na, Mn and Cu were significant, only Na significantly influenced the EC_a measurements at the other 60 ha (NW) centre pivot. Moreover, models for parameters pH_e, Mg and Fe had moderate R^2 values (0.53 - 0.67) but were not significant.

The results from the statistical analysis of the MLR models for soil properties and EC_a at the end of the 2016 winter season in December 2016 are presented in Table 4.14. No EC_a survey data for the 40 ha centre pivot at Douglas and the lower 55 ha centre pivot (SE) at Hofmeyr were available. At the Hofmeyr 55 ha upper centre pivot (NW), even though MLR models for EC_e, P, Zn, Mn and Fe were significant, only EC_e significantly influenced the EC_a measurements. Furthermore, even though at this centre pivot models for parameters K, GΘ and clay had moderately high R^2 values (0.71, 0.60 and 0.79 respectively), these models were not significant. The parameters EC_e, K, Mg, Zn, GΘ and clay had significant models at the 20 ha centre pivot of Luckhoff and most of these soil properties significantly influenced the EC_a measurements except GΘ. Moreover, models for C, N, Ca, Cu and Fe had moderately high R^2 values (0.64 – 0.85) but these models were not significant. At the Luckhoff 40 ha centre

pivot, moderate to high R^2 values were obtained for parameters pH_w, pH_e, N, P, K, Ca, Cu, Fe and Gϴ but only models for K, Cu and Gϴ were significant ($p < 0.05$). Additionally, none of the measured soil properties significantly influenced EC_a at this centre pivot. Moderate to high R^2 values (0.56 – 0.83) were obtained for MLR models of pH_w, N, Na and Mn at the Luckhoff's 60 ha centre pivot (NE) that but none of these models were significant. Furthermore, none of the measured soil parameters significantly influenced EC_a at this centre pivot. At the other 60 ha centre pivot (NW), models for pH_w, Zn, Cu, Fe and Gϴ had moderately high R^2 values (R^2 = 0.61 – 0.80). However, only Zn, Cu and Fe significantly influenced EC_a measurements at this centre pivot.

The results from the statistical analysis of the MLR models for soil properties and last EC_a surveys in June 2017 are reported in Table 4.15. Data of EC_a was available for only four of the centre pivots. For Douglas, models for soil parameters EC_e, C, P, Mg, Na, Zn, Cu, and Fe had moderate to high R^2 values (0.63 – 0.98). However, only models for EC_e, P, Na, Zn, and Cu were significant. Moreover, soil parameters Na, and Cu significantly influenced EC_a survey readings at this site. The MLR models for parameters pH_w, EC_e, C, N, Zn and Mn at Luckhoff's 20 ha centre pivot had moderate to high R^2 values (0.54 – 0.99) but only models for pH_w, Zn and Mn were significant. Furthermore, these three soil properties (pH_w, Zn and Mn) also significantly influenced EC_a at this centre pivot. At Luckhoff's 40 ha centre pivot, the models for Ca and Cu were significant with only Ca significantly influencing the EC_a survey measurements at this centre pivot. Although, models for pH_w, EC_e, C, K, Ca, Cu, Fe and clay had moderate to high R^2 values (R^2 = 0.56 – 0.98) at the 60 ha centre (NE) pivot of Luckhoff, only models for pH_w, C and Fe were significant. Additionally, none of the measured soil properties significantly influenced EC_a at this centre pivot in June 2017.

Table 4.13 Statistical analysis and summary statistics of the MLR models between EC_a and soil parameters in June 2016

Field		Statistic	pH_w	pH_e	EC_e	C	N	P	K	Ca	Mg	Na	Zn	Mn	Cu	Fe	GΘ	Clay
Douglas	40ha	model	ns	ns	*	*	*	*	*	**	ns	ns	ns	ns	ns	ns	**	ns
		β_1	ns	ns	**	*	ns	ns	ns	**	ns	ns	ns	ns	ns	ns	**	ns
		R^2	0.04	0.10	0.92	0.44	0.63	0.72	0.50	0.82	0.28	0.27	0.02	0.05	0.43	0.20	0.93	0.28
Hofmeyr	55ha NW	model	ns	ns	**	ns	**	ns	ns	ns	ns	ns	ns	ns	ns	ns	ns	*
		β_1	ns	ns	*	ns	*	ns	ns	ns	ns	ns	ns	ns	ns	ns	ns	*
		R^2	0.50	0.29	0.85	0.56	0.58	0.21	0.11	0.27	0.10	0.31	0.24	0.17	0.07	0.34	0.27	0.62
	55ha SE	model	**	ns	ns	ns	ns	ns	ns	ns	ns	ns	ns	ns	ns	ns	*	ns
		β_1	ns	ns	ns	ns	ns	ns	ns	ns	ns	ns	ns	ns	ns	ns	ns	ns
		R^2	0.94	0.24	0.13	0.41	0.06	0.20	0.22	0.08	0.04	0.26	0.84	0.74	0.43	0.25	0.61	0.20
Luckhoff	20ha	model	ns	ns	ns	ns	ns	ns	ns	ns	ns	ns	ns	ns	ns	ns	ns	ns
		β_1	ns	ns	ns	ns	ns	ns	ns	ns	ns	ns	ns	ns	ns	ns	ns	ns
		R^2	0.46	0.79	0.82	0.39	0.28	0.23	0.77	0.80	0.12	0.44	0.22	0.03	0.28	0.11	0.64	0.68
	40ha	model	*	ns	ns	**	***	*	ns	ns	ns	ns	ns	*	ns	*	*	ns
		β_1	ns	ns	ns	*	***	**	ns	ns	ns	ns	ns	*	ns	ns	ns	ns
		R^2	0.62	0.43	0.69	0.75	0.91	0.75	0.50	0.35	0.22	0.45	0.65	0.52	0.23	0.60	0.75	0.41
	60ha NE	model	ns	**	ns	ns	ns	**	*	ns	*	**	ns	ns	ns	ns	ns	ns
		β_1	ns	ns	ns	ns	ns	ns	ns	ns	ns	ns	ns	ns	ns	ns	ns	ns
		R^2	0.91	0.97	0.18	0.04	0.10	0.82	0.91	0.67	0.72	0.85	0.02	0.33	0.01	0.16	0.12	0.001
	60ha NW	model	ns	ns	ns	*	**	ns	ns	ns	ns	*	ns	*	***	ns	ns	ns
		β_1	ns	ns	ns	ns	ns	ns	ns	ns	ns	*	ns	ns	ns	ns	ns	ns
		R^2	0.21	0.67	0.01	0.95	0.90	0.33	0.21	0.35	0.54	0.34	0.02	0.49	0.99	0.53	0.16	0.01

GΘ – gravimetric water content; β_1 – constant parameter in the MLR model related to EC_a ; *, **,*** - model or β_1 significant at 0.05, 0.01 and 0.001 probability level respectively.

Table 4.14: Statistical analysis and summary statistics of the MLR models between EC_a and soil parameters in December 2016

Field		Statistic	pH_w	pH_e	EC_e	C	N	P	K	Ca	Mg	Na	Zn	Mn	Cu	Fe	GΘ	Clay
Hofmeyr	55ha NW	model	ns	ns	***	ns	ns	*	ns	ns	ns	ns	*	*	ns	*	ns	ns
		β_1	ns	ns	**	ns	ns	ns	ns	ns	ns	ns	ns	ns	ns	ns	ns	ns
		R^2	0.02	0.06	0.99	0.48	0.13	0.67	0.71	0.08	0.01	0.29	0.51	0.49	0.24	0.95	0.60	0.79
Luckhoff	20ha	model	ns	ns	*	ns	ns	ns	**	ns	*	ns	*	ns	ns	ns	**	*
		β_1	ns	ns	**	ns	ns	ns	***	ns	*	ns	**	ns	ns	ns	ns	*
		R^2	0.03	0.33	0.98	0.64	0.66	0.09	0.99	0.56	0.92	0.01	0.95	0.003	0.79	0.85	0.93	0.69
	40ha	model	ns	ns	ns	ns	ns	ns	**	ns	ns	ns	ns	ns	**	ns	*	ns
		β_1	ns	ns	ns	ns	ns	ns	ns	ns	ns	ns	ns	ns	ns	ns	ns	ns
		R^2	0.67	0.54	0.48	0.26	0.68	0.55	0.79	0.54	0.07	0.34	0.27	0.47	0.83	0.60	0.89	0.19
	60ha NE	model	ns	ns	ns	ns	ns	ns	ns	ns	ns	ns	ns	ns	ns	ns	ns	ns
		β_1	ns	ns	ns	ns	ns	ns	ns	ns	ns	ns	ns	ns	ns	ns	ns	ns
		R^2	0.56	0.45	0.11	0.05	0.73	0.18	0.47	0.45	0.11	0.64	0.05	0.83	0.24	0.10	0.34	-
	60ha NW	model	ns	ns	ns	ns	ns	ns	ns	ns	ns	ns	*	ns	*	ns	ns	ns
		β_1	ns	ns	ns	ns	ns	ns	ns	ns	ns	ns	*	ns	*	*	ns	ns
		R^2	0.61	0.22	0.18	0.43	0.13	0.41	0.19	0.45	0.45	0.26	0.77	0.04	0.72	0.80	0.61	-

GΘ – gravimetric water content; β_1 – constant parameter in the MLR model related to EC_a ; *, **,*** -model or β_1 significant at 0.05, 0.01 and 0.001 probability level respectively.

Table 4.15: Statistical analysis and summary statistics of the spatial MLR models between EC_a and soil parameters in June 2017

Field		Statistic	pH_w	pH_e	EC_e	C	N	P	K	Ca	Mg	Na	Zn	Mn	Fe	Cu	clay
Douglas	40ha	model	ns	ns	*	ns	ns	*	ns	ns	ns	**	**	ns	ns	*	ns
		β_1	ns	ns	ns	ns	ns	ns	ns	ns	ns	*	ns	ns	ns	*	-
		R^2	0.26	0.16	0.89	0.90	0.02	0.81	0.46	0.36	0.28	0.98	0.90	0.27	0.08	0.63	-
Luckhoff	20ha	model	*	ns	ns	ns	ns	ns	ns	ns	ns	ns	*	*	ns	ns	ns
		β_1	*	ns	ns	ns	ns	ns	ns	ns	ns	ns	*	*	ns	ns	ns
		R^2	0.97	0.30	0.57	0.58	0.54	0.11	0.31	0.01	0.05	0.004	0.88	0.99	0.40	0.49	0.21
	40ha	model	ns	ns	ns	ns	ns	ns	ns	*	ns	ns	ns	ns	ns	*	ns
		β_1	ns	ns	ns	ns	ns	ns	ns	*	ns	ns	ns	ns	ns	ns	ns
		R^2	0.29	0.13	0.02	0.002	0.001	0.25	0.18	0.96	0.03	0.05	0.45	0.30	0.04	0.53	0.07
	60ha NE	model	*	ns	ns	*	ns	ns	ns	ns	ns	ns	ns	ns	**	ns	ns
		β_1	ns	ns	ns	ns	ns	ns	ns	ns	ns	ns	ns	ns	ns	ns	ns
		R^2	0.91	0.44	0.77	0.91	0.12	0.23	0.56	0.74	0.44	0.07	0.15	0.11	0.98	0.86	0.76

β_1 – constant parameter in the MLR model related to EC_a ; *, **,*** -model or β_1 significant at 0.05, 0.01 and 0.001 probability level respectively.

The regression models of EC_a with soil properties at the study sites across the two growing seasons suggested that most of the models were not suitable for predictive purposes over time. At the Douglas site, none of the measured soil parameters significantly influenced EC_a in both June 2016 and June 2017 (Table 4.13 and 4.15). Only EC_e significantly influenced EC_a at the 55 ha upper pivot (NW) at both sampling times at Hofmeyr site (Table 4.13 and Table 4.14). At the 20 ha centre pivot of Luckhoff, none of the measured soil properties significantly influenced EC_a across three different sampling times; however, Zn was significantly modelled by EC_a measurements in both December 2016 and June 2017 (Table 4.14 and Table 4.15). At the Luckhoff's 40 and 60 ha (NE and NW) centre pivots; none of the soil parameters were significantly modelled by EC_a measurements across all the different sampling times. These observations are not unexpected since they reflect the complex and dynamic nature of EC_a measurements with EMI. As suggested by Corwin *et al.* (2006), these observations also reveal the need for ground truth soil samples to be collected during each EC_a survey to sufficiently infer temporal changes in spatial patterns. Furthermore, these observations show that EC_a correlates to some degree with soil properties and the strength of the estimated correlations can vary widely from one survey to the next (Corwin and Lesch, 2003). This is especially the case in non-saline fields where the dominant factors influencing EC_a are not easily identifiable (Farahani *et al*., 2004).

Generally, model results from the spatial regression between EC_a and soil properties obtained using spatial multiple linear regression (MLR) across the study sites showed that only a few soil properties were significantly modelled with EC_a measurements from site to site. In some cases, high R^2 was observed yet the specific soil property did not significantly influence EC_a measurements suggesting that other factors such as terrain had stronger influence on the EC_a variability at that particular site. Results from this study suggest that for the irrigated non-saline fields in South Africa where salinity is not dominant, EC_a measurements can probably be used as a surrogate measurement for some soil fertility properties on account of strong correlations.

In spite of some soil parameters significantly modelled by EC_a measurements at each measurement date, there was only a few observations that would suggest model stability over time. This therefore demonstrates that most of the EC_a and soil property models in this study are inadequate for predictive purposes over time. The lack of temporal stability between EC_a and soil property relationships calls for the necessity to re-calibrate the EMI for each EC_a survey. The EC_a-soil property relationships from this study collectively demonstrated that these relationships are mostly site- and time-specific and the model interpretation should only be restricted to the findings of this nature.

4.4 Conclusions

Most of the soil fertility parameters from the seven centre pivots at three study sites showed medium to high variability except for pH_w, pH_e and Na. This presents an opportunity for site-specific management. At all centre pivots except for one at Douglas, the soil fertility parameters fall within a satisfactory range for cropping. At Douglas, challenges with some nutrients such as Mg, Fe and Mn maybe experienced due to high pH. Furthermore, low C, P and N were also noted on all the centre pivots.

Most of the measured soil fertility properties were accurately modelled by MIR spectral data. The MIR model results from this study showed that MIR attenuated total reflectance spectroscopy is an effective technique with high applications in quantitative analysis of soils under irrigation for prediction purposes useful in site-specific soil fertility management. However, in some cases predictions were better per site than when the sites were grouped. Particularly, the MIR prediction of pH_e, P, K, Fe and Zn were significantly reduced when all the soils from the study sites were combined. This observation may imply that developing site-specific models may be the better option in some cases. The comparisons of multi-variate

techniques *viz.* CLSR, SMLR, PLSR and PCR in predicting soil properties related to soil fertility showed that PLSR as the best technique for modelling soil fertility properties with MIR spectra.

Generally, model statistics obtained from the spatial regression between EC_a and soil fertility properties across the study sites showed that only a few measured parameters were significantly modelled with EC_a measurements and the models were mostly site-specific. Measurements of EC_a at the study sites explained EC_e, C, N, P, K, Ca, Mg, Na, Zn, Mn, Fe, Cu, clay and GϴW best in some specific cases. Regardless of the strong models observed between EC_a and some soil parameters at a specific sampling date, there were only a few models that would suggest model stability over time. Study results suggest that for the irrigated non-saline and non-sodic fields, EC_a measurements can be used as a surrogate measurement for some soil fertility properties due to strong correlations observed using spatial MLR in the ESAP software.

CHAPTER 5: QUANTIFYING ACCUMULATION OF PLANT NUTRIENTS IN WHEAT AND MAIZE UNDER IRRIGATION USING CONVENTIONAL CHEMISTRY PROCEDURES, INFRARED REFLECTANCE SPECTROSCOPY AND ELECTROMAGNETIC INDUCTION

5.1 Introduction

Nutrient management is a major concern for the future of intensive crop production in South Africa (Sosibo *et al*., 2017). In these systems, producers tend to use excessive fertilizers which often lead to severe environmental damage. Improved nutrient management practices to optimize crop productivity and quality are more relevant than ever as pressure on food supply increases. Enhancement of soil fertility is a key point in obtaining the most profitable yields in irrigated agriculture. To optimize nutrient management, it is essential for irrigation farmers to assess the plant nutrient availability in the soil as well as to monitor crop performance throughout the growing season. In so doing, it is possible to act in accordance with crop requirements instead of relying only on fertilization by tradition or interpretations of soil analyses, which may not be able to reflect the true plant available concentrations of nutrients (Van Maarchalkerweerd and Husted, 2015). Routine plant analyses used as a guidance tool for fertilization is less common. However, plant analysis findings can be used to determine if the soil fertility level and applied fertilizers are sufficient to meet the crop requirements (Jones *et al.,* 1991). One barrier to the increased use of plant analyses as a fertilization tool is the price versus the perceived value by farmers (Van Maarchalkerweerd and Husted, 2015). Therefore, cheaper, accurate and more easily accessible methods for plant nutrient analysis are urgently needed.

Much effort has been put into developing methods for diagnosing nutritional disorders in plants. This is usually done by determining the total nutrient concentrations in plants or plant parts using tedious colorimetric methods or more accurate and faster methods such as Atomic Absorption Spectroscopy (AAS), multi-elemental techniques such as Inductively Coupled

Plasma Emission Spectrometry (ICP-OES) or Inductively Coupled Plasma Mass Spectrometry (ICP-MS). However, on the other hand, alternative techniques for plant analysis based on secondary indices are being recognized. Infrared spectroscopic techniques such as near infrared (NIR) and mid infrared (MIR) can be routinely used for fast plant nutrient analysis. These techniques are useful tools in quantitative and qualitative plant analysis with their advantages such as being rapid, non-destructive, reproducible, easy to use and cost-effective (Türker-Kaya and Huck, 2017). However, these measurements of nutrient concentrations are usually indirect. Instead, compounds that relate to physiological effects derived from the plant nutritional status are measured and these may correlate with the plant nutrient concentrations. Therefore, it is essential that these methods are thoroughly tested to ensure that they provide information specifically about the status of the given nutrient. Many research attempts have been made to use NIR spectroscopy to determine concentrations of most essential plant nutrients in numerous plant species, commonly using chemometrics to relate spectral data to nutrient concentrations (Chen *et al.*, 2002; Cozzolino and Moron, 2004; Huang *et al*., 2009). Only a few attempts were made for the same purpose using MIR spectroscopy (Van Maarchalkerweerd and Husted, 2015), therefore, this study investigates the use of the MIR spectroscopic technique to predict nutrients in wheat and maize crops.

Fast, inexpensive and accurate measurement of within-field variation of soil properties and crop yields is essential for the site-specific management of the agricultural fields. An electromagnetic induction sensor that delivers dense apparent electrical conductivity (EC_a) datasets can be used to achieve this objective. The EM38 meter is the most widely used EMI sensor in agriculture (Sudduth *et al.*, 2001; Heil and Schmidhalter, 2017). Several researchers have related EC_a to a number of different soil properties either within an individual field or across the entire landscape. Currently, areas of application include the estimation of nutrient levels and other soil chemical and physical properties, soil sampling points, the determination of soil types and their boundaries, the prediction of yield and the delineation of crop management zones (Heil and Schmidhalter, 2017).

Field-scale variation in crop yields is affected by many factors such as climate, soil properties, management practices and topographic position of the field (Singh *et al.,* 2016). A complete knowledge of factors and their interactions that affect yield is required for site specific yield management. Measurements of EC_a can be used to reflect crop yields. Although EC_a has no direct relationship to the growth and yield of plants, the spatial variation of EC_a is partly correlated with soil properties that do affect crop yields. This connection is clearly illustrated in literature. The advantage of EC_a in comparison to yield measurements is its relative temporal stability, which offers a better basis for the delineation of management zones than variable yield mapping information does (Heil and Schmidhalter, 2017). A number of studies have investigated the use of EC_a measurements in studying crop yields variation at field scale. Little information is available in literature on the potential use of EC_a measurements in investigating total nutrient uptake by wheat and maize crops at field scale. The main aim of this study was to quantify the accumulation of plant nutrients in wheat and maize grown under irrigation. Specific objectives were to (i) quantify the accumulation of nutrients by wheat during the 2016 winter growing season and maize during the 2016/2017 summer growing season, (ii) measure total nutrient uptake, nutrient harvest index and nutrient partitioning of the wheat and maize under site climate and typical soil and crop management conditions, (iii) examine whether MIR can predict plant nutrients in wheat and maize and compare the models in precision and robustness, (iv) investigate whether EC_a can be useful in studying total nutrient uptake and grain yields in fields under irrigation.

5.2 Procedure

The study sites' characteristics, soil sampling and analysis, plant sampling and analysis, data processing and statistical analysis are described in Chapter 3, and therefore not repeated in this chapter.

5.3 Results and Discussion

5.3.1 Nutrient concentrations in wheat and maize components

The nutrient concentrations in wheat and maize varied significantly among the various tissues at harvest. Tables 5.1 to 5.7 and Tables 5.8 to 5.11 shows the descriptive statistics for the nutrient concentrations in various parts of the wheat and maize at the study sites, respectively. At the Douglas 40 ha field, higher concentrations of K, Ca, Na and S in the stem and leaves component of wheat was measured (Table 5.1). However, higher concentrations of P, Cu and Zn were found in the seed component of the wheat whereas the husk component had higher concentrations of Mg, B, Fe and Mn. The two fields at Hofmeyr had higher concentrations of K, Ca, Na and S in the stem and leaves component whereas the husk component had higher concentrations of B and Fe. The seed component had higher concentrations of P, Cu, Mn and Zn. For wheat, the concentration of Mg was higher in the seed component at the 55 ha NW field and in the stem-leaves component at the 55 ha SE field (Tables 5.2 and 5.3). For the four fields at the Luckhoff site, concentrations of Ca, B, Fe and Mn were higher in the husk component of wheat whereas P, Cu and Zn concentrations were higher in the seed component. The concentrations of K and Na were higher in the stem and leaves component of wheat for all the fields at the Luckhoff site except Na at the 60 ha NE field where the husk component had higher Na concentration than other components (Table 5.4 to Table 5.7). The concentrations of Mg and S were highly variable in wheat components at the Luckhoff fields. Concentrations of Mg were higher in the seed component at the 40 ha, 60 ha NE and 60 ha NW fields whereas at the 20 ha fields the concentration of this nutrient was higher in the husk component. The concentrations of S was higher in the stem and leaves component at the 20 ha and 40 ha fields whereas at the 60 ha NE and 60 ha NW fields the same nutrient was higher in the seed component (Table 5.4 to Table 5.7).

The nutrients K, Ca, Mg, Na, S, B, Cu, Fe, Mn and Zn in maize at the Douglas 40 ha field were more concentrated in the stem and leaves as shown in Table 5.8. However, P behaved differently with a higher concentration observed in the grain component. The same trends were also observed at the Luckhoff fields with most of the measured nutrients more concentrated in the stem and leaves except for P which was concentrated in the maize seed component (Table 5.9 to Table 5.11).

At the harvest stage, the average concentration of all the nutrients at all sites in wheat and maize exceeded the critical values suggested by Campbell (2000) at physiological crop maturity below which retardation of crop growth may occur (Table 5.12). The average concentration of P, K, B and Fe in wheat at most of the study sites exceeded the sufficient ranges of Campbell (2000) as shown in Table 5.12. The rest of the nutrients (Ca, Mg, S, Cu, Mn and Zn) fall within the optimum concentration ranges. The concentrations of P, K, Ca, Mg and B in maize at the study sites exceeded the suggested optimum ranges by Campbell (2000). The concentrations of Mn and Zn exceeded the sufficient ranges at two of the study sites whereas these respective concentrations were within the optimum ranges at the other two sites. Only S and Cu concentrations in maize were within the suggested sufficient ranges as shown in Table 5.12. The reason for the concentrations of some of the measured nutrients in exceeding the suggested optimum ranges in literature could have been due to the sampling time differences. The suggested sufficient ranges by Campbell (2000) are more relevant at the crop's physiological maturity stage. A common misconception in nutrient assimilation is that nutrient accumulation stops upon the maturity stage (Bender, 2012). However, Sayre (1948) and Karlen *et al.* (1988) suggest that as much as 50% of dry weight, P, Mg, and S accumulation is still ongoing at flowering stage of maize growth which justifies sampling at post-physiological maturity stage.

The measured total nutrient concentrations in wheat and maize were also compared with the accepted nutrient concentrations in these crops in South Africa (FSSA, 2007). There is limited information on the total nutrient concentration in wheat with only N, P, K, Mg and S having received more attention. However, there is more information on maize with almost all the macronutrients and micronutrients information accessible in FSSA (2007). The total concentrations of P and K in wheat at the study sites exceeded the published values with S fairly within the reported range. The measured concentrations of P, Mg, S, B and Cu in maize at the study sites were fairly within the range as reported in FSSA (2007). However, the concentrations of K, Ca and Mn were significantly higher than the reported values. The concentrations of Zn in maize at the Luckhoff fields were moderately within the range with the concentrations significantly higher at the Douglas 40 ha field. Iron (Fe) concentrations in maize at Douglas 40 ha, Luckhoff 20 ha and 60 ha NE fields were also reasonably within the reported range with the concentrations at the Luckhoff 40 ha significantly higher than the reported values by the FSSA (2007).

5.3.2 Crop yield parameters, nutrient uptake and partitioning by wheat and maize during the two growing seasons at study sites

The amounts of nutrients accumulated by wheat and maize during the winter 2016 and summer 2016/17 seasons are presented in Table 5.14 and Table 5.15, respectively. The ANOVAs for the biomass, grain yield, harvest index and nutrient uptake by wheat showed significant differences ($p < 0.05$) between locations for all the variables (Table 5.14). Similar observations were also made with maize except Fe uptake which was not significant across the study sites (Table 5.15). The Hofmeyr 55 ha SE field had significantly higher wheat biomass and grain yield as well as P, K, Ca, S, Cu, Fe and Zn uptake by wheat when compared to some of the other fields at Douglas and Luckhoff sites (Table 5.14). These differences could be due to the different agronomic practices being used by the farmers at these sites. An important agronomic practice is the higher wheat density at the Hofmeyr fields as compared

to the other fields at Douglas and Luckhoff sites (Tables 3.2 and 3.3). Gao *et al* (2009) found higher wheat yield, N uptake and N use efficiency in higher wheat density treatments as compared to lower wheat density treatments in a study which investigated the effects of mulching, N fertilizer application rate and plant density in a winter wheat-fallow system. Remarkably, the 55 ha SE field has significantly higher biomass, grain yield, harvest index as well as higher total P, K, Ca, Mg, S, B, Cu, Fe and Zn uptake by wheat as compared to the other 55 ha NW field yet these fields are at the same location and were managed similarly. The reason for this observation can be attributed to the significant differences between the two fields in some of the important soil properties such as C and K at the beginning of the winter 2016 season (Table 4.8). The exploratory analysis of soil fertility at the two Hofmeyr fields showed that the 55 ha SE field was more fertile than the other 55 ha NW field in June 2016. Contrastingly, significantly higher Mg and B uptake by wheat was observed at the Douglas 40 ha field as compared to other fields at Hofmeyr and Luckhoff sites.

The average wheat grain yield at the 7 experimental fields was 7.39 t ha^{-1} higher than the average grain yield reported by Gregory *et al.* (1979) and Du Preez and Bennie (1991), *viz.* 6.45 t ha^{-1} and 5.80 t ha^{-1}, respectively. Research on wheat cultivar trials conducted in South Africa have documented potential yields of up to 12 t ha^{-1} under controlled field experiments (ARC-SGI, 2015; Sosibo *et al.,* 2017). These observations show that there may be opportunity to increase wheat yield in the study areas through refinements of crop and resource management strategies. Significantly higher maize biomass and grain yield as well as total P, K, Ca, Mg, S, Na, B, Cu, Mn and Zn uptake ($p < 0.05$) was observed at the Douglas 40 ha field as compared to the fields at Luckhoff at the end of the 2016/17 summer season (Table 5.15). The observed significant differences at these fields is most probably due to the differences in the crop and soil management practices at these fields. Primarily, the Douglas 40 ha field was fertilized more heavily than the fields at the Luckhoff site (Table 3.2). Furthermore, most of the soil fertility properties were significantly higher at the Douglas 40 ha

field which may also have contributed to the observed significant differences (See Tables 4.8 – 4.10).

The lower maize biomass and grain yield as well as total nutrient uptake observed at the Luckhoff 40 ha field was probably due to the smaller popcorn cultivar grown at this field as compared to maize cultivars grown in other fields (Table 3.2 and Table 3.3). The average grain yield for the standard maize cultivars at the study sites was 14.4 t ha^{-1}. The average grain yield for maize in this study was higher than the average maize yields under irrigation in South Africa reported by Schulze and Walker (2007), Wettstein *et al*. (2017) and USDA (2018) , *viz* 6.05 , 8.13 and 11.0 t ha^{-1} respectively, demonstrating impressive yields at the study sites. The improvements in the maize yield trends across years can be mainly attributed to more refined management practices and improved seed varieties with increased plant populations. Moreover, the latest advances in GPS technology allows the farmers in South Africa to plant crops with greater precision and speed, higher plant populations and at more uniform depths, thus allowing the farmers to achieve greater yields (USDA, 2018).

Table 5.1: Descriptive statistics for the concentration of nutrients in various parts of wheat harvested on the 40 ha centre pivot at Douglas in November 2016

Component	Seeds						Husks						Stem and leaves					
	Mean	Min	Max	SD	CV	Range	Mean	Min	Max	SD	CV	Range	Mean	Min	Max	SD	CV	Range
Macronutrient (%)																		
P	0.357	0.216	0.458	0.054	15.1	0.242	0.135	0.044	0.209	0.043	31.9	0.165	0.081	0.042	0.179	0.024	29.6	0.137
K	0.392	0.272	1.50	0.170	43.4	1.23	0.906	0.283	2.80	0.429	47.4	2.52	2.29	0.717	2.93	0.312	13.6	2.22
Ca	0.038	0.030	0.057	0.006	15.8	0.027	0.226	0.175	0.457	0.047	20.8	0.283	0.244	0.124	0.384	0.047	19.3	0.261
Mg	0.146	0.101	0.357	0.037	25.3	0.256	0.158	0.113	0.261	0.026	16.5	0.148	0.153	0.095	0.201	0.023	15.0	0.106
Na	0.034	0.027	0.060	0.005	14.7	0.034	0.192	0.113	0.390	0.043	22.4	0.276	0.279	0.040	0.434	0.072	25.8	0.395
S	0.136	0.102	0.195	0.019	14.0	0.092	0.114	0.067	0.270	0.034	29.8	0.203	0.177	0.032	0.263	0.045	25.4	0.231
Micronutrient (mg/kg)																		
B	1.47	1.08	2.41	0.324	22.0	1.33	12.1	5.50	20.6	3.09	25.5	15.1	6.38	3.59	10.1	1.59	24.9	6.51
Cu	2.71	1.72	4.18	0.527	19.4	2.46	1.47	0.940	3.33	0.512	34.8	2.39	1.82	1.07	5.73	0.741	40.7	4.66
Fe	21.3	13.5	72.8	8.31	39.0	59.3	61.6	32.6	96.7	15.4	25.0	64.2	45.3	15.8	81.4	13.6	30.0	65.7
Mn	40.5	25.1	55.8	7.01	17.3	30.7	69.6	29.2	116	20.4	29.3	87.2	33.6	16.4	63.8	10.0	29.8	47.4
Zn	25.8	17.7	34.8	3.87	15.0	17.1	11.1	4.19	19.3	3.10	27.9	15.1	11.6	4.93	21.4	4.21	36.3	16.5

Table 5.2: Descriptive statistics for the concentration of nutrients in various parts of wheat harvested on the 55 ha NW centre pivot at Hofmeyr in November 2016

Component	Seeds						Husks						Stem and leaves					
	Mean	Min	Max	SD	CV	Range	Mean	Min	Max	SD	CV	Range	Mean	Min	Max	SD	CV	Range
Macronutrient (%)																		
P	0.426	0.358	0.541	0.045	10.6	0.183	0.135	0.072	0.220	0.038	28.1	0.149	0.082	0.040	0.186	0.029	35.4	0.146
K	0.540	0.485	0.766	0.059	10.9	0.281	1.08	0.109	1.66	0.285	26.4	1.55	2.81	1.95	4.20	0.488	17.4	2.25
Ca	0.062	0.047	0.079	0.008	12.9	0.032	0.273	0.203	0.397	0.045	16.5	0.194	0.318	0.229	0.549	0.078	24.5	0.320
Mg	0.149	0.120	0.186	0.017	11.4	0.066	0.097	0.057	0.167	0.021	21.6	0.110	0.088	0.054	0.149	0.023	26.1	0.095
Na	0.028	0.019	0.032	0.002	7.14	0.013	0.043	0.033	0.061	0.005	11.5	0.027	0.054	0.039	0.123	0.015	27.8	0.084
S	0.183	0.157	0.214	0.014	7.65	0.057	0.125	0.086	0.155	0.017	13.6	0.068	0.196	0.102	0.337	0.052	26.5	0.234
Micronutrient (mg/kg)																		
B	1.65	1.24	2.22	0.236	14.3	0.980	6.73	4.88	9.28	1.09	16.2	4.40	4.22	2.63	7.30	0.981	5.51	4.67
Cu	4.03	2.07	15.3	2.12	52.6	13.2	2.20	1.26	3.35	0.420	19.1	2.09	2.24	1.10	6.06	0.724	32.3	4.96
Fe	46.8	32.2	225.7	27.2	58.1	193.5	177.5	91.6	298.3	42.8	24.1	206.7	101.8	53.8	145.2	22.6	22.2	91.4
Mn	33.8	19.5	46.3	6.17	18.3	26.8	29.6	14.7	59.4	7.80	26.4	44.7	19.1	5.94	48.9	8.57	44.9	43.0
Zn	45.1	29.8	67.3	8.96	19.9	37.5	21.7	9.05	58.8	8.57	39.5	49.8	16.8	5.37	38.0	6.60	39.3	32.6

Table 5.3: Descriptive statistics for the concentration of nutrients in various parts of wheat harvested on the 55 ha SE centre pivot at Hofmeyr in November 2016

Component	Seeds						Husks						Stem and leaves					
	Mean	Min	Max	SD	CV	Range	Mean	Min	Max	SD	CV	Range	Mean	Min	Max	SD	CV	Range
Macronutrient (%)																		
P	0.432	0.360	0.491	0.030	6.94	0.131	0.142	0.068	0.229	0.030	21.1	0.160	0.090	0.054	0.141	0.021	23.3	0.087
K	0.648	0.517	0.771	0.062	9.57	0.254	1.17	0.687	2.57	0.332	24.3	1.89	2.73	0.256	3.79	0.659	24.1	3.53
Ca	0.062	0.045	0.085	0.010	16.1	0.40	0.255	0.151	0.326	0.038	14.9	0.175	0.268	0.172	0.369	0.041	15.3	0.196
Mg	0.143	0.119	0.170	0.011	7.69	0.051	0.088	0.053	0.185	0.022	25.0	0.132	0.748	0.044	0.127	0.016	2.14	0.082
Na	0.028	0.025	0.031	0.001	3.57	0.007	0.043	0.032	0.135	0.015	34.9	0.102	0.047	0.027	0.111	0.014	29.8	0.084
S	0.170	0.142	0.208	0.013	7.65	0.066	0.107	0.065	0.178	0.022	20.6	0.113	0.167	0.101	0.239	0.029	17.4	0.138
Micronutrient (mg/kg)																		
B	1.43	1.00	1.90	0.182	12.7	0.900	6.25	3.53	9.68	1.42	22.7	6.15	3.94	2.10	5.87	0.801	20.3	3.77
Cu	3.70	2.50	6.93	0.764	20.6	4.43	2.47	1.42	4.92	0.630	25.5	3.50	2.99	1.54	9.90	1.58	52.8	8.36
Fe	39.6	31.0	57.5	5.26	13.3	26.5	167.2	95.1	239.3	30.3	18.1	144.2	98.0	33.7	168.9	26.7	27.2	135.2
Mn	31.0	19.9	50.5	6.89	22.2	40.6	23.3	8.19	42.1	7.10	30.5	33.9	14.2	6.55	30.8	5.21	36.7	24.2
Zn	38.8	29.3	49.3	4.59	11.8	20.0	15.9	5.31	27.1	4.21	26.5	21.8	12.3	5.57	18.3	3.26	26.5	12.8

Table 5.4: Descriptive statistics for the concentration of nutrients in various parts of wheat harvested on the 20 ha centre pivot at Luckhoff in November 2016

Component	Seeds						Husks						Stem and leaves					
	Mean	Min	Max	SD	CV	Range	Mean	Min	Max	SD	CV	Range	Mean	Min	Max	SD	CV	Range
Macronutrients (%)																		
P	0.388	0.296	0.572	0.053	13.7	0.277	0.116	0.063	0.191	0.035	30.2	0.128	0.074	0.048	0.106	0.015	20.3	0.058
K	0.426	0.361	0.630	0.055	12.9	0.268	1.32	0.846	2.16	0.362	27.4	1.32	2.65	1.85	3.17	0.300	11.3	1.31
Ca	0.046	0.037	0.061	0.006	13.0	0.024	0.369	0.221	0.549	0.086	23.3	0.328	0.287	0.148	0.415	0.071	24.7	0.267
Mg	0.141	0.116	0.189	0.015	10.6	0.073	0.190	0.070	0.277	0.051	26.8	0.208	0.141	0.061	0.280	0.050	35.5	0.219
Na	0.008	0.002	0.038	0.011	137.5	0.036	0.076	0.021	0.204	0.038	50.0	0.183	0.088	0.017	0.234	0.053	60.2	0.217
S	0.141	0.117	0.197	0.020	14.2	0.080	0.139	0.098	0.196	0.027	19.4	0.098	0.196	0.097	0.318	0.046	23.5	0.221
Micronutrients (mg/kg)																		
B	0.166	0.030	0.920	0.257	154.8	0.890	6.85	4.44	13.4	2.66	38.8	9.00	3.75	1.94	6.78	1.40	10.0	4.84
Cu	4.57	1.53	18.6	4.33	94.7	17.1	1.28	0.86	2.28	0.368	28.8	1.42	1.72	0.94	4.47	0.947	55.1	3.53
Fe	27.5	19.8	39.7	5.63	20.5	19.9	106.4	55.4	145.5	25.4	24.0	90.1	80.9	39.2	167.7	29.7	36.7	128.5
Mn	48.5	26.4	89.5	17.9	36.9	63.1	111.8	19.7	472.2	116.8	104.5	452.5	58.6	5.94	277.0	71.8	126.9	271.1
Zn	26.0	15.6	49.0	7.79	30.0	33.4	8.44	4.53	18.1	3.81	45.1	13.6	7.73	2.78	15.3	3.83	49.5	12.5

Table 5.5: Descriptive statistics for the concentration of nutrients in various parts of wheat harvested on the 40 ha centre pivot at Luckhoff in November 2016

Component	Seeds						Husks						Stem and leaves					
	Mean	Min	Max	SD	CV	Range	Mean	Min	Max	SD	CV	Range	Mean	Min	Max	SD	CV	Range
Macronutrient (%)																		
P	0.420	0.298	0.542	0.045	10.7	0.245	0.130	0.071	0.236	0.039	30.0	0.166	0.088	0.048	0.135	0.020	22.7	0.087
K	0.435	0.363	0.610	0.046	10.6	0.247	1.00	0.433	2.13	0.316	31.6	1.70	2.39	1.84	2.83	0.255	10.7	0.993
Ca	0.048	0.039	0.069	0.006	12.5	0.030	0.268	0.167	0.399	0.061	22.8	0.232	0.210	0.145	0.349	0.045	21.4	0.204
Mg	0.145	0.111	0.199	0.016	11.0	0.088	0.120	0.061	0.207	0.033	27.5	0.145	0.088	0.057	0.180	0.027	30.7	0.124
Na	0.035	0.017	0.049	0.005	16.4	0.032	0.044	0.038	0.065	0.005	11.2	0.032	0.047	0.031	0.076	0.010	21.3	0.045
S	0.150	0.044	0.186	0.020	13.3	0.141	0.090	0.008	0.141	0.029	32.2	0.133	0.132	0.007	0.211	0.041	31.1	0.203
Micronutrient (mg/kg)																		
B	0.479	0.250	0.970	0.142	29.6	0.720	4.83	2.25	11.9	1.96	40.6	9.67	2.14	1.33	5.67	0.728	34.0	4.34
Cu	2.30	1.47	4.69	0.51	22.2	3.22	1.13	0.720	1.89	0.250	22.1	1.17	1.24	0.890	2.22	0.266	21.5	1.33
Fe	32.3	21.8	63.7	7.09	22.0	41.9	125.0	65.8	238.6	35.7	28.6	172.8	76.7	42.9	115.8	18.5	24.1	72.8
Mn	45.2	25.6	70.4	9.69	21.4	44.8	54.4	13.3	125.0	27.0	49.6	111.7	20.1	10.4	46.9	8.44	42..0	36.5
Zn	27.9	16.7	45.0	6..30	22.6	28.4	6.92	3.67	16..8	2.86	41.3	13.1	6.20	3.25	10.9	1.83	29.5	7.67

Table 5.6: Descriptive statistics for the concentration of nutrients in various parts of wheat harvested on the 60 ha NE centre pivot at Luckhoff in November 2016

Component	Seeds						Husks						Stem and leaves					
	Mean	Min	Max	SD	CV	Range	Mean	Min	Max	SD	CV	Range	Mean	Min	Max	SD	CV	Range
Macronutrient (%)																		
P	0.432	0.375	0.485	0.030	6.94	0.110	0.143	0.076	0.219	0.045	31.5	0.142	0.084	0.056	0.112	0.016	19.0	0.056
K	0.557	0.358	0.476	0.030	5.39	3.20	0.105	0.074	0.185	0.027	25.7	0.112	2.38	1.83	2.71	0.208	9.74	0.878
Ca	0.048	0.042	0.056	0.004	8.33	0.014	0.243	0.179	0.323	0.035	14.4	0.114	0.180	0.107	0.282	0.002	1.11	0.176
Mg	0.147	0.121	0.170	0.013	8.84	0.050	0.105	0.074	0.185	0.027	25..7	0.112	0.076	0.051	0.146	0.020	26.3	0.095
Na	0.029	0.026	0.034	0.002	6.90	0.008	0.045	0.040	0.054	0.004	8.89	0.014	0.041	0.034	0.049	0.003	7.32	0.015
S	0.131	0.120	0.148	0.008	6.11	0.028	0.071	0.050	0.107	0.014	19.7	0.057	0.090	0.068	0.116	0.014	15.6	0.048
Micronutrient (mg/kg)																		
B	0.542	0.410	0.690	0.072	13.3	0.280	4.62	1.94	7.36	1.35	29.2	5.42	2.44	1.53	4.78	0.755	30.9	3.25
Cu	1.95	1.42	3.55	0.465	23.8	2.13	1.23	0.670	2.08	0.316	25.7	1.41	1.18	0.830	1.67	0.180	15.3	0.840
Fe	27.1	20.7	45.1	6.16	22.7	24.4	121.3	56.3	202.8	37.5	30.9	146.5	59.9	29.7	91.3	15.7	26.2	61.6
Mn	38.2	30.6	48.8	5.30	13.9	18.3	45.6	18.3	119.3	28.7	62.9	100.9	17.8	11.2	37.5	7.45	41.9	26.3
Zn	25.8	19.3	43.5	5.10	19.8	24.2	8.57	4.50	25.4	4.81	56.1	20.9	5.91	3.33	10.3	1.73	29.3	6.92

Table 5.7: Descriptive statistics for the concentration of nutrients in various parts of wheat harvested on the 60 ha NW centre pivot at Luckhoff in November 2016

Component	Seeds						Husks						Stem and leaves					
	Mean	Min	Max	SD	CV	Range	Mean	Min	Max	SD	CV	Range	Mean	Min	Max	SD	CV	Range
Macronutrient (%)																		
P	0.427	0.355	0.517	0.041	9.60	0.163	0.117	0.086	0.184	0.021	17.9	0.097	0.095	0.058	0.167	0.026	27.4	0.109
K	0.454	0.384	0.515	0.038	8.37	0.131	1.22	0.747	1.51	0.219	18.0	0.767	2.39	1.70	2.68	0.247	10.3	0.980
Ca	0.047	0.039	0.057	0.004	8.51	0.018	0.260	0.183	0.342	0.039	15.0	0.159	0.200	0.136	0.285	0.040	20.0	0.149
Mg	0.150	0.125	0.183	0.016	10.7	0.058	0.111	0.074	0.137	0.017	15.3	0.062	0.083	0.052	0.118	0.018	21.7	0.065
Na	0.029	0.026	0.039	0.003	10.3	0.013	0.044	0.039	0.047	0.002	4.55	0.008	0.049	0.040	0.078	0.008	16.3	0.038
S	0.130	0.102	0.151	0.012	9.23	0.049	0.067	0.050	0.094	0.010	14.9	0.044	0.100	0.068	0.139	0.018	18.0	0.071
Micronutrient (mg/kg)																		
B	0.552	0.440	0.690	0.083	15.0	0.250	4.16	2.11	5.28	0.815	19.6	3.17	2.34	1.53	4.86	0.651	27.8	3.33
Cu	1.67	1.17	2.83	0.362	21.7	1.66	1.03	0.67	1.25	0.143	13.9	0.580	1.20	0.830	1.33	0.117	9.75	0.500
Fe	23.8	18.6	29.9	3.67	15.4	11.3	109.2	63.0	159.0	26.7	24.5	96.0	70.2	31.1	131.2	22.2	31.6	100.1
Mn	37.8	21.3	54.8	10.2	27.0	33.6	40.6	13.0	76.0	21.6	53.2	63.0	14.2	4.00	23.7	5.82	41.0	19.7
Zn	22.3	16.9	28.4	3.52	15.8	11.5	5.99	3.75	11.9	1.74	29.0	8.17	5.37	2.50	10.1	2.07	38.5	7.58

Table 5.8: Descriptive statistics for the concentration of nutrients in various parts of maize harvested on the 40 ha centre pivot at Douglas in May 2017

	Seeds						Cobs						Husks						Stem and leaves					
	Mean	Min	Max	SD	CV	Range	Mean	Min	Max	SD	CV	Range	Mean	Min	Max	SD	CV	Range	Mean	Min	Max	SD	CV	Range
Macronutrient (%)																								
P	0.283	0.188	0.416	0.045	15.9	0.228	0.054	0.026	0.095	0.014	25.9	0.068	0.042	0.028	0.059	0.007	16.7	0.031	0.142	0.099	0.408	0.058	40.8	0.309
K	0.333	0.232	0.413	0.034	10.2	0.182	0.450	0.270	0.550	0.067	14.9	0.279	0.860	0.549	1.29	0.158	18.4	0.741	3.88	3.01	5.14	0.477	12.3	2.13
Ca	0.003	0.002	0.006	0.001	29.9	0.005	0.008	0.005	0.017	0.003	37.5	0.012	0.084	0.053	0.145	0.019	22.6	0.092	0.779	0.663	0.964	0.065	8.34	0.302
Mg	0.106	0.069	0.159	0.018	17.0	0.090	0.026	0.017	0.040	0.006	23.1	0.023	0.085	0.055	0.147	0.021	24.7	0.092	0.483	0.318	0.677	0.071	14.7	0.359
Na	0.026	0.016	0.039	0.004	15.4	0.023	0.025	0.022	0.029	0.001	4.00	0.007	0.025	0.022	0.029	0.001	4.00	0.007	0.115	0.091	0.151	0.012	10.4	0.060
S	0.101	0.083	0.141	0.012	11.9	0.058	0.039	0.018	0.058	0.010	25.6	0.040	0.036	0.027	0.049	0.006	16.7	0.022	0.192	0.161	0.297	0.027	14.1	0.136
Micronutrient (mg/kg)																								
B	2.07	1.47	2.46	0.235	11.4	0.99	2.41	1.68	3.15	0.365	15.1	1.47	5.77	4.19	7.53	0.705	12.2	3.34	25.9	20.8	33.4	2.70	10.4	12.6
Cu	1.52	0.64	5.40	0.759	49.9	4.76	3.06	1.79	4.56	0.645	21.1	2.77	3.00	1.56	9.15	1.38	46.0	7.59	13.1	9.34	22.1	2.10	16.0	12.8
Fe	9.97	5.15	23.9	4.23	42.4	18.8	31.8	9.40	91.7	15.6	49.1	82.3	25.3	9.66	82.8	13.9	54.9	73.2	150.3	87.5	400.7	54.6	36.3	313.3
Mn	3.09	1.37	6.65	1.11	35.9	5.28	5.80	3.59	10.2	1.27	21.9	6.56	27.0	15.0	55.0	8.94	33.1	40.0	132.4	96.7	171.8	17.2	13.0	75.1
Zn	18.8	12.6	27.3	2.77	14.7	14.8	17.2	9.00	26.00	3.84	22.3	17.0	27.1	7.85	49.7	9.41	34.7	41.8	47.1	22.0	86.3	12.5	26.5	64.3

Table 5.9: Descriptive statistics for the concentration of nutrients in various parts of maize harvested on the 20 ha centre pivot at Luckhoff in May 2017

	Seeds						Cobs						Husks						Stem and leaves					
	Mean	Min	Max	SD	CV	Range	Mean	Min	Max	SD	CV	Range	Mean	Min	Max	SD	CV	Range	Mean	Min	Max	SD	CV	Range
Macronutrient (%)																								
P	0.226	0.186	0.288	0.028	12.4	0.102	0.034	0.015	0.085	0.020	58.8	0.069	0.038	0.022	0.062	0.012	31.6	0.041	0.092	0.060	0.140	0.022	23.9	0.080
K	0.306	0.243	0.375	0.030	9.80	0.132	0.703	0.537	0.886	0.077	11.0	0.349	0.736	0.490	0.953	0.102	13.9	0.462	3.64	2.47	4.60	0.518	14.2	2.03
Ca	0.004	0.002	0.015	0.002	50.0	0.012	0.012	0.006	0.023	0.004	33.3	0.017	0.075	0.056	0.109	0.013	22.6	0.0530	0.822	0.647	1.13	0.110	13.3	0.487
Mg	0.096	0.074	0.112	0.011	11.5	0.038	0.034	0.017	0.054	0.008	23.5	0.037	0.095	0.069	0.162	0.018	18.9	0.093	0.440	0.269	0.689	0.097	22.0	0.420
Na	0.011	0.004	0.012	0.002	18.2	0.009	0.026	0.005	0.032	0.005	19.2	0.027	0.010	0.004	0.021	0.004	40.0	0.034	0.115	0.067	0.295	0.050	43.5	0.228
S	0.078	0.066	0.101	0.007	8.97	0.035	0.032	0.020	0.051	0.008	25.0	0.030	0.040	0.026	0.058	0.007	17.5	0.032	0.145	0.100	0.233	0.027	18.6	0.133
Micronutrient (mg/kg)																								
B	1.36	0.940	1.92	0.225	16.5	0.980	2.81	1.69	4.13	0.631	22.5	2.44	4.49	3.61	6.03	0.478	10.6	2.42	18.2	11.7	28.2	3.57	19.6	16.5
Cu	1.18	0.440	2.94	0.654	55.4	2.50	2.16	1.50	3.00	0.446	20.6	1.50	1.69	0.940	5.78	0.944	55.9	4.84	6.89	3.92	16.6	3.06	44.4	12.7
Fe	11.4	9.25	17.3	1.79	15.7	8.08	54.5	35.6	74.8	10.9	20.0	39.2	30.6	21.9	43.5	5.47	17.9	21.6	139.7	94.7	262.3	40.3	28.8	167.6
Mn	4.24	2.86	6.86	1.07	25.2	4.00	6.07	3.25	15.6	3.17	52.2	12.3	25.1	9.44	60.8	15.6	62.2	51.3	140.7	49.1	496.4	120.9	85.9	447.3
Zn	11.7	8.69	15.5	1.68	14.4	6.84	6.27	3.58	9.67	1.70	27.1	6.09	3.67	1.78	9.36	1.93	52.6	7.58	12.3	7.70	23.5	3.85	31.3	15.8

Table 5.10: Descriptive statistics for the concentration of nutrients in various parts of maize harvested on the 40 ha centre pivot at Luckhoff in May 2017

	Seeds						Cobs						Husks						Stem and leaves					
	Mean	Min	Max	SD	CV	Range	Mean	Min	Max	SD	CV	Range	Mean	Min	Max	SD	CV	Range	Mean	Min	Max	SD	CV	Range
Macronutrient (%)																								
P	0.307	0.175	0.452	0.057	18.6	0.278	0.062	0.049	0.084	0.009	14.5	0.035	0.070	0.023	0.138	0.020	28.6	0.115	0.236	0.109	0.499	0.085	36.0	0.390
K	0.270	0.182	0.386	0.043	15.9	0.204	0.546	0.415	0.735	0.079	14.5	0.320	0.613	0.274	1.33	0.214	34.9	1.06	4.81	3.77	5.71	0.510	10.6	1.94
Ca	0.005	0.003	0.010	0.001	20.0	0.007	0.016	0.010	0.038	0.006	37.5	0.028	0.097	0.065	0.138	0.017	17.5	0.073	0.808	0.244	1.00	0.143	17.7	0.756
Mg	0.133	0.071	0.210	0.026	19.5	0.139	0.048	0.029	0.080	0.010	20.8	0.051	0.132	0.063	0.167	0.020	15.2	0.104	0.449	0.272	0.727	0.106	24.3	0.456
Na	0.027	0.025	0.029	0.001	3.70	0.004	0.028	0.025	0.030	0.001	3.57	0.005	0.026	0.015	0.043	0.003	11.5	0.028	0.067	0.045	0.079	0.005	7.46	0.034
S	0.103	0.039	0.128	0.017	16.5	0.089	0.038	0.023	0.053	0.006	15.8	0.030	0.046	0.027	0.074	0.009	19.6	0.047	0.168	0.066	0.245	0.033	19.6	0.180
Micronutrient (mg/kg)																								
B	1.46	0.810	4.64	0.901	61.7	3.83	1.73	1.25	3.25	0.398	23.0	2.00	3.81	2.75	6.50	0.606	15.9	3.75	13.1	5.50	17.5	2.54	19.4	12.0
Cu	1.68	0.594	3.69	0.661	39.3	3.10	1.32	0.560	2.140	0.351	26.6	1.58	1.21	0.470	3.06	0.541	44.7	2.59	4.73	2.36	7.95	1.39	29.4	5.59
Fe	18.9	9.89	43.2	6.43	34.0	33.3	52.6	29.9	90.6	12.6	24.0	60.7	29.8	15.1	81.8	10.6	35.6	66.7	221.3	127.7	750.0	121.2	54.8	622.3
Mn	8.93	4.67	13.8	1.81	20.3	9.11	7.71	5.67	11.2	1.38	17.9	5.55	22.2	10.7	44.5	7.53	33.9	33.8	82.9	19.4	178.5	29.7	35.8	159.1
Zn	20.5	13.2	35.8	5.35	26.1	22.6	4.13	2.08	9.25	1.29	31.2	7.17	10.7	2.92	39.9	7.05	65.9	37.0	20.8	8.00	68.4	12.3	59.1	60.4

Table 5.11: Descriptive statistics for the concentration of nutrients in various parts of maize harvested on the 60 ha NE centre pivot at Luckhoff in November 2016

	Seeds						Cobs						Husks						Stem and leaves					
	Mean	Min	Max	SD	CV	Range	Mean	Min	Max	SD	CV	Range	Mean	Min	Max	SD	CV	Range	Mean	Min	Max	SD	CV	Range
Macronutrient (%)																								
P	0.271	0.230	0.322	0.023	8.48	0.092	0.062	0.041	0.100	0.016	25.8	0.059	0.049	0.027	0.083	0.014	28.6	0.055	0.137	0.094	0.275	0.044	32.1	0.181
K	0.332	0.292	0.400	0.025	7.53	0.109	0.796	0.647	0.954	0.094	11.8	0.307	0.699	0.415	0.989	0.149	21.3	0.574	3.17	2.64	3.77	0.331	10.4	1.12
Ca	0.004	0.003	0.008	0.001	25.0	0.005	0.012	0.007	0.019	0.003	25.0	0.012	0.069	0.052	0.104	0.011	15.9	0.051	0.735	0.522	0.937	0.091	12.4	0.416
Mg	0.100	0.085	0.116	0.009	9.00	0.031	0.032	0.018	0.045	0.007	21.9	0.027	0.072	0.060	0.090	0.009	12.5	0.030	0.294	0.163	0.417	0.070	23.8	0.254
Na	0.026	0.017	0.029	0.002	7.69	0.012	0.026	0.023	0.028	0.001	3.85	0.005	0.027	0.024	0.035	0.002	7.41	0.011	0.064	0.060	0.072	0.003	4.69	0.012
S	0.078	0.067	0.100	0.006	7.69	0.033	0.034	0.023	0.054	0.009	26.5	0.031	0.034	0.025	0.054	0.007	20.6	0.029	0.113	0.086	0.197	0.022	19.5	0.111
Micronutrient (mg/kg)																								
B	1.80	1.53	2.36	0.164	9.09	0.830	2.24	1.72	3.14	0.372	16.6	1.42	4.19	3.72	4.97	0.373	8.90	1.25	14.5	10.0	19.1	2.18	15.0	9.08
Cu	1.11	0.670	2.33	0.371	33.4	1.66	2.11	1.44	3.94	0.619	29.3	2.50	1.46	0.750	2.78	0.468	32.1	2.03	5.15	3.22	7.22	0.876	17.0	4.00
Fe	12.3	8.64	19.7	2.81	22.8	11.1	55.0	26.4	116.9	18.6	33.8	90.5	29.6	20.6	46.1	6.45	21.8	25.5	153.9	111.9	282.6	44.2	28.7	170.8
Mn	4.33	3.58	8.00	0.918	21.2	4.42	4.67	3.36	6.61	0.891	19.1	3.25	14.8	10.8	17.7	1.59	10.7	6.92	74.8	43.6	99.3	12.5	16.7	55.8
Zn	12.0	8.42	19.0	2.19	18.3	10.6	5.84	2.67	12.0	2.28	39.0	9.33	3.49	1.58	7.08	1.55	44.4	5.50	11.3	6.33	33.8	6.11	54.1	27.5

Table 5.12: Measured, critical and sufficient concentration values for the nutrients in wheat and maize at the study sites

Field		Crop	Nutrients										
			P	K	Ca	Mg	S	Na	B	Cu	Fe	Mn	Zn
			%								mg/kg		
Douglas	40ha	wheat	0.57	3.58	0.51	0.46	0.43	0.50	20.0	6.00	128.2	143.7	48.5
Hofmeyr	55haNW	wheat	0.64	4.55	0.65	0.33	0.51	0.13	12.6	8.53	324.8	82.6	83.0
	55haSE	wheat	0.66	4.51	0.58	0.30	0.44	0.12	11.6	10.5	317.3	69.1	67.2
	20ha	wheat	0.58	4.40	0.70	0.47	0.48	0.17	10.8	7.58	214.7	218.9	42.2
Luckhoff	40ha	wheat	0.64	3.82	0.53	0.35	0.37	0.12	7.45	4.67	234.0	119.7	41.0
	60NE	wheat	0.66	2.90	0.47	0.33	0.29	0.12	7.60	4.36	208.3	101.6	40.3
	60NW	wheat	0.64	4.06	0.51	0.20	0.30	0.12	7.05	3.89	203.2	92.6	33.6
*critical value		wheat	0.15	2.00	0.15	0.10	0.10	-	1.00	3.00	25.0	15.0	15.0
*sufficient range		wheat	0.2-0.50	2.0-4.0	0.2-1.0	0.14-1.0	0.15-0.65	-	1.5-4.0	4.5-15	30-200	20-150	18-70
Douglas	40ha	maize	0.52	5.53	0.87	0.70	0.37	0.19	36.1	20.6	217.3	168.2	110.2
Luckhoff	20ha	maize	0.40	5.36	0.91	0.63	0.29	0.17	26.6	12.2	236.3	176.1	33.9
	40ha	maize	0.68	6.24	0.93	0.76	0.35	0.15	20.1	9.46	320.6	121.8	56.6
	60haNE	maize	0.52	5.00	0.82	0.50	0.26	0.14	22.8	9.83	253.3	100.5	32.6
**critical value		maize	0.25	2.00	0.40	0.25	0.12	-	10.0	5.00	15.0	15.0	15.0
*sufficient range		maize	0.25-0.40	1.6-2.5	0.2-0.8	0.12-0.5	0.12-0.40	-	3.0-20	4.0-20	30-250	15-150	16-50

*nutrient concentrations at maturity; **critical values at maize tasselling stage (Campbell, 2000)

The partitioning of Mg followed a similar pattern on 5 of the 7 sites with most of the accumulated Mg partitioned in the wheat grain component. On the Douglas 40 ha and Luckhoff 20 ha fields, most of the accumulated Mg was partitioned in the wheat's stem and leaves components. The partitioning of Na followed the order of stem and leaves > seeds > husks accumulation at 5 sites. The exception was the Douglas 40 ha and Luckhoff 20 ha fields where the Na partitioning followed the order of stem and leaves > husks > seed. The partitioning of Cu followed the same order on 5 study fields with most of the accumulated Cu at these sites partitioned in the wheat grain at harvest. The order of partitioning was seed > stem and leaves > husks. However, at the Luckhoff 60 ha NE and 60 ha NW fields, the order of Cu partitioning was stem and leaves > seed > husks. Likewise, at 5 of the 7 study fields, most of the accumulated Mn was partitioned in the grain component with the partitioning following the order of seed > stem and leaves > husks. Interestingly, Mn partitioning at Douglas 40 ha and Luckhoff 20 ha fields followed a different partitioning order with most of the Mn in the stem and leaves component. The Mg, Na and Mn partitioning observations at the 7 study sites at crop harvest shows that partitioning behaviour of these nutrients were affected by the agronomic properties at the Douglas 40 ha and Luckhoff 20 ha fields which resulted in the site x component interaction significant effect. The reasons for this could be the occurrence of nutrient imbalances at these study sites. The average total nutrient accumulation in the dry matter of wheat at harvest was approximately 206.8, 42.0, 318.4, 34.7, 23.8, 13.4, 29.2, 0.07, 0.05, 1.38, 0.64 and 0.36 kg ha^{-1} for N, P, K, Ca, Mg, Na, S, B, Cu, Fe, Mn and Zn at the study sites, respectively. Approximately similar findings for the macronutrients were found by Du Preez and Bennie (1991) who reported an average removal of 214.0, 39.9, 326.3, 32.7, 20.6 and 17.8 kg $ha^{-`1}$ for N, P, K, Ca, Mg and S, respectively, by winter wheat at 13 study sites situated in the central semi-arid region of South Africa. A large amount of the accumulated nutrients such as K, Ca, B and Fe would normally be returned to the soil by decomposition of the wheat residues if not removed after harvest. However, the farmers at the study sites

usually burn residues after crop harvest which may compromise the recycling of these nutrients in the soil.

The partitioning of the nutrients in maize shows that most of the measured nutrients were partitioned in the stem and leaves of the crop at harvest stage. Only P, Zn and S were partitioned significantly higher in the grain component at some of the sites. At harvest, an average of 71, 89, 62, 54, 67, 57, 65 and 74% of the total accumulated K, Ca, Mg, Na, B, Cu, Fe and Mn in maize were partitioned in the stem plus leaves components, respectively. The partitioning of K, Ca, B and Mn followed the order of stem and leaves > husks > cobs > seed with the grain component accounting for 6, 17, 7 and 5% of the total accumulation, respectively. The partitioning of Mg and S in maize followed a similar pattern at all the study sites with the order of stem and leaves > seeds > husk > cobs. An average of 17 and 28 % of the total Mg and S were accumulated in the grain component at the study sites, respectively. Accumulation of Na in maize followed the partitioning order of stem and leaves > cobs > seeds > husks with the grain component removing an average of 15% of the total Na accumulated at harvest stage. The partitioning pattern of Fe and Cu were similar at all the study sites with the order of stem and leaves > cobs > husks > seed. The grain component removed 6 and 12% of the accumulated Fe and Cu, respectively.

The grain component partitioned an average of 52% of the total P uptake by maize at all the study sites. An average 29, 10 and 9% of the remaining P was segregated into the stem and leaves, cobs and husks components, respectively. The partitioning of the Zn by maize showed different patterns from one field to the other. At the Luckhoff fields, 37% of the total accumulated Zn was partitioned in the grain component and 35% was partitioned in the stem and leaves. Partitioning at the Douglas 40 ha field showed that 43% of the total Zn uptake by maize was accumulated in the stem and leaves, while 24, 16 and 18% of the Zn was segregated into the husks, cobs and seed of maize at harvest, respectively. The partitioning patterns of Zn could be attributed to the Zn imbalances as well as the different maize cultivars

grown at the study sites. The average total nutrient accumulation in the dry matter of maize at harvest was approximately 228.3, 46.9, 352.3, 60.5, 46.8, 10.7, 24.5, 0.18, 0.09, 1.35, 0.92 and 0.45 kg ha^{-1} for N, P, K, Ca, Mg, Na, S, B, Cu, Fe, Mn and Zn at the experimental fields, respectively. Most of the accrued K, Ca, Mg, Na, B, Cu, Fe and Mn by the maize crop were integrated in the stem and leaves at harvest. A larger fraction of these nutrients can be remobilized back into the soil by leaving the maize residues in the field after harvest.

5.3.3 Correlation of MIR spectra with nutrient concentrations in wheat and maize

Table 5.16 and 5.17 show calibration and prediction statistics for nutrients using MIR spectra of both wheat and maize samples from the study sites, respectively. Classical least square regression (CLSR), principal component regression (PCR) and partial least square regression (PLSR) were performed to develop the calibration models. The CLS method is a regression technique that is based on the least square algorithm. This method can handle MIR spectral baselines that may vary from sample to sample. The PLSR method performs a principal component analysis decomposition in such a way that reference data is used for optimization of MIR data and then performs regression equations; while PCR uses only MIR spectral information in constructing principle components for regression purposes. Calibration statistics including the root mean square error of calibration (RMSEC), the coefficient of determination in calibration (R^2), root mean square error of prediction (RMSEP), coefficient of determination in prediction R^2_v, and residue prediction deviation (RPD) were employed for the statistical evaluation of the prediction models.

Using the CLSR method, excellent R^2 (>0.75) were obtained for N, P, K, Na, B, Fe, Mn and Zn of wheat samples (Table 5.16). Moderate to good R^2 (0.50-0.75) were estimated for Ca,

Mg, S and Cu. In contrast, low R^2 (<0.50) were found for C. Excellent R^2 (>0.75) were found for the concentrations of N, P, K, Mg, Na, B, Cu, Fe, Mn and Zn of wheat using the PCR technique. Moreover, moderately well fitted models with R^2 in the range of 0.65-0.75 were established for C, Ca and S concentrations. Using the PLSR technique, excellent models (R^2>0.75) were built for the concentrations of C, N, P, K, Na, B, Cu, Fe and Zn of wheat samples. Poor models (R^2<0.5) were found for Ca, Mg, S and Mn.

Table 5.13: ANOVA for the seasonal accumulation and partitioning of nutrients in different components of wheat and maize at the study sites for the 2016 winter and 2016/17 summer seasons

Source of variation	P	K	Ca	Mg	Na	S	B	Cu	Fe	Mn	Zn
Wheat											
Component	***	***	***	***	***	***	***	***	***	***	***
Site	***	***	***	***	***	***	***	***	***	***	***
Component x Site	***	0.005**	0.002**	***	***	***	***	0.007**	0.017*	**	***
Maize											
Component	***	***	***	***	***	***	***	***	***	***	***
Site	***	***	***	***	***	***	***	***	0.058ns	***	***
Component x Site	***	***	***	***	***	***	***	***	0.068ns	***	***

*, **,***- source of variation significant on the nutrient partioning at 0.05, 0.01 and 0.001 probability level respectively

Table 5.14: Biomass, grain yield, harvest index and total nutrient uptake of wheat at the study sites at the end of the 2016 winter season

Field		Biomass	Yield	HI	Total nutrient uptake (kg/ha)										
		t/ha			P	K	Ca	Mg	Na	S	B	Cu	Fe	Mn	Zn
Douglas	40ha	21.2ab	8.02ab	0.38b	40.4b	293.3b	34.4bc	32.0a	37.1a	32.4ab	0.11a	0.044bc	0.806c	0.870b	0.354c
Hofmeyr	55ha NW	16.7c	6.92bc	0.42a	37.6bc	280.7b	32.3bc	18.4c	6.80c	28.9b	0.058c	0.048b	1.54b	0.431d	0.455b
	55ha SE	23.6a	8.83a	0.38b	52.9a	399.2a	43.9a	24.3b	9.00bc	36.7a	0.080b	0.087a	2.20a	0.524cd	0.518a
Luckhoff	20ha	17.9bc	6.08c	0.33c	32.3c	321.5b	38.4ab	26.0b	10.4b	30.8bc	0.051cd	0.046bc	1.19bc	1.05a	0.246d
	40ha	19.4bc	7.32bc	0.36bc	41.2b	297.5b	30.7c	21.9b	7.63bc	25.9cd	0.036e	0.032c	1.28bc	0.643c	0.276d
	60ha NE	20.2abc	6.89bc	0.34c	42.4b	300.2b	28.7c	20.9c	7.59bc	20.6d	0.041de	0.029c	1.10c	0.558cd	0.260d
	60ha NW	20.6a	6.72bc	0.32c	42.3b	338.7ab	32.2bc	22.3bc	8.72bc	21.9d	0.040de	0.028c	1.20bc	0.498cd	0.223d
P-value		0.001**	0.002**	***	***	0.003**	***	***	***	***	***	***	***	***	***

,*- mean differences significant at 0.01 and 0.001 probability level respectively

Table 5.15: Biomass, grain yield, harvest index and total nutrient uptake of maize at the study sites at the end of the 2016/17 summer season

Field		Biomass	Yield	HI	Total nutrient uptake (kg/ha)										
		t/ha			P	K	Ca	Mg	Na	S	B	Cu	Fe	Mn	Zn
Douglas	40ha	28.6a	15.6a	0.547a	58.8a	425.4a	71.9a	61.6a	15.3a	34.5a	0.280a	0.153a	1.60ab	1.30a	0.802a
	20ha	24.8b	13.6b	0.549a	40.2c	348.8b	65.5ab	46.9b	11.6b	23.0b	0.168b	0.076b	1.39ab	1.09b	0.267b
Luckhoff	40ha	14.8c	7.23c	0.487b	36.2c	235.8c	44.6c	35.2d	6.06c	16.8c	0.086c	0.042c	1.39b	0.535d	0.278b
	60ha NE	25.4b	13.8b	0.544a	51.1b	342.8b	64.6b	40.5c	9.93b	21.6b	0.158b	0.065b	1.68a	0.734c	0.276b
P-value		***	***	***	***	***	***	***	***	***	***	***	0.087ns	***	***

ns,***- mean differences not significant at 0.05 and significant at 0.001 probability level respectively

For maize, R^2 values for the regression models were also deduced after model development using the three regression techniques. The CLSR produced excellent models (R^2>0.75) for the concentrations of N, P, K, Ca, Mg, Na, B, Cu, Fe and Mn of maize samples. However, models fitted for S and Zn concentrations were moderate. Only C was poorly modelled (R^2<0.50) with the CLSR technique. The PCR technique was as robust with models for the concentrations of C, N, P, K, Ca, Mg, Na, S, B, Cu and Fe of maize having R^2 >0.75. A moderately fitted model was deduced for the prediction of Mn with R^2 of 0.70. Only Zn concentrations were poorly modelled with R^2 of 0.47. The PLSR technique produced excellent models (R^2>0.75) for C, N, P, K, Ca, Mg, Na, and B of maize. Moderately fitted models were produced for the prediction of the concentrations of S, Cu, Fe and Mn in maize plants using the same method. Only Zn was poorly modelled with R^2 of 0.37.

However, R^2 as a determination of the amount of variation in the data that is adequately modelled by the calibration equation, is not a convincing indicator evaluating MIR models of nutrients in plants. This is because MIR is not used to directly measure the nutrient concentrations. Instead, residue of percentage deviation (RPD) which is the ratio of standard error of performance to standard deviation was employed further to assess the MIR models. RPD is the standard deviation (SD) of data divided by the root mean square error of prediction (RMSEP), thus representing the average error on predicted or cross-validated values respectively. Therefore, the RPD value relates calibration performance to the range of measurements and is often used as a quality indicator of the calibration models (Ward *et al.*, 2011; Williams, 2014). An approach suggested by Chang *et al*., (2001)was used to interpret the RPD values. Three categories were distinguished: category A with a RPD >2.0 for excellent models, category B with RPD between 1.4 and 2.0 for models with acceptable accuracy that could be improved, and category C with RPD <1.4 for models that may not be reliable for prediction.

Comparisons of the RPD values across the regression techniques show that higher RPD values were observed when using PCR and PLSR methods. Values of RPD for the concentrations of N, P, K, B, Cu, Fe, Mn and Zn of wheat were all above 2.0 when using both the PCR and PLSR methods which indicated excellent models (Table 5.16). The RPD for C was between 1.4 and 2.0, suggesting that the PCR and PLSR models for C have acceptable accuracy that could be improved through different strategies (Huang *et al*., 2009). For Ca, Mg, Na and S in the wheat components, RPD values were less than 1.4 which showed poor reliability of the MIR models when using the PCR technique (Table 5.16). However, the RPD for the PSLR model for Mg was 1.77 which indicated acceptable accuracy that can be improved. As shown in Table 5.17, RPD values for C, P, K and Fe concentrations of maize components were above 2.0 suggesting excellent PCR and PLSR models of these nutrients for predictive purposes. The RPD for the concentrations of N, Ca, S, B and Cu of maize were between 1.4 and 2.0 which shows that PCR models for these nutrients have acceptable accuracy that could still be improved. Furthermore, PLSR models of Na, Mn, Cu and Zn also had RPD values between 1.4 and 2.0 indicating acceptable model accuracy. For Mg in the maize crop, RPD was less than 1.4 with all three techniques which suggest that the MIR model for Mg is unreliable. These results demonstrated the applicability of MIR as a predictive tool for rapid analysis of nutrients in wheat and maize samples. Particularly with the wheat samples, about 8 of the 13 investigated nutrients were excellently predicted by MIR equations with more room for improvement for the models of the other five nutrients which had acceptable accuracy. However, models developed from spectra of maize samples were not as accurate as their counterpart equations derived from wheat samples. Only 4 of the 13 nutrients showed excellent prediction capabilities while the other 6 showed acceptable accuracy. The reason for this observation could be due to the dilution effect from high maize biomass as compared to the wheat at harvest. Most plant nutrient concentrations decrease with increasing plant biomass and development (Davis, 2009). This inverse relationship between biomass accumulation and nutrient concentration is termed the dilution effect (Jarrell and Beverly, 1981). Haung *et al.* (2009) reported difficulties in measurements of absorption

changes of nutrient concentrations when low concentration of nutrients encountered large spectral variation. In their study, R^2 for prediction increased with mean nutrient concentration suggesting that stronger response may be interpreted from the spectra with higher concentration of nutrients, thus providing better correlations. Nonetheless, MIR was still an acceptable approach for satisfactory analysis of nutrients in maize with little to no sample preparation.

5.3.4 Correlation of EC_a with crop yield parameters and total nutrient uptake at study sites

The Pearson correlation coefficient (*r*) was used to study the relationships of EC_a with biomass, grain yield, harvest index as well as the total nutrient removed by wheat and maize during the winter 2016 and summer 2016/17 seasons, respectively. The correlation coefficient was interpreted using the guide provided by Evans (1996). Wheat biomass yield, grain yield and harvest index at Hofmeyr 55 ha NW, Luckhoff 20 ha, 40 ha and 60 ha NW fields showed no significant correlation ($p < 0.05$) with EC_a. These variables were weak to moderately correlated with EC_a as shown in Table 5.18. Wheat biomass and grain yield were strongly correlated ($r > 0.6$) with EC_a at both Luckhoff 60 ha fields (Table 5.18). However, only the biomass and grain yield at the Luckhoff 60 ha NE field was significantly correlated with EC_a. At the Hofmeyr 55 ha (NW) field, the measured nutrients accrued in wheat showed no significant correlations with EC_a. The accumulated K, Ca, Mg, Na, S, B, Cu and Mn in wheat were moderately correlated to EC_a while P and Zn weakly correlated.

.

Table 5.16 Regression statistics between MIR and nutrient concentration in wheat sampled from the study sites

Regression method	Statistic	C	N	P	K	Ca	Mg	Na	S	B	Cu	Fe	Mn	Zn
CLSR	R^2	0.01	0.98	0.96	0.93	0.65	0.75	0.86	0.74	0.93	0.72	0.78	0.78	0.89
	RMSEC	5.40	0.16	0.04	0.34	0.31	0.29	0.04	0.04	1.18	0.87	45.0	19.3	6.42
	R_v^2	0.50	0.95	0.94	0.96	0.92	0.58	0.080	0.45	0.76	0.89	0.91	0.34	0.67
	RMSEP	2.33	0.230	0.048	0.481	0.134	0.325	0.118	0.065	1.54	0.505	32.0	19.1	8.31
	RPD	0.49	3.15	3.08	1.92	0.83	0.12	0.61	0.71	2.08	4.72	1.70	1.75	1.49
PCR	R^2	0.73	0.98	0.95	0.95	0.65	0.82	0.83	0.69	0.92	0.76	0.87	0.79	0.89
	RMSEC	0.77	0.153	0.046	0.271	0.202	0.019	0.040	0.028	1.17	0.580	28.4	14.9	5.33
	R_v^2	0.85	0.98	0.99	0.97	0.80	0.60	0.15	0.60	0.69	0.92	0.83	0.37	0.92
	RMSEP	0.62	0.177	0.034	0.293	0.090	0.265	0.102	0.041	1.26	0.364	24.6	14.4	5.85
	RPD	1.84	6.44	4.35	3.15	1.23	0.15	0.71	1.12	2.55	6.62	2.22	2.32	2.12
PLSR	R^2	0.81	0.99	0.91	0.99	0.46	0.47	0.94	0.45	0.99	0.76	0.97	0.16	0.84
	RMSEC	0.676	0.081	0.060	0.100	0.244	0.029	0.024	0.035	0.453	0.588	13.0	24.5	6.52
	R_v^2	0.81	0.96	0.99	0.99	0.87	0.35	0.04	0.53	0.68	0.84	0.90	0.58	0.96
	RMSEP	0.706	0.167	0.025	0.383	0.669	0.022	0.116	0.041	1.21	0.345	18.9	10.6	3.31
	RPD	1.61	4.34	5.92	2.41	0.17	1.77	0.62	1.12	2.65	6.99	2.88	3.15	3.74

R^2- coefficient of determination in calibration; R_v^2- coefficient of determination in prediction; RMSEC – root mean square error of calibration; RMSEC – root mean square error of calibration; RPD-ratio of standard error of performance to standard deviation; CLSR – classical least square regression; PCR – principal components regression; PLSR – principal least square regression

Table 5.17 Regression statistics between MIR and nutrient concentration in maize sampled from the study sites

Regression method	Statistic	C	N	P	K	Ca	Mg	Na	S	B	Cu	Fe	Mn	Zn
CLSR	R^2	0.20	0.87	0.85	0.92	0.92	0.88	0.78	0.68	0.88	0.80	0.76	0.77	0.69
	RMSEC	11.5	0.237	0.058	0.327	0.103	0.050	0.014	0.044	3.82	1.97	36.4	56.4	18.1
	R_v^2	0.56	0.71	0.96	0.91	0.93	0.71	0.54	0.53	0.91	0.69	0.82	0.85	0.12
	RMSEP	5.10	0.348	0.026	0.304	0.182	0.104	0.017	0.040	4.59	2.30	32.9	63.8	14.5
	RPD	0.41	1.53	3.69	2.78	1.30	0.90	1.06	1.03	1.22	1.52	2.28	0.62	0.71
PCR	R^2	0.95	0.88	0.91	0.92	0.90	0.86	0.89	0.78	0.86	0.76	0.81	0.70	0.47
	RMSEC	0.695	0.208	0.040	0.288	0.109	0.048	85.8	0.027	3.54	1.74	25.3	48.9	15.5
	R_v^2	0.84	0.81	0.98	0.90	0.94	0.82	0.72	0.76	0.92	0.78	0.92	0.90	0.10
	RMSEP	0.948	0.273	0.025	0.360	0.149	0.080	0.014	0.028	3.38	1.81	20.2	33.4	9.99
	RPD	2.18	1.53	3.84	2.35	1.58	1.18	1.26	1.46	1.66	1.93	3.72	1.19	1.03
PLSR	R^2	0.95	0.82	0.89	0.93	0.84	0.82	0.82	0.72	0.77	0.68	0.73	0.72	0.37
	RMSEC	0.660	0.246	0.044	0.273	0.135	0.053	0.011	0.029	4.43	1.96	29.3	48.0	16.3
	R_v^2	0.82	0.77	0.99	0.90	0.92	0.84	0.81	0.74	0.94	0.77	0.91	0.93	0.19
	RMSEP	1.01	0.303	0.027	0.357	0.200	0.076	0.010	0.031	3.37	2.00	26.9	22.7	7.00
	RPD	2.05	1.38	3.56	2.37	1.18	1.24	1.80	1.32	1.67	1.75	2.79	1.75	1.47

R_l^2- coefficient of determination in calibration; R_v^2- coefficient of determination in prediction; RMSEC – root mean square error of calibration; RMSEC – root mean square error of calibration ; RPD-ratio of standard error of performance to standard deviation; CLSR – classical least square regression; PCR – principal components regression; PLSR – principal least square regression

Total nutrient accumulation by wheat at the Luckhoff 20 ha, 40 ha and 60 ha (NW) fields did not significantly correlate with EC_a. Nutrients like P, K, Ca and Fe were weakly correlated with EC_a whereas Mg, S, B, Cu and Mn showed moderate correlations with EC_a at the Luckhoff 20 ha field. Only total Na and Zn uptake by wheat correlated strongly with EC_a at the Luckhoff 20 ha field. All the nutrients at harvesting of wheat at the Luckhoff 40 ha field were weakly correlated with EC_a (Table 5.18). Total P, K, Mg, Na, S, Cu, Mn and Zn uptake strongly correlated with EC_a ($r > 0.7$) at Luckhoff 60 ha (NE) field. However, only P, Na, S and Mn were significantly correlated with EC_a and Ca, B and Fe were weakly correlated.

Maize biomass yield, grain yield and harvest index at Douglas 40 ha and Luckhoff 40 ha fields showed weak and non-significant correlations with EC_a. Biomass and harvest index were moderately correlated with EC_a at the Luckhoff 20 ha field while the grain yield at this field was weakly correlated. Biomass and grain yields at the Luckhoff 60 ha (NE) field were significantly correlated with EC_a with very strong correlation coefficient values ($r > 0.90$). The harvest index at this field was not significantly correlated with EC_a and the coefficient value was weak. Total uptake of P, Mg, S, B, Cu, Fe, Mn and Zn by maize at the Douglas 40 ha field showed weak correlations with EC_a whereas K, Ca and Na were moderately correlated. All the correlation coefficients for total nutrient removal at this field were not significant. At the Luckhoff 20 ha field, total P, Mg, Cu and Mn accumulation by the maize crop were weakly correlated with EC_a. Furthermore, total uptake of Ca, Na and Fe were moderately correlated whereas K, S, B and Zn were strongly correlated with EC_a. The P, Mg, Na, S, B, Cu, Mn and Zn removed by the popcorn at the Luckhoff 40 ha field showed weak correlations with EC_a whereas K, Ca and Fe were moderately correlated. None of the correlations between EC_a and total nutrients removed at the Luckhoff 40 ha field were significant. Remarkably, most of the measured nutrients removed by the maize crop at the Luckhoff 60 ha NE field showed strong correlations with only Mg showing a moderate correlation with EC_a (Table 5.18). Total P, K, Na, S, B, Fe and Mn accrued by maize at this field showed significant correlations with EC_a.

A number of researchers have found moderate to strong correlations between EC_a and crop yield (Kitchen *et al*., 2003). However, a more recent study by Singh *et al.* (2016) found weak to moderate correlations between EC_a and yield of maize and soybean. Kitchen *et al.* (2003) reported high correlations between EC_a and yields though the values of the correlation coefficients varied from year to year. These variations were attributed to the differences in crop type and climate which may have varied from year to year (Kravchenko and Bullock, 2000; Kitchen *et al*., 2003). In this study, the correlation coefficients of EC_a with grain yields and total nutrient removed by the wheat and maize crops varied from field to field. Significantly strong and negative correlation coefficients were observed at the Luckhoff 60 ha NE field for both the grain yield and total nutrients accumulated during both the winter 2016 and summer 2016/17 seasons (Table 5.18). Generally, while the correlation coefficients of EC_a with grain yields at the Luckhoff 60 ha NE field was negative they were mostly positive for the Douglas 40 ha, Hofmeyr 55 ha NW, Luckhoff 20 ha, 40 ha and 60 ha NW fields (Table 5.18). Increasing EC_a is often associated with the increasing clay content (McNeil, 1992). This may be the case with the positive correlation coefficients at the Douglas 40 ha and Hofmeyr 55 ha NW fields where the soils have generally high clay content. The soils at the Luckhoff 20 ha, 40 ha and 60 ha NW fields were generally well-drained hence the observed trend may be due to slightly improved soil properties with higher EC_a than Luckhoff 60 ha NE field (Kitchen *et al*., 2003). The observed trends at the Luckhoff 60 ha NE field maybe due to poor soil internal drainage, slope and elevation of the landscape that may have had strong and significant association with yield variability.

Table 5.18: Pearson correlation coefficient between EMI EC_a and yield parameters and total nutrient uptake at the study sites

Field		Crop	Biomass	Yield	HI	P	K	Ca	Mg	Na	S	B	Cu	Fe	Mn	Zn
Douglas	40ha	Maize	-0.13	0.03	0.16	0.25	-0.49	-0.50	0.16	-0.42	-0.29	0.32	-0.17	-0.34	-0.23	0.36
Hofmeyr	55ha NW	Wheat	0.44	0.33	-0.25	0.38	0.52	0.50	0.46	0.54	0.49	0.50	0.56	0.28	0.45	0.32
Luckhoff	20ha	wheat	-0.36	0.02	0.23	-0.01	-0.38	0.38	0.40	0.78	0.58	0.54	-0.44	-0.21	0.54	0.66
		maize	0.54	0.38	-0.53	0.16	0.73	0.50	0.35	0.53	0.65	0.67	-0.10	0.47	0.06	0.68
Luckhoff	40ha	wheat	0.15	0.07	-0.07	-0.14	0.22	0.09	0.37	0.16	0.15	0.09	-0.17	-0.09	0.07	-0.24
		maize	-0.13	0.08	0.34	0.22	-0.36	-0.39	-0.30	-0.25	0.16	-0.20	0.13	-0.45	0.13	0.24
Luckhoff	60ha NE	wheat	-0.88*	-0.88*	-0.77	-0.85*	-0.69	-0.38	-0.70	-0.88*	-0.93*	-0.22	-0.62	0.21	-0.87*	-0.70
		maize	-0.96**	-0.91*	-0.18	-0.91*	-0.93**	-0.70	-0.46	-0.92**	-0.94**	-0.89*	-0.72	-0.97**	-0.85*	-0.67
Luckhoff	60ha NW	wheat	-0.72	0.75	-0.13	-0.53	-0.48	-0.50	-0.36	-0.40	-0.35	-0.42	-0.76	-0.66	-0.25	-0.30

*, **- correlation significant at 0.05 and 0.01 probability level respectively

5.4 Conclusions

Biomass and grain yield together with nutrient accumulation for wheat and maize as well as the distribution among the crop components at the study sites provided important information that could be useful for crop producers in improving nutrient management. Generally, the concentrations of the nutrients in wheat and maize at harvest exceeded the critical and optimum ranges which are mostly reliable to use at the crop's physiological maturity. The partitioning of the nutrients in the wheat and maize components were highly variable from one field to the other. Generally, higher amounts of the majority of the nutrients accumulated by wheat were partitioned in the stem and leaves components. In contrast, P and Zn were partitioned highly in the grain component at all the fields. For the maize, most of the nutrients were partitioned in the stem and leaves components, with only P, Zn and S partitioned mostly in the grain component at all the study sites.

The MIR calibration and validation statistics results obtained from this study demonstrated the potential of MIR as a predictive tool for rapid analysis of nutrient concentrations in wheat and maize samples. Particularly with the wheat samples, majority of the measured nutrients were excellently predicted by MIR models. Other nutrients were modelled by MIR techniques with acceptable accuracy. However, models developed from spectra of maize samples were not as accurate as models derived from spectra of wheat samples. Nonetheless, MIR was still an acceptable approach for acceptable and quick analysis of nutrients in maize with little to no sample preparation. Hence, further work still needs to be done in this regard to improve the accuracy of the MIR technique.

The correlation of crop grain yields and total nutrient uptake with EC_a showed some strong relationships that could be further interpreted with more rigorous spatial analysis. While strong and significant relationships of EC_a with grain yield and total nutrient removal by wheat and

maize were shown in some instances, climate, crop type and specific site characterization information is generally required to interpret the relationship for any given site and season.

CHAPTER 6: SPATIAL CHARACTERIZATION OF SOIL FERTILITY PROPERTIES AND CROP YIELDS UNDER IRRRIGATION USING APPARENT SOIL ELECTRICAL CONDUCTIVITY IN WHEAT-MAIZE CROPPING SYSTEMS

6.1 Introduction

Accurate characterization of field variability of important soil properties such as texture, organic matter and plant nutrients are needed to develop site-specific management strategies and assess yield variability (Farahani *et al.,* 2004). Spatial variability of soil properties are important in agriculture for evaluating soil quality, planning land use and determining the suitability of cropping patterns (Lesch *et al.,* 2005). Generally traditional soil sampling methods such as grid sampling have been used to characterize soil spatial variability. However, these methods are labour-intensive, time consuming and expensive. Recent developments in sensor technology have provided the opportunity to characterize and map soil spatial variability for the purpose of site-specific management. Apparent electrical conductivity (EC_a) measurements have been widely used in agriculture for describing various soil properties. The principal assumption in the use of EC_a survey data is that quantitative relationships between a soil parameter and soil EC_a would allow mapping of the spatial variability of that soil parameter using the spatial EC_a data (Corwin and Lesch, 2005b; Farahani *et al*., 2004). This minimizes the need for intensive soil sampling and the accompanying labour and cost. Moreover, EC_a measurements are reliable, easy to take and easy to organize, making this measurement a valuable tool in site-specific management.

The intensive spatial data acquired from spatial EC_a measurements is applicable for supplying comprehensive information on various agricultural management practices as well as detailed baseline data for precision agriculture strategies and applications (Rhoades *et al*., 1997; Triantafilis *et al*., 1998; Corwin and Lesch, 2003; Lesch *et al*., 2005). Methods for predicting

and mapping soil salinity from EC_a measurements have been thoroughly discussed by numerous authors (Rhoades *et al*., 1989, 1999; Rhoades 1992, 1996; Lesch *et al.,* 2005). EC_a survey data have also been successfully used to map other soil properties such as clay content, depth to clay layers, and water content (Kitchen *et al.,* 2000; Doolittle *et al.,* 2002; Schmidhalter *et al*., 2001). Other studies have also related EC_a survey data to some properties related to soil fertility such as C, N, exchangeable Ca, Mg, Na, K and CEC (Kitchen *et al*., 2000; Farahani *et al*., 2004; Bronson *et al*., 2005). Moreover, yield potential have been directly linked to EC_a measurements in many applications (Johnson *et al.*, 2001; Lesch *et al*., 2005). The effectiveness of EC_a mapping for predicting crop yields appears to depend upon the degree to which soil properties affecting yield are correlated with the factors affecting EC_a (Johnson *et al.,* 2001). However, few of these studies related EC_a survey data to the spatial characterization of the full spectrum of the soil properties related to soil fertility and crop yield.

As much as EC_a sensors have provided the opportunity to rapidly map spatial variability of soil properties, identifying the drivers of the variability has remained difficult especially in non-saline fields where the dominant causes of the variability are not easily identifiable (Farahani *et al*., 2004). In fields with high salt concentrations, EC_a survey information can be used effectively to demonstrate that salinity is the dominant factor influencing field-scale EC_a variability. However, in non-saline fields it is likely that other soil properties such as water, clay and organic matter content are influencing the EC_a in a significant manner. In this case, the interpretation of the EC_a measurement can only be established from ground-truth soil samples from which a relationship between EC_a and all potential soil properties can be established (Corwin and Scudiero, 2016). Farahani *et al*. (2004) argued that the main obstacle in the use of EC_a mapping techniques is the lack of more in-depth studies of the spatial and temporal variability of EC_a and an appreciation of its complex interactions with stable and dynamic soil properties in fields with low salt concentrations. There is little information regarding the use of EC_a sensors to characterize spatial variability of overall soil characteristics of agricultural fields

where soil condition incorporates both soil properties that affect EC_a and other soil characteristics influencing yield potential with which they may be correlated (Johnson *et al*., 2001). The objectives of this study were to (i) identify the main causes of the observed EC_a variability of the non-saline soils under irrigation at three study sites (ii) and evaluate the use of EC_a survey information for the characterization and mapping of within-field variability of soil fertility parameters related to grain yields. This is important for monitoring the impact of management decisions on temporal trends in soil properties and for effective application of site-specific management strategies.

6.2 Procedure

The study sites' characteristics, soil EC_a measurements, soil sampling and analysis, data processing and statistical analysis are described in detail in Chapter 3, and therefore not repeated in this chapter.

6.3 Results and discussions

The prediction of site-specific soil properties from EC_a survey data can be achieved using statistical calibration and prediction techniques. In the regression-based calibration approach suggested by Lesch *et al.* (1995a), a suitable spatially referenced regression model (MLR) will relate soil property of interest with both trend surface parameters and EC_a (z_1, z_2) readings as shown in Equation 6.1, where x and y are easting and northing UTM coordinates (m) and β_0, β_1, β_2, β_3, β_4 empirical regression model coefficients and ε representing the random error component associated with the model (Corwin and Scudiero, 2016).

$$\text{Soil property of interest} = \beta_0 + \beta_1 z_1 + \beta_2 z_2 + \beta_3 x + \beta_4 y + \varepsilon \qquad \text{Equation 6.1}$$

At all the fields the EC_a deep readings (z_1) were used to model the targeted soil fertility parameters variability with the EC_a shallow readings (z_2) removed from the Equation 6.1. EC_a deep readings (z_1) proved to be the most reliable in modelling the soil properties of interest at the study sites (Barnard *et al*., 2020).

6.3.1 The prediction and mapping of soil properties from EC_a survey data

The model parameters for the soil properties that correlated with EC_a at the study sites during the study period are reported in Tables 6.1 to 6.5. The results also show the statistical analysis of the spatial MLR models and their respective final parameter combinations. Table 6.1 shows the regression model summary statistics for the soil properties that were significantly modelled by the EC_a survey data in both June 2016 and 2017 at the Douglas 40 ha centre pivot. The regression statistics show that the EC_a survey data explains about 90% of the observed variation of Ca and Θ_v in June 2016. Additionally, at least one trend surface parameter significantly influenced the prediction power of Ca and Θ_v models. In June 2017, the EC_a survey data explains about 98 and 71% of the observed variation of Na and Cu, respectively. The prediction model of Na shows that both trend surface parameters were statistically significant. However, only the y trend parameter was significant in the Cu model. Figure 6.1 shows the spatial interpolated maps of EC_a with highlighted sampling points as well as the soil properties that were significantly modelled by the EC_a survey data in both June 2016 and 2017. Comparing the EC_a spatial patterns from June 2016 to June 2017 shows that EC_a values increased during this period with generally no changes in the spatial patterns across the 40 ha field. The spatial patterns of Ca in June 2016 shows that the north-western part of the field had relatively higher Ca which coincides with higher EC_a. However, the y-coordinates seems to have a significantly higher influence on the spatial variation of Ca at the time of the EC_a survey. The spatial variation of Na and Cu shows that the southern part of the Douglas 40 ha centre pivot had relatively lower amounts of these elements as compared to the northern part of the field.

Table 6.2 shows the regression summary statistics of the soil parameters that significantly influenced the EC_a readings at the 55 ha NW centre pivot at Hofmeyr in June and December 2016. The regression statistics shown that the June 2016 EC_a survey data explains about 85, 58 and 62% of the observed variation in ln (EC_e), N and clay respectively. The R^2 value of the EC_e model in December 2016 is 0.94, suggesting that about 94% of the observed spatial variation of the EC_e at the 0.3 m depth can be explained by the log transformed EC_a signal data from the survey. The x and y co-ordinates did not significantly influence the modelling of N and clay in June 2016. However, both trend surface parameters were found to be statistically significant in the improvement of the EC_e prediction models in both June and December 2016. Figure 6.2 and 6.3 present the interpolated spatial maps for the soil properties that were successfully interpreted by the EC_a survey data obtained in both June and December 2016 at the 55 ha NW upper pivot at Hofmeyr. There seems to be a decrease in the EC_a mean values from June to December 2016. However, the spatial trend of the EC_a during the same period shows the increase of EC_a from the wider areas towards the centre of the field. The EC_a circular patterns observed at the Hofmeyr 55 ha NW centre pivot in December 2016 are not natural under normal field conditions. These patterns were a result of instrument drift which was not corrected during the EC_a survey (Barnard *et al*., 2020). Higher EC_a in the south eastern parts of the fields in June 2016 corresponds with relatively higher clay content, N and EC_e as shown by their corresponding spatial maps. The spatial patterns of EC_e from June to December was highly dynamic with an overall decrease of salts in northern portions of the field.

Table 6.3 presents the regression model statistics for the soil parameters at the Luckhoff's 20 ha field which significantly influenced the EC_a readings in December 2016 and June 2017. The R^2 values for the EC_e, K, Mg and Zn show that more than 95% of the observed field-scale variation of these soil parameters at the Luckhoff's 20 ha centre pivot can be explained from the EC_a survey data in December 2016. However, only 79 and 68% of the variation of Cu and

clay can be accounted for using the same survey data. In June 2017, 97, 88 and 99% of the observed spatial variability of pH_w, Zn and Mn can be elucidated from the EC_a survey data. In December 2016, the trend surface parameters were not significant on the prediction model of Mg and clay. However, the x-co-ordinate was significant in the prediction models of K and Zn and the y co-ordinate was only significant on the EC_e model.

Furthermore, in June 2017, only the x-coordinate was significant on all prediction models of all the soil parameters that significantly correlated with EC_a. Figures 6.4-6.5 displays the spatial maps for the soil parameters that were successfully mapped at the Luckhoff's 20 ha centre pivot using the EC_a survey data in December 2016 and June 2017. The spatial patterns and magnitude of EC_a survey data remained relatively constant during the same period. The spatial patterns of the mapped soil properties in December 2016 show that areas with higher EC_a values corresponds with relatively higher levels of clay, EC_e, K, Mg and Zn. In June 2017, spatial patterns of pH_w, Zn and Mn show that areas with higher pH_w corresponded with areas that had lower Mn and higher Zn levels. Remarkably, Zn was successfully mapped in both December 2016 and June 2017 using the EC_a survey data and the spatial patterns of this nutrient were not altered by the farmer's management decisions during the summer of 2016/17 season. However, there was a general decrease of Zn during the same period probably due to removal through crop harvest.

Table 6.1: Regression model summary statistics for Douglas 40 ha centre pivot in June 2016 and 2017

Model statistic	June 2016		June 2017	
	Ca	Θ_v	Na	Cu
R^2	0.86	0.92	0.98	0.71
RMSE	181.7	1.53	18.2	0.46
Variable	Estimate	Standard Error	t-Score	Prob > |t|
June 2016				
Ca, mg/kg				
	Model parameters: Ca = $\beta_0 + \beta_1 z_1 + \beta_2 x + \beta_3 y + \beta_3 x^2$			
β_0	3249	211.8	16.3	0.0001***
β_1	160.9	45.2	3.56	0.009**
β_2	-1717	775.0	-2.22	0.062ns
β_3	813.5	212.4	3.83	0.006**
β_4	1007	731.1	1.38	0.211ns
Θ_v, %				
	Model parameters: $\Theta_v = \beta_0 + \beta_1 z_1 + \beta_2 x + \beta_3 y + \beta_4 xy + \beta_5 x^2 + \beta_6 y^2$			
β_0	32.2	3.76	8.58	0.0004***
β_1	-1.83	0.60	-3.04	0.029*
β_2	-32.1	8.36	-3.84	0.012*
β_3	-21.6	10.4	-2.08	0.092ns
B_4	10.9	13.2	0.83	0.444ns
B_5	19.7	7.46	2.65	0.046*
B_6	13.2	7.84	1.69	0.152ns
June 2017				
Na, $mgkg^{-1}$				
	Model parameters: Na = $\beta_0 + \beta_1 z_1 + \beta_2 z_1^2 + \beta_3 x + \beta_4 y + \beta_5 xy + \beta_6 x^2 + \beta_7 y^2$			
β_0	-284.1	72.8	-3.90	0.018*
β_1	-28.2	8.72	-3.24	0.032*
β_2	104.8	9.27	11.3	0.0003***
β_3	397.0	102.1	3.89	0.018*
β_4	1102	195.8	5.63	0.005**
β_5	289.7	162.5	1.78	0.149ns
β_6	-431.3	90.2	-4.78	0.009**
β_7	-740.0	142.7	-5.18	0.007**
Cu, $mgkg^{-1}$				
	Model parameters: Cu = $\beta_0 + \beta_1 z_1 + \beta_2 z_1^2 + \beta_3 y + \beta_4 y^2$			
β_0	-0.97	1.32	-0.73	0.488ns
β_1	-0.52	0.15	-3.56	0.009**
β_2	0.76	0.22	3.39	0.012*
β_3	13.1	3.99	3.27	0.014*
B_4	-9.58	3.09	-3.10	0.017*

Θ_v – volumetric water content; *, **, *** - model parameter in the spatial MLR significant at 0.05, 0.01 and 0.001 probability level

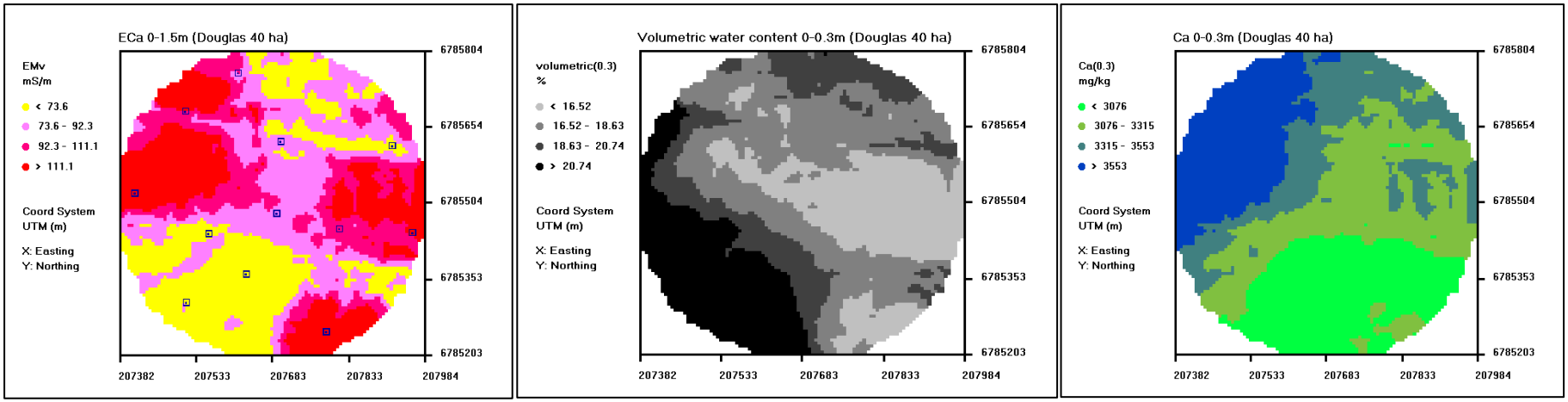

a) June 2016

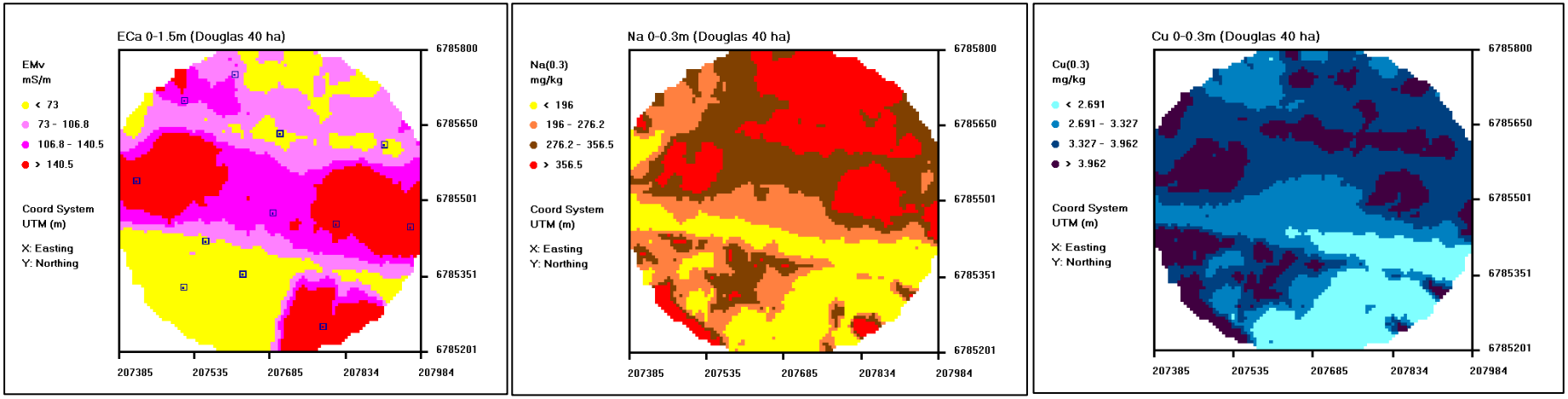

b) June 2017

Figure 6.1: Interpolated maps showing the spatial patterns of soil properties at Douglas 40 ha centre pivot in June 2016 and 2017

Table 6.2: Regression model summary statistics for Hofmeyr upper 55 ha (NW) centre pivot in June and December 2016

Model statistic	June 2016			December 2016
	EC_e	N	Clay	EC_e
R^2	0.85	0.58	0.62	0.94
RMSE	0.56	0.02	4.24	9.20
Variable	Estimate	Standard Error	t-Score	Prob > |t|
June 2016				
EC_e, mS/m				
	Model parameters: $Ln(EC_e) = \beta_0 + \beta_1 z_1 + \beta_2 x + \beta_3 y + \beta_4 x^2$			
β_0	3.24	0.65	4.99	0.002**
β_1	-0.46	0.16	-2.77	0.028*
β_2	9.69	2.28	4.25	0.004**
β_3	-3.83	0.88	-4.34	0.003**
β_4	-9.26	2.30	-4.03	0.005**
N, %				
	Model parameters: $N = \beta_0 + \beta_1 z_1$			
β_0	0.12	0.004	27.2	0.0001***
β_1	0.01	0.003	3.71	0.004**
Clay, %				
	Model parameters: $Clay = \beta_0 + \beta_1 z_1 + \beta_2 y + \beta_3 y^2$			
β_0	38.9	4.83	8.05	0.0001***
β_1	2.94	1.22	2.41	0.043*
β_2	-26.7	18.5	-1.45	0.186ns
β_3	28.0	16.7	1.68	0.132ns
December 2016				
EC_e, mSm^{-1}				
	Model: $LnEC_e = \beta_0 + \beta_1 z_1 + \beta_2 z_1^2 + \beta_3 x + \beta_4 y + \beta_5 xy + \beta_6 x^2 + \beta_7 y^2$			
β_0	-158.2	55.6	-2.84	0.047*
β_1	-60.8	14.9	-4.09	0.015*
β_2	35.9	8.34	4.30	0.013*
β_3	378.4	113.8	3.32	0.029*
β_4	669.3	171.3	3.91	0.017*
β_5	103.9	49.6	2.10	0.010*
β_6	-449.2	104.5	-4.30	0.011*
B_7	-854.7	187.6	-4.56	0.010**

*, **, *** - model parameter in the spatial MLR significant at 0.05, 0.01 and 0.001 probability level

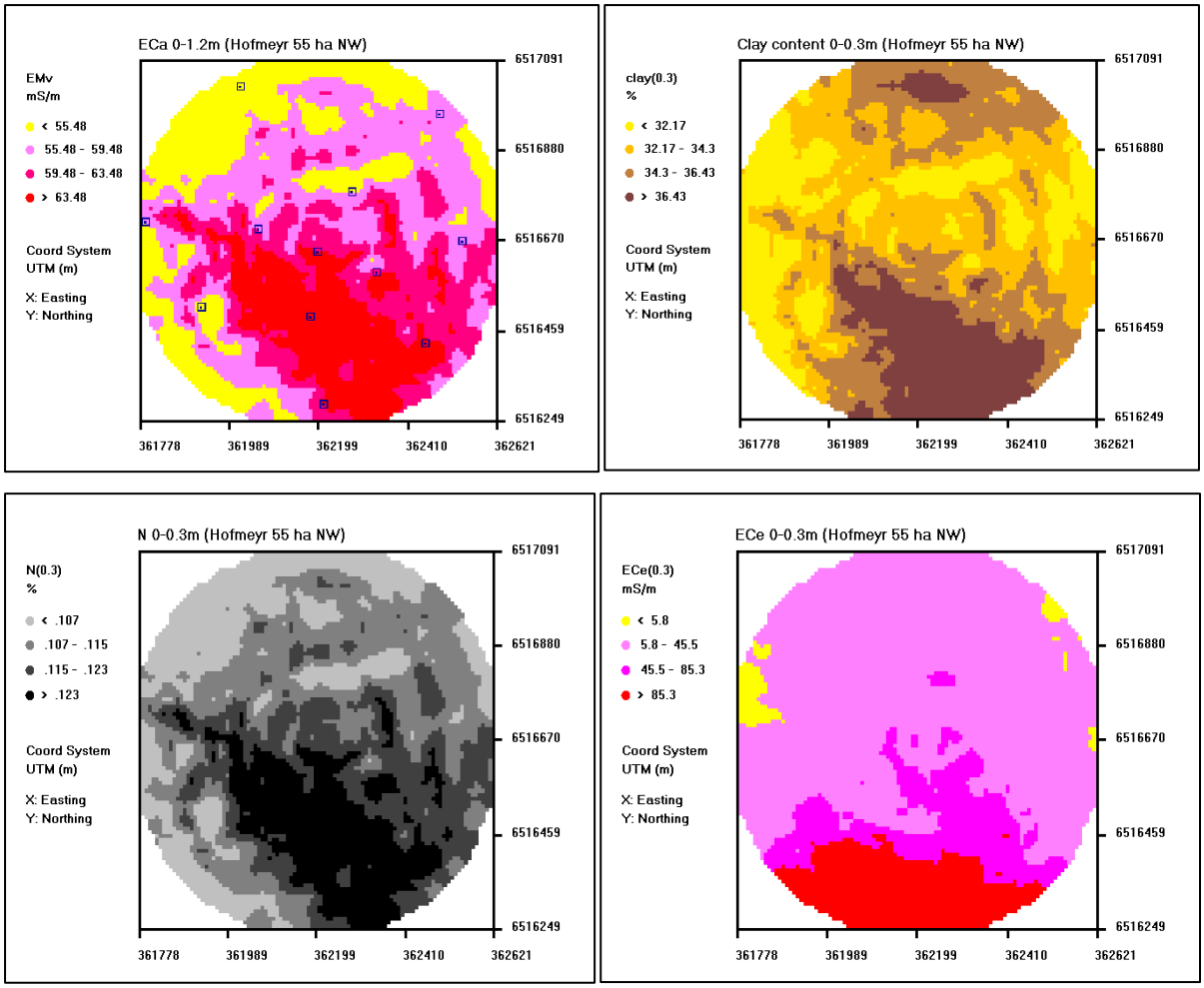

Figure 6.2: Interpolated maps showing the spatial patterns of soil properties at Hofmeyr 55 ha centre pivot NW in June 2016

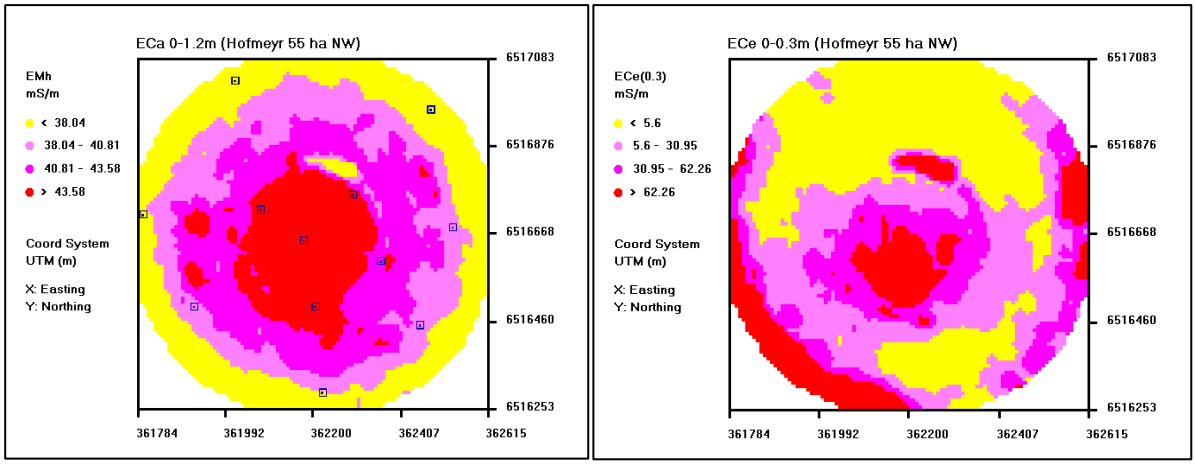

Figure 6.3: Interpolated maps showing the spatial patterns of soil properties at Hofmeyr 55 ha centre pivot NW in December 2016

Table 6.3: Regression model summary statistics for Luckhoff 20 ha centre pivot in December 2016 and June 2017

Model statistic	December 2016							June 2017	
	ECe	K	Mg	Zn	Cu	Clay	pH_w	Zn	Mn
R^2	0.99	0.99	0.89	0.95	0.79	0.68	0.97	0.88	0.99
RMSE	7.87	20.8	28.9	0.65	0.12	0.20	0.15	0.09	2.90

Variable	Estimate	Standard Error	t-Score	Prob > |t|
December 2016				
EC_e, mSm^{-1}				
	Model parameters: $EC_e = \beta_0 + \beta_1 z_1 + \beta_2 y$			
β_0	125.7	8.83	14.2	0.0008***
β_1	49.6	4.54	10.9	0.002**
β_2	-67.7	12.1	-5.58	0.012*
K, $mgkg^{-1}$				
	Model parameters: $K = \beta_0 + \beta_1 z_1 + \beta_2 x$			
β_0	486.4	18.4	26.5	0.0001***
β_1	190.6	13.3	14.4	0.0007***
β_2	-325.6	36.7	-8.86	0.003**
Mg, $mgkg^{-1}$				
	Model parameters: $Mg = \beta_0 + \beta_1 z_1 + \beta_2 z_1^2$			
β_0	343.3	24.3	14.1	0.0008***
β_1	100.5	21.0	4.79	0.017*
β_2	126.6	29.7	-4.26	0.024*
Zn, $mgkg^{-1}$				
	Model parameters: $Zn = \beta_0 + \beta_1 z_1 + \beta_2 x$			
β_0	8.56	0.52	16.6	0.0005***
β_1	2.24	0.37	6.00	0.009**
β_2	-7.99	1.03	-7.74	0.005**
Clay, %				
	Model parameters: $LnClay = \beta_0 + \beta_1 z_1$			
β_0	1.99	0.11	19.0	0.0001***
β_1	0.32	0.11	2.93	0.043*
June 2017				
pH_w				
	Model parameters: $pH_w = \beta_0 + \beta_1 z_1 + \beta_2 x$			
β_0	7.80	0.14	54.8	0.0001***
β_1	0.46	0.06	7.40	0.005**
β_2	-2.86	0.29	-9.95	0.002**
Zn, $mgkg^{-1}$				
	Model parameters: $LnZn = \beta_0 + \beta_1 z_1 + \beta_2 x$			
β_0	2.00	0.09	22.2	0.0002***
β_1	0.13	0.04	3.26	0.047*
β_2	-0.86	0.18	-4.75	0.018*
Mn, $mgkg^{-1}$				
	Model parameters: $Mn = \beta_0 + \beta_1 z_1 + \beta_2 x$			
β_0	7.77	2.84	2.74	0.072ns
β_1	-13.5	1.25	-10.8	0.002**
β_2	106.1	5.73	18.5	0.0003***

*, **, *** - model parameter in the spatial MLR significant at 0.05, 0.01 and 0.001 probability level

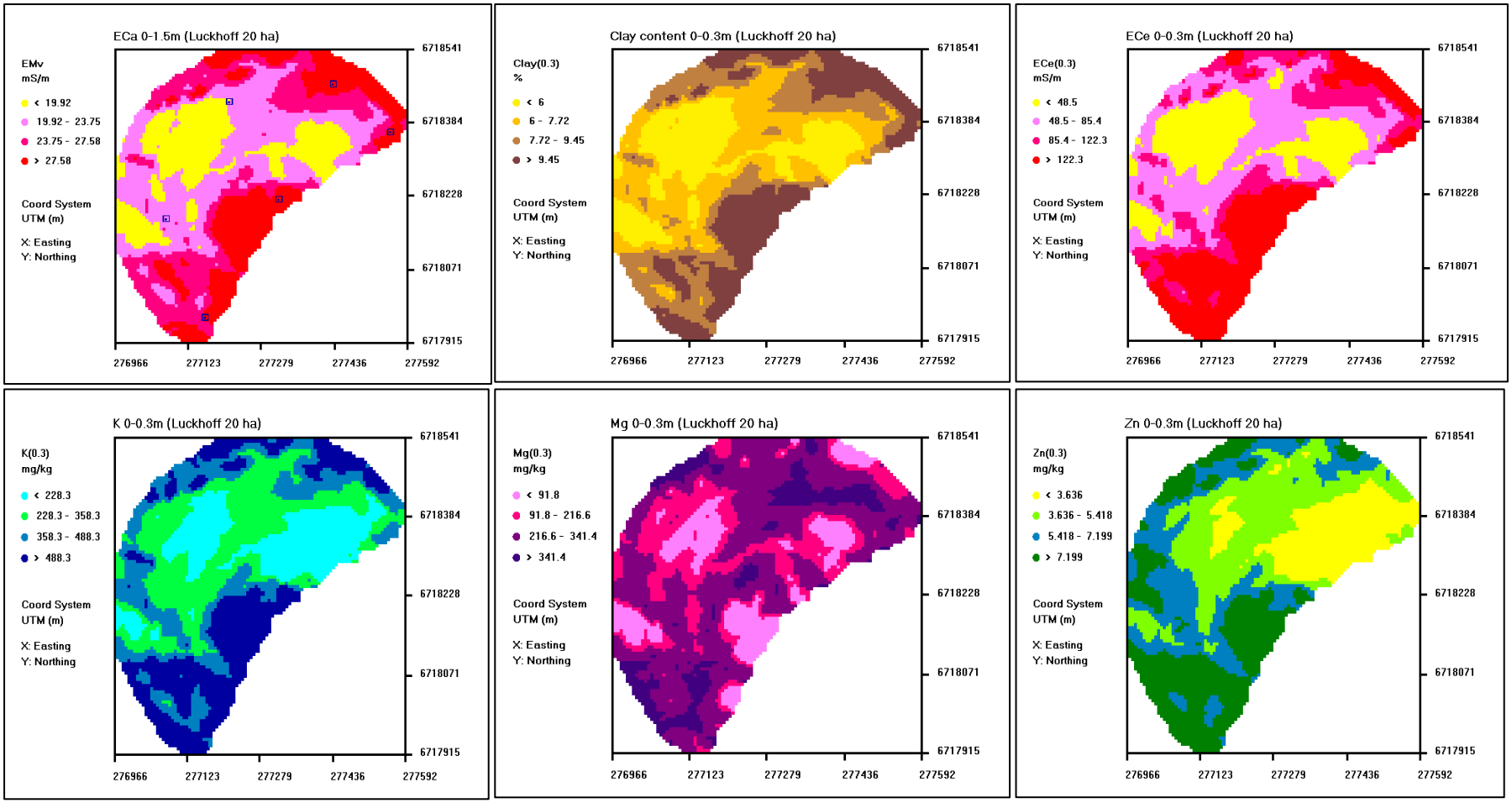

Figure 6.4: Interpolated maps showing the spatial patterns of soil properties at Luckhoff's 20 ha centre pivot in December 2016

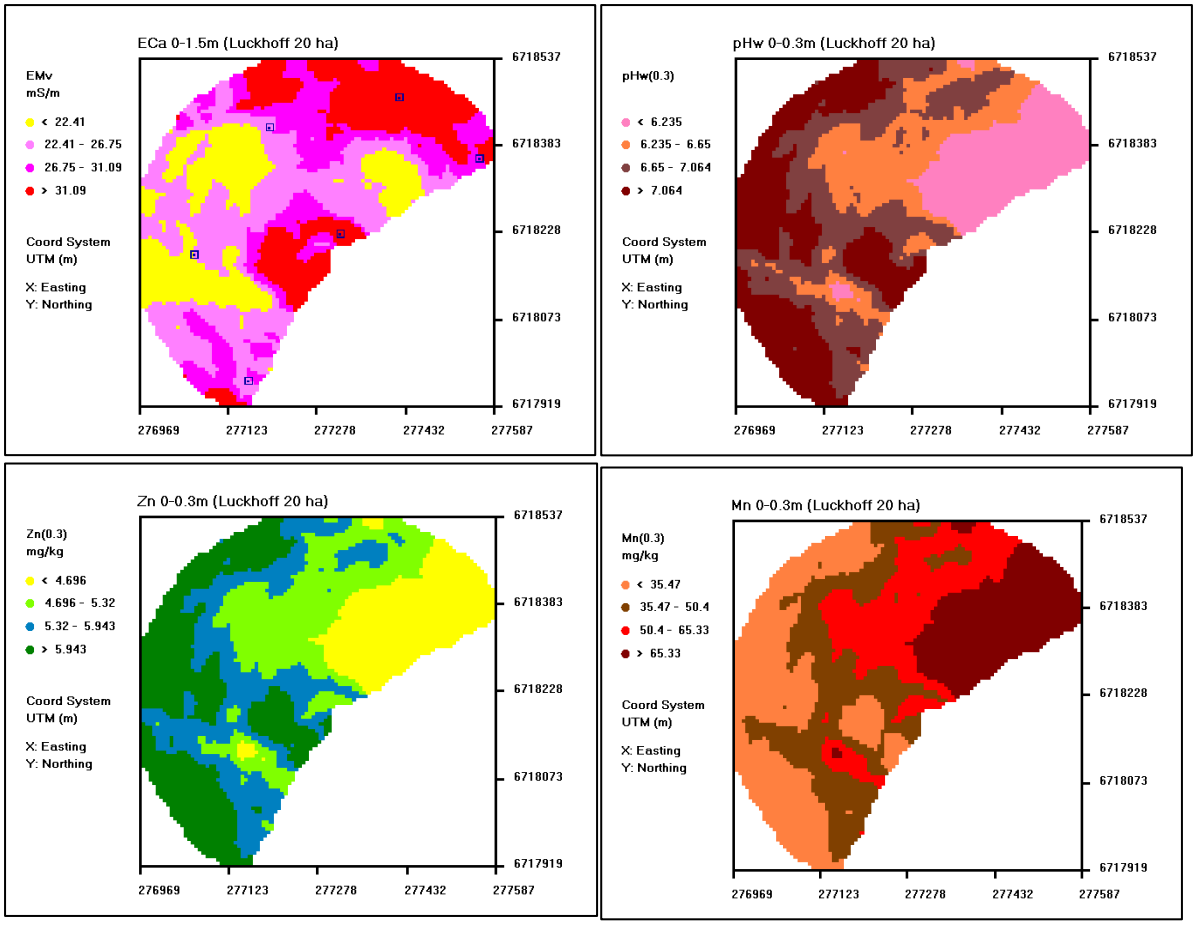

Figure 6.5: Interpolated maps showing the spatial patterns of soil properties at Luckhoff's 20 ha centre pivot in June 2017

Table 6.4 shows the spatial MLR model statistics of the soil parameters that were significantly modelled with EC_a survey data at Luckhoff's 40 ha centre pivot in June 2016 and 2017. In June 2016, the spatial MLR statistics show that 75, 91, 75 and 52% of the observed variation of C, N, P and Mn can be described using the EC_a survey data, respectively. Furthermore, about 96% of the observed variation of Ca can explained by the EC_a survey data obtained in June 2017. Additionally, the trend surface parameters were found to be significant on the models for C, N, P and Ca at this field. However, only the y co-ordinate significantly improved the prediction power of the Mn model. The spatial patterns of EC_a remained relatively constant from June 2016 to June 2017 (Figures 6.6 and 6.7). However, lower values of EC_a were obtained in June 2017. In June 2016, the spatial patterns of C and N were relatively similar with higher C and N contents observed in the northern parts of the field. The areas of the field

with higher C and N values corresponded with generally lower EC_a values. Relatively higher P levels were observed in south western part of field as compared to other areas. Coincidentally, lower Mn levels were observed in the western section of the field. In June 2017, spatial Ca map shows generally higher Ca levels in the south-western sections of the Luckhoff 40 ha field. Some smaller sections in the northern part of the field also have higher Ca levels.

Table 6.5 presents the spatial MLR model summary statistics for the plant nutrients that were successfully modelled by the EC_a survey data in December 2016 at half of the 60 ha NW centre of Luckhoff. The R^2 and root mean square error estimates for Zn and Cu are 0.83, 0.10, and 0.72, 0.30, respectively. These R^2 estimates suggest that the EC_a deep readings describes about 83 and 72% of the apparent Zn and Cu variation in this field. Additionally, the trend surface parameters did not significantly improve the prediction power of the Zn and Cu models. Figure 6.8 displays the spatial patterns of the EC_a and nutrients at half of the 60 ha NW of Luckhoff. The spatial maps of EC_a and the modelled nutrients look relatively similar. The spatial patterns show that areas with relatively higher EC_a corresponded with higher levels of Zn and Cu.

Table 6.4: Regression model summary statistics for 40 ha centre pivot of Luckhoff in June 2016 and 2017

Model Statistic	June 2016				June 2017
	C	N	P	Mn	Ca
R^2	0.75	0.91	0.75	0.52	0.96
RMSE	0.29	0.17	0.23	23.3	102.6

Variable	Estimate	Standard Error	t-Score	Prob > |t|
June 2016				
C, %				
	Model parameters: $Ln(C) = \beta_0 + \beta_1 z_1 + \beta_2 x + \beta_3 y$			
β_0	-0.79	0.26	-3.02	0.016*
β_1	-0.28	0.09	-3.30	0.011*
β_2	-1.05	0.37	-2.88	0.021*
β_3	0.91	0.31	2.93	0.019*
N, %				
	Model parameters: $Ln(N) = \beta_0 + \beta_1 z_1 + \beta_2 z_1^2 + \beta_3 x + \beta_4 y$			
β_0	-2.78	0.16	-17.9	0.0001***
β_1	-0.32	0.05	-5.98	0.0006***
β_2	0.10	0.04	2.80	0.026*
β_3	-0.94	0.22	-4.30	0.004**
β_4	0.66	0.20	3.24	0.014*
P, $mgkg^{-1}$	Model parameters: $Ln(P) = \beta_0 + \beta_1 z_1 + \beta_2 z_1^2 + \beta_3 x + \beta_4 y$			
β_0	2.88	0.20	14.2	0.0001***
β_1	-0.28	0.07	-3.91	0.006**
β_2	0.09	0.05	1.90	0.099ns
β_3	-0.71	0.29	-2.48	0.042*
β_4	-0.81	0.27	-3.01	0.020*
Mn, $mgkg^{-1}$				
	Model parameters: $Mn = \beta_0 + \beta_1 z_1 + \beta_2 y$			
β_0	83.0	14.9	5.57	0.0003***
β_1	-16.3	5.79	-2.81	0.021*
β_2	-46.7	25.2	-1.85	0.094ns
June 2017				
Ca, $mgkg^{-1}$				
	Model parameter: $Ca = \beta_0 + \beta_1 z_1 + \beta_2 z_1^2 + \beta_3 x + \beta_4 y + \beta_5 xy + \beta_6 x^2 + \beta_7 y^2$			
β_0	5725	574.1	9.97	0.0006***
β_1	623.5	113.1	5.51	0.005**
β_2	-858.7	130.1	-6.60	0.003**
β_3	-8401	1298	-6.47	0.003**
β_4	-12837	1983	-6.47	0.003**
β_5	3064	715.5	4.28	0.013*
β_6	6484	1112	5.83	0.004**
β_7	10815	1719	6.29	0.003**

*, **, *** - model parameter in the spatial MLR significant at 0.05, 0.01 and 0.001 probability level

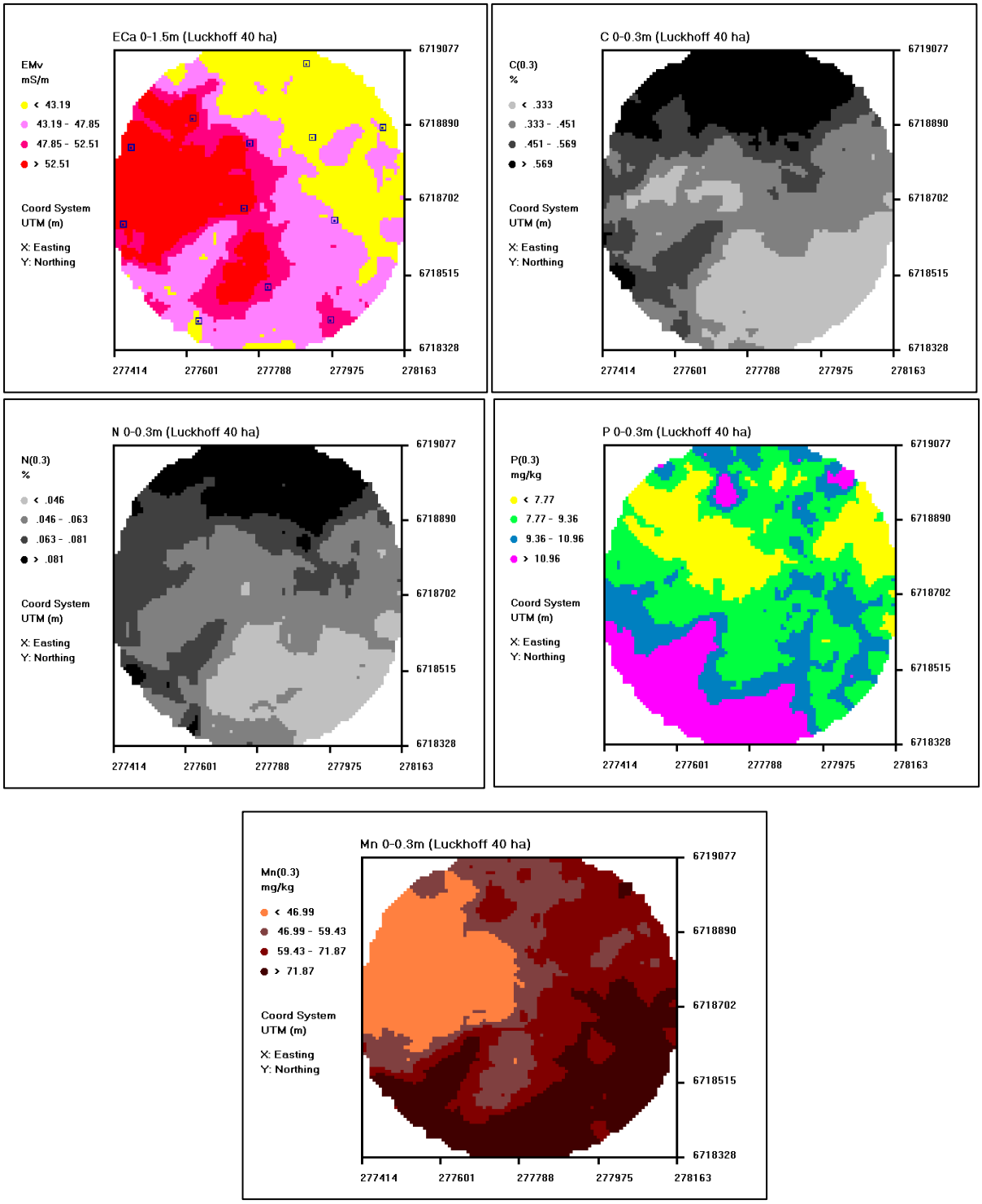

Figure 6.6: Interpolated maps showing the spatial patterns of soil properties at Luckhoff's 40 ha centre pivot in June 2016

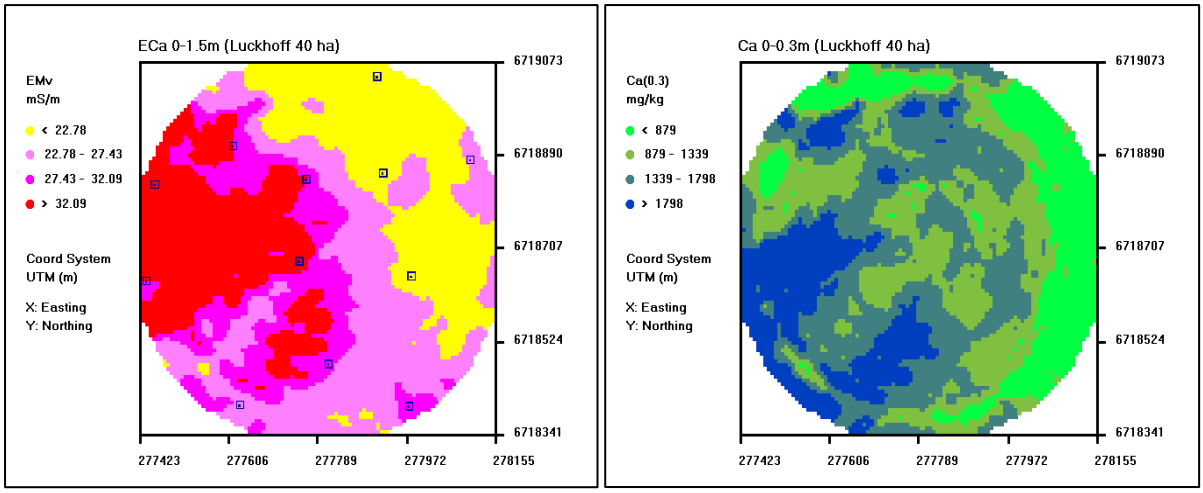

Figure 6.7: Interpolated maps showing the spatial patterns of soil properties at Luckhoff's 40 ha centre pivot in June 2017

Table 6.5: Regression model summary statistics for the 60 ha NW centre pivot at Luckhoff in December 2016

Model Statistic	Zn			Cu
R^2	0.83			0.72
RMSE	0.10			0.30
Variable	**Estimate**	**Standard Error**	**t-Score**	**Prob > |t|**
Zn, $mgkg^{-1}$				
	Model parameters: $LnZn = \beta_0 + \beta_1 z_1$			
β_0	2.16	0.04	52.3	0.0001***
β_1	0.14	0.03	4.43	0.011*
Cu, $mgkg^{-1}$				
	Model parameters: $LnCu = \beta_0 + \beta_1 z_1$			
β_0	1.10	0.12	8.96	0.0009***
β_1	0.31	0.10	3.20	0.033*

*, **, *** - model parameter in the spatial MLR significant at 0.05, 0.01 and 0.001 probability level

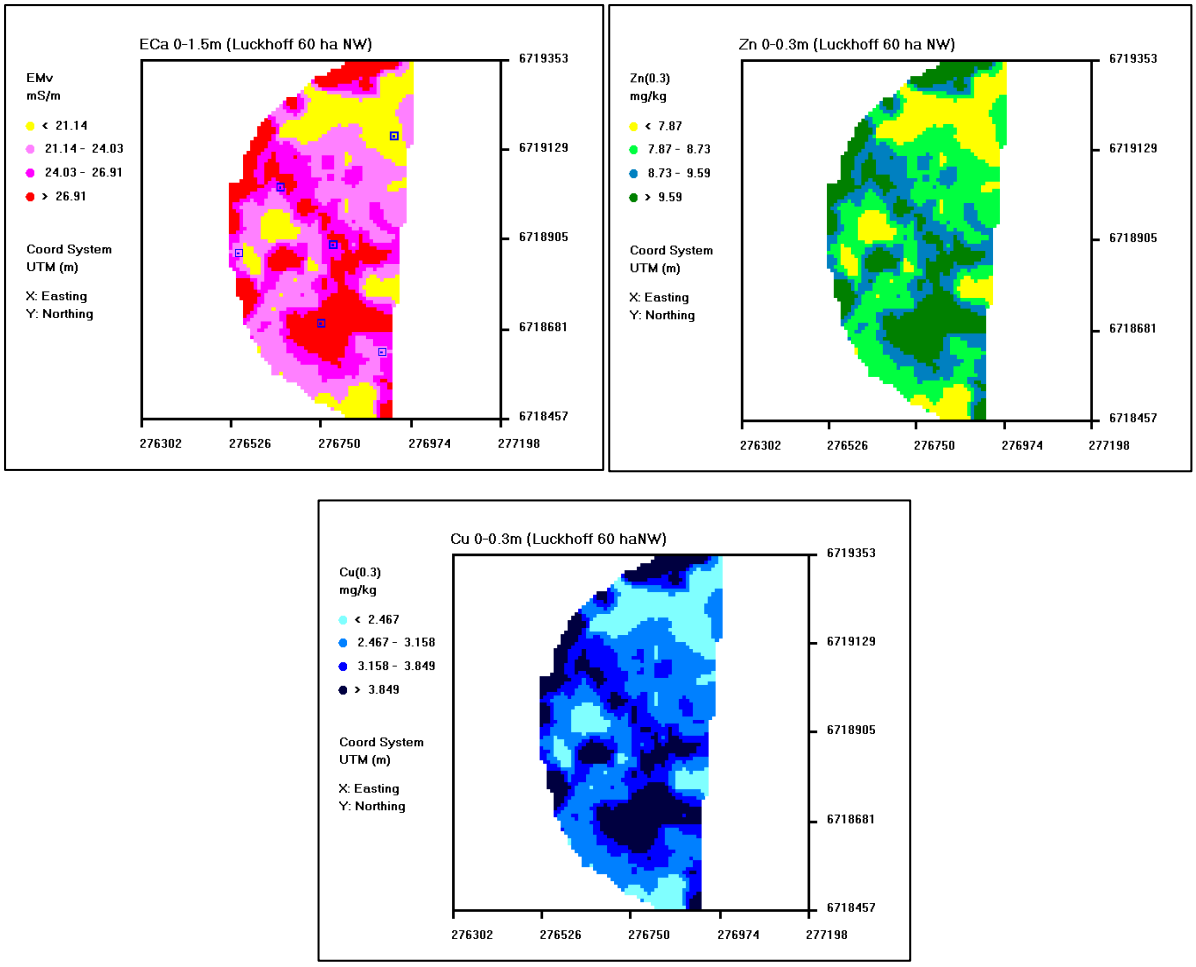

Figure 6.8: Interpolated maps showing the spatial patterns of Zn and Cu at half of Luckhoff's 60 ha NW centre pivot in December 2016

Site-specific measured EC_a synthesizes the effects of particular static and dynamic soil factors, which include soil salinity, clay content and mineralogy, water content, bulk density and temperature (Corwin and Lesch, 2005). Generally, the magnitude and spatial patterns of EC_a measurements in a field are dominated by one or two of these factors which also varies from field to field. However, the results of this study demonstrated that at some fields, most of the primary factors were not dominant drivers of EC_a measurements. Most of the measured soil properties at the study sites did not significantly influence the EC_a variability. In such cases, field scale EC_a can be useful as a tool for delineation of overall soil condition (Johnson *et al*., 2001). Some of the primary factors such as EC_e, water and clay content significantly influenced the spatial EC_a measurements at specific fields at Hofmeyr and Luckhoff sites.

Particularly, the clay content at the 55 ha NW field at Hofmeyr significantly correlated with both EC_e (r = 0.6*) and N (r = 0.6*) showing that the soil texture at this field was the dominant driver of EC_a measurements in June 2016. At the Luckhoff 20 ha field, clay content moderately correlated ($r < 0.6$) with the secondary properties that were significantly correlated with EC_a. However, these moderate correlations were not significant, suggesting that significant EC_a relationships of these secondary properties were not primarily influenced by soil texture at this field. The results from the study suggest that EC_a measurements in most of the experimental fields were dominated by dynamic factors and other properties that might not have been considered in this study. It is recognised that the distribution efficiency of the irrigation system and management of irrigation scheduling can also influence the magnitude and spatial pattern of soil properties at these fields (Barnard *et al*., 2020). Furthermore, the application of commercial fertilizers can influence EC_a to the point where static dominated fields are altered to dynamic dominated fields (Johnson *et al*., 2003) which may have been the case in this study.

6.3.2 The prediction and mapping of crop yield from EC_a survey data

The studies relating crop yield to EC_a have been met with inconsistent results. Corwin and Lesch (2003) highlights the complex interaction of the soil properties that influence EC_a and complex interaction of biological, anthropogenic and climatological factors that influence yield beyond the soil-related factors as the causes. The objective of this study was to see if the EC_a survey data can be used to model and deduce spatial patterns of wheat and maize crop yields for the purpose of site-specific management. The Pearson correlation coefficient (r) was used in Chapter 5 to see if there was a significant linear relationship between crop yields and EC_a. Significant correlations (r) between crop yields and EC_a were observed at half of the Luckhoff's 60 ha NE centre pivot (Table 5.18). In instances where yield correlates with EC_a, spatial measurements of EC_a can be used in a site-specific crop management context (Corwin and Lesch, 2003). However, it is important to establish the soil properties that most significantly

influence the EC_a measurements within a field in order to establish the soil properties that are influencing yield.

The Pearson correlation coefficient (*r*) was used to find the predominant soil factors influencing the spatial EC_a measurements in-order to establish the factors that influenced the crop yields at the Luckhoff's 60 ha NE centre pivot in December 2016 and June 2017. Unfortunately, none of the measured soil properties registered any strong and significant correlation with EC_a in December 2016 (results not shown). This shows that the factors that significantly influenced the EC_a and wheat grain yields were beyond the measured soil properties in this study. Hence, soil properties such as internal drainage, slope and elevation of the field could have had stronger association with the EC_a and yield variability. In June 2017, clay content strongly and significantly correlated with both maize grain yield (r = -0.87*) and EC_a (r = 0.86*) at Luckhoff's 60 ha NE centre pivot. In this scenario, EC_a survey data can be used in a site-specific management context to address crop yield variation in this field. In this chapter, the spatial MLR analysis in the ESAP software was used to model the spatial variation of the crop yield parameters with EC_a survey data at the study fields especially in the Luckhoff's 60 ha NE where significant yield-EC_a relationships were observed. Total nutrient removal for elements such as Ca, Mg, K, Na, S, P, Fe and Mn were strongly and significantly correlated (r > 0.7) with both wheat and maize crop yields at this field. Hence, the study also attempted to use the spatial MLR models in the ESAP software to study the spatial patterns of the crop nutrient removals at the study fields.

Table 6.6 presents summary of the spatial MLR statistics and parameter estimates of the models of wheat and maize yield parameters at half of the Luckhoff's 60 ha NE centre pivot. The R^2 values for the wheat and maize grain yield models are 0.86 and 0.89 respectively, suggesting that approximately 90% of the observed yield variation in the Luckhoff's 60 ha NE centre pivot can be described by the EC_a survey data. Furthermore, the results of the spatial

MLR statistics for the maize biomass yield model show that approximately 89% of the spatial variation of the maize biomass yield can be explained using the EC_a survey data. Additionally, only the x co-ordinates were significant in the wheat grain yield model whereas no trend surface parameters were found to significantly improve the predictions in the maize grain yield model. On the other hand, only the y co-ordinates were significant in the maize biomass yield model. Table 6.7 shows the spatial MLR summary statistics of the models of total nutrient removed from the Luckhoff fields by wheat. The results presented are for the nutrients that correlated significantly with EC_a in the spatial MLR model. Total K, S, Cu and Mn removed by the wheat crop in the Luckhoff 60 ha NE field were significantly correlated with EC_a in the spatial MLR model and the regression statistics show that the EC_a survey in December 2016 at this site can explain 99, 87, 88 and 76% of the within-field variation of the nutrient removed respectively (Table 6.7). Remarkably, total Ca, Mg, K, S and Fe removed by the maize crop at half of the 60 ha NE field at the Luckhoff site were significantly correlated with EC_a survey data in June 2017 at this site (Table 6.8). The R^2 values of their respective models show that 88, 91, 68, 97 and 90% of the within-field variation of the removal of these nutrients can be elaborated from the corresponding EC_a survey data respectively

Figure 6.9 shows the interpolated spatial maps for the EC_a with highlighted 6 sampling points and wheat grain yield at half of the 60 ha NE field at Luckhoff site in December 2016. The spatial EC_a map shows the presence of a linear belt in the middle of the Luckhoff 60 ha NE field with lower EC_a values. The occurrence of the belt in the middle of the field is not natural under normal field conditions. This unnatural pattern was caused by errors associated with conducting an EC_a survey for more than a day without proper instrument set-up (Barnard *et al*., 2020). Nonetheless, the spatial maps of EC_a and wheat yield show that there was an inverse relationship between EC_a and wheat grain yields at this field. Figure 6.10 displays the spatial maps for total nutrients removed by the wheat crop at this field. High removal of K, S, Cu and Mn occurred in the areas with corresponding high yields such as the north-western

and middle sections of half of the 60 ha NE centre pivot of Luckhoff. This spatial trend can be expected since there is a significantly positive correlation ($r > 0.70$) between crop yields and total nutrient removed by the wheat crop at this field

Spatial patterns for the clay content, EC_a with highlighted sampling points and maize yield parameters are shown in Figure 6.11 in June 2017. The spatial patterns of the EC_a from December 2016 to June 2017 shows that EC_a was variable across some sections of the field where comparatively lower EC_a were observed. However, generally higher EC_a values were obtained with the EC_a survey in June 2017 as compared to December 2016. The spatial maps of the clay content and maize yield parameters show that there was an inverse relationship between these variables. Areas with higher clay content such as the north western portions of the half of Luckhoff's 60 ha NE field concurred with lower grain and biomass yields. These puzzling observations could be a reflection of the effects of complex interactions of soil texture with other soil properties such as soil drainage and terrain.

Figure 6.12 shows the interpolated spatial maps for the total nutrient removed by the maize crop at half of the 60 ha NE centre pivot at the Luckhoff site. The spatial patterns of the removal of Ca, Mg, S and Fe follows the spatial pattern of the maize yield parameters. South eastern sections of the field with high yields concurred with high removal of these four nutrients. On the other hand, the removal of K seems to inversely follow the spatial patterns of the clay content in some sections of the fields and crop yields in other sections. The north-western part of the fields with high clay content and low yields concurred with high K removal. Furthermore, the south-eastern part of the field with high yields and low clay content concurred with high K removal. These observations furthermore confirm the complexity of field studies where the interaction of several factors often cause confounding results (Corwin and Lesch, 2003). Nonetheless, the spatial characterization of the nutrient removals can serve as useful supplementary information in the formulation of site-specific nutrient replacement strategies

in precision agriculture. Nutrient removal maps formulated at the half of the Luckhoff's 60 ha NE can be used as the basis for nutrient replacement rates in this field.

Table 6.6: Regression model summary statistics for wheat and maize crop yield parameters of the Luckhoff's 60 ha NE centre pivot

		Crop yield parameters		
Model Statistic		wheat	maize	
		yield	biomass	yield
R^2		0.86	0.89	0.89
RMSE		0.58	1.21	0.74
Variable	Estimate	Standard Error	t-Score	Prob > |t|
Wheat yield, t ha^{-1}				
	Model parameters: yield = $\beta_0 + \beta_1 z_1 + \beta_2 x$			
β_0	7.69	0.56	13.6	0.0009***
β_1	-0.79	0.19	-4.27	0.024*
β_2	-1.68	1.00	-1.68	0.192
Maize biomass, t ha^{-1}				
	Model parameters: biomass = $\beta_0 + \beta_1 z_1 + \beta_2 y$			
β_0	28.0	1.39	20.2	0.0003
β_1	-2.44	0.57	-4.27	0.024*
β_2	-9.37	5.54	-1.69	0.190
yield, t ha^{-1}				
	Model parameters: Fe = $\beta_0 + \beta_1 z_1 + \beta_2 z_1^2$			
β_0	16.0	0.84	19.0	0.0003***
β_1	-1.59	0.34	-4.57	0.020*
β_2	-8.48	3.37	-2.51	0.087

*, **, *** - model parameter in the spatial MLR significant at 0.05, 0.01 and 0.001 probability level respectively

Table 6.7: Regression model summary statistics for nutrient uptake by wheat crop at Luckhoff 60 ha NE centre pivot

Model statistic	K	S	Cu	Mn
R^2	0.99	0.87	0.88	0.76
RMSE	4.68	1.11	0.001	0.09
Variable	**Estimate**	**Standard Error**	**t-Score**	**Prob > |t|**
K, $kgha^{-1}$				
	Model parameters: $K = \beta_0 + \beta_1 z_1 + \beta_2 x$			
β_0	342.6	4.53	75.7	0.0001***
β_1	-18.5	1.49	-12.4	0.001**
β_2	-85.6	8.06	-10.6	0.002**
S, $kgha^{-1}$				
	Model parameters: $S = \beta_0 + \beta_1 z_1$			
β_0	20.5	0.45	45.1	0.0001***
β_1	-1.77	0.34	-5.15	0.007**
Cu, $kgha^{-1}$				
	Model parameters: $Cu = \beta_0 + \beta_1 z_1 + \beta_2 x$			
β_0	0.03	0.001	31.2	0.0001***
β_1	-0.001	0.0003	-3.31	0.046*
β_2	-0.008	0.002	-4.09	0.027*
Mn, $kgha^{-1}$				
	Model parameters: $Mn = \beta_0 + \beta_1 z_1$			
β_0	0.55	0.035	15.8	0.0001***
β_1	-0.09	0.027	-3.58	0.023*

*, **, *** - model parameter in the spatial MLR significant at 0.05, 0.01 and 0.001 probability level respectively

Table 6.8: Regression model summary statistics for nutrient uptake by maize crop at Luckhoff''s 60 ha NE centre pivot

Model statistic	Luckhoff 60 ha NE				
	Ca	Mg	K	S	Fe
R^2	0.88	0.91	0.68	0.97	0.90
RMSE	3.85	2.63	0.09	0.63	0.13
Variable	Estimate		Standard Error	t-Score	Prob > |t|
Ca, kg ha^{-1}	Model parameters: $Ca = \beta_0 + \beta_1 z_1 + \beta_2 x + \beta_3 y + \beta_2 y^2$				
β_0	80.1		4.42	18.1	0.0004***
β_1	-8.53		1.82	-4.69	0.018*
β_2	-62.9		17.7	-3.56	0.038*
Mg, kg ha^{-1}					
	Model parameters: $Mg = \beta_0 + \beta_1 z_1 + \beta_2 y$				
β_0	55.8		3.01	18.5	0.0003***
β_1	-6.03		1.24	-4.85	0.017*
β_2	-64.8		12.0	-5.38	0.013*
K, kg ha^{-1}					
	Model parameters: $LnK = \beta_0 + \beta_1 z_1$				
β_0	5.84		0.04	159.0	0.0001***
β_1	-0.08		0.03	-2.89	0.044*
S, kg ha^{-1}					
	Model parameters: $S = \beta_0 + \beta_1 z_1$				
β_0	25.1		0.72	34.5	0.0001***
β_1	-2.63		0.30	-8.77	0.003**
β_2	-13.3		2.91	-4.56	0.020*
Fe, kg ha^{-1}					
	Model parameters: $Mn = \beta_0 + \beta_1 z_1$				
β_0	1.99		0.15	13.5	0.0009***
β_1	-0.28		0.06	-4.61	0.019*
β_2	-1.16		0.59	-1.96	0.145

*, **, *** - model parameter in the spatial MLR significant at 0.05, 0.01 and 0.001 probability level respectively

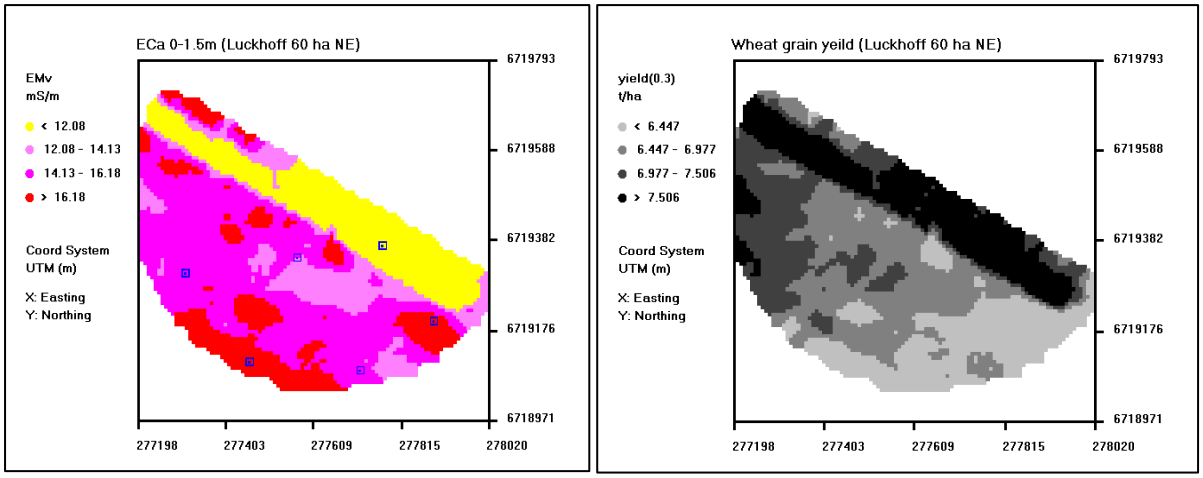

Figure 6.9: Interpolated maps showing the spatial patterns of EC_a with highlighted sampling points and wheat grain yield at half of Luckhoff's 60 ha NE centre pivot in December 2016.

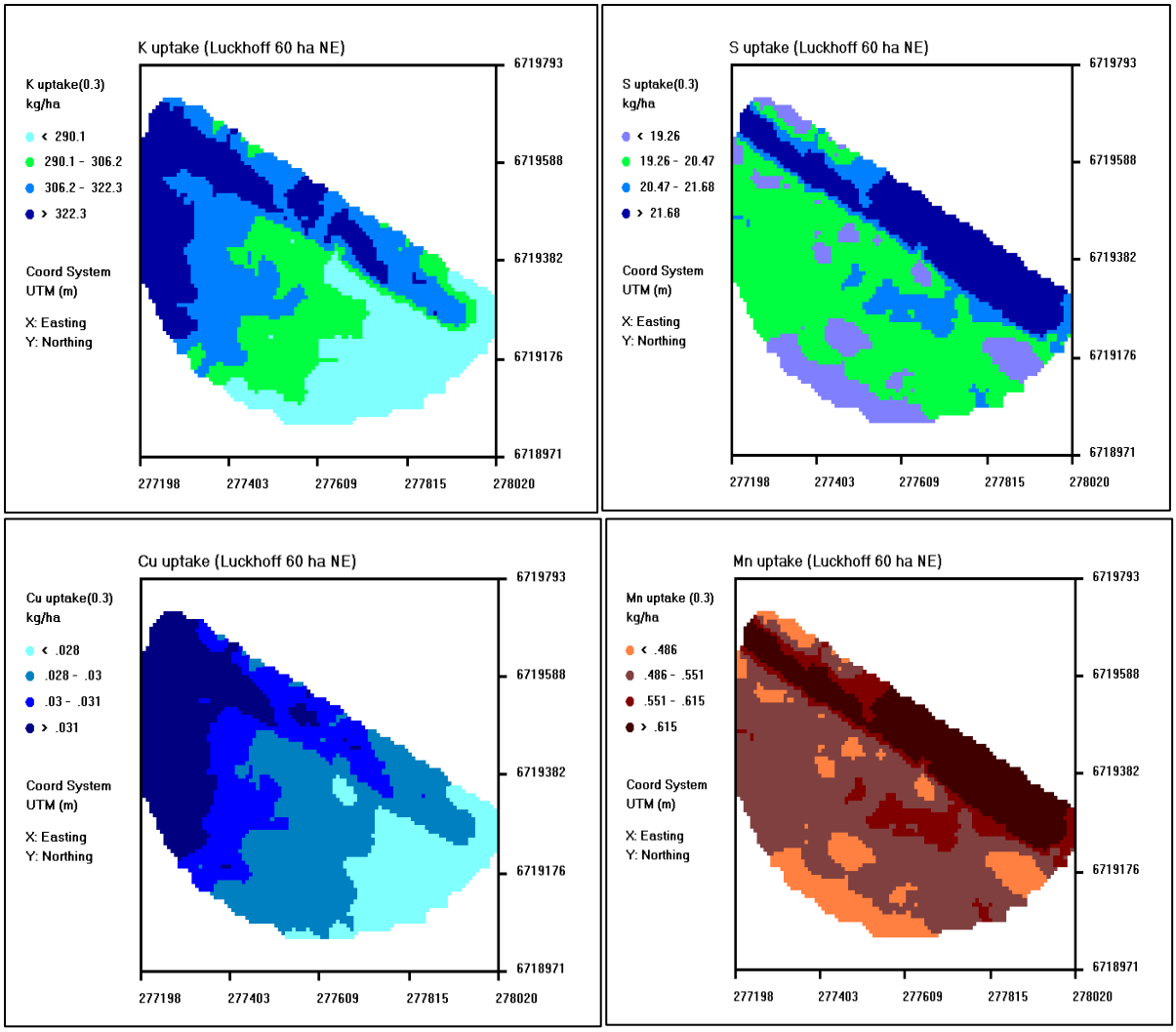

Figure 6.10: Interpolated maps showing the spatial patterns of nutrient uptake by the wheat crop at half of Luckhoff's 60 ha NE centre pivot in December 2016

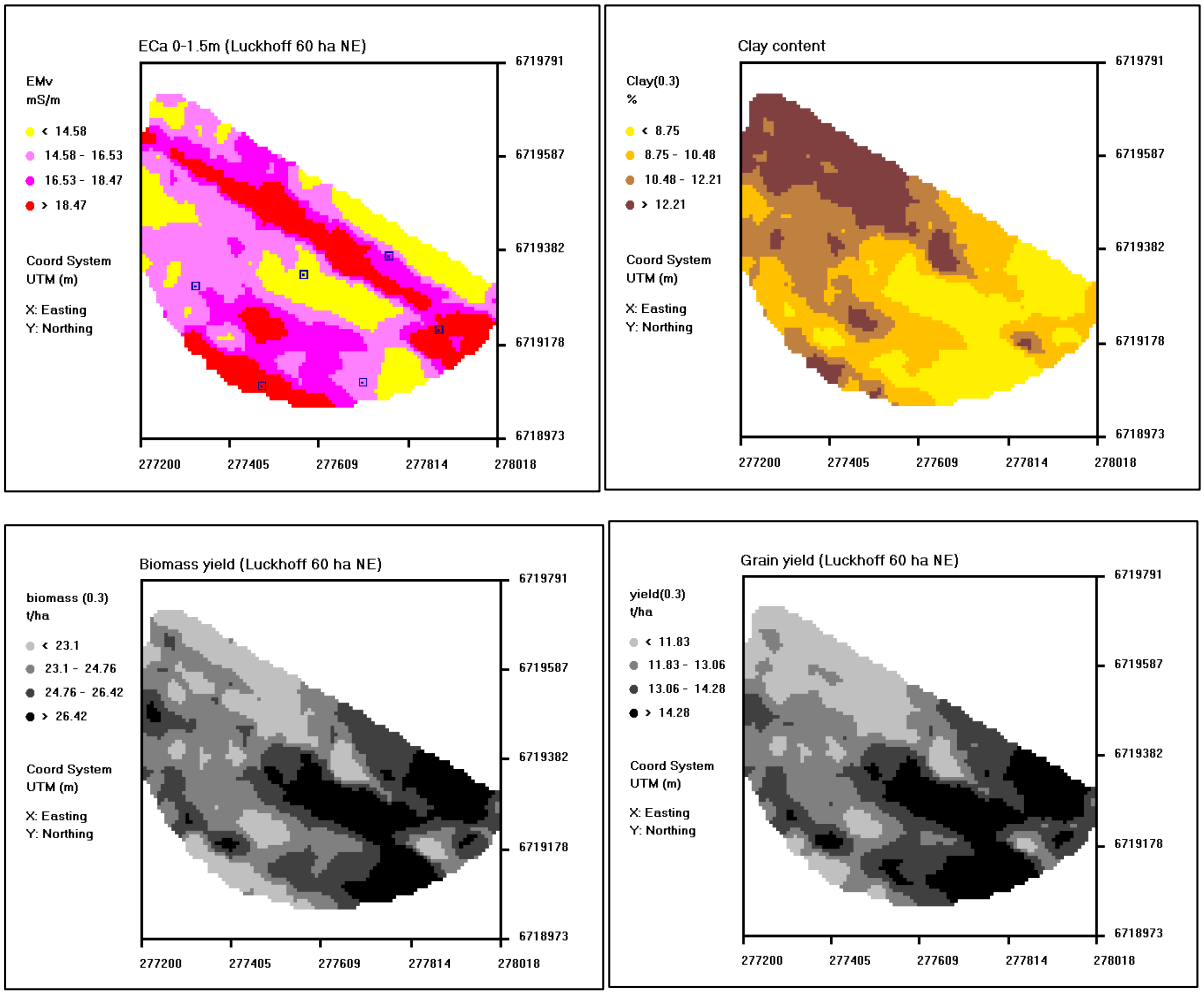

Figure 6.11: Interpolated maps showing the spatial patterns of EC_a with highlighted sampling points, clay content and maize yield parameters at half of Luckhoff's 60 ha NE centre pivot in June 2017

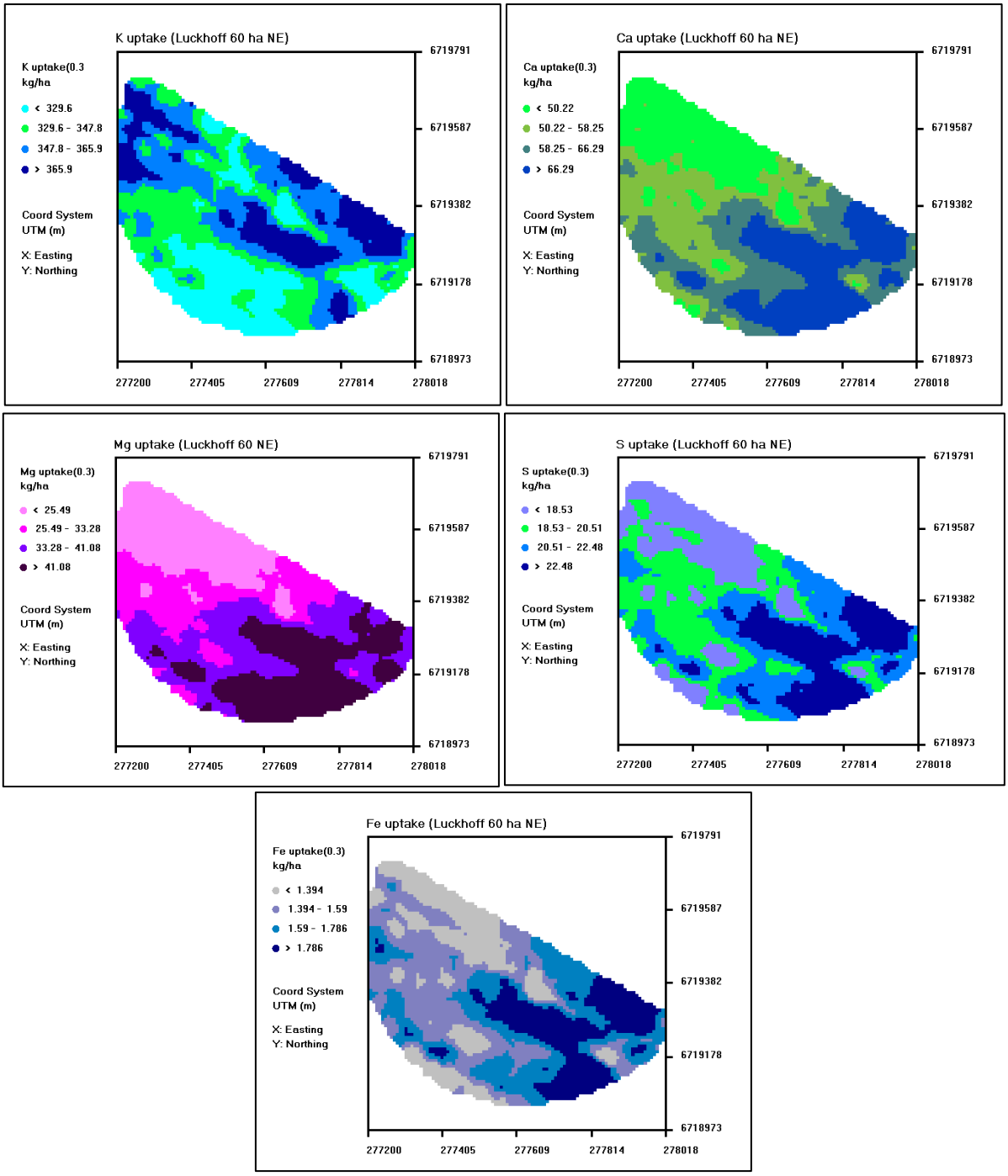

Figure 6.12: Interpolated maps showing the spatial patterns of nutrient uptake by the maize crop at half of Luckhoff's 60 ha NE centre pivot in June 2017

6.4 Conclusions

The use of EC_a survey data to map within-field spatial patterns of soil properties such as salinity, clay and water content has been well-documented in soil research fraternity (Lesch *et al*., 2005; Misra & Padhi, 2014). However, this technology has progressed from a basic mapping procedure into a more comprehensive tool for supplying detailed feedback on various agricultural management practices (Lesch *et al*., 2005). Furthermore, most published research applies this technology to the assessment of few specific factors contributing to soil production (Johnson *et al*., 2001). This study aimed to assess EC_a mapping for spatially demarcating a full spectrum of soil fertility properties related to grain yield in three irrigation systems for the purpose of site-specific management. The regression-based statistical modelling and prediction approach was used to achieve the objective. As long as the EC_a survey data is well correlated with the measured soil parameter of interest, accurate quantification and prediction of that soil parameter is generally possible using this approach (Lesch *et al*., 2005).

At Douglas 40 ha field, Ca, Θ_v, Na and Cu were well modelled and spatially mapped using their corresponding EC_a survey data. EC_e, N and clay were successfully modelled and spatially mapped with EC_a measurements at the 55 ha NW centre pivot at Hofmeyr site. Soil parameters associated with soil fertility at Luckhoff 20 ha field *viz* EC_e, K, Mg, Zn and clay were positively and significantly modelled with EC_a except Mn in June 2017 which showed significant negative correlation. The spatial representation of most of these soil properties show that site-specific management of these soil properties can be implemented at this field using the EC_a survey data. For the Luckhoff 40 ha centre pivot, C, N, P, Ca and Mn were successfully modelled and mapped using the spatial MLR models. However, most of these properties with the exception of Ca, were negatively associated with EC_a. Micronutrients Zn and Cu were positively correlated with EC_a at half of the 60 ha NW centre pivot of Luckhoff and they were spatially represented using the EC_a survey data.

ECa – crop yield interactions vary widely among published research and inconsistent correlations have been reported across years. In this study, the results were not different with low EC_a-crop yields correlations observed in most of the study fields except at half of the 60 ha NE centre pivot of Luckhoff where both wheat and maize yields negatively and significantly correlated with EC_a. Consequently, substantial removals of some of the nutrients by both crops significantly correlated with the EC_a survey data when modelled using spatial MLR analysis. The spatial characterization of the nutrient removals may be useful as supplementary information in the formulation of site-specific nutrient replacement strategies. The results from this study demonstrate that soil spatial information derived from EC_a survey data can be used in some site-specific cases to help improve the management of some soil fertility parameters in irrigated systems.

CHAPTER 7: SENSOR DATA FUSION APPROACH FOR SOIL QUALITY ASSESSMENT

7.1 Introduction

Soil quality is defined as the capacity of a soil to function as a living system within natural or managed ecosystem boundaries for sustainable plant and animal productivity, maintenance of environmental quality, and support of plant and animal health (Karlen *et al.,* 1997). It reflects how efficiently a soil accepts, holds and releases both water and nutrients to plants, maintains suitable soil biotic environment and respond to different sets of management systems. In an agricultural context, a soil with high quality equates to a soil with high productivity without significant soil or environmental degradation (Fuentes *et al*., 2009). In an effort to comprehend the broad categories of soil function, evaluation and quantification of soil quality necessitates measurement of multiple physical, chemical and biological soil properties (Karlen *et al*., 1997; Veum *et al.,* 2017). Measurements of these soil properties often involve costly and tedious laboratory analyses, which limits the production of dense field-scale spatial information which is critical in site-specific management.

Advances in soil sensor technology have made it possible to provide high-resolution spatial data useful for efficient and effective resource management (Mohamood *et al*., 2012). Soil sensors have been widely used to estimate individual soil properties and sensor fusion technology has been investigated and applied to improve the prediction of multiple soil properties (Mahmood *et al.,* 2012; Wetterlind *et al*., 2015; Veum *et al.,* 2017). Generally, no single soil sensor is capable of capturing the wide range of soil properties related to soil quality evaluation due to the multifaceted nature of soils. The inability of the single sensor can be overcome by combining different sensing methods and incorporating data from multiple sensors holds more promise for providing complementary and more robust soil parameter estimates (Mahmood *et al*., 2012). Therefore, soil quality assessment in irrigated fields

represents an ideal platform to apply the sensor data fusion approach to obtain soil quality data with better quality and reliability.

Mid-infrared spectroscopy (MIR) has been used successfully to predict soil quality indicators such as soil organic carbon (SOC), total carbon (TC), soil organic matter (SOM), cation exchange capacity (CEC), Ca, Mg, clay and others (Viscarra Rossel *et al., 2006*; Knox *et al.,* 2015; Terra *et al.,* 2015; Ma *et al.,* 2019). Estimation of other important soil quality indicators such as pH_w, P, K, Na, Cu, Fe, Mn and Zn has been less consistent (Viscarra Rossel *et al.,* 2006; Du and Zhou, 2009; Ma *et al.,* 2019). To augment MIR for improved estimation of the important soil quality indicators, complementary in-field sensors such as electrical conductivity (EC_a) sensors may be combined with MIR sensors. Apparent electrical conductivity (EC_a) reflects various soil attributes such as texture, mineralogy, CEC and water content (Sudduth *et al*., 2013). The fusion of the MIR sensor and EC_a sensor data may perform extrapolations that are potentially more accurate than if they are achieved by an individual sensor.

A few studies have been attempted to evaluate the effectiveness of the sensor data approach. Wong *et al.* (2010) successfully used a dual EM38-gamma-ray soil sensing approach with a rule-based method to estimate topsoil depth and soil pH with better accuracy than the single-based sensor approach. Taylor *et al.* (2010) used the fusion of gamma-ray spectrometer and an EM38 sensor to estimate topsoil clay content and concluded that soil property models based on both sensors predicted topsoil clay content better than models based on either of the sensors. Schirrmann *et al.* (2011) investigated a sensor fusion approach comprising a pH sensor, a VIS-NIR spectrometer and an EC_a sensor for mapping plant macro-nutrients in soil. The conclusion was that only the prediction of pH was improved by combining the data from all three sensors. These reviews showed that there is potential to get better soil property estimates using sensor data fusion, although this approach has not been extensively tested for evaluating multiple soil properties. Mahmood *et al*. (2012) applied sensor fusion of data

from a VIS-NIR spectrometer and EM38 sensor for prediction of multiple soil properties. The study used three data fusion methods *viz* partial least regression (PLSR), step-wise multiple linear regression (SMLR) and principal component regression combined with step-wise multiple linear regression (PCR + SMLR). From the study, they concluded that generally soil property models based on fusion methods significantly improved the prediction of soil properties. Furthermore, the PLSR fusion method performed the best among the data fusion methods. Although a few attempts have been made to complement the VIS-NIR sensors with supplementary sensors to improve estimation of multiple soil properties, the fusion of MIR sensors with additional sensors have received even less attention.

Several soil attributes contribute to soil function and a soil quality index (SQI) provides an opportunity to monitor changes in soil function due to management changes over time. The Soil Management Assessment Framework (SMAF) is a conceptual framework that has been designed to make quantitative assessment of soil quality (Andrews *et al*., 2004). This framework was developed to integrate multiple soil quality indicators into a comprehensive SQI to assess the impact of soil management decisions on soil functions. The SQI computed using the SMAF algorithms have been successfully used at various scales for different purposes such as assessing impacts of soil and crop management on soil quality and crop production (Veum *et al*., 2014; Gelaw *et al.,* 2015; Cherubin *et al*., 2016; Veum *et al*., 2017; Gura and Mnkeni, 2019; Nabiollahi *et al*., 2020). The SMAF evaluation is site-specific and uses a three step process to make assessment that includes indicator selection, indicator interpretation, and integration into an index (Stott *et al*., 2010). Currently, the SMAF integrates up to 13 indicators with scoring curves consisting of interpretation algorithms. These management-sensitive indicators include soil physical, chemical, and biological characteristics *viz* macroaggregate stability (AGS), plant-water-holding capacity (PWHC), water-filled pore space (WFPS), bulk density, electrical conductivity (EC), soil pH, sodium adsorption ratio (SAR), extractable P and K, soil organic carbon (SOC), microbial biomass carbon (MBC),

potentially mineralizable nitriogen (N_{min}) and β-glucosidase (BG) activity (Andrews *et al*., 2004; Wienhold *et al*., 2009; Stott *et al*., 2010; 2011; 2013).

Fewer studies have attempted the concurrent estimation of a wide range of soil properties using VIS-NIR-MIR sensors and supplementary sensors for the purpose of soil quality assessment. Veum *et al*. (2015) attempted to estimate SMAF soil quality indicators and scores using VNIR spectra and ancillary laboratory data. The study found that in some cases, augmenting VIS-NIR data with supplementary laboratory data improved SMAF estimation models. Veum *et al.* (2017) applied a sensor fusion approach to assess soil quality indicators and SMAF scores using VIS-NIR spectroscopy in conjunction with EC_a and penetration resistance measured by cone penetrometer *viz* cone index (CI). Models integrating VIS-NIR reflectance data with EC_a and CI data improved the estimates of soil quality indicators and SMAF scores with reduction of RMSE values for the estimates. The conclusion from these studies seems to suggest that data from complementary sensors may overcome limitations of the VIS-NIR technique in soil quality assessment by improving the prediction of the soil quality indicators that are not well captured by the VIS-NIR sensor alone. In general, the MIR technique in multiple soil property quantification is considered as superior to VIS-NIR (Pirie *et al*., 2005; Viscarra Rossel *et al.,* 2006; Vohland *et al.,* 2014). Therefore improved estimation of soil quality indicators and SMAF-SQI using the data fusion from MIR sensor and other contemporary sensors holds more promise for providing more accurate soil quality estimates, leading to more robust management and increased acceptance of sensor-based soil and crop management.

Irrigation presents an effective tool that can be used to increase the maize and wheat yield potential of the arable lands in South Africa. However, a systematic overall soil quality assessment of the irrigated fields where these two grain crops are mostly grown is essential to develop appropriate soil management strategies and to enhance the grain yield. Moreover,

due to the dynamic nature of the irrigation systems, monitoring and assessment of soil quality is critical at field scale and the development of rapid, low-cost methods using in-field sensors to facilitate soil quality evaluation should be a priority. Therefore, the objectives of this study were to evaluate a sensor fusion approach on irrigated soils from three sites using MIR spectra in conjunction with EC_a sensor data to estimate (a) multiple soil quality indicators and (b) SMAF soil quality scores (c) overall SMAF soil quality index (SMAF-SQI).

7.2 Procedure

The study sites' characteristics, soil sampling and analysis, data processing and statistical analysis are described in detail in Chapter 3, and therefore not repeated in this chapter. For this chapter, only pertinent data from three centre pivots, one per study site were used *viz* 40 ha, 20 ha and 55 ha NW centre pivots at Douglas, Luckhoff and Hofmeyr, respectively. The reason for choosing only one field per site to investigate the sensor fusion approach was the demanding nature of the MIR data retrieving phase involved prior to sensor data fusion. Hence only one field per site was considered sufficient for comparative analysis of the sensor fusion technique across the study sites.

7.3 Results and discussions

7.3.1 SMAF soil quality assessment

The descriptive statistics for the measured soil parameters of the centre pivots used in soil quality assessment are presented in Chapter 4. However, the summary statistics of the SMAF scores of the selected soil quality indicators and the overall SMAF soil quality index are presented in Table 7.1. At the Douglas 40 ha centre pivot, most of the SMAF indicators scored moderate to high (0.60 - 0.99) except for P which scored very low (0.11). EC_e scored zero in some areas of the centre pivot confirming the problem of salinity existing in some areas of the 40 ha field. Of the scored indicators, the coefficient of variation (CV) for the SMAF scores was

highest for P (81.8%), followed by EC_e (49.0%) and SOC (38.7). Overall, the SMAF soil quality index (SQI) score indicated that mean soil function at the Douglas 40 ha centre pivot during the study period was 66% and was ranging from 52% up to 72%, indicating that the soil has moderate ability to support plant growth and development (Andrews *et al*., 2004). Lower SMAF scores for P were more influential in the moderate overall SMAF score at the Douglas 40 ha centre pivot confirming the need to supplement P for optimum plant growth. At the Hofmeyr 55 ha NW centre pivot, pH, EC_e and K scored high whereas SOC and P scored fairly low. The coefficient of variation of the SMAF scores at this centre pivot followed the same pattern as at the Douglas 40 ha centre pivot. SMAF P scores resulted in the highest CV (93.3%) followed by SOC (50.0%) and EC_e (37.1%). The overall SMAF score for the Hofmeyr centre pivot could not be deduced due to the lack of scores for the soil physical properties. Nonetheless, the scoring of the individual soil quality indicators at this site still provides much needed information in evaluating the impact of recent soil and crop management practices and to provide guidance in development of appropriate soil and crop management strategies.

Most of the selected soil quality indicators at the Luckhoff 20 ha centre pivot scored moderately high to high (0.68-0.99) except SOC which scored quite low (0.08). SMAF P scores resulted in the highest CV (46.7%), followed by SOC (37.5%) and bulk density (pb) (22.1%). The average SMAF score for P was fairly high (0.75), ranging from 0.01 to 1.00. The high range for the P scores suggests the need to apply site-specific P management at this field to ensure efficient use of P by the growing crops. The SMAF SQI score for the Luckhoff 20 ha centre pivot ranged from 0.62 to 0.81. Overall the soil in this field was found to be performing moderately high with respect to soil quality, functioning at 74% of optimum when compared with similar soils reported by Andrews *et al*., (2004). Across the study sites, the SMAF scores suggest the need to address the following soil quality indicators *viz* EC_e, SOC and P in some areas of the selected fields. The overall SMAF soil quality index at the Douglas and Luckhoff

fields suggest that an opportunity to improve the soil quality performance at these fields still exists through appropriate soil and crop management strategies.

7.3.2 Identifying optimal spectral bands from MIR spectra

Robust identification of MIR wavebands or wavenumbers from MIR spectra data (4000 - 400 cm^{-1}) for sensor data fusion was achieved using derivative analysis (Melendez-Pastor *et al*., 2008; Mahmood *et al*., 2012). This analysis perform a baseline correction and improve weak features of the relevant peaks in the spectra (Duckworth, 1998). The original soil absorbance spectra and their corresponding first derivative spectra of the soils from the centre pivots are shown in Figures 7.1 to 7.3. The first derivative spectrum clearly shows the peaks and dips which are the discrete absorption features caused by the intrinsic soil characteristics or/and by the presence of other elements. Signs of spectrum noise are observed for the first derivative spectra at lower and higher MIR wavenumbers. The selected MIR wavenumbers to be used as predictor variables in the sensor fusion for the prediction of soil properties and SMAF scores are shown in Tables 7.2 to 7.5. These spectral bands are highly correlated with respect to soil properties and the SMAF scores. All the correlated wavebands have significant bilateral correlations ($p < 0.01$) for the soil properties and the SMAF scores. Only wavebands for SMAF P scores were identified at $p < 0.05$ for the Hofmeyr 55 ha NW field.

At the Douglas 40 ha field, a large number of wavebands were selected for C, Mg, Na and Mn. However, at Hofmeyr 55 ha NW field more wavebands were observed for pH_e, Mg and GΘ. Interestingly at the Luckhoff 20 ha field, soil quality indicators *viz* N, P, Zn and Cu correlated with more wavebands as compared to other soil properties.

Table 7.1: Descriptive statistics for the SMAF scores and overall soil quality index (SQI) at three study sites

Indicator score	mean	min	max	SD	CV	range
Douglas 40 ha						
pH	0.60	0.56	0.65	0.03	5.00	0.09
ECe	0.83	0	1.00	0.41	49.0	1.00
SOC	0.75	0.24	0.98	0.29	38.7	0.74
P	0.11	0.04	0.27	0.09	81.8	0.23
K	0.99	0.99	1.00	0.001	0.08	0.002
ρb	0.70	0.50	0.90	0.16	22.9	0.40
SQI	0.66	0.52	0.72	0.08	12.1	0.20
Hofmeyr 55 ha NW						
pH	0.98	0.94	1.00	0.02	2.04	0.06
ECe	0.78	0.34	1.00	0.29	37.1	0.66
SOC	0.30	0.09	0.51	0.15	50.0	0.42
P	0.15	0.002	0.33	0.14	93.3	0.33
K	0.99	0.96	1.00	0.02	2.02	0.04
Luckhoff 20 ha						
pH	0.93	0.79	1.00	0.08	8.60	0.21
ECe	0.99	0.96	1.00	0.02	2.02	0.04
SOC	0.08	0.03	0.13	0.03	37.5	0.10
P	0.75	0.01	1.00	0.35	46.7	0.999
K	0.99	0.93	1.00	0.02	2.02	0.06
ρb	0.68	0.52	0.85	0.15	22.1	0.33
SQI	0.74	0.62	0.81	0.06	8.11	0.19

ρb – bulk density; SQI – overall SMAF soil quality index

Different wavebands were selected by the correlation analysis for each soil quality indicator and the SMAF scores in the three fields depending on differences in soil properties (Table 7.2to 7.5). For example, C has a peak around 2052 at Douglas 40 ha field. The closest selected wavebands to 2052 for C from the other two fields is 1872 and 1749 cm^{-1} at Hofmeyr 55 ha NW and Luckhoff 20 ha fields, respectively. Similarly, K have an absorption waveband around 2067 cm^{-1} at the Douglas 40 ha field, but the closest wavenumbers correlating with K

at the other two fields is 1391 and 1812 cm^{-1} at Hofmeyr 55 ha NW and Luchoff 20 ha fields, respectively. This shows that soils from different fields have different spectral characteristics for correlating with a certain soil parameter (Mahmood *et al.,* 2012). The same observation is also true with respect to SMAF scores of the selected soil quality indicators. However, the overall SMAF SQI peaked around 1912 cm^{-1} at Douglas 40 ha centre pivot which was quite close to SQI peak of 1908 cm^{-1} at Luchoff 20 ha centre pivot.

7.3.3 SMLR fusion of soil quality indicators

Multiple linear regression (MLR) is the most widely used method to establish relationships between a dependent variable and more than one independent variables. In step-wise multiple linear regression (SMLR), the independent variables are entered one by one in the model and only those variables that significantly explain variance in the dependant variable are retained. To evaluate the sensor fusion approach to predict soil quality indicators and SMAF scores, SMLR fusion method was used and soil parameters were regressed to both MIR spectra and EC_a measurements. Regression summary statistics for SMLR models estimating the measured multiple soil quality indicators are presented in Table 7.6. Both MIR and EM38 sensors showed different levels of accuracy to predict soil properties and the reason for that observation is that these sensors respond differently to diverse soil properties based on their fundamental principles. Generally, the MIR sensor produced better predictions for all soil properties than the EM38 sensor. This observation was not unexpected since the sensed soil depth using the EM38 was about 0 - 1.5 m whereas soil measurements were restricted to the top 0.30 m soil depth. This suggests that EM38 is not effective in measuring soil properties in the top 0.3 m soil depth. Better prediction results may be obtained when the entire soil profile is considered to incorporate the effective sensitivity of the EM38 sensor (Mahmood *et al*., 2012; McNeill, 1980). Furthermore, the MIR sensor captures soil attributes information better than the EM38 sensor because soil physical, chemical and biological properties have specific absorption dips on the MIR spectra (Pirie *et al.,* 2005; Viscarra Rossel *et al.,* 2006). Generally,

the accuracy of the MIR sensor obtained using specific absorption wavebands identified after first derivative analysis of the spectrum was higher than when using the full MIR region. This observation may be significant as hundreds of redundant wavebands in the full MIR region may interfere in the prediction of a specific soil property. Hence, better and more robust MIR models could be obtained by identifying specific wavebands at which a specific soil property is significantly correlated (Melendez-Pastor *et al.,* 2008). The same observation was also made by Ma *et al*. (2019) who used uninformative variable elimination algorithm to identify MIR wavenumbers for the prediction of soil pH, SOM, total N and available P. Their results demonstrated that reliable selected wavenumbers could improve model accuracy because of avoidance of over- and under-fitting to some extent by the elimination of interference and irrelevant wavebands.

The results in Table 7.6 show that model performance of individual sensors were improved after using SMLR fusion for many soil properties of the centre pivots. At the Douglas 40 ha field, the SMLR fusion method improved the MIR models of pH_w, pH_e, P, Mg, Na, Zn, Mn and sand, reducing the RMSE by 25%, 57%, 12%, 23%, 36%, 9%, 52% and 38%, respectively. Marginal improvement was also observed for the MIR models of EC_e, N, Ca, Cu, GΘ, ρb and clay with only the R^2 of the models slightly improved by the sensor fusion. MIR models of C, K and silt were not substantially improved with the addition of the EC_a data. Both R^2 and RMSE values of these models were not enhanced by the SMLR fusion. Remarkably, at the Hofmeyr 55 ha NW centre pivot, MIR models of many of the measured soil parameters *viz* pH_e, C, N, P, Ca, Na, Zn, Fe, GΘ, clay and sand were improved reflecting 14%, 75%, 33%, 21%, 18%, 57%, 21%, 56%, 42%, 55% and 33% reduction in RMSE values, respectively. MIR models of EC_e, K and Mg were slightly improved with the fusion of MIR and EC_a data with the R^2 values of the models slightly improved by the SMLR fusion. However, the R^2 and RMSE values of the MIR models of pH_w, Mn, Cu and silt were not improved by the fusion of data from both MIR and EC_a sensors. At the Luckhoff 20 ha centre pivot, the SMLR fusion of MIR and EC_a data

improved the MIR models of N, K, Ca, P, Na, Zn, Cu, silt and sand, recording a reduction of the RMSE of the models by 60%, 19%, 29%, 11%, 15%, 24%, 40%, 18% and 26%, respectively. Furthermore, MIR models of pH_w, pH_e, C, P, Mg, GΘ and ρb were slightly improved with the SMLR fusion of MIR and EC_a data. However, MIR model performance of EC_e, Mn, Fe and clay were not improved by the fusion of MIR and EC_a data.

Incidentally, MIR models of Na, Zn and sand from all the three centre pivots from the study sites were substantially improved by the SMLR fusion. The lack of improvement of the MIR models for some of the measured soil properties may indicate the poor ability of the SMLR fusion method to deal with the multi-collinearity among the independent variables. The SMLR is not able to handle a large number of predictor variables than the response variable. The partial least square regression (PLSR) technique can be used to improve the MIR models of the soil properties that could not be improved with the SMLR method. This technique has the ability to handle multi-collinearity among sensor outputs and thus enhances the effectiveness of the sensor data fusion (Viscarra Rossel *et al.,* 2006; Mahmood *et al*., 2012). However, in this preliminary study, the SMLR fusion method has sufficiently demonstrated the effectiveness of applying the sensor fusion approach in improving the models of soil property estimates from single soil sensors.

Absorbance spectrum of Douglas 40 ha soil

First derivative spectrum of relative absorbance for Douglas 40 ha soil

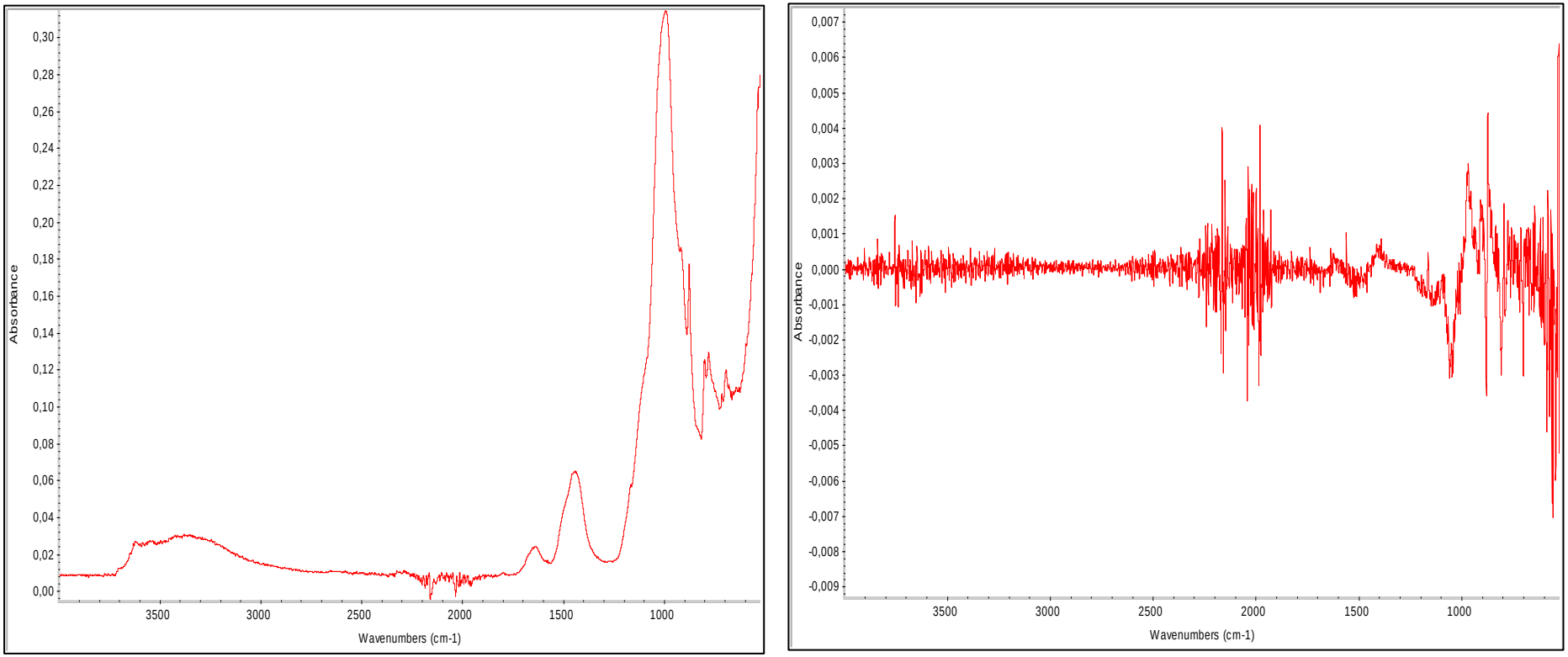

Figure 7.1: Examples of absorbance spectra and first derivative of the absorbance spectra for the Douglas soil

Absorbance spectrum of Hofmeyr 55 ha NW soil

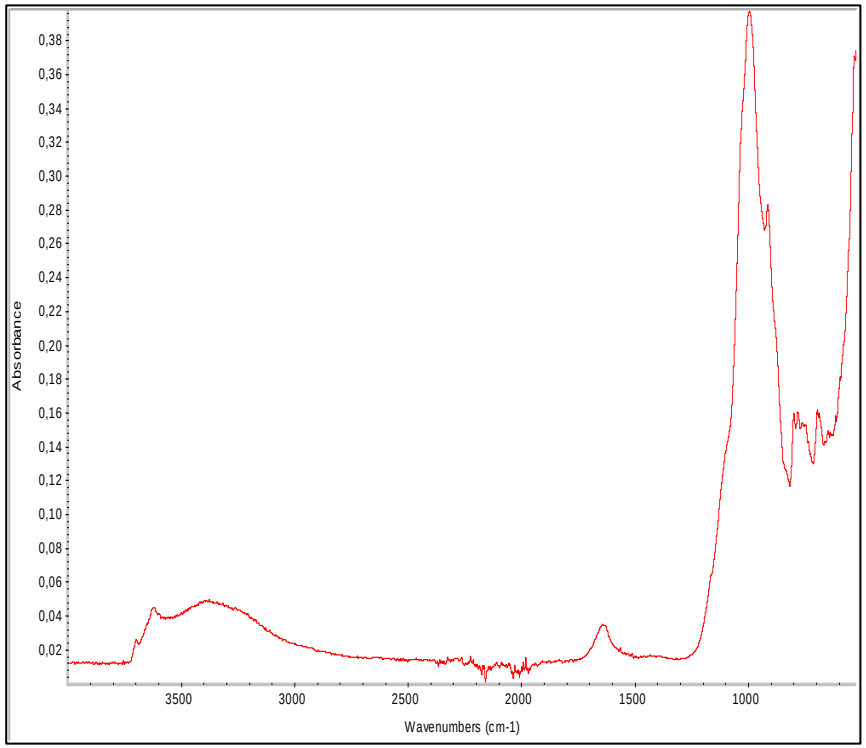

First derivative spectrum of relative absorbance for Hofmeyr 55 ha NW soil

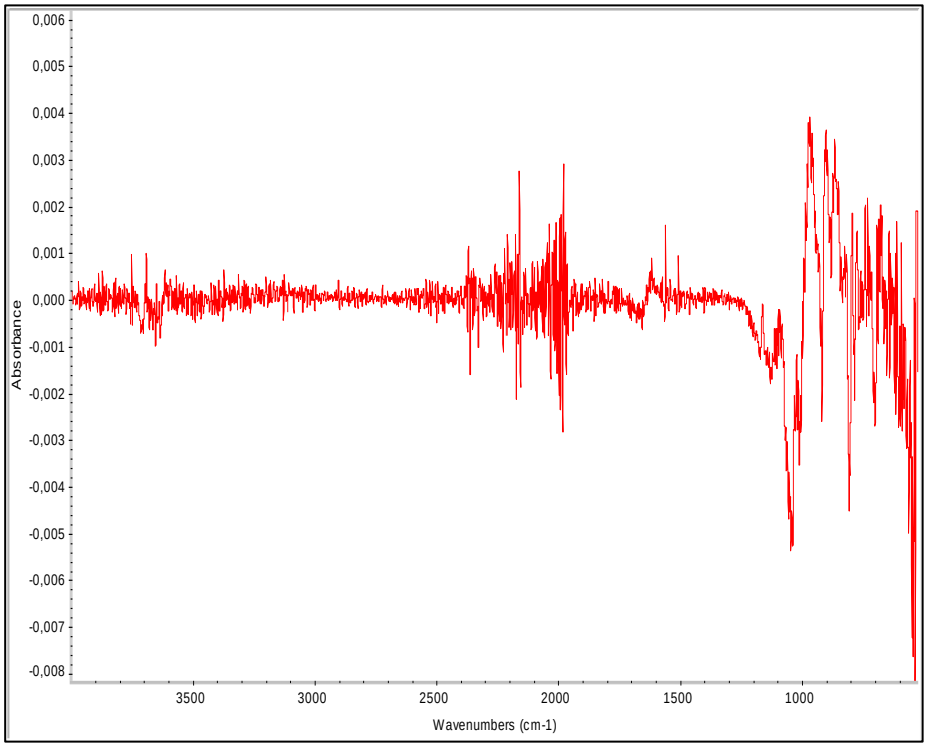

Figure 7.2: Examples of absorbance spectra and first derivative of the absorbance spectra for the Hofmeyr 55 ha NW soils.

Absorbance spectrum of Luckhoff 20 ha soil

First derivative spectrum of relative absorbance for Luckhoff 20 ha soil

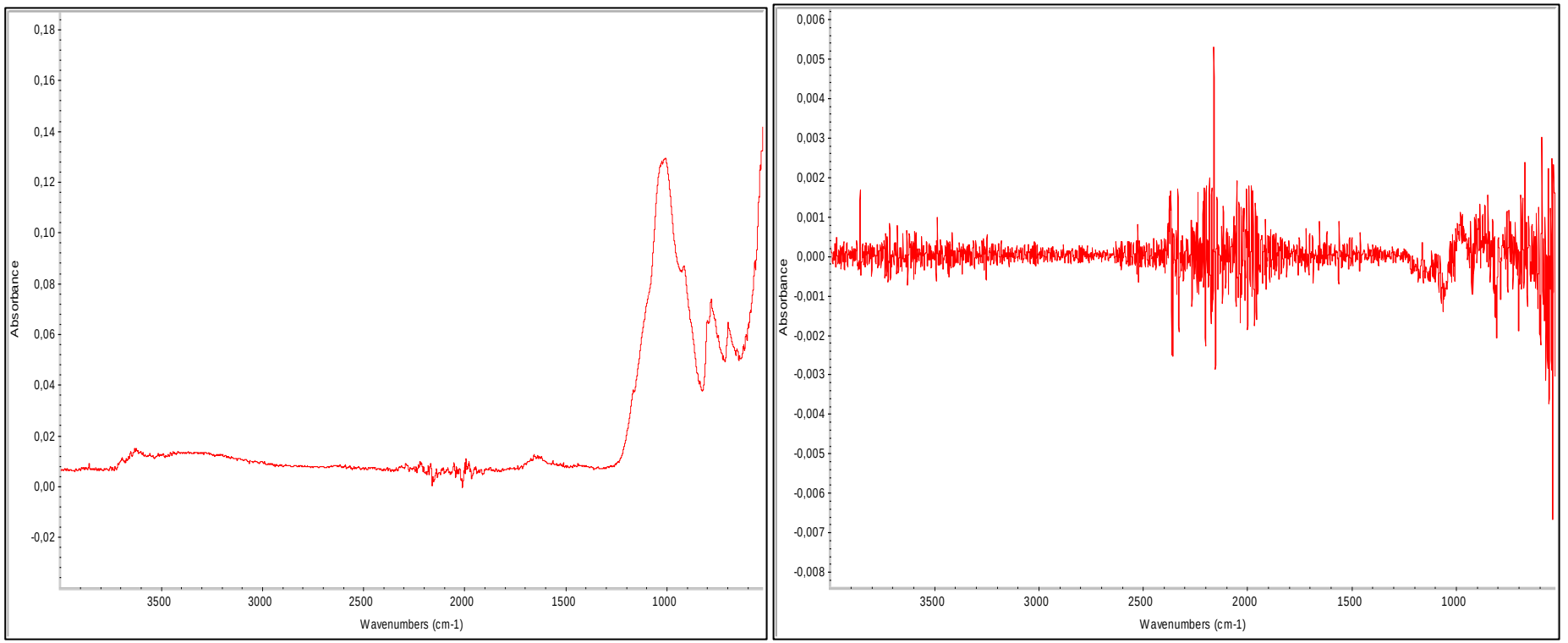

Figure 7.3: Examples of absorbance spectra and first derivative of the absorbance spectra for the Luckhoff 20 ha soil.

Table 7.2: Selected first derivative absorbance bands with high correlation coefficient with respect to soil properties at Douglas 40 ha field.

High Pearson correlation ($r^{**} > 0.75$)												
pH_w	ṽ (cm^{-1})	813	2216									
		-0.947	-0.922									
pH_e	ṽ (cm^{-1})	1055	2139									
	r	-0.934	0.936									
EC_e	ṽ (cm^{-1})	713	2114	2028	2366							
	r	-0.951	-0.971	-0.938	-0.978							
C	ṽ (cm^{-1})	871	872	875	876	877	882	1510	1509	1508	1507	2052
	r	0.940	0.958	0.947	-0.951	-0.939	-0.950	-0.967	-0.940	-0.919	-0.985	-0.950
N	ṽ (cm^{-1})	2237										
	r	-0.955										
P	ṽ (cm^{-1})	808	986	2144	2218	2287						
	r	-0.980	-0.921	0.955	0.937	-926						
K	ṽ (cm^{-1})	1058	2067									
	r	-0.949	0.922									
Ca	ṽ (cm^{-1})	972	1057									
	r	0.950	-0.956									
Mg	ṽ (cm^{-1})	964	969	975	994	1051	1052	1053	1160			
	r	0.975	0.938	0.918	-0.948	-0.931	-0.934	-0.919	0.926			
Na	ṽ (cm^{-1})	965	967	968	971	972	1056	1057	2255			
	r	0.955	0.925	0.939	0.928	0.970	-0.925	-0.962	-0.986			
Zn	ṽ (cm^{-1})	2199	2140	2250								
	r	0.918	0.940	-950								
Mn	ṽ (cm^{-1})	965	967	968	972	973	1057	1058				
	r	0.930	0.922	0.938	0.942	0.967	-0.973	-0.930				
Cu	ṽ (cm^{-1})	960	964	965	968	994						
	r	0.956	0.925	0.938	0.945	-0.990						
GΘ	ṽ (cm^{-1})	2197	2041									
	r	0.918	0.931									
ρb.	ṽ (cm^{-1})	968	2258	2285								
	r	0.937	0.920	-0.972								
Clay	ṽ (cm^{-1})	566										
	r	-0.920										
Sand	ṽ (cm^{-1})	711	712	1503	2260							
	r	0.934	0.935	0.927	0.925							
Silt	ṽ (cm^{-1})	968	2286									
	r	0.951	-0.933									

GΘ – gravimetric water content; ρb – bulk density; ṽ - MIR wavenumber; **-correlation significant at 0.01 probability level.

Table 7.3: Selected first derivative absorbance bands with high correlation coefficient with respect to soil properties at Hofmeyr 55 ha NW field.

High Pearson correlation ($r^{**} > 0.75$)														
pH_w	$\tilde{\nu}$ (cm^{-1})	3374												
	r	-0.923												
pH_e	$\tilde{\nu}$ (cm^{-1})	668	1960	1964	2053	2114	2137	2411	3885					
	r	0.895	-0.902	0.904	0.878	0.968	-0.909	0.889	-0.893					
EC_e	$\tilde{\nu}$ (cm^{-1})	778	1947	2036	2283	3135								
	r	-0.875	0.944	0.915	0.960	0.879								
C	$\tilde{\nu}$ (cm^{-1})	726	1754	1872	3355									
	r	-0.972	-0.934	-0.876	0.946									
N	$\tilde{\nu}$ (cm^{-1})	1391	3355											
	r	-0.923	0.880											
P	$\tilde{\nu}$ (cm^{-1})	570	594											
	r	0.944	0.950											
K	$\tilde{\nu}$ (cm^{-1})	769	1391											
	r	0.955	-0.912											
Ca	$\tilde{\nu}$ (cm^{-1})	570	594	686										
	r	-0.932	-0.913	-0.892										
Mg	$\tilde{\nu}$ (cm^{-1})	570	594	918	1089	1898	2164							
	r	-0.986	-0.908	-0.889	-0.891	-0.882	-0.928							
Na	$\tilde{\nu}$ (cm^{-1})	709	1474	2460	3822									
	r	-0.875	-0.878	0.936	-0.911									
Zn	$\tilde{\nu}$ (cm^{-1})	635	1947											
	r	-0.895	-0.884											
Mn	$\tilde{\nu}$ (cm^{-1})	726	814	1872	3355									
	r	-0.979	-0.927	-0.895	0.888									
Cu	$\tilde{\nu}$ (cm^{-1})	726	814											
	r	-0.892	-0.953											
Fe	$\tilde{\nu}$ (cm^{-1})	570	594											
	r	0.882	0.916											
GΘ	$\tilde{\nu}$ (cm^{-1})	715	703	755	859	960	968	970	1061	1119	1716	1953	2384	3712
	r	0.895	-0.910	-0.877	0.922	0.923	0.895	0.890	-0.997	-0.912	0.887	-0.913	-0.881	-0.888
Clay	$\tilde{\nu}$ (cm^{-1})	916	2165	3820										
	r	-0.882	-0.879	0.876										
Sand	$\tilde{\nu}$ (cm^{-1})	570	918	1042	1898	2164								
	r	0.936	0.926	0.878	0.893	0.895								
Silt	$\tilde{\nu}$ (cm^{-1})	3132												
	r	-0.923												

GΘ – gravimetric water content; ρb – bulk density; $\tilde{\nu}$ - MIR wavenumber; **-correlation significant at 0.01 probability level.

Table 7.4: Selected first derivative absorbance bands with high correlation coefficient with respect to soil properties at Luckhoff 20 ha field.

High Pearson correlation ($r^{**} > 0.75$)																
pH_w	$\tilde{\nu}$ (cm^{-1})	901	2060													
	r	0.876	0.895													
pH_e	$\tilde{\nu}$ (cm^{-1})	555	734	2600	2603	3734										
	r	0.896	-0.930	0.972	-0.975	-0.911										
EC_e	$\tilde{\nu}$ (cm^{-1})	667	2310													
	r	0.917	0.888													
C	$\tilde{\nu}$ (cm^{-1})	701	750	1749	3480											
	r	-0.901	0.900	-0.883	-0.907											
N	$\tilde{\nu}$ (cm^{-1})	750	1393	1435	1515	1560	1618	2178	3630	3651	3671	3861				
	r	0.908	0.878	0.895	0.942	-0.882	-0.917	-0.910	-0.905	-0.921	-0.878	0.935				
P	$\tilde{\nu}$ (cm^{-1})	1364	1425	1486	1505	1506	1538	1575	1615	1652	1655	1682	3566	3737	3868	3879
	r	-0.962	-0.924	0.924	0.908	0.898	0.928	0.891	0.986	0.911	-0.895	0.912	0.880	-0.885	0.875	0.893
K	$\tilde{\nu}$ (cm^{-1})	1438	1682	1812	2124	3897										
	r	-0.952	0.876	-0.943	0.928	0.913										
Ca	$\tilde{\nu}$ (cm^{-1})	719	804	2016	2095	2131										
	r	0.949	-0.896	-0.900	-0.923	-0.965										
Mg	$\tilde{\nu}$ (cm^{-1})	2131														
	r	-0.912														
Na	$\tilde{\nu}$ (cm^{-1})	798	2141	2198												
	r	-0.896	-0.914	0.913												
Zn	$\tilde{\nu}$ (cm^{-1})	750	1645	1648	1682	2304	3671	3855	3879	3897						
	r	0.899	0.899	-0.925	0.914	0.934	-0.936	-0.895	0.892	0.882						
Mn	$\tilde{\nu}$ (cm^{-1})	883	1159	2060												
	r	-0.889	-0.882	-0.911												
Cu	$\tilde{\nu}$ (cm^{-1})	596	602	806	905	1953	1962	2168	2563	3838						
	r	0.931	0.945	-0.940	0.935	0.879	0.943	-0.926	-0.931	0.963						
Fe	$\tilde{\nu}$ (cm^{-1})	1115	1900	1963	2266	3722	3768									
	r	-0.893	-0.911	0.975	-0.907	0.881	0.881									
GΘ	$\tilde{\nu}$ (cm^{-1})	1648														
	r	-0.895														
VΘ	$\tilde{\nu}$ (cm^{-1})	1648														
	r	-0.900														
ρb	$\tilde{\nu}$ (cm^{-1})	701	1000	3480	3484											
	r	-0.944	-0.894	0.902	-0.928											
Clay	$\tilde{\nu}$ (cm^{-1})	910	1157	2093	2226	3462	3806									
	r	0.911	-0.878	0.876	0.888	-0.973	-0.880									
Sand	$\tilde{\nu}$ (cm^{-1})	1794	2225	2226	3462	3944										
	r	-0.935	-0.893	-0.919	0.917	-0.888										
Silt	$\tilde{\nu}$ (cm^{-1})	782	2291													
	r	-0.885	-0.932													

GΘ – gravimetric water content; VΘ – volumetric water content; ρb – bulk density; $\tilde{\nu}$ - MIR wavenumber; **-correlation significant at 0.01 probability level.

Table 7.5: Selected first derivative absorbance bands of SMAF scores of soil quality indicators and soil quality index (SQI) at study sites.

High Pearson correlation ($r^{**} > 0.75$)															
Douglas 40 ha															
pH_w	$\tilde{\nu}$ (cm^{-1})	813													
	r	0.936													
EC_e	$\tilde{\nu}$ (cm^{-1})	2114	2256	2366											
	r	0.958	0.938	0.996											
SOC	$\tilde{\nu}$ (cm^{-1})	1507	2052	2248											
	r	-0.943	-0.948	0.971											
P	$\tilde{\nu}$ (cm^{-1})	2005	2235	2236											
	r	0.922	-0.940	-0.931											
K	$\tilde{\nu}$ (cm^{-1})	620	2053	2182	2192										
	r	-0.951	0.947	-0.952	0.958										
ρb	$\tilde{\nu}$ (cm^{-1})	967	968	2255	2258	2285									
	r	-0.925	-0.944	0.831	-0.925	0.966									
SQI	$\tilde{\nu}$ (cm^{-1})	1912	2088	2179											
	r	-0.923	0.926	0.979											
Hofmeyr 55 ha NW															
pH_w	$\tilde{\nu}$ (cm^{-1})	3751	3374												
	r	-0.882	0.953												
EC_e	$\tilde{\nu}$ (cm^{-1})	800	874	1372	1716	1831	1913	1914	2249						
	r	-0.900	0.889	-0.885	0.895	-0.952	0.915	0.910	0.905						
SOC	$\tilde{\nu}$ (cm^{-1})	726	1872												
	r	-0.934	-0.892												
P	$\tilde{\nu}$ (cm^{-1})	570	594	635	657	814									
	r	0.837	0.775	-0.874	-0.785	-0.839									
K	$\tilde{\nu}$ (cm^{-1})	1391	1534	2004	2008	2065	2210	2292	2296	2370	2382	3457	3815		
	r	-0.893	-0.930	-0.889	0.880	-0.884	-0.933	-0.947	0.902	-0.887	-0.947	-0.904	0.889		
Luckhoff 20 ha															
pH_w	$\tilde{\nu}$ (cm^{-1})	558	766	773	1161	2020	2021	3423							
	r	0.875	0.876	0.911	0.932	0.876	0.922	-0.877							
EC_e	$\tilde{\nu}$ (cm^{-1})	1364	1425	1491	1505 - 1508		1537	1538	1557	1615	1634	1652	1655	3737	3868
	r	0.965	0.906	0.937	-0.877 - 0.937		-0.893	-0.972	-0.877	0.960	-0.875	-0.893	0.882	0.908	-0.916
SOC	$\tilde{\nu}$ (cm^{-1})	750	1515	1682	3671	3861									
	r	0.923	0.886	0.896	-0.886	0.882									
P	$\tilde{\nu}$ (cm^{-1})	1990	2117												
	r	-0.882	0.879												
K	$\tilde{\nu}$ (cm^{-1})	701	2117	2194	2332	3484									
	r	-0.914	0.957	-0.901	-0.888	-0.886									
ρb	$\tilde{\nu}$ (cm^{-1})	561	654	910	2071	2225	3462	3480							
	r	0.925	-0.884	-0.901	0.957	-0.935	0.908	-0.878							
SQI	$\tilde{\nu}$ (cm^{-1})	1908	1960												
	r	0.854	-0.892												

ρb – bulk density; SQI – SMAF soil quality index $\tilde{\nu}$ - MIR wavenumber; ** - correlation significant at 0.01 probability level.

Table 7.6: Regression statistics for models of measured soil properties with MIR spectra and EC_a sensor combinations at three study sites

Sensor	Statistic	pH_w	pH_e	EC_e	C	N	P	K	Ca	Mg	Na	Zn	Mn	Cu	Fe	GΘ	ρb	Clay	Silt	Sand
Douglas 40ha																				
MIR	R^2	0.90	0.88	0.96	0.97	0.91	0.96	0.90	0.91	0.86	0.94	0.84	0.93	0.89	-	0.87	0.95	0.85	0.85	0.87
	RMSE	0.04	0.07	29.5	0.01	0.004	0.08	39.1	121.3	13.1	12.7	0.79	2.14	0.25	-	0.76	0.01	1.62	0.89	2.51
MIR + EC_a	R^2	0.93	0.99	0.97	0.97	0.93	0.97	0.90	0.94	0.94	0.98	0.90	0.99	0.90	-	0.88	0.98	0.88	0.85	0.93
	RMSE	0.03	0.03	29.3	0.01	0.004	0.07	45.0	125.6	10.1	8.11	0.72	1.03	0.28	-	0.82	0.01	1.73	1.03	1.55
Hofmeyr 55 ha NW																				
MIR	R^2	0.85	0.94	0.92	0.90	0.77	0.89	0.91	0.87	0.97	0.88	0.80	0.96	0.91	0.78	0.993	-	0.78	0.85	0.88
	RMSE	0.08	0.07	7.79	0.04	0.009	0.42	8.21	253.5	21.7	10.1	1.51	8.71	0.31	16.9	0.19	-	2.21	1.09	1.94
MIR + EC_a	R^2	0.85	0.97	0.93	0.99	0.90	0.95	0.92	0.93	0.98	0.98	0.88	0.96	0.91	0.97	0.998	-	0.96	0.85	0.96
	RMSE	0.09	0.06	7.93	0.01	0.006	0.33	8.64	206.7	23.2	4.33	1.2	9.14	0.36	7.50	0.11	-	0.99	1.21	1.30
Luckhoff 20 ha																				
MIR	R^2	0.77	0.95	0.84	0.83	0.77	0.97	0.91	0.93	0.83	0.83	0.88	0.83	0.88	0.95	0.80	0.86	0.95	0.87	0.79
	RMSE	0.31	0.09	13.6	0.05	0.01	2.15	35.9	88.3	17.8	7.57	0.67	12.2	0.20	9.42	0.89	0.004	0.48	0.39	1.20
MIR + EC_a	R^2	0.81	0.96	0.84	0.84	0.97	0.98	0.95	0.97	0.85	0.90	0.94	0.83	0.96	0.95	0.85	0.88	0.95	0.93	0.91
	RMSE	0.32	0.09	15.4	0.06	0.004	1.91	29.1	63.1	19.1	6.46	0.51	13.7	0.12	10.5	0.85	0.004	0.50	0.32	0.89

GΘ – gravimetric water content; ρb – bulk density; MIR – mid-infrared sensor; MIR + EC_a – sensor fusion of mid-infrared sensor and apparent electrical conductivity sensor; R^2 – co-efficient of determination; RMSE – root mean square error

7.3.4 SMLR fusion of SMAF scores and overall SMAF SQI

Regression summary statistics for the SMLR models estimating the SMAF scores and the overall SMAF soil quality index are presented in Table 7.7. MIR models for the SMAF scores and SQI were compared with models developed from fusion of both MIR spectra in conjunction with EC_a data. At the Douglas 40 ha centre pivot, ample improvement was noted for the MIR models of only K and ρb SMAF scores which was appropriately reflected by 40% and 33% reduction of their RMSE values, respectively. Slight improvement of the MIR models of pH_w and SOC scores was observed which was reflected with a small improvement of the R^2 values. However, SMLR fusion did not improve the MIR model performance of EC_e and P scores as well as the overall SQI at the Douglas 40 ha field.

At the Hofmeyr 55 ha NW field, the performance of the MIR models of EC_e, SOC and P scores were improved with reduction of RMSE by 40%, 16% and 33%, respectively. Moreover, the MIR model of pH_w SMAF scores was slightly improved as shown by the increase of the associated R^2 from 0.91 to 0.92. However, SMLR fusion did not improve the performance of the model for the SMAF K score. Remarkably, MIR models of EC_e, SOC, P, K and ρb SMAF scores at Luckhoff 20 ha field were improved by combining the MIR spectra and EC_a data as reflected by the reduction of 33%, 50%, 15%, 33% and 20% in their associated RMSE values. For the overall SMAF soil quality index, combining MIR spectra with the EC_a data reduced the RMSE value of the SQI model by 67% and increased the R^2 from 0.73 to 0.94. The SMAF soil quality assessment combines the impact of the soil physical, chemical and biological properties on the overall soil function (Andrews *et al*., 2004). Several factors related to the measurement of these soil properties likely contributed to performance differences among the models. The substantial improvement of the overall SMAF-SQI model indicates that adding EC_a to the MIR spectra provided supplementary information that related to one or more of the SMAF scoring categories. Adding EC_a data improved most of the scored soil parameters related to the soil function categories as reflected by the improved models of the SMAF scores

of EC_e, SOC, P, K and ρb. This significant observation at the Luckhoff 20 ha field provides preliminary evidence that evaluation of alternative sensor combinations may lead to improved and more robust estimations of soil quality. The unsuccessful improvement of the overall SMAF-SQI model at the Douglas 40 ha centre pivot is reflected by the inability of the SMLR fusion to substantially improve model performance of most of the scored individual soil quality indicators. However, generally across the three centre pivots the MIR models of the SMAF scores were improved by the SMLR fusion of MIR spectra and EC_a sensor data. The sensor fusion results from this study demonstrates that sensor fusion is more robust and provides extended attribute coverage and complementary information on certain soil properties and overall soil quality.

Table 7.7: Regression statistics for models of SMAF scores and soil quality index (SQI) with MIR spectra and EC_a sensor combinations at three study sites

Sensor	Statistic	pH_w score	EC_e score	SOC score	P score	K score	ρb score	SQI
Douglas 40ha								
MIR	R^2	0.87	0.99	0.94	0.98	0.90	0.93	0.96
	RMSE	0.01	0.03	0.05	0.01	0.0002	0.03	0.02
MIR + EC_a	R^2	0.89	0.99	0.96	0.98	0.98	0.98	0.96
	RMSE	0.01	0.03	0.05	0.01	0.0001	0.02	0.02
Hofmeyr 55 ha NW								
MIR	R^2	0.91	0.82	0.87	0.76	0.90	-	-
	RMSE	0.005	0.10	0.043	0.06	0.004	-	-
MIR + EC_a	R^2	0.92	0.95	0.93	0.89	0.90	-	-
	RMSE	0.005	0.06	0.036	0.04	0.004	-	-
Luckhoff 20 ha								
MIR	R^2	0.87	0.93	0.78	0.78	0.92	0.82	0.73
	RMSE	0.02	0.003	0.014	0.13	0.006	0.05	0.03
MIR + EC_a	R^2	0.88	0.97	0.88	0.88	0.97	0.94	0.94
	RMSE	0.02	0.002	0.007	0.11	0.004	0.04	0.01

ρb – bulk density; SQI – overall SMAF soil quality index; MIR – mid-infrared sensor; MIR + EC_a – sensor fusion of mid-infrared sensor and apparent electrical conductivity sensor; R^2 – co-efficient of determination; RMSE – root mean square error

7.4 Conclusions

Irrigation presents an effective tool that can be used to increase the grain yields in South Africa. However, efficient overall soil quality assessment of the irrigated fields is essential to develop appropriate soil and crop management strategies and to enhance the grain yield. A comprehensive assessment of soil quality requires the concurrent measurement of soil physical, chemical and biological properties. High-resolution, rapid and cost-effective techniques for the measurement of soil properties and overall soil quality are highly valuable for soil conservation and to improve soil productivity of irrigation systems. This study presents the use of the sensor fusion approach to estimate several soil quality indicators and overall SMAF soil quality index of irrigated soils from three study sites using the MIR spectra data in conjunction with EC_a data.

Generally, models for measured soil parameters based on SMRL fusion of data from MIR and EC_a sensor measurements were more robust as compared to the models developed from individual sensors. Furthermore, SMLR fusion also improved models of SMAF scores of the selected soil quality indicators across the selected centre pivot fields from the study sites. The sensor fusion approach using the SMLR fusion technique did not improve the MIR model performance of the overall soil quality index (SQI) at the Douglas 40 ha field. However, there was a substantial improvement of the MIR model performance of the overall SQI of the Luckhoff 20 ha field. The study concludes that sensor data fusion approach can enhance the efficient and robust measurement of soil properties and overall soil quality using soil sensors in irrigated agriculture. Sensor fusion has the potential to reliably estimate comprehensive SQI for environmental protection, improved sustainability and productivity of irrigation systems.

CHAPTER 8: GENERAL CONCLUSIONS AND RECOMMENDATIONS

8.1 General conclusions

The efficiency and environmental safety of agricultural production systems that have been engaged to meet the rapid rise in global demand for food have been questioned (Adamchuk *et al.,* 2011). Sustainable agriculture is considered the most feasible means of meeting the increasing future global demand for food through its goal of delicately balancing crop productivity, profitability, natural resource use and environmental effects (Corwin *et al*., 1999). One of the key approaches for achieving sustainable agriculture is site-specific management through precision agriculture (Lowenberg-DeBoer and Erickson, 2000). However, the achievement of sustainable agriculture through the application of precision agriculture requires the development and adaptation of innovative new methodologies to assess and quantify soil properties as well as their spatial and temporal variability at field scale. The aim of the study was to investigate the use of soil sensors in assessing multiple soil fertility parameters and their variability under irrigation using infrared reflectance spectroscopy and electromagnetic induction for the purpose of site-specific management. The study also aimed to evaluate the use of a sensor fusion approach to evaluate multiple soil properties and the overall soil quality using the Soil Management Assessment Framework (SMAF). The contributions from this study will assist irrigation farmers, researchers, educators and policymakers in the soil science fraternity in South Africa to embrace, develop and implement site-specific sensor-based soil and crop management.

Although the literature review (Chapter 2) shows that numerous attempts have been made to evaluate the use of sensors in evaluating soil fertility parameters, model prediction accuracy and scale has been identified as critical factors. Moreover, most studies did not investigate the use of soil sensors on a full spectrum of soil properties. Even though studies on individual sensors show promising findings, no single sensor has been able to fully characterize the spatial and temporal complication of soils. As a result, the studies of the fusion of

measurements from different sensors have become a subject of on-going research in recent times (Karlen *et al.,* 2019). On that note, research on soil sensor technology with a particular emphasis on improving model performance through sensor fusion technology is urgently required. Therefore this study was positioned on following a set of specific objectives: (i) to determine the predictive capabilities of the mid-infrared (MIR) spectral datasets obtained with an iS50 FTIR spectrophotometer for predicting nutrients in soil and plant samples under irrigation, (ii) to determine whether EC_a can serve as an estimator of plant nutrient levels for the demarcation of site-specific management zones in irrigated fields, (iii) to spatially characterize within-field variability of plant nutrients and crop yield under irrigation in wheat-maize cropping sequence, (iv) to characterize the spatial variability of seasonal nutrient removal by wheat and maize crops for formulating nutrient replacement strategies under irrigation, and (v) to evaluate a sensor data fusion approach on soils from irrigated fields using MIR spectra in conjunction with EC_a data to estimate multiple soil quality indicators, SMAF scores and overall soil quality.

The soil sensors used in this study *viz* MIR sensor and EM38 sensor showed different levels of accuracy with respect to predicting soil fertility properties under irrigation (Chapter 4). The predictive models obtained from data from the MIR sensor showed good accuracy with respect to most of the measured soil properties. The study results demonstrated the effectiveness and usefulness of the MIR attenuated reflectance technique in quantitative analysis of soil fertility properties. However, unstable models were identified for some soil properties such as P, K, Fe and Zn when all the samples from the study sites were grouped. This observation may suggest that in some cases, developing site-specific models may be more appropriate to achieve more accurate models for some soil fertility properties (Shaviv *et al.,* 2003; Linker *et al*., 2004; 2005). However, this may reduce the efficiency of developing more robust models that incorporate multiple soil types. The same observation was also noted with the EM38 sensor, where most of the soil properties that were modelled accurately with the EM38 sensor

were site-specific (Chapter 4). However, the EM38 sensor modelled accurately only a few soil properties per site at a given sampling time. Moreover, most of the EC_a models were not stable over two seasons. Hence, for site-specific management using EC_a survey data, ground-truth samples at a site for each given EC_a survey is a necessity. The model results for both sensors show that the MIR sensor produced better prediction models for all soil properties than the EM38 sensor. This observation could be attributed to the principle of measurement of the EM38. The EM38 sensor is designed to measure soil properties in the entire soil profile up to 1.5 m. Hence, better models could have been obtained if the entire soil profile per site was considered (McNeill, 1980). Moreover, EC_a measurement is a complex measurement which reflects the interaction of several site-specific soil properties. Hence, interpreting the EC_a measurement at a given site requires the knowledge of many site-specific factors which may not have been considered in this study.

The use of sensors in quantifying nutrient accumulation in wheat and maize components was attempted in Chapter 5. The study also endeavoured to quantify the accumulation of nutrients by each crop during the growing season. At harvest, most of the nutrients, *viz* K, Ca, Mg, Na, B, Cu, Fe and Mn accumulated in the stem and leaves of wheat and maize. Hence, most of these nutrients could be remobilized back in the soil through retaining the residues of these crops after harvest. In contrast, P and Zn were partitioned the most in the grain component of wheat and maize. Consequently, most of the total P and Zn taken up by the wheat and maize are harvested with the grain component. Generally for most nutrients, total nutrient removal by maize was more as compared to the total nutrient removal by wheat at each field at the study sites. Maize is generally a high biomass crop as compared to wheat which explains its propensity to harvest more nutrients than wheat. These observations may be significant for the formulation of nutrient replacement strategies after each growing season.

The MIR technique produced excellent predictive models for the nutrient concentrations in wheat samples (Chapter 5). However, the models for the nutrient concentrations in maize samples were not as accurate as those derived from the wheat samples. The reason for this observation could be due to the dilution effect of high maize biomass as compared to the wheat at harvest. Haung *et al.,* (2009) reported difficulties in measurements of NIR absorption changes of nutrient concentrations when low concentration of nutrients encountered large spectral variation due to issues such as low signal-to-noise ratio and repack error. Their study findings showed that R^2 for prediction increased with mean nutrient concentration. They concluded that stronger response may be interpreted from the spectra with higher concentration of nutrients, thus providing better correlations. Lower MIR model accuracy for some nutrient concentrations in maize suggests that further work is still required to improve the accuracy of the MIR technique in this regard using different strategies. However, the MIR technique provided acceptable results for a rapid analysis of nutrient concentrations in wheat and maize without sample pre-treatment.

The Pearson correlation coefficient was used to study the relationships of EC_a with crop yields and total nutrient uptake at each study site (Chapter 5). Strong and significant correlation was only observed at Luckhoff 60 ha NE field for wheat and maize. Generally, studies on EC_a-crop yield relationships have been met with inconsistent results which were also the case in this study. The reasons for these inconsistences have been highlighted as the complex interactions of biological, anthropogenic and climatological factors that affect crop yields beyond the site-specific soil factors (Corwin and Lesch, 2003).

The findings in Chapter 6 on the in-field spatial characterization of plant nutrient levels and crop yields at the study sites showed that although EC_a readings may be useful for the spatial characterization of some soil fertility properties in non-saline and non-sodic soils, the results showed many inconsistencies between sites and between the centre pivots. These findings

most certainly confirm the site-specific nature of the application of EC_a measurements and that the interpretation of the EC_a measurements is restricted by findings of this nature. Moreover, the study findings confirm that more research is required for application over larger spatial scales. However, taking the nature of the findings of this study, this may not be feasible.

Robustness of a single sensor is often less than ideal because practically most of the sensors respond to more than one soil parameter of interest (Adamchuk *et al*., 2011). A sensor fusion approach that integrates measurements from different sensors has the potential to improve the measurement accuracy of important soil properties and overall soil quality. The findings in Chapter 7 demonstrated that models obtained based on fusion of data from MIR sensor and EM38 sensor measurements were more robust as compared to models from individual sensors. The SMLR fusion method failed to improve the models of some soil properties at the selected fields as well as the overall SMAF soil quality index at the Douglas 40 ha field. A more robust fusion technique such as PLSR can be used to implement the data fusion for these properties. It is of particular importance to note that the performance of the sensor fusion approach in soil property assessments is mostly affected by the type of the sensors used for data fusion. More superior findings are expected where individual sensors also show good correlation with soil properties. In this study, the MIR sensor showed good correlations with most soil properties when specific MIR wavebands that correlated highly with soil properties were identified. Hence, despite low correlations between EC_a measurements and most soil properties at the study sites, the estimations of the soil quality indicators and SMAF scores were mostly improved by sensor fusion. Other studies also observed the same findings, howbeit mostly using NIR in conjunction with EC_a and other sensors (Schirrmann *et al.,* 2011; Mahmood *et al.,* 2012; Veum *et al*., 2015; 2017). These observations may also indicate that the poor correlation of EC_a with soil properties can also enhance the model performance during sensor fusion. Despite many potential benefits of employing the sensor fusion approach in overall soil quality assessments, the approach may be hindered due to the difficulty of handling

large volumes of sensory data from multiple sensors, lack of accuracies in positioning systems using multiple sensors real-time and complex statistical techniques to be used for the sensor data fusion (Mahmood *et al.,* 2012). Nevertheless, the benefits of the sensor fusion have been recognized by researchers and developers and more research on sensor fusion for precision agriculture is expected in the near future.

8.2 Recommendations for further research

The MIR technique has been demonstrated to be efficient in quantifying soil fertility properties and nutrient accumulation in wheat and maize. A major advantage of the spectroscopic techniques for soil and plant analysis is that from a single spectrum many properties may be determined, thus offering an opportunity to reduce costs and increased efficiency over conventional techniques. Combining MIR technique with PLSR presents an attractive option that can be recommended for in-field monitoring, modelling and site-specific management of soil and crop properties in irrigation systems.

The findings of this study showed the inconsistency of using EC_a measurements in evaluating and quantifying soil fertility properties and their variability in irrigated agriculture. Therefore, it is highly recommended to evaluate the use of EC_a sensors as complementary sensors to supplement other sensors such as electrochemical sensors. The electrochemical sensors use ion-selective membranes to detect the activity of ions such as H^+, K^+ or NO_3^-. These sensors have been successfully used to directly evaluate some soil fertility properties (Adamchuk *et al*., 2011). Since EC_a is primarily related to the physical soil characteristics such as texture, water content and minerology, complementing EC_a measurements with electrochemical sensors will improve the potential of EC_a measurements in the evaluation of soil fertility properties and their variability in irrigated agriculture.

The study findings also showed that the accuracy of the MIR models obtained after identifying the specific wavebands where a certain soil property is highly correlated was higher than when the whole MIR region was considered. However, the process of identifying the highly correlated wavebands was strenuous since the process involved obtaining a few wavenumbers from spectral data consisting of more than 3000 wavenumbers. In that regard, more efficient spectral data handling techniques are essential. Moreover, sensor fusion involves handling large volumes of sensory data from multiple sensors. Hence, more efficient statistical techniques are still required in handling and processing large volume of data effectively for sensor data fusion.

The use of the sensor fusion approach in assessing and quantifying soil quality indicators and overall soil quality using MIR sensor and EM38 sensor has been demonstrated to be superior. However, the MIR spectra data was obtained in the laboratory. Only the EC_a measurements were taken under field conditions. Fusing sensor-based techniques in the field has the potential to reliably estimate comprehensive overall in-field soil quality assessments. Therefore, it is recommended to test the use of the MIR technique under field conditions to enhance the efficiency of the MIR and EC_a fusion technique for in-field use and environmental monitoring.

This study was only limited to the use of the MIR sensor and EM38 sensor for evaluation of soil fertility and its variability in irrigated agriculture. Other sensors exist such as mechanical, gamma ray and X-ray sensors. These presents an opportunity to further study the soil characteristics and overall soil quality using the sensor fusion of the MIR, EC_a and/or one or two of these contemporary sensors depending on availability and efficiency.

9.0 REFERENCES

ABDU H., ROBINSON D.A., SEYFRIED M. & JONES S.B. 2008. Geophysical imaging of watershed subsurface patterns and prediction of soil texture and water holding capacity. *Water Resource Research* 44, W00D18.

ADAMCHUK V.I. & CHRISTENSEN P.T. 2005. An integrated system for mapping soil physical properties on-the-go: the mechanical sensing component. In: *Precision Agriculture: Papers from the Fifth European Conference on Precision Agriculture*, Uppsala, Sweden, 9-12 June 2005, ed. J. Stafford, 449-456. Wageningen Academic Publishers, Wageningen, The Netherlands.

ADAMCHUK V.I., HUMMEL J.W., MORGAN M.T. & UPADHYAYA S.K. 2004. On-the-go soil sensors for precision agriculture. *Computers and Electronics in Agriculture* 44:71–91.

ADAMCHUK V.I., LUND E.D., SETHURAMASAMYRAJA B., MORGAN M.T., DOBERMANN A. & MARX D.B. 2005. Direct measurement of soil chemical properties on-the-go using ion-selective electrodes. *Computers and Electronics in Agriculture* 48: 272-294.

ADAMCHUK, V.I., VISCARRA ROSSEL, R.A., SUDDUTH, K.A., SCHULZE & LAMMERS, P. 2011. Sensor fusion for precision agriculture. In: Thomas, C. (Ed.), *Sensor Fusion - Foundation and Applications.* In Tech, Rijeka, Croatia, pp. 27–40.

AGRICULTURAL RESEARCH COUNCIL SMALL GRAIN INSTITUTE (ARC–SGI). 2015. Wheat production guidelines: *Production of the small grains in the summer rainfall area.* Pretoria: South Africa.

AL-GAADI K.A. 2012. Employing electromagnetic induction technique for the assessment of soil compaction. *American Journal of Agricultural and Biological Sciences* 7: 425-434.

ANDREWS S.S., KARLEN D.L. & CAMBARDELLA C.A. 2004. The soil management assessment framework: a quantitative soil quality evaluation method. *Soil Science Society of America Journal* 68:1945–1962.

AGRI LABORATORY ASSOCIATION OF SOUTHERN AFRICA (AgriLASA). 2004. Soil Handbook. Pretoria (South Africa): *Agri Laboratory Association of Southern Africa.* Pretoria, South Africa.

ATHERTON B.C., MORGAN M.T., SHEARERE S.A., STOMBAWGH T.S. & WARD A.D. 1999. Site-specific farming: a perspective on information needs, benefits and limitations. *Journal of Soil and Water Conservation* 54 (2): 455–461.

BARNARD J.H., VAN RENSBURG L.D., VAN ANTWERPEN R., VAN HEERDEN P.S., JUMMAN A., STEENEKAMP D., GROVÉ B., & DU PREEZ C.C. 2020. On-farm water and salt management guidelines for irrigated crops: Level three decision support. *Water Research Commission*, *Report No*: K5/2499/4, Pretoria, South Africa.

BARRIOS, M. DOS R., MARQUES JUNIOR, J., PANOSSO A.R., SIQUEIRA D.S., & LA SCALA JR. N., 2012. Magnetic susceptibility to identify landscape segments on a detailed scale in the region of Jaboticabal. Sao Paulo, Braz. Rev. Bras. *Ciênco Solo* 36:1073-1082.

BATTEN G.D., 1998. Plant analysis using near-infrared reflectance spectroscopy: the potential and the limitations. *Australian Journal of Experimental Agriculture* 38:697-706. doi: 10.1071/EA97146

BAUER R., NIEUWOUDT H., KOSSMANN J., KOCH R.K. & ESBENSEN K.H. 2008. FTIR Spectroscopy for grape and wine analysis. *Analytical chemistry.* American Chemical Society 2008.

BEN-DOR E. & BANIN A. 1995. Near-infrared analysis as a rapid method to simultaneously evaluate several soil properties. *Soil Science Society of America Journal* 59, 364– 372.

BENDER R. 2012. Nutrient uptake and partitioning in high-yielding corn. *Master Thesis, Crop Sciences*, University of Illinois, Urbana, Illinois, USA.

BOGREKCI I. & LEE W. S. 2005b. Spectral Soil Signatures and sensing Phosphorus. *Biosystems Engineering* 92:527–533.

BROCCA L., MELONE F. & MORAMARCO R. 2009. Soil moisture temporal stability over experimental areas in central Italy. *Geoderma* 148: 364-374.

BROCCA L., MELONE F., MORAMARCO T. & MORBIDELLI R. 2010. Spatial- temporal variability of soil moisture and its estimation across scales. *Water Resource Res*earch 46, p. W02516.

BRONSON K.F., BOOKER J.D., OFFICER S.J., LASCANO R.J., MAAS S.J., SEARCY S.W. & BOOKER J. 2005. Apparent Electrical Conductivity, Soil Properties and Spatial Covariance in the U.S. Southern High Plains. *Precision Agriculture* 6:297-311.

BULLOCK D.S. & BULLOCK D.G. 2000. Economic optimality of input application rates in precision farming. *Precision Agriculture* 2:71–101.

BYLER D. M., GERASIMOWICZW. V., SUSI H. & SCHNITZER M. 1987. FTIR spectra of soil constituents: fulvic acid and fulvic acid complex with ferric ions. *Applied Spectroscopy* 41:1428–1430.

CAMPBELL C.R. 2000. Reference sufficiency ranges for plant analysis in the Southern Region of the United States. www.ncagr.gov/agronomi/saaesd/scsb394.pdf [Accessed: 24 September 2020].

CHANG J., CLAY D.E., CARLSON C.G., CLAY S.A. & REESE C. 2001. Determining the impact of approaches to classify nutrient management zones. *In* P.C. Robert et al. (ed.) *Precision agriculture - Proceeding of the 5th International Conference Minneapolis, MN, 16–19 July 2000.* ASA, CSSA, and SSSA, Madison, WI.

CHANG C.W., LAIRD D.A., MAUSBACH M.J. & HURBURGH C.R. 2001. Near-infrared reflectance spectroscopy-principal components regression analysis of soil properties. *Soil Science Society of America Journal* 65:480-490.

CHANGWEN D., ZHAOYANG M., JIANMIN Z. & GOYNE K.W. 2013. Application of mid-infrared photoacoustic spectroscopy in monitoring carbonate content in soils. *Sensors & Actuators B*: *Chemical* 188:1167-1175.

CHEN M., GLAZ B., GILBERT R.A., DAROUB S.H., BARTON F.E. & WAN Y. 2002. Near-infrared reflectance spectroscopy analysis of phosphorus in sugarcane leaves. *Agronomy Journal* 94:1324 –1331. doi:10.2134/agronj2002.1324

CHERUBIN M.R., KARLEN D.L., FRANCO A.L.C., CERRI C.E.P., TORMENA C.A. & CERRI C.C., 2016. A Soil Management Assessment Framework (SMAF) evaluation of Brazilian sugarcane expansion on expansion on soil quality. *Soil Science Society of America Journal* 80:215–226. https://doi.org/10.2136/sssaj2015.09.0328.

CHRISTY C. D. 2008. Real-time measurement of soil attributes using on-the-go near infrared reflectance spectroscopy. *Computers and Electronics in Agriculture* 61:10–19.

CORWIN D.L., KAFFKA S.R., HOPMANS J.W., MORI Y., Van GROENIGEN J.W., Van KESSEL C. LESCH S.M. & OSTER J.D. 2003a. Assessment and field-scale mapping of soil quality properties of a saline-sodic soil. *Geoderma* 114: 231 - 259.

CORWIN D.L. & LESCH S.M. 2003. Application of soil electrical conductivity to precision agriculture: theory, principles, and guidelines. *Agronomy Journal* 95: 455 – 471.

CORWIN D.L. & LESCH S.M. 2005. Characterizing soil spatial variability with apparent soil electrical conductivity: Part II. Case study. *Computers and Electronics in Agriculture* 46: 103–133.

CORWIN D.L. & LESCH S.M. 2005a. Apparent soil electrical conductivity measurements in agriculture. *Computers and Electronics in Agriculture* 46:11–43.

CORWIN, D.L., & LESCH, S.M., 2005b. Characterizing soil spatial variability with apparent soil electrical conductivity: I. survey protocols. *Computers and Electronics in Agriculture* 46:103–133.

CORWIN D.L. & LESCH S.M. 2005c. Characterizing soil spatial variability with apparent soil electrical conductivity: Part II. Case study. *Computers and Electronics in Agriculture* 46:135–152. doi:10.1016/j.compag.2004.11.003

CORWIN D.L. & LESCH S.M. 2010. Delineating site-specific management units with proximal sensors. In: Oliver M.O. (Ed.), *Geostatistical Applications for Precision Agriculture.* Springer, New York, NY, USA, pp. 139–165.

CORWIN D.L., LESCH S.M., OSTER J.D. & KAFFKA S.R. 2006. Monitoring management induced spatio-temporal changes in soil quality through soil sampling directed by apparent electrical conductivity*. Geoderma* 131:369–387.

CORWIN D.L., LOAGUE K. & ELLSWORTH T.R. 1999. Assessing non-point source pollution in the vadose zone with advanced information technologies. In: Corwin D.L. *et al.* (Eds.), Assessment of Nonpoint Source Pollution in the Vadose Zone. *Geophysical Monograph Series* 108:1–20. AGU, Washington, D.C., USA.

CORWIN D.L. & SCUDEIRO E. 2016. Field-Scale Apparent Soil Electrical Conductivity. *In Methods of Soil Analysis* doi:10.2136/methods-soil.2015.0038

COZZOLINO D. & MORON A. 2004. Exploring the use of near infrared reflectance spectroscopy (NIRS) to predict trace minerals in legumes. *Animal Feed Science Technology* 111:161–173. doi:10.1016/j.anifeedsci.2003.08.001

DAVIS, D. R. (2009): Declining fruit and vegetable nutrient composition: What is the evidence? *Horticulture Science* 44:15–19.

DEMATTE J. A. M., CAMPOS R. C., ALVES M. C., FIORIO P. R. & NANNI M. R. 2004. Visible-NIR reflectance: a new approach on soil evaluation. *Geoderma* 121:95–112.

DESBIEZ A., MATTHEWSA R., TRIPATHI B. & ELLIS-JONES J. 2004. Perceptions and assessment of soil fertility by farmers in the mid-hills of Nepal. *Agriculture, Ecosystems and Environment* 103:191–206.

DIERKE C. & WERBAN U. 2013. Relationships between gamma-ray data and soil properties at an agricultural test site. *Geoderma* 199:90-98.

DJAMAN K., IRMAK S., MARTIN D. L., FERGUSON R. B. & BERNARDS M. L. 2013. Plant Nutrient Uptake and Soil Nutrient Dynamics under Full and Limited Irrigation and Rain-fed Maize Production. *Agronomy Journal* 105(2):527-538.

DOOLITTLE J.A., INDORANTE, S.J., POTTER D.K., HEFNER S.G. & MCCAULEY W.M. 2002. Comparing three geophysical tools for locating sand blows in alluvial soils of southeast Missouri. *Journal of Soil Water Conservation* 57:175–182.

DOOLITTLE J.A., SUDDUTH K.A., KITCHEN N.R. & INDORANTE S.J. 1994. Estimating depths to clay pans using electromagnetic induction methods. *Journal of Soil and Water Conservation* 49:572 - 575.

DU C W. & ZHOU J. M. 2007. Prediction of soil available phosphorus using Fourier Transform infrared photoacoustic spectroscopy. *Chinese Journal of Analytical Chemistry* 35:119–122.

DU C.W. & ZHOU J.M. 2009. Evaluation of Soil Fertility Using Infrared Spectroscopy – A Review. *Environmental Chemistry Letters* 7:97-113.

DU C. W., ZHOU J. M., WANG H. Y., CHEN X. Q., ZHU A. N. & ZHANG J. B. 2009. Determination of soil properties using infrared photoacoustic spectroscopy using techniques of partial least square (PLS). *Vibrational Spectroscopy* 49:32–37.

DU PREEZ C. C. & BENNIE A. T.P. 1991. Concentration, accumulation and uptake rate of macro-nutrients by winter wheat under irrigation. *South African Journal of Plant and Soil* 8(1):31-37. doi:10.1080/02571862.1991.10634576

DUCKWORTH J. H. 1998. Spectroscopic qualitative analysis. In J. Workman Jr & A. Springsteen (Eds.). *Applied spectroscopy: A compact reference for practitioners* (pp. 93–163). London: Academic Press.

EDEH J.A. 2017. Quantifying spatio-temporal soil water content using electromagnetic induction. MSc dissertation, University of the Free State, Bloemfontein, South Africa.

EIGENBERG, R.A., DORAN, J.W., NIENABER, J.A., FERGUSON, R.B. & WOODBURY, B.L., 2002. Electrical conductivity monitoring of soil condition and available N with animal manure and a cover crop. *Agriculture, Ecosystems & Environment* 88:183 - 193.

EKWUE E.I. & BARTHOLOMEW J. 2011. Electrical conductivity of some soils in Trinidad as affected by density, water and peat content. *Bio system Engineering* 108:95-103.

ESBENSEN K. H. 2002. Multivariate Data Analysis–In Practice. 5th ed.; Camo ASA: Oslo, 2002.

EVANS J. D. 1996. Straightforward statistics for the behavioral sciences. Pacific Grove, CA: Brooks/Cole Publishing.

FAINTHFULL N. T. 2002. Methods in Agricultural Chemical Analysis. CABI Publishing, pp. 57–104.

FARAHANI H.J., BUCHLEITER G.W. & BRODAHL M.K. 2004. Characterization of apparent electrical conductivity variability in irrigated sandy and non-saline fields in Colorado. *American Society of Agricultural Engineers* 48(1):155-168.

FENG Y.W., YOSHINAGA I., SHIRATANI E., HITOMI T. & HASEBE H. 2005. Nutrient balance in a paddy field with a recycling irrigation system. *Water Science & Technology* 51:3-4,151–157 @ IWA Publishing 2005.

FERGUSON, R.B., G.W. HERGERT, J.S. SCHEPERS, C.A. GOTWAY, J.E. CAHOON, & PETERSON T.A. 2002. Site-specific nitrogen management of irrigated maize: Yield and soil residual nitrate effects. *Soil Science Society of America Journal* 66:544–553. doi:10.2136/sssaj2002.0544

FERTILIZER SOCIETY OF SOUTH AFRICA (FSSA). 2007. FSSA Fertilizer Handbook. Fertilizer Society of South Africa, Pretoria, South Africa

FOOD AND AGRICULTURAL ORGANIZATION (FAO). 2002. Food security in Africa. *Rome*, 2002. 51p. (Water Reports, n.7).

FOOD AND AGRICULTURAL ORGANIZATION (FAO). 2006. Nutrient management guidelines for some major field crops. *Plant Nutrition and Environmental Issues* 11: 301– 302.

FOTH H.D. & ELLIS B.G. 1988. Soil fertility. Wiley, New York, New York.

FRAISSE, C.W., SUDDUTH K.A., KITCHEN N.R., & FRIDGEN J.J. 1999. Use of unsupervised clustering algorithms for delineating within-field management zones. *American Society of Agricultural Engineers Meetings Papers No.* 993043. International lines, CO Meeting, Toronto, Ontario, Canada. July 18–21.

FRANCIOSO O., FERRARI E., SALADINI M., MONTECCHIO D., GIOACCHINI P. & CIAVATTA C. 2007. TG–DTA, DRIFT and NMR characterisation of humic-like fractions from olive wastes and amended soil. *Journal of Hazardous Materials* 149:408–417.

FRANZEN D.W. & KITCHEN N.R. 1999. Developing management zones to target nitrogen applications*. Site-Specific Management Guidelines.* SSMG-5. Potash and Phosphate Inst., Norcross, GA.

FRIEDMAN S.P. 2005. Soil properties influencing apparent electrical conductivity: A review. *Computers and Electronics in Agriculture* 46: 45 - 70.

FUENTES M., GOVAERTS B., DE LEÓN F., HIDALGO C., DENDOOVEN L., SAYRE K.D. & ETCHEVERS J. 2009. Fourteen years of applying zero and conventional tillage, crop rotation and residue management systems and its effect on physical and chemical soil quality. *European Journal of Agronomy* 30(3): 228-237.

GAO Y., YUN L., ZHANG J., LIU W., DANG Z., CAO W. & QIANG Q. 2009. Effects of mulch, N fertilizer, and plant density on wheat yield, wheat nitrogen uptake, and residual soil nitrate in a dryland area of China. *Nutrient Cycling Agroecosystem* 85:109–121 doi 10.1007/s10705-009-9252-0

GELAW A.M., SINGH B.R. & LAL R. 2015. Soil quality indices for evaluating smallholder agricultural land uses in northern Ethiopia. *Sustainability* 7:2322–2337. https://doi.org/10.3390/su7032322.

GEONICS LIMITED. 2008. EM38-MK2 ground conductivity meter operational manual, Mississauga, Ontario, Canada.

GREGORY P.J., CRAWFORD D.V. & McGOWAN M. 1979. Nutrient relations of winter wheat. 1. Accumulation and distribution of Na, K, Ca, Mg, P, S and N. *Journal of Agricultural Science Cambridge* 93:485--494.

GRUNWALD S., THOMPSON J.A. & BOETTINGER J.L. 2011. Digital soil mapping and modelling at continental scales: finding solutions for global issues. *Soil Science Society of America Journal* 75:1201-1213

GRUNWALD S., VASQUES G. M., & RIVERO G.R. 2015. Fusion of Soil and Remote Sensing Data to Model Soil Properties. *Advances in Agronomy* 131

GURA I. & MNKENI P.N.S. 2019. Crop rotation and residue management effects under no till on the soil quality of a Haplic Cambisol in Alice, Eastern Cape, South Africa. *Georderma* 337:927-934

HAVLIN J. L., TISDALE S.L., NELSON W.L., & BEATON J.D. 2014. Soil fertility and nutrient management*: An introduction to nutrient management*. 8th ed. Pearson, Upper Saddle River, New York.

HE Y., SONG H. Y., PEREIRA A. G. & GÓMEZ A. H. 2005. A new approach to predict N, P, K and OM content in a loamy mixed soil by using near infrared reflectance spectroscopy. In: Huang *et al.* (Eds.), *ICIC, Part I, LNCS* 3644:859–867.

HE Y., HUANG M., GARCIA A., HERNANDEZ A. & SONG H. 2007. Prediction of soil macronutrients content using near-infrared spectroscopy. *Computers and Electronics in Agriculture* 58:144–153.

HEIL K., & SCHMIDHALTER U. 2012. Characterization of soil texture variability using the apparent soil electrical conductivity at a highly variable site. *Computers in Geoscience.* 39:98-110.

HEIL K. & SCHMIDHALTER U. 2017. The Application of EM38: Determination of Soil Parameters, Selection of Soil Sampling Points and Use in Agriculture and Archaeology. *Sensors* 17: 2540 doi:10.3390/s17112540

HEINIGER R.W., MCBRIDE R.G., & CLAY D.E. 2003. Using Soil Electrical Conductivity to Improve Nutrient Management. *Agronomy Journal* 95:508–519.

HENDRICKX J. 1992. Soil Salinity assessment by electromagnetic induction of irrigated land. *Soil Science Society of America Journal* 56:1933-1941.

HUANG C.J., HAN L.J., YANG Z.L., & LIU M. 2009. Exploring the use of near infrared reflectance spectroscopy to predict minerals in straw. *Fuel* 88:163–168. doi:10.1016/j.fuel.2008.07.031

HUIZENGA J.M., SILBERBAUER M., DENNIS R. & DNNIS I. 2013. An inorganic chemistry dataset (1972-2011) of rivers, dams and lakes in South Africa. *Water South Africa* 39(2):335-340.

HUMMEL J.W., GAULTNEY L.D. & SUDDUTH K.A. 1996. Soil property sensing for site-specific crop management. *Computer and Electronics in Agriculture* 14:121–136.

HUSSAINI K., ASHRAF M., & ASHRAF M.Y. 2008. Relationship between growth and ion relation in pearl millet (*Pennisetum glaucum* (L.) R. Br.) at different growth stages under salt stress. *Africa Journal Plant Sciences.* 2(3):23–27.

ISLAM K., SINGH B. & MCBRATNEY A. 2003. Simultaneous estimation of several soil properties by ultra-violet, visible and near-infrared spectroscopy. *Australian Journal of Soil Research* 41:1101-1114.

ISLAM K., SINGH B., SCHWENKE G. & MCBRATNEY A. 2004a. Evaluation of Vertisol soil fertility using ultra-violet, visible and near-infrared spectroscopy. In '*Proceedings of Supersoil 2004, the 3rd Australian New Zealand Soils Conference*'. University of Sydney, Australia, 5-9 December 2004. (Ed. B Singh)(CD-Rom)

JARRELL W. M. & BEVERLY R. B. 1981. The dilution effect in plant nutrition studies. *Advances in Agronomy* 34:197–224

JAYNES D.B., COLVIN T.S. & AMBUEL J. 1995. Yield mapping by electromagnetic induction. p. 383–394. *In* P.C. Robert et al. (ed.) *Site-specific management for agricultural systems. Proceedings of 2nd International Conference Minneapolis, MN. 27–30 Mar. 1994.* ASA, CSSA, and SSSA, Madison, WI.

JAYNES D.B., COLVIN T.S. & KASPAR T.C. 2005. Identifying potential soybean management zones from multi-year yield data. *Computers and Electronics in Agriculture* 46:309–327.

JONG E., DE NESTOR P.A. & PENNOCK D.J. 1998. The use of magnetic susceptibility to measure long-term soil redistribution. *Catena* 32: 23-35.

JOHNSON C.K., DORAN J.W., DUKE H.R., WEINHOLD B.J., ESKRIDGE K.M. & SHANAHAM J.F., 2001. Field-scale Electrical Conductivity Mapping for Delineating Soil Condition. *Soil Science Society of America Journal* 65: 1829 - 1837.

JOHNSON C.K., MORTENSEN D.A., WIENHOLD B.J., SHANAHAN J.F. & DORAN J.W. 2003. Site-specific management zones based upon soil electrical conductivity in a semiarid cropping system. *Agronomy Journal* 95:303–315.

JONES J.B., WOLF B. & MILLS H.A. 1991. Interpretation of results. In: *Plant Analysis Handbook – a practical sampling, preparation, analysis, and interpretation guide.* Micro-Macro Publishing Inc., USA.

KAFFKA S.R., LESCH S.M., BALI K.M. & CORWIN D.L. 2005. Site-specific management in salt-affected sugar beet fields using electromagnetic induction. *Computers and Electronics in Agriculture* 46:329–350.

KARLEN D. L., FLANNERY R. L., & SADLER E. J. 1988. Aerial Accumulation and Partitioning of Nutrients by Corn. *Agronomy Journal* 80:232-242.

KARLEN D.L., MAUSBACH M.J., DORAN J.W., CLINE R.G., HARRIS R.F. & SCHUMAN G.E. 1997. Soil quality: A concept, definition and framework for evaluation. *Soil Science Society of America Journal* 61: 4–10. 6(1):3-14.

KARLEN D.L., VEUM K.S., SUDDUTH K.S., OBRYCKIC J.F. & NUNES M.R. 2019. Soil health assessment: Past accomplishments, current activities, and future opportunities. S*oil & Tillage Research* 195:104365. https://doi.org/10.1016/j.still.2019.104365

KITCHEN N. R., SUDDUTH K. A., BIRRELL S.J. & BORGELT S. C. 1996. Missouri precision agriculture research and education. *Precision Agriculture, Proceedings of the 3rd International Conference,* 23-26 June, pp. 1091-1099. ASA/CSSA/SSSA, Minneapolis, Minnesota.

KITCHEN N.R., DRUMMOND S.T., LUND E.D., SUDDUTH K.A. & BUCHLEITER G.W. 2003. Soil electrical conductivity and topography related to yield for three contrasting soil–crop systems. *Agronomy Journal* 95:483–495.

KITCHEN N.R., SUDDUTH K.A. & DRUMMOND S.T. 2000. Characterizing soil physical and chemical properties influencing crop yield using soil electrical conductivity. In *Second International Geospatial Information in Agriculture and Forestry Conference* 2:122−131. Ann Arbor, Mich. ERIM International.

KITCHEN N.R., SUDDUTH K.A., MYERS D.B., DRUMMOND S.T. & HONG S.Y. 2005. Delineating productivity zones on claypan soil fields using apparent soil electrical conductivity. *Computers and Electronics in Agriculture* 46: 285–308.

KNOX N.M., GRUNWALD S., MCDOWELL M.L., BRULAND G.L., MYERS D.B. & HARRIS W.G. 2015. Modelling soil carbon fractions with visible near infrared (VNIR) and mid-infrared (MIR) spectroscopy. *Geoderma* 239–240, 229–239.

KODAIRA M. & SHIBUSAWA S. 2013. Using a mobile real-time soil visible-near infrared sensor for high resolution soil property mapping. *Geoderma* 199:64-79.

KRAVCHENKO, A.N., AND D.G. BULLOCK. 2000. Correlation of corn and soybean grain yield with topography and soil properties. *Agronomy Journal* 92:75–83.

KUCHENBUCH R., CLAASSEN N. & JUNGK A. 1986. Potassium availability in relation to soil moisture. Plant Soil 95:221–231. doi:10.1007/ BF02375074

KUMAR S. & DEY P. 2011. Effects of different mulches and irrigation methods on root growth, nutrient uptake, water-use efficiency and yield of strawberry. *Science Horticulture* 127:318–324. doi:10.1016/j.scienta.2010.10.023

KUMARAVEL V., SANGODE S.J., SIDDAIAH N.S. & KUMAR R. 2010. Interrelation of magnetic susceptibility, soil color and elemental mobility in the Pliocenee Pleistocene Siwalik paleosol sequences of the NW Himalaya, India. *Geoderma* 154: 267-280.

LANDON J.R. 1991. Booker Tropical Soil Manual: *A Handbook of Soil Survey and Agricultural Land Evaluation in the Tropics and Subtropics.* Longman Scientific Technical and Booker Tate Limited, London, U.K.

LECO. 2003. Truspec CN Carbo/Nitrogen Determinator Instructions Manual. LECO Corporation, St Joseph, U.S.A.

LESCH S.M., CORWIN D.L. & ROBINSON D.A. 2005. Apparent soil electrical conductivity mapping as an agricultural management tool in arid zone soils. *Computers and Electronics in Agriculture* 46: 351–378.

LESCH S.M., RHOADES J.D. & CORWIN D.L. 2000. ESAP-95 version 2.10R: User and tutorial guide. *Research Report* 146. USDA-ARS, US Salinity Laboratory, Riverside, CA.

LESCH S.M., STRAUSS D.J. & RHOADES J.D. 1995a. Spatial prediction of soil salinity using electromagnetic induction techniques. 1. Statistical prediction models: A comparison of multiple linear regression and cokriging. *Water Resources Research* 31:373–386.

LESCH, S.M., STRAUSS, D.J. & RHOADES J.D. 1995b. Spatial prediction of soil salinity using electromagnetic induction techniques. 2. An efficient spatial sampling algorithm suitable for multiple linear regression model identification and estimation. *Water Resources Research* 31:387–398.

LI H.Y., SHI Z., WEBSTER R. & TRIANTAFILIS J. 2013. Mapping the three-dimensional variation of soil salinity in a rice-paddy soil. *Geoderma* 195-196, 31-41.

LINKER R., KENNY A., SHAVIV A., SINGHER L. & SHMULEVICH L. 2004. FTIR/ATR nitrate determination of soil pastes using PCR, PLS and cross-validation. *Applied Spectroscopy* 58: 516–520.

LINKER R., SHMULEVICH I., KENNY A. & SHAVIV A. 2005. Soil identification and chemometrics for direct determination of nitrate in soils using FTIR-ATR mid-infrared spectroscopy. *Chemosphere* 61:652–658.

LINKER R., WEINER M., SHMULEVICH I. & SHAVIV A. 2006. Nitrate determination in soil pastes using attenuated Total reflectance mid-infrared spectroscopy: Improved Accuracy via Soil Identification. *Biosystems Engineering* 94:111–118.

LOWENBERG-DEBOER J. & ERICKSON K. 2000. Precision Farming Profitability. Purdue University, West Lafayette, IN.

LU S.G., BAI S.Q. & FU L.X. 2008. Magnetic properties as indicators of Cu and Zn contamination in soils. *Pedosphere* 18: 479-485.

LUND E.D., COLIN P.E., CHRISTY D., & DRUMMOND P.E. 1999. Applying soil electrical conductivity technology to precision agriculture. p. 1089–1100. In Robert P.C. et al. (ed.) *Precision agriculture - Proceedings at 4th International Conference, St. Paul, MN. 19–22 July 1998*. ASA, CSSA, and SSSA, Madison, WI.

LYNAM J.K. & HERDT R.W. 1989. Seeds and sustainability: sustainability as an objective in international agricultural research. *Agricultural economics* 3(4): 381-397

MA F., DU C. W., Z H O U J. M. & S H E N Y. Z. 2019. Investigation of soil properties using different techniques of mid-infrared spectroscopy. *European Journal of Soil Science* 70:96–106. doi: 10.1111/ejss.12741

MAHMOOD H. S., HOOGMOED W. B., & VAN HENTEN E. J. 2009. Combined sensor system for mapping soil properties. In Van Henten E. J. *et al.* (Eds.), *Precision agriculture 2009: Proceedings of the 7th European conference on precision agriculture, The Netherlands (pp. 423–430).* The Netherlands: Wageningen Academic Publishers.

MAHMOOD S. H., HOOGMOED W.B., & VAN HENTEN E.J. 2012. Sensor data fusion to predict multiple soil properties. *Precision Agriculture* 13:628-645

MAHMOOD S.H., HOOGMOED W.B. & VAN HENTEN E.J. 2013. Proximal gamma-ray spectroscopy to predict soil properties using windows and full-spectrum analysis methods. *Sensors* 13:16263-16280.

MALEKI M.R., MOUAZEN A.M., RAMON H. & BAERDEMAEKER J. DE. 2007. Optimization of soil VIS-NIR sensor-based variable rate application system of soil phosphorus. *Soil Tillage Research* 94: 239-250.

MALICKI M.A. & WALCZAK R.T. 1999. Evaluating soil salinity status from bulk electrical conductivity and permittivity. *European Journal of Soil Science* 50(3):505–514.

MARTIN M.Z., LABBÉ N., ANDRÉ N., WULLSCHLEGER S.D., HARRIS R.D. & EBINGER M.H., 2010. Novel multivariate analysis for soil carbon measurements using laser-induced breakdown spectroscopy. Soil Science Society of America Journal 74: 87-93.

McDOWELL M.L., BRULAND G.L., DEENIK J.L., GRUNWALD S., & KNOX N.M. 2012. Soil total carbon analysis in Hawaiian soils with visible, near-infrared and mid-infrared diffuse reflectance spectroscopy. *Geoderma* 189-190, 312-320.

McCARTY G. W. & REEVES J. B. 2006. Comparison of near infrared and mid infrared diffuse reflectance spectroscopy for field-scale measurement of soil fertility parameters. *Soil Science Society of America* 171:94–102.

MCCARTY G.W., REEVES III J.B., REEVES V.B., FOLLETT R.F. & KIMBLE J.M. 2002. Mid-infrared and near-infrared diffuse reflectance spectroscopy for soil carbon measurements. *Soil Science Society of America Journal* 66:640– 646.

McNEILL J.D. 1980. Electromagnetic terrain conductivity measurement at low induction numbers. Technical Note TN-6.

MCNEIL J.D. 1992. Rapid, accurate mapping of soil salinity by electromagnetic ground conductivity meters. *In Advances in measurements of soil physical properties: Bringing theory into practice. Soil Science Society of America* 30:201–229. SSSA, Madison, WI.

MELENDEZ-PASTOR I., NAVARRO-PEDRENO J., GOMEZ I. & KOCH M. 2008. Identifying optimal spectral bands to assess soil properties with VNIR radiometry in semi-arid soils. *Geoderma* 147(3–4): 126–132.

MILORI D.M.B.P., GALETI H.V.A., MARTIN-NETO L., DIECKOW J., GONZALEZ-PÉREZ, M., BAYER C. & SALTON J. 2006. Organic matter study of whole soil samples using laser-induced fluorescence spectroscopy. *Soil Science Society of America Journal* 70: 57-63.

MINASNY B., MCBRATNEY A.B., PICHON L., SUN W. & SHORT M.G. 2009a. Evaluating near infrared spectroscopy for field prediction of soil properties. *Australian Journal of Soil Research* 47: 664.

MISRA R.K. & PADHI J. 2014. Assessing field-scale soil water distribution with electromagnetic induction meter. *Journal of Hydrology* 516: 200 - 209.

MORAL F.J., TERRÓN J.M. & MARQUES DA SILVA J.R. 2010. Delineation of management zones using mobile measurements of soil apparent electrical conductivity and multivariate geostatistical techniques. *Soil Tillage Research* 106:335–343.

MOUAZEN A.M., KUANG B., DE BAERDEMAEKER J. & RAMON H. 2010. Comparison among principal component, partial least squares and back propagation neural network analyses for accuracy of measurement of selected soil properties with visible and near infrared spectroscopy. *Geoderma* 158: 1–2, 23-31

MOUAZEN A. M., MALEKI M. R., BAERDEMAEKER J. D. & RAMON H. 2007. On-line measurement of some selected soil properties using a VIS-NIR sensor. *Soil & Tillage Research* 93:13–27.

MUSINGUZI P., EBANYAT P., TENYWA J.S., BASAMBA T.A., TENYWA M.K. & MUBIRU D. 2016. Critical soil organic carbon range for optimal crop response to mineral fertiliser nitrogen on a ferralsol. Experimental Agriculture 52(4):635-653. doi:10.1017/S0014479715000307

MUTUO P.K., SHEPHERD K.D., ALBRECHT A. & CADISCH G. 2006. Prediction of carbon mineralization rates from different soil physical fractions using diffuse reflectance spectroscopy. *Soil Biology & Biochemistry* 38:1658–1664.

NABIOLLAHI K.; HESHMAT E.; MOSAVI A.; KERRY R.; ZERAATPISHEH M. & TAGHIZADEH-MEHRJARDI R. 2020. Assessing the Influence of Soil Quality on Rainfed Wheat Yield. *Agriculture 10*, 469. doi:10.3390/agriculture10100469

NADLER A. 1982. Estimating the soil water dependence of the electrical conductivity soil solution/electrical conductivity bulk soil ratio. *Soil Science Society of America Journal* 46:722–726.

NANNI M. R. & DEMATTE J. A. W. 2006. Spectral reflectance methodology in comparison to traditional soil analysis. Soil Science Society of America Journal 70:393–407.

ORTEGA R. A. & SANTIBANEZ O. A. 2007. Determination of management zones in corn (*Zea mays* L.) based on soil fertility. Computers and Electronics in Agriculture 58, 49–59.

PANDEY R.K., MARANVILLE J.W., & ADMOU A. 2000. Deficit irrigation and nitrogen effects on maize in a Sahelian environment: I. Grain yield and yield components. *Agricultural Water Management.* 46:1–13. doi:10.1016/S0378-3774(00)00073-1

PERALTA N.R. & COSTA J.L. 2013. Delineation of management zones with soil apparent electrical conductivity to improve nutrient management. Computers and Electronics in Agriculture 99 (2013) 218–226

PIRIE A., SINGH B. & ISLAM K. 2005. Ultra-violet, visible, near-infrared, and mid-infrared diffuse reflectance spectroscopic techniques to predict several soil properties. *Australian Journal of Soil Research* 43:713-721.

REEVE R.C. & FIREMAN M. 1967. Salt problems in relation to irrigation. Hagan R.M. et al (Ed) *In: Irrigation of agricultural lands.* https://doi.org/10.2134/agronmonogr11.c56

REEVES J.B., McCARTY G.W. & REEVES V.B. 2001. Mid-infrared diffuse reflectance spectroscopy for the quantitative analysis of agricultural soils. *Journal of Agricultural and Food Chemistry* 49:766-772. doi:10.1021/jf0011283

RENZULLO L., BARRETT D., MARKS A., HILL M., GUERSCHMAN J., MU Q. & RUNNING S. 2008. Multi-sensor model-data fusion for estimation of hydrologic and energy flux parameters. *Remote Sensing of Environment 112*:1306-1319.

RIDINGS M., SHORTER A.J. & SMITH J.B. 2000. Strategies for the investigation of contaminated sites using field portable x-ray fluorescence (FPXRF) techniques. *Communications in Soil Science and Plant Analysis* 31: 1785-1790.

RHOADES J.D. 1992. Instrumental field methods of salinity appraisal. In Topp G.C. *et al.* (Eds.), *Advances in Measurement of Soil Physical Properties: Bring Theory into Practice. Soil Science Society of America 30:*231–248*. SSSA*, Madison, WI, USA.

RHOADES J.D. 1996. Salinity: Electrical conductivity and total dissolved salts. In: Sparks D.L. (Ed.), *Methods of Soil Analysis. Part 3—Chemical Methods. Soil Science Society of America Book Series 5, pp. 417–435.* Soil Science Society of America, Madison, WI, USA.

RHOADES J.D., CHANDUVI F. & LESCH, S.M. 1999. Soil salinity assessment: Methods and interpretation of electrical conductivity measurements. *FAO Irrigation and Drainage Paper No* 57. Food and Agriculture Organization of United Nations, Rome, Italy.

RHOADES J.D., LESCH S.M., LEMERT R.D. & ALVES W.J. 1997. Assessing irrigation/drainage/salinity management using spatially referenced salinity measurements. *Agricultural water management* 35:147–165.

RHOADES J.D., MANTEGHI N.A., SHOUSE P.J. & ALVES W.J. 1989. Soil electrical conductivity and soil salinity: New formulations and calibrations. *Soil Science Society of America Journal* 53:433–439.

RHOADES J.D., MANTEGHI N.A., SHOUSE P.J. & ALVES W.J. 1989a. Estimating soil salinity from saturated soil-paste electrical conductivity. *Soil Science Society of America Journal* 53: 428 - 433.

RHOADES J.D., MANTEGHI N.A., SHROUSE P.J. & ALVES W.J. 1989b. Soil electrical conductivity and soil salinity: new formulations and calibrations. *Soil Science Society of America Journal* 53:433 - 439.

RHOADES J.D., RAATS P.A. & PRATHER R.J. 1976. Effect of liquid-phase electrical conductivity, water content and surface conductivity on bulk soil electrical conductivity. *Soil Science Society of America Journal* 40: 651 - 655.

SAEY T., MEIRVENNE M., VAN SMEDT P., DE COCKX L., MEERSCHMAN E., ISLAM M.M. & MEEUWS F. 2011. Mapping depth-to-clay using fitted multiple depth response curves of a proximal EMI sensor. *Geoderma* 162:151-158.

SAYRE J.D. 1948. Mineral accumulation in corn. *Plant Physiology* 23:267–281. doi:10.1104/pp.23.3.267

SCHMIDHALTER U.A., ZINTEL A. & NEUDECKER E. 2001. Calibration of Electromagnetic Induction Measurements to Survey the Spatial Variability of Soils. *In Proceedings of the 3rd European Conference on Precision Agriculture pp. 479–484*. 18–20 June 2001, Montpellier, France.

SCHULZE R.E. & WALKER N.J. 2007. Maize Yield Estimation. *In:* Schulze R.E. (Ed). 2007. *South African Atlas of Climatology and Agro-hydrology.* Water Research Commission, Pretoria, RSA, WRC Report 1489/1/06, Section 16.2.

SHAINBERG I., RHOADES J.D. & PRATHER R.J.1980. Effect of exchangeable sodium percentage, cation exchange capacity, and soil solution concentration on soil electrical conductivity. *Soil Science Society of America Journal* 44:469–473.

SHAVIV A., KENNY A., SHMULEVICH I., SINGHER L., REICHLIN Y. & KATZIR A. 2003. IR fiber-optic systems for in situ and real time monitoring of nitrate in water and environmental systems. *Environmental Science and Technology* 37:2807–2812.

SHIBUSAWA S., IMADE ANOM S.W., SATO S., SASAO A. & HIRAKO S. 2001. Soil mapping using the real-time soil spectrophotometer. In: Grenier G., Blackmore S. (Eds.), *ECPA 2001, Third European Conference on Precision Agriculture* 1:497–508. Agro Montpellier.

SCHIRRMANN M., GEBBERS R., KRAMER E., & SEIDEL J. 2011. Evaluation of soil sensor fusion for mapping macronutrients and soil pH. In Adamchuk V. I., Viscarra Rossel R. A. (Eds.), *Proceedings of the second global workshop on proximal soil sensing*, Canada (pp. 48–51). Montreal, Canada: McGill University press.

SHEPHERD K. D. & WALSH M. G. 2002. Development of reflectance spectral libraries for characterization of soil properties. *Soil Science Society of America Journal* 66:988–998.

SHIRATSUCHI L.S., FERGUSON R.B., ADAMCHUK V.I., SHANAHAN J.F. & SLATER G.P. 2009. Integration of ultrasonic and active canopy sensors to estimate the in-season nitrogen content for corn. In: *Proceedings of the 39th North Central Extension- Industry Soil Fertility Conference, Des Moines, Iowa, 18-19 November 2009.* International Plant Nutrition Institute, Norcross, Georgia, USA.

SIMONE G., FARINA A., MORABITO F.C., SERPICO S.B. & BRUZZONE L. 2002. Image fusion techniques for remote sensing applications. *Information Fusion* 3:3-15.

SINGH G., WILLIARD K. J. W. & SCHOONOVER J. E. 2016. Spatial Relation of Apparent Soil Electrical Conductivity with Crop Yields and Soil Properties at Different Topographic Positions in a Small Agricultural Watershed. *Agronomy 6:5.* doi: 10.3390/agronomy6040057

SOIL CLASSIFICATION WORKING GROUP, 1991. Soil classification, a taxonomic system for South Africa. Memoirs concerning the natural agricultural resources of South Africa.

SOSIBO N.Z., MUCHAONYERWA P., VISSER L., BARNARD A., DUBE E. & TSILO T.J. 2017. Soil fertility constraints and yield gaps of irrigation wheat in South Africa. *South African Journal of Soil Plants and Soil* http://dx.doi.org/10.17159/ sajs.2017/20160141

SMITH R.J., RAINE S., MCCARTHY A.C. & HANCOCK N. 2009. Managing spatial and temporal variability agriculture through adaptive control. *Australian Journal of Multi-Disciplinary Engineering* 7(1): 79-89

SPADONI M. & VOLTAGGIO M. 2013. Contribution of gamma ground spectrometry to the textural characterization and mapping of floodplain sediments. *Journal of Geochemical Exploration* 125:20-33.

STAFFORD J. V. 1996. Essential technology for precision agriculture. *Precision Agriculture*, *Proceedings of the 3rd International Conference,* pp. 595-604. 23-26 June, *ASA/CSSA/SSSA*, Minneapolis, Minnesota.

STOTT D.E., ANDREWS S.S., LIEBIG M.A., WIENHOLD B.J. & KARLEN D.L. 2010. Evaluation of β-glucosidase activity as a soil quality indicator for the Soil Management Assessment Framework (SMAF). *Soil Science Society of America Journal* 74:107–119. doi:10.2136/sssaj2009.0029.

STOTT D.E., CAMBARDELLA C.A., TOMER M.D., KARLEN D.L. & ROJER W. 2011. A Soil Quality Assessment within the Iowa River South Fort Watershed. *Soil Science Society of America Journal* 75:2271–2282.

STOTT D.E., KARLEN D.L. & HARMEL R.D. 2013. A Soil Quality and Metabolic Activity Assessment after Fifty-Seven Years of Agricultural Management. *Soil Science Society of America Journal 77*:903–913.

SUDDUTH K.A., DRUMMOND S.T. & KITCHEN N.R. 2001. Accuracy issues in electromagnetic induction sensing of soil electrical conductivity for precision agriculture. *Computers and Electronics in Agriculture* 31: 239-264.

SUDDUTH K.A., KITCHEN N.R. & DRUMMOND S.T. 1999. Soil conductivity sensing on claypan soils: Comparison of electromagnetic induction and direct methods. In Robert P.C*. et al.* (Ed.) p. 979–990. *Precision agriculture – Proceedings of the 4th International Conference, St. Paul, MN.* 19–22July 1998. ASA, CSSA, and SSSA, Madison, WI.

SUDDUTH K.A., KITCHEN N.R., HUGHES D.F & DRUMMOND S.T. 1996. Electromagnetic induction sensing as an indicator of productivity on clay-pan soils. In P.C. Robert *et al.* (Ed.) p. 671–681. *Precision agriculture – Proceedings at the 3rd International Conference, Minneapolis, MN. 23–26 June 1996.* ASA, CSSA, and SSSA, Madison, WI.

SUDDUTH K.A., KITCHEN N.R., WIEBOLD W.J., BATCHELORC W.D., BOLLEROD G.A., BULLOCK D.G., CLAYE D.E., PALM H.L., PIERCE F.J., SCHULER R.T. & THELEN K.D. 2005. Relating apparent electrical conductivity to soil properties across the north-central USA. *Computers and Electronics in Agriculture* 46:263–283. doi:10.1016/j.compag.2004.11.010

SUDDUTH K.A., MYERS D.B., KITCHEN N.R. & DRUMMOND S.T. 2013. Modeling soil electrical conductivity-depth relationships with data from proximal and penetrating EC_a sensors. *Geoderma* 199:12-21.

TANDON H.L.S. & MURALIDHARUDU Y. 2010. Nutrient uptake, removal and recycling by crops. *Fertilizer Development and Consultation Organization*, 2010

TAYLOR J., SHORT M., MCBRATNEY A. B., & WILSON J. 2010. Comparing the ability of multiple soil sensors to predict soil properties in a Scottish potato production system. In Viscarra Rossel R. A. *et al.* (Eds.), *Proximal soil sensing* 387–396. Dordrecht: Springer.

TERRA F.S., DEMATTÊ J.A.M. & VISCARRA ROSSEL R.A. 2015. Spectral libraries for quantitative analyses of tropical Brazilian soils: comparing vis–NIR and mid–IR reflectance data. *Geoderma* 255–256, 81–93.

THE NON-AFFILIATED SOIL ANALYSIS WORK COMMITTEE. 1990. Handbook of standard soil testing methods for advisory purposes. *Soil Science Society of South Africa*, Sunnyside, Pretoria.

THOMPSON G.A. 1995. A comparison of methods used for the extraction of K in soils of the Western Cape. *South African Journal of Plant and Soil* 12(1): 20-26

TOWETT E.K., SHEPHERD K.D. & CADISCH, G. 2013. Quantification of total element concentrations in soils using total X-ray fluorescence spectroscopy (TXRF). *Science for Total Environment* 463-464, 374-388.

TÜRKER-KAYA S. & HUCK C.W. 2017. A Review of Mid-Infrared and Near-Infrared Imaging: Principles, Concepts and Applications in Plant Tissue Analysis. *Molecules* 22:168. doi:10.3390/molecules22010168

TRIANTAFILIS J., HUCKEL A.I. & MCBRATNEY A.B. 1998. Estimating deep drainage on the field scale using a mobile EM sensing system and Sodium-SaLF. *In: Proceedings of the Ninth Australian Cotton Growers Research Association Conference,* pp. 61–64. August 12–14, 1998, Broadbeach, Queensland, Australia.

UNITED STATES DEPARTMENT OF AGRICULTURE (USDA), 2018. Commodity Intelligence Report. *Foreign Agricultural Service, July 2, 2018*. https://ipad.fas.usda.gov/highlights/2018/07/SouthAfrica/index.pdf [Accessed: 15 April 2021

UNITED STATES SALINITY LABORATORY STAFF. 1954. Diagnosis and improvement of saline and alkali soils. Richards L.A. (Ed.), *Handbook No.* 60. United States Department of Agriculture, United States of America.

VAN HEERDEN P.S. & WALKER S. 2016. Upgrading of SAPWAT3 as a management tool to estimate the irrigation water use of crops. *Revised edition SAPWATT4. Water Research Commission Report No* TT662/16. Pretoria, South Africa.

VAN MAARSCHALKERWEERD M. & HUSTED S. 2015. Recent developments in fast spectroscopy for plant mineral analysis. *Frontiers in Plant Science* 6:169. doi: 10.3389/fpls.2015.00169

VASQUES G.M., GRUNWALD S. & SICKMAN J.O. 2008. Comparison of multivariate methods for inferential modeling of soil carbon using visible/near-infrared spectra. *Geoderma* 146:14-25.

VAUGHAN B. 1999. How to determine an accurate soil testing laboratory. In: Clay et al. (Ed.) *Site Specific Management Guidelines (SSMG)* 4. Potash and Phosphate Institute, Norcross, Georgia.

VENTER A., BEUKES D. J., CLAASSENS A.S. & VAN MEIRVENNE M. 2004. Temporal and spatial relations of plant element uptake and yield of a lucerne stand. *South African Journal of Plant and Soil* 21(3):157-165. doi: 10.1080/02571862.2004.10635042

VERMA S. K. & DEB M. K. 2007b. Non-destructive and rapid determination of nitrate in soil, dry deposits and aerosol samples using KBr-matrix with diffuse reflectance Fourier transform infrared spectroscopy (DRIFTS). *Analytica Chimica Acta* 582: 382–389.

VEUM K.S., GOYNE K.W., KREMER R.J., MILES R.J. & SUDDUTH K.A. 2014. Biological indicators of soil quality and soil organic matter characteristics in an agricultural management continuum. *Biogeochemistry* 117: 81–99.

VEUM K.S., SUDDUTH K.A., KREMER R.J. & KITCHEN N.R. 2015. Estimating a Soil Quality Index with VNIR Reflectance Spectroscopy. *Soil Science Society of America Journal* 305:53-61

VEUM K.S., SUDDUTH K.A., KREMER R.J. & KITCHEN N.R. 2017. Sensor data fusion for soil health assessment. *Geoderma* 305:53-61

VISCARRA ROSSEL R. A. & MCBRATNEY A. B. 1998. Laboratory evaluation of a proximal sensing technique for simultaneous measurement of clay and water content. *Geoderma* 85:19–39.

VISCARRA ROSSEL, R.A., WALVOORT, D.J.J., MCBRATNEY, A.B., JANIK, L.J., SKJEMSTAD, J.O., 2006. Visible, near infrared, mid infrared or combined diffuse reflectance spectroscopy for simultaneous assessment of various soil properties. *Geoderma* 131:59-75.

VISCARRA ROSSEL R.A., TAYLOR, H.J. & MCBRATNEY A.B. 2007. Multivariate calibration of hyperspectral gamma-ray energy spectra for proximal soil sensing. *European Journal of Soil Science* 58:343-353.

VISCARRA ROSSEL R.A., CATTLE S.R., ORTEGA A. & FOUAD Y. 2009. In situ measurements of soil color, mineral composition and clay content by VIS-NIR spectroscopy. *Geoderma* 150:253-266.

VISCARRA ROSSEL R.A., ADAMCHUK V.I., SUDDUTH K.A., MCKENZIE N.J. & LOBSEY C. 2011. Proximal soil sensing: an effective approach for soil measurements in space and time. *Advances in Agronomy.* 113:243-291.

VOHLAND M. & EMMERLING C. 2011. Determination of total soil organic C and hot water extractable C from VIS–NIR soil reflectance with partial least squares regression and spectral feature selection techniques. *European Journal of Soil Science* 62: 598–606.

VOHLAND M., LUDWIG M., THIELE-BRUHN S. & LUDWIG B., 2014. Determination of soil properties with visible to near-and mid-infrared spectroscopy: effects of spectral variable selection. *Geoderma* 223:88–96. doi: 10.1016/j.geoderma.2014.01.013.

WANG J.S., GRIMLEY D.A., XU C. & DAWSON J.O. 2008. Soil magnetic susceptibility reflects soil moisture regimes and the adaptability of tree species to these regimes. *Forest Ecological Management* 255:1664-1673.

WARD A., NIELSEN A.L. & MOLLER H. 2011. Rapid assessment of mineral concentration in meadow grasses by near infrared reflectance spectroscopy. *Sensors* 11:4830–4839. doi:10.3390/s110504830

WETTERLIND J., STENBERG B. & SODERSTROM M. 2008b. The use of near infrared (NIR) spectroscopy to improve soil mapping at the farm scale. *Precision Agriculture* 9:57–69.

WETTERLIND J., PIIKKI K., STENBERG B., & SÖDERSTRÖM M. 2015. Exploring the predictability of soil texture and organic matter content with a commercial integration soil profiling tool. *European Journal of Soil Science* 66:631-638. doi: 10.1111/ejss.12228

WETTSTEIN S., MUIR K., SCHARFY D. & STUCKI M. 2017. The environmental mitigation potential of photovoltaic-powered irrigation in the production of South African maize. *Sustainability* 9:1772. doi:10.3390/su9101772

WHEAL M. S., FOWLES T.O. & PALMER L.T. 2011. A cost-effective acid digestion method using closed polypropylene tubes for inductively coupled plasma optical emission spectrometry (ICP-OES) analysis of plants essential elements. *Analytical methods.* 3:2854-2863

WHELAN B. & TAYLOR J. 2013. Precision agriculture for grain production systems. CSIRO PUBLISHING, Australia.

WIELOPOLSKI L., CHATTERJEE A., MITRA S. & LAL R. 2011. In situ determination of soil carbon pool by inelastic neutron scattering: comparison with dry combustion. *Geoderma* 160:394-399.

WIENHOLD B.J., KARLEN D.L., ANDREWS S.S. & STOTT D.E. 2009. Protocol for Soil Management Assessment Framework (SMAF) soil indicator scoring curve development. *Renewable Agriculture Food Systems* 24:260–266. doi: 10.1017/S1742170509990093.

WILDING L.P., BOUMA J. & GOSS D.W. 1994. Impact of spatial variability on interpretive modeling. In: Bryant R.B., Arnold R.W. (Eds.), *Quantitative modeling of soil forming processes. Soil Science Society of America* 39:61–75. ASA, CSSA, and SSSA, Madison, WI, USA

WILLIAMS P. 2014. Tutorial: the RPD statistic: a tutorial note. *NIR News* 25, 22–26.

WONG M. T. F., WITTER K., OLIVER Y. & ROBERTSON K. J. 2010. Use of EM38 and gamma ray spectrometry as complementary sensors for high-resolution soil property mapping. In Viscarra Rossel R. A. *et al.* (Eds.) *Proximal soil sensing* (pp. 343–349). Dordrecht: Springer.

WU C.M., TSAI H.T., YANG K.H. & WEN J.C. 2012. How reliable is X-ray fluorescence (XRF) measurement for different metals in soil contamination? *Environmental Forensics* 13:110-121.

ZENG Q. & BROWN P. 2000. Soil potassium mobility and uptake by corn under differential soil moisture regimes. *Plant Soil* 221:121–134. doi:10.1023/A:1004738414847

ZHU Y., WEINDORF D.C. & ZHANG W. 2011. Characterizing soils using a portable X-ray fluorescence spectrometer: 1. Soil texture. *Geoderma* 167-168, 167-177.